SYNTHESIS, STRUCTURAL, EPR, MAGNETIC AND OPTICAL SPECTRAL STUDIES OF HIGHER VALENT MANGANESE COMPLEXES

A THESIS
SUBMITTED FOR THE DEGREE OF

DOCTOR OF PHILOSOPHY

BY

K. RAJENDER REDDY

SCHOOL OF CHEMISTRY
UNIVERSITY OF HYDERABAD
HYDERABAD -500 134, INDIA
NOVEMBER 1993

CONTENTS

STATEMENT

I hereby declare that the matter embodied in this thesis is the result of investigations carried out by me in the School of Chemistry, University of Hyderabad, Hyderabad, under the supervision of Dr. M.V. Rajasekharan.

In keeping with the general practice of reporting scientific observations, due acknowledgement has been made wherever the work described is based on the findings of other investigators.

KR Reddy

K. Rajender Reddy

CERTIFICATE

Certified that the work contained in this thesis entitled "SYNTHESIS, STRUCTURAL, EPR, MAGNETIC AND OPTICAL SPECTRAL STUDIES OF HIGHER VALENT MANGANESE COMPLEXES " has been carried out by Mr. K. Rajender Reddy under my supervision and the same has not been submitted elsewhere for a degree.

Hyderabad

November, 1993

M.V. RAJASEKHARAN

(Thesis Supervisor)

DEAN

SCHOOL OF CHEMISTRY

Professor P.S. Zacharias
Dean, School of Chemistry
University of Hyderabad
Hyderabad-500 134, India

ACKNOWLEDGEMENTS

I take this opportunity to thank my research supervisor, **Dr. M. V. Rajasekharan** for suggesting me this problem and for valuable guidance.

I thank all my teachers of the school for their inspiring lectures, help and encouragement. I also thank the present and former Deans for extending all the facilities of the department.

I thank Prof. P. T. Manoharan (IIT, Madras), Prof. Animesh Chakravorty (IACS, Calcutta), Prof. D. J. Hodgson (Univ of Wyoming, USA), Prof. J. P. Tuchagues (Institut National Polytechinque, Toulouse Cedex, France) and Prof. S. Padhye (Univ of Poona) for their help in providing X-ray data.

I thank Prof. K. V. Reddy, PSO, CIL and the CIL staff for their help in recording the spectra. I also thank all the non-teaching staff of the school for their help.

I thank my labmates Dr G. Swarnabala, Dr N. Venkata Laxmi, Dr C. Balagopala Krishna, Miss Sindhu Menon and Miss Ramalakshmi for their help and cooperation.

I would like to extend my heartfelt thanks to my friends Messers Rama Reddy, Bhaskar Kanth, Prabhakar, Hari, Venkat, Prem, Kishan, Narender, Jagdeesh, Sekhar, Satish, Bhanu, Ramkishan, Ramakrishna, Murali, Peddi reddi, Dharma Rao, Chandra, Shastry, Raghu, Soma Sekhar, Sambasiva Rao, Arul Samy, K. M. Sharma, Bheema

Rao, Bhaskar Raju and other colleagues for their cooperation.

It is my pleasure to thank Messers Prem Kumar (Anna), Prem Kumar (Chotte), Narender Rao Jayender and my hostel friends Suresh, Srinivas, Murali, Purendra, Nagesh, A.K.Singh and Kranti who made my stay a memorable one.

I wish to express my profound gratitude to my mother, sisters, Uncle and beloved friend Srikanth Sharma for their love and affection.

It is the time to recall my beloved father and grand father whom I am missing at this time.

Financial Assitance from UGC is greately acknowledged.

ABBREVIATIONS

acac	acetylacetone
bpy	2,2'-bipyridine
phen	1,10-phenanthroline
H_2sal	salicylic acid
py(pyr)	pyridine
DMF	dimethylformimide
CH_3CN	acetonitrile
DCM	dichloromethane
THF	tetrahydrofuran
picH	picolinic acid
hqnH	8-hydroxyquinoline
HIm	imidazole
dbm	dibenzolmethane
H_2phth	phthalicacid
hmpH	2-(hydroxymethyl)pyridine
EPR	electron paramagnetic resonance
EXAFS	extended X-ray absorption fine structure
XAS	X-ray absorption spectroscopy
PS-II	photosystem-II
OEC	oxygen evolving complex
WOC	water oxidation center
por	porphyrin
TPP	tetraphenylporphyrin
biphenH_2	2,2'-biphenol
Hpyro	1-aza-2-keto-3,5-cyclohexadiene
tpa	tris(2-methylpyridyl)amine 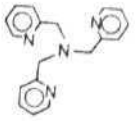
tren	2,2',2''-triaminoethylamine 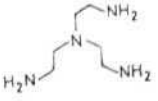

tacn 1,4,7-triazacyclononane

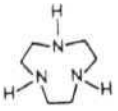

N_3O-py N,N-bis(2-pyridylmethyl)glycinate

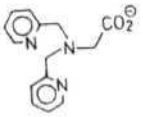

cyclam (14-aneN_4) 1,4,8,11-tetraazacyclotetradecane

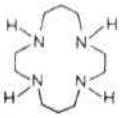

salen N,N'-bis(salicylidine)ethylenediaminato

H_2salpn N,N-bis(salicylidene)-1,3-diaminopropane

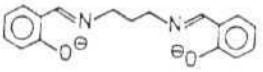

salmp 2-(bis(salicylideneamino)-methyl)-phenolate

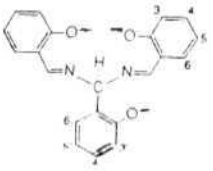

H_2salahp 1-hydroxy-3-(salicylideneamino)-propane

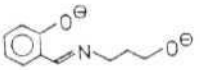

H_2saladhp 2-(salicylideneamino)-1,3-di-hydroxy-2-methylpropane

H_2salathm tris(hydroxymethyl)-salicylideneamino-methane

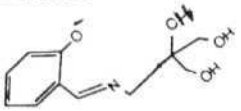

bispicen N,N'-bis(2-pyridylmethyl)-1,2-ethanediamine

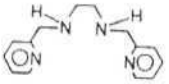

bispictn N,N'-bis(2-pyridylmethyl)-1,3-propanediamine

bispicbn N,N'-bis(2-pyridylmethyl)-2,3-butanediamine

bispichxn N,N'-bis(2-pyridylmethyl)-1,2-cyclohexanediamine

tpen N,N,N',N'-tetrakis(2-pyridylmethyl)-1,2-ethanediamine

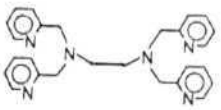

bpea N,N'-bis(2-pyridylmethyl)ethylamine

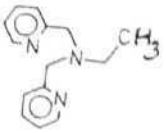

$HB(pz)_3$ hydrotris(pyrazol-1-yl)borate

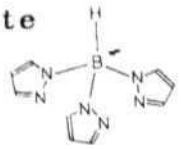

tmip tris(N-methylimidazol-2-yl)phosphine

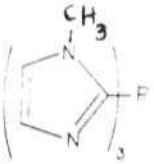

Htphpn(Htpdp) N,N,N',N'-tetrakis(2-pyridylmethyl)-1,3-diamino-2-propanol

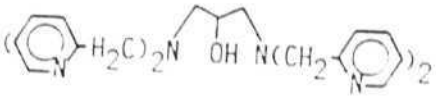

H_3L-1 1,5-bis(salicylideneamino)-3-pentanol

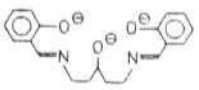

H_2L-2 salicylaldehyde anthraniloylhydrazone

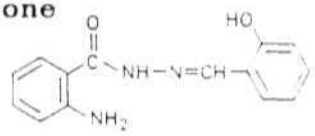

H_3L-3 1-salicylideneamino-3-salicylamino-2-propanol

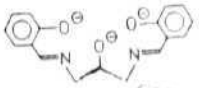

H_3L-4 Bis(benzoylacetone)-1,3-diimino-propane-2-ol

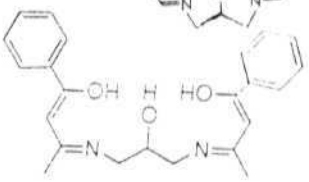

H_3L-8 3,5-bis((salicylideneamino)methyl)-pyrazole

HL-10 2,6-bis[N-(2-pyridylethyl)iminomethyl]-4-methylphenol

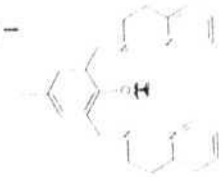

Hbpmp 2,6-bis[bis(2-pyridylmethyl)aminomethyl]-4-methylphenol

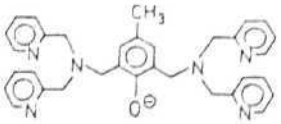

Hbcmp 2,6-bis(1,4,7-triazacyclonon-1-ylmethyl)-4-methylphenol

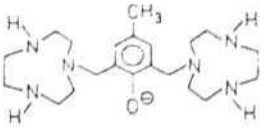

L-Im 2,6-bis[(bis((1-methylimidazol-2-yl)methyl)-amino)methyl]-4-methylphenol

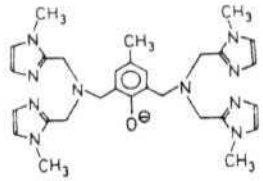

L-6

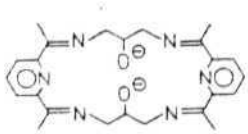

L-7

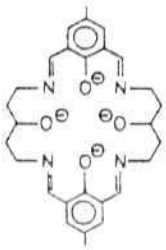

L-9

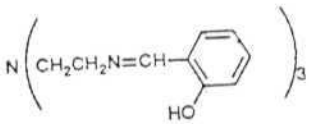

L-5

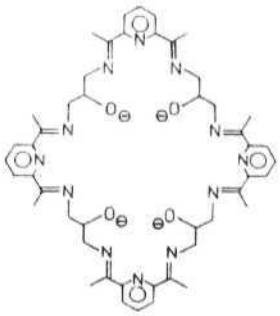

PREFACE

High-valent polynuclear complexes of manganese have drawn much attention of inorganic-chemists. Apart from their interesting electronic and magnetic properties, these units are found at the active site of some bio-systems. Many synthetic attempts are focussed now to prepare simple inorganic compounds which mimic the native systems. One such system currently under study is "Water Oxidation Center" (WOC) of photosystem-II (PS-II). It is found that a polynuclear unit is responsible for catalysing the water oxidation reaction in WOC.

With the interest in water oxidation, initially we carried out oxidation of water by Ce(IV) with di-μ-oxo Mn(III,IV) complexes as catalyst. Under the heterogeneous conditions Mn(III,IV) complexes are found to be good catalysts as reported earlier by Ramraj *et al.* (Angew. Chem. Int. Ed. Engl. 1986, 25, 826). However we also found that as the reaction proceeds, permanganate ion accumulates in solution. This complicates the total heterogeneous proposal for water oxidation. At this stage we thought the manganese species present in solution may also have an effect on water oxidation. Then we shifted our attention towards manganese oxidation by Ce(IV). All the reactions are carried out in aqueous solutions in an attempt to isolate water bound complexes.

The present thesis deals primarily with the synthesis and characterisation of higher-valent manganese complexes by Ce(IV) oxidation. Our attempts with HNO_3 oxidation and disproportionation of Mn(III) resulted in the isolation of two other complexes which are also discussed.

The first chapter gives a brief introduction on the importance of transition metal ions in bio-chemistry and is followed by a review on high-valent polynuclear manganese complexes.

Next two chapters contain, synthesis and structural characterisation of di- and tri- nuclear compounds prepared by Ce(IV) oxidations. Structures are compared with the known compounds and formation of different bridging units are explained by aqueous chemistry. Explanations are given for magnetic behavior with temperature variation for a (IV,IV) dimer (Chapter 2) and compared with the known (IV,IV) complexes.

Chapter 4 deals with the synthesis and structural studies on Mn(III) monomers formed by Ce(IV) and HNO_3 oxidations. Comparisons are made with the analogous compounds.

The final chapter describes the synthesis and structural studies on a (III,IV) complex obtained from the disproportionation of $Mn(OAc)_3$ in aqueous solution and preliminary investigations on other systems.

Some of the results in this thesis have been published or communicated:

1. A mononuclear bis-chelate complex of manganese(III) with 1,10-phenanthroline. Crystal and molecular structure of $[Mn(phen)_2Cl_2]NO_3 \cdot 2.5CH_3COOH$.

   K. Rajender Reddy and M. V. Rajasekharan Polyhedron (in press)

2. Modelling the photosynthetic water oxidation center: synthesis, structure and magnetic properties of $[Mn_2(\mu\text{-}O)_2(\mu\text{-}OAc)(H_2O)_2(bpy)_2](ClO_4)_3 \cdot H_2O$

   K. Rajender Reddy, M. V. Rajasekharan, Subhash Padhye, F. Dahan and J.-P. Tuchagues Inorg Chem (in press).

3. Mononuclear Mn(III) aquo complexes. Crystal and molecular structures of $Mn(phen)(H_2O)Cl_3$ and $[Mn(acac)_2(H_2O)_2]ClO_4 \cdot 2H_2O$ (acacH = acetylacetone, phen = 1,10-phenanthroline).

   G. Swarnabala, K. Rajender Reddy, T. Jyotsna and M. V. Rajasekharan Transition Met Chem (communicated).

CHAPTER 1.

BIO-INORGANIC MODELS: A BRIEF REVIEW ON POLYNUCLEAR MANGANESE COMPLEXES IN HIGHER VALENT STATES.

1.1 Introduction:

Over the past two decades there has been a growing interest n the study of a wide range of metallic and non-metallic elements ›resent in biological systems.[1-6] About 30 elements are recognized as essential for life in living organisms. Depending on the amount utilized, they are categorized into two types: one, in which they are used in bulk or macroscopic amounts (e.g., H, Na, K, Mg, Ca, N, O, P, S, and Cl) and the other, in which they are used in trace or microscopic quantities (e.g., Fe, Cu, Zn, Li, B, F, Si, V, Cr, Mn, Co, Ni, As, Se, Mo, I and W). Elements of the first category are mainly s- and p-block elements while trace elements are mainly transition elements.

One of the major roles played by metallic elements in bio-chemistry is in the active sites of metalloproteins which are involved in various bio-processes in the form of metalloenzymes like nitrogenases, oxidases, hydrogenases, reductases; respiratory proteins like hemoglobin and myoglobin; electron

transport proteins such as cytochromes and ferredoxins and metal storage proteins. Known metalloproteins now number several hundred and a vast field of research lies waiting for detailed explorations.

Development of spectroscopic and isolating techniques have led to the understanding of structural conformations at the active sites of some of the metalloproteins. The living systems are so complex that the understanding of structural and mechanistic aspects are often hampered by experimental and spectroscopic limitations. On the other hand, a combination of spectroscopic results on the bio-molecules and available knowledge of spectroscopic and coordination properties of low molecular weight complexes can lead to reasonable and likely structural proposals. This is one of the active areas of research in which inorganic chemists all over the world are involved. Making simple compounds which can possibly serve as models for bio-systems can help in understanding the complex bio-mechanisms.

1.2 Transition Metals in Bio-Chemistry:

Several transition metals are known to be involved in biology,[1-6] all of which, with the exception of molybdenum and possibly tungsten, belong to the 3d-series. Iron, zinc and copper

are the early elements to be recognized in bio-systems and much work has been done to understand their biological role.

Of all the transition elements iron is the most important and much is known about it.[7-11] It is at the active center of molecules responsible for oxygen transport[9] and electron transport.[10] Studies on ferritin,[11] an iron storage protein show that it consists of a shell of protein surrounding a core that contains iron ions having an approximate composition $(FeOOH)_8 . FeO.H_2PO_4$. From Mössbauer and magnetic studies it has been observed that all ferric ions are high spin and are subjected to strong antiferromagnetic interactions. The other important function of iron is to bind molecular oxygen in hemoglobin (Hb) and myoglobin (Mb).[9,12] From X-ray studies on both $Mb(O_2)$ and $Hb(O_2)$ it is clear that O_2 binds in an end-on-bent fashion. Model studies on Fe(II) porphyrins show that they can react reversibly with dioxygen (eq. 1) where B is an axial base.[13-16]

$$Fe^{II}(Por)(B)_2 + O_2 \rightleftharpoons Fe(Por)(B)(O_2) + B \qquad .....(1)$$

One of the difficulties encountered in attempts to obtain oxygen carriers based on iron(II) complexes is the large driving force towards the irreversible formation of the μ-oxo dimer (eq. 2)

$$Fe^{II} + O_2 \rightleftharpoons Fe(O_2) \xrightarrow{Fe(II)} Fe^{III}\text{-}O\text{-}Fe^{III} \qquad .....(2)$$

Considerable research has been done in overcoming this problem and three approaches have been successful, (a) the use of steric constraints in such a way that dimerization is inhibited, (b) the use of low temperature so that the reaction leading to dimerization is very slow and (c) rigid surface attachment of the iron complex to a surface (e.g., silica gel) so that dimerization is prevented. "Picket Fence" concept (Fig. 1.1) is one such steric approach in which one side of the porphyrin is substituted by bulky organic groups leaving the other side unhindered. A suitable ligand such as N- alkyl imidazole is coordinated on the unhindered side of the porphyrin thus leaving a hydrophobic pocket for the reaction with O_2. Hemerythrin, the other oxygen binding protein has been studied by X-ray and spectroscopic methods.[17-20] These studies show that it forms an $Fe_2^{III}(O_2^{2-})$ type of complex

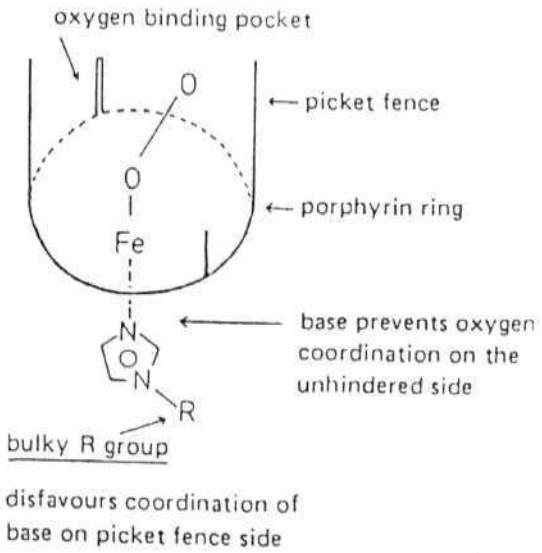

Fig. 1.1. "Picket fence" concept (Ref. 1. p.120)

in which two non-equivalent ferric ions are coupled with strong antiferromagnetic interactions. The peroxo state of the bound O_2 is clearly shown by the resonance Raman spectrum where ν (O-O) is found at 844 cm^{-1}, a value typical for the O-O single bond of peroxide. Understanding of hemerythrin has been enhanced by the characterization and study of several interesting model systems.[21-23] These are helpful in studying the electronic and structural properties of deoxy- hemerythrin and proposals have been made for the possible mode of molecular oxygen coordination for deoxy form.

Zinc is the other transition element which has been recognized as essential for all forms of life, and a large number of diseases and congenital disorders have been traced to zinc deficiency. It has many different bio-functions including its role in alcohol dehydrogenase, aldoses, peptidases, carboxypeptidases, proteases, DNA- and RNA- polymerase etc. Some have been characterized by X-ray and one such example is bovine carboxypeptidase[24] which has zinc ion in tetrahedral environment coordinated by two histidine nitrogen atoms, an oxygen atom of the carboxyl side chain of glutamate residue and a water molecule coordinated weakly at the fourth coordination site.

Carbonic anhydrase catalyzes the reversible hydration of CO_2 as shown in the following equation.

$$CO_2 + H_2O \rightleftharpoons HCO_3^- + H^+ \qquad \text{.....(3)}$$

This involves a proton, which is proposed to be bound to the enzyme at some step of the catalytic pathway,

$$CO_2 + H_2O + E \rightleftharpoons HCO_3^- + EH^+ \rightleftharpoons HCO_3 + E + H^+ \qquad \text{..(4)}$$

where EH^+ and E represent the acidic and basic forms of the enzyme. In order to understand the mechanism of the enzyme action, metal substitutions were carried out. In this approach cobalt substituted metal enzymes[25-28] were proved to be good functional models for the native systems because of similarities in the chemistry of the two metal ions. The activity of these derivatives are similar to that of the natural products. Cobalt(II) which has well defined electronic spectra allowed researchers to monitor the pH-dependent properties and interactions with substrates and inhibitors. Another characterstic of cobalt(II) is that the NMR signals of protons of residues coordinated to the metal ion can be detected outside the diamagnetic protein region. In this way coordinated histidines can be counted and monitored easily under the various chemical conditions. Manganese(II) and copper(II) derivatives are also often studied, although the latter does not show any activity and the former shows only slight activity. Nevertheless they provided structural information mainly through EPR[29,30] and NMR[31,32] relaxation studies.

Copper is the third most abundant transition metal in the human body. A number of important proteins and enzymes contain copper at their active sites.[33-36] These copper proteins are associated with a variety of biological functions including oxygen transport and activation, electron transfer, iron metabolism and superoxide dismutation. The protein ligand imposes unusual geometric and electronic structures at the copper site. Based on spectral features they are classified into three types:[37] blue copper, normal copper and coupled binuclear copper. A reasonable understanding has been achieved for a number of copper proteins from optical and EPR spectroscopy.[38] Most of the known active sites of the copper proteins are 'intrinsic', that is, they are formed only through the intimate interaction of copper ions with the ligating protein residues. This generates a copper site which is quite different, both in geometry and ligation, from small molecule copper complexes. It is generally difficult to synthesize model complexes which will mimic the intrinsic protein site; however a number of complexes have been synthesized to study specific protein functions.

Cobalt [39] has only one important biochemical function in vitamin B_{12}, whose structure has been determined by X-ray crystallography as well as chemical studies.

Molydbneum,[40] vanadium,[41,42] chromium [43,44] and nickel [45] are the other transition elements whose chemical behavior in life

process is currently becoming well defined. Manganese is another example in this list.

1.3 Manganese in Bio-Chemistry:

Manganese is an essential trace element and is involved in a number of metal proteins.[46,47] Some are isolated in the pure state and structurally well characterized. Apart from photosystem-II (PS-II), on which much research activity is going on currently, catalases, pseuodocatalases and superoxide dismutases are the other examples in which manganese is involved at the active site.

1.3.1 Photosystem -II:

Much development in manganese model chemistry is attributed to its involvement in PS-II,[48-51] a subcomponent of natural photosynthetic apparatus.

PS-II is a complex natural system in which water is oxidized to molecular oxygen. This redox reaction which involves a $4e^-$ transfer occurs at the active site called "water oxidation center (WOC) " or "oxygen evolving complex (OEC)" within the thylakoid membrane of green plants and also in algae and cyanobacteria. Experimental evidences suggest that the active site consists of a polynuclear manganese aggregate which oxidizes coordinated

water molecules to molecular oxygen. The exact nature of the manganese complex has not been established despite the fact that it has been characterized extensively with a variety of spectroscopic (EXAFS, XAS, EPR and Optical) and magnetic techniques.[52-59]

A minimal quantity of 4Mn ions per PS-II unit appears to be required for O_2 evolution and Mn extraction studies on native system satisfies this number.[60,61] Kok *et al.* have identified five oxidation states ("S-states") (Fig. 1.2) during water oxidation from the periodic observation of O_2 evolution from dark adapted choloroplast when they are irradiated with a series of light flashes. They have been designated as S_0 - S_4.[62] In each case the absorption of one quantum of light raises the oxidation level by one unit and drives the system from S_0 to S_4. Each state

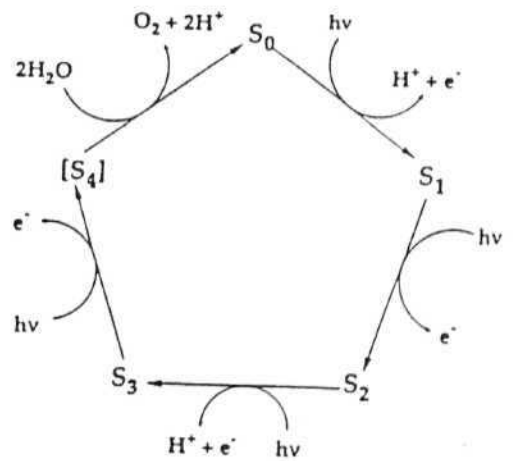

Fig. 1.2. S-state mechanism (Ref. 62)

acts as a biological capacitor by storing one oxidizing equivalent, discharge of the capacitor occurs during the $S_4 \longrightarrow S_0$ transition upon oxidation of the substrate water molecule to O_2.

A complex EPR multiline signal reported by Dismukes and Siderer [63] provided the first evidence that at least a portion of manganese is involved in the redox chemistry. Based on its behavior during the periodic flashes the multiline EPR was assigned to the S_2 state. The spectrum was similar to that of μ-oxo dimers (Fig. 1.3) and are characteristic of mixed-valence

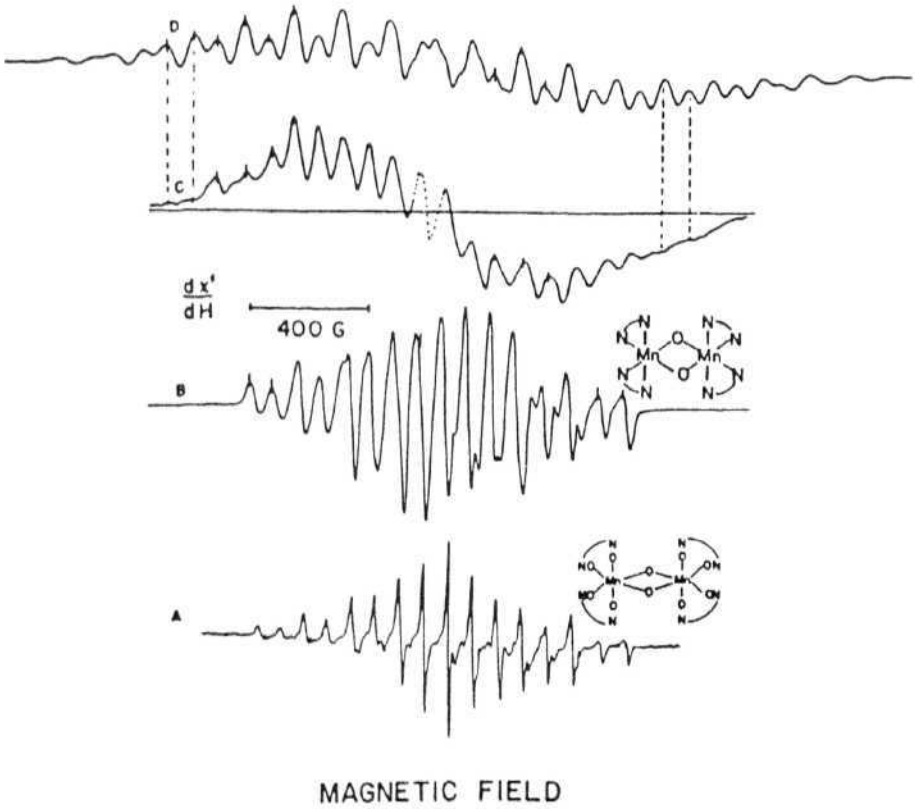

Fig. 1.3. EPR spectra of (A) $L_2Mn^{III}(O)_2Mn^{IV}L_2$, L=2,2'-bypyidine-N,N'-oxide at 15K, (B)L=2,2'-bypyridine at 77K, (C) difference 1-0 flashes of EDTA-washed broken chloroplasts at 10K, (D) computer simulation of Mn(3III,IV) tetramer. (Ref. 63b)

systems with S = 1/2 ground state.[64,65] A broad EPR signal associated with S_1 state has recently been discovered by using parallel polarization techniques,[66] indicating that the S_1 state is also paramagnetic.

An even more direct measure of the participation of manganese in the oxidant accumulation has been provided by X-ray absorption spectroscopy (XAS). XAS data obtained for S_1, S_2 and S_3 states,[53] and indirect information on the S_0 state, which was extracted from the S_0^* state induced by hydroxylamine, indicate that each Mn possess 4-6 N or O atoms between 1.8-2.2 Å, 1-1.5 Mn atoms at 2.7Å and 0.5 Mn or Ca atoms at 3.3 Å. Little change has been found in the EXAFS spectrum for $S_1 \rightarrow S_2 \rightarrow S_3$ transition, indicating that no significant rearrangement of ligands occurs in these steps. However, structural changes are found for the S_0^*, suggesting that the same would be true for S_0.[54] The EPR and XAS studies propose an average oxidation state of 3+ for manganese in the S_1 state. No structural information is available for the unstable $[S_4]$ state which is responsible for the release of oxygen. The stoichiometry of 4Mn per complex and the multiline EPR signals are consistent with a multinuclear complex in which Mn atoms are close to one another to share the unpaired electron of the S_2-state. This eliminates the model mononuclear manganese involved in the redox reaction.

Based on the current state of our understanding from

different experimental sources some suggestions have been made for the structure and reaction mechanism for the water oxidation complex. In a single center proposal, a tetranuclear manganese assembly accumulates oxidizing equivalents and oxidizes water directly; the cubane proposal of Brudvig[67] and double-pivot mechanism of Christou[68] are two examples (Fig. 1.4). In the double center model,[69] two possibilities arise, one involving two sets of dimers and the other involving a monomer and a trimer. In both these cases the two centers are redox coupled with one another.

1.3.2 Superoxide Dismutase:

Observations on superoxide dismutase isolated from *Thermus thermophilus* HB8[47] have shown that it contains one Mn^{III} monomer per subunit. X-ray studies show that it has a trigonal bipyramidal geometry in which Mn is coordinated by N- and O- donor atoms of the amino acids of the polypeptide chain.

1.3.3 Catalase and Pseudocatalase:

Catalase, a hexamer isolated from *Thermus thermophilus* consists of two Mn^{III} ions per subunit.[47] X-ray observations made it clear that each Mn^{III} ion is at a distance of 3.6 Å and optical spectra are consistent with the μ-oxo-bis(μ-acetato)

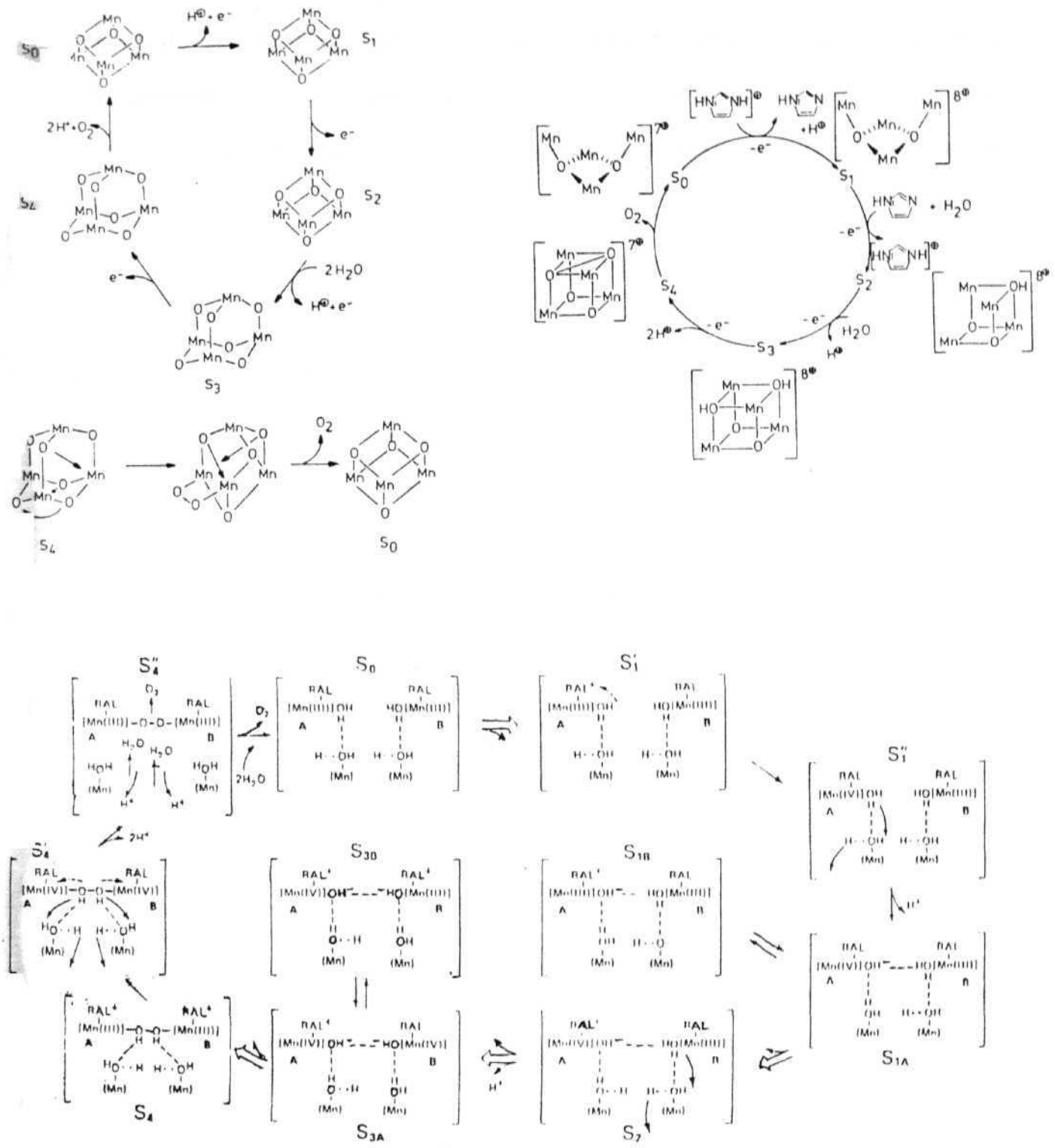

Fig. 1.4. (A)Brudvig's 'Cubane' mechanism (Ref. 67) (B)Christou's 'Double pivot' mechanism (Ref. 68) (C)Kambara's 'Double centered' mechanism (Ref. 69).

dimanganese(III) core. Similar structural unit was proposed for pseudocatalase isolated from *Lactobacillus plantarum*, but EPR spectra contradicts the oxidation state assignment by showing the multiline spectra characteristic of the mixed-valence state.

1.4 Model Complexes of Manganese:

Except possible involvement of Cl^- in the coordination sphere, all the biomolecules of manganese are coordinated by O- and N- donor atoms. These are generally from carboxylate, alkoxy or phenoxy and imidazole groups of the protein chain. Observed oxidation states of the metal ion are in the range 2-4. With the purpose of mimicking biomolecules, inorganic chemists synthesized a number of high valent polynuclear complexes,[47,70-72] with a special emphasis on PS-II. Efforts in this direction led to many higher valent polynuclear manganese complexes, which are characterized by X-ray, magnetic and spectroscopic techniques. For simplicity they can be categorized depending on nuclearity of metal ions and the core structure.

1.4.1 Dinuclear:

Depending on the bridging unit these are further categorized and are shown in the Fig. 1.5

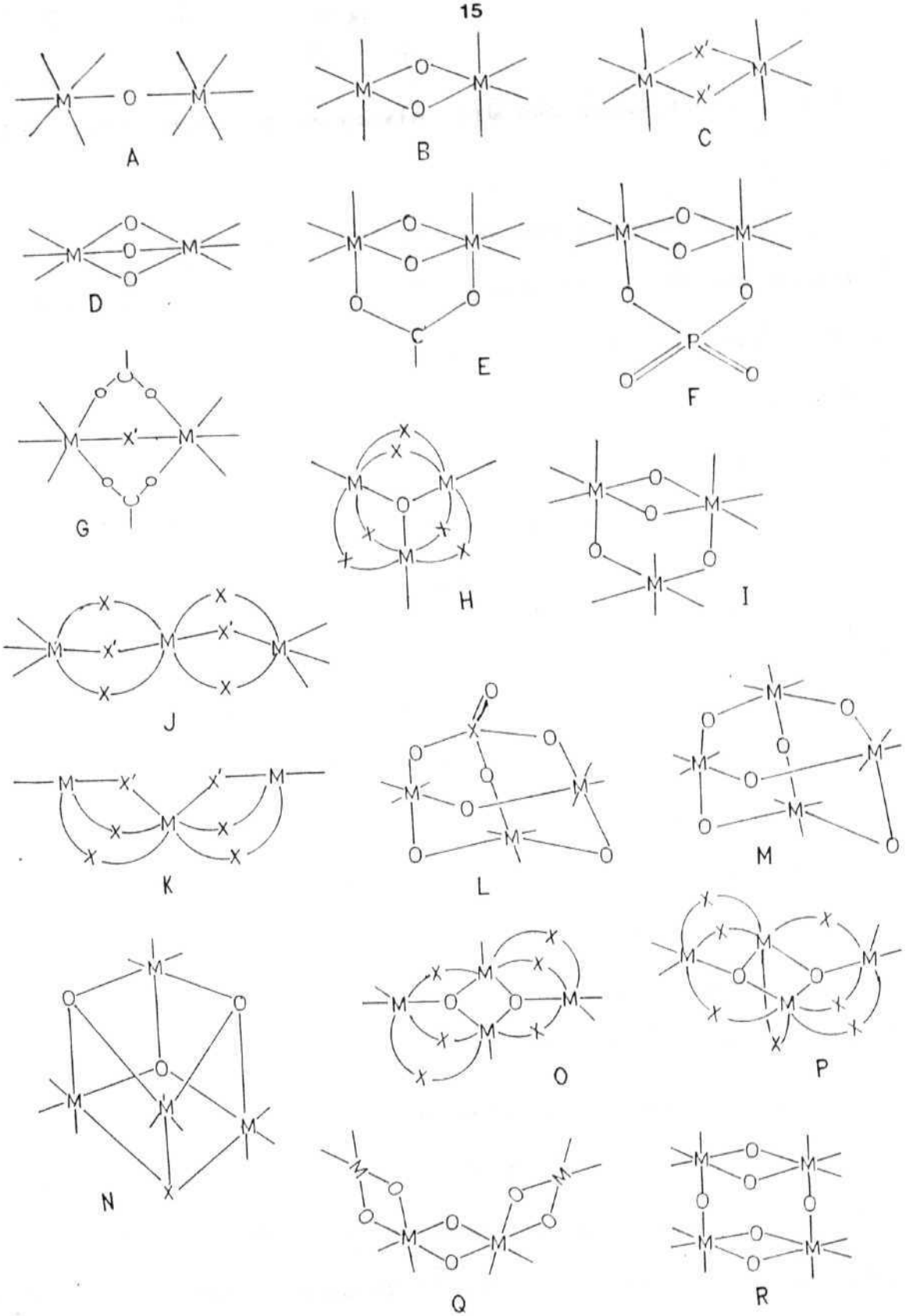

Fig. 1.5. Commonly observed core structures of higher valent manganese compounds. (X = $RCOO^-$ or $PhCOO^-$ and X' = alkoxy or phenoxy oxygen of ligand)

1.4.1(a) di(μ-oxo) and di(μ-alkoxy or phenoxy): (Fig. 1.5B,1.5C)

The di(μ-oxo) species are the first generation complexes for mimicking PS-II and shows a Mn-Mn distance of 2.7 Å comparable to that found in the native system. Mixed-valence complexes of this dimeric core show a 16-line EPR spectrum which is consistent with the S_2 state of PS-II. Structurally characterized complexes with their properties are shown in Table 1.1

In 1960, Nyholm and Turco[73] in an attempt to synthesize $Mn(bpy)_3^{3+}$ ended up with an unexpected μ-oxo dimer, $[Mn_2O_2(bpy)_4]^{3+}$ (1) by persulphate oxidation of Mn^{2+} in the presence of ligand. Later Plaksin *et al.*[74] characterized this by X-ray crystallography. Analogous complexes of phen, phen-N-oxide and bpy-N-oxide were reported by Uson *et al.*[75] and crystal structure of 2 at 100 and 200 K was determined by Stebler *et al.*[76] Detailed studies of 1 and 2 were made by Calvin and co-workers.[65,77] Electro-chemical studies on these complexes show two redox waves corresponding to (III,IV)/(III,III) and (III,IV/IV,IV) couple. Crystal structure of the oxidized form of the phen complex 3 synthesized by Goodwin and Sylva,[78] was determined by Stebler *et al.*[76] Related complexes in which the diamine ligand is replaced by a tetradentate ligand and their substituted analogs have been synthesized (4 - 16). All these

Table. 1.1 Di(μ-oxo) dimeric complexes of manganese.

Complex		O.S.	Mn--Mn (Å)	Mag§ (J in cm^{-1})	EPR (A in Gauss)	Optical nm($\varepsilon/M^{-1}cm^{-1}$)	Ref
$[Mn_2O_2(bpy)_4](ClO_4)_3$	(1)	III,IV	2.716(2)	g = 2.003	g = 2.002	525(530), 555(455)	65, 74, 77
				J = −150	A_1 = 167	684(561), 830(430)	
					A_2 = 79		
$[Mn_2O_2(phen)_4](PF_6)_3$	(2)	III,IV	2.695(9)	g = 1.999	g = 2.003	523(580), 550(460)	65, 76, 77
				J = −148	A_1 = 167	680(550), 800(sh)	
					A_2 = 79		
$[Mn_2O_2(phen)_4](ClO_4)_4$	(3)	IV,IV	2.748(2)	g = 1.96			76, 78
				J = −144			
$[Mn_2O_2(bispicen)_2](ClO_4)_3$	(4)	III,IV	2.659(2)	g = 2.00	g = 2.00	553(569), 655(526)	79, 81
				J = −140	A = 78	805(250)	
$[Mn_2O_2(bispicen)_2](ClO_4)_4$	(5)	IV,IV	2.672(1)	J = −125.6		544(843), 632(657)	81
$[Mn_2O_2(bispicen)_2](ClO_4)_2$ [a]	(6)	III,III	2.676(3)	J = −86.4		461(141)	80
$[Mn_2O_2(bispicen)_2](ClO_4)_2$ [b]	(7)	III,III	2.686(1)				80
$[Mn_2O_2(tpa)_2](S_2O_6)_{3/2}$	(8)	III,IV	2.643(1)				82
$[Mn_2O_2(tpa)_2](ClO_4)_3$	(9)	III,IV	2.693(3)	J = −176†	g = 2.00	668(891), 557(903)	83
				J = −221	A = 76		
$[Mn_2O_2(tpa)_2](ClO_4)_4$ [c]	(10)	IV,IV	2.747(18)	J = −131		640(1394), 538(1466)	83

§ J refers to $\mathcal{H} = -2J\ S_1.S_2$

† the structural data are for the unsubstituted tpa, while the magnetic data are for two different ring substituted derivatives

Table. 1.1 contd...

Complex		O.S.	Mn--Mn (Å)	Mag (J in cm^{-1})	EPR (A in Gauss)	Optical nm($\varepsilon/M^{-1}cm^{-1}$)	Ref
$[Mn_2O_2(tpa)_2](NO_3)_2$	(11)	III,III	2.674(4)			443(361), 575(249)	80
$[Mn_2O_2(tren)_2](CF_3SO_3)_3$	(12)	III,IV	2.679(1)	g = 1.958	A_1 = 150	680(570), 548(440)	84
				J = −146	A_2 = 78		
$[Mn_2O_2(14\text{-}aneN_4)_2](CF_3SO_3)_3$	(13)	III,IV	2.741(1)		$A_1 \cong 2A_2$	646(760), 560(889)	85
$[Mn_2O_2(N_3O\text{-}py_2)](ClO_4)$	(14)	III,IV	2.656(2)	g = 2.00	g = 2.00		86
				J = −151	A ≅ 70		
$[Mn_2O_2(cyclam)_2]Br_3$ [d]	(15)	III,IV	2.731(2)	J = −118.5	A = 80	550(847), 640(889)	87
$[Mn_2O_2(salpn)_2]$	(16)	IV,IV	2.728(1)	g = 2.0			88
				J = −82			
$[Mn_2(L\text{-}1)(CH_3O)Cl_2(CH_3OH)_2]$	(17)	III,III	3.006(2)	g = 2.0			89
				J = −15.5			
$[Mn_2(salen)_2(H_2O)_2](ClO_4)_2$	(18)	III,III	3.361(2)				90
$[Mn_2(salmp)_2]$	(19)	III,III	3.111(1)	J = −3.25			91
$(Ph_4P)[Mn_2(salmp)_2]$	(20)	II,III	3.140(1)				91
$[Mn_2(sal)_4(pyr)_2]$	(21)	III,III	3.247(1)			522(215), 460(274)	92
$[Mn(EtOH)_4]$						424(336)	
$[Mn_2(L\text{-}2)_2(OMe)_2]$	(22)	III,III	3.144				93

Table. 1.1 contd...

Complex		O.S.	Mn--Mn (Å)	Mag (J in cm^{-1})	EPR (A in Gauss)	Ref
$[Mn_2(2\text{-}OH\text{-}3,5\text{-}Cl_2\text{-}salpn)_2(THF)_2](ClO_4)$	(23)	III,IV	3.65	g = 2.00 J = −10	g = 2.0 A ≅ 103−112	94
$[Mn_2O_2(salpn)_2]$	(24)	IV,IV	2.731(2)			95
$[Mn_2(salahp)_2Cl_2(CHOH)_2]$	(25)	III,III	3.011(1)			95
$[Mn_2(L\text{-}3)_2]$	(26)	III,III	3.243(2)	g = 2.00 J = +4.5		96
$[Mn_2(biphen)_2(biphenH_2)(bpy_2)]$	(27)	II,III	3.182(6)	J = +0.89		97
$[Mn_2O_2(pic)_4]$	(28)	IV,IV	2.747(2)	J = −86.5, g = 1.83		98
$[Mn_2(2\text{-}OH\text{-}5\text{-}Cl_2\text{-}salpn)_2(MeOH)]$	(29)	III,III	3.808(1)	g = 1.95 J = −3.55		99
$[Mn_2O_2(bispictn)_2]^{4+}$	(30)	IV,IV	2.719(3)	J = −105		100
$[Mn_2O_2(bispicbn)_2]^{4+}$	(31)	IV,IV				
$[Mn_2O_2(bispichxn)_2]^{4+}$	(32)	IV,IV				

[a] [N,N-bis(6-methylpyrid-2-yl)methyl]ethane-1,2-diamine; [b] N,N-bis(2-methylpyrazyl)-ethane-1,2-diamine; [c] [(6-methyl-2-pyridyl)methyl)(2-(2-pyridyl)ethyl))(2-pyridylmethyl)amine; [d] dithionate salt was also prepared.

complexes have Mn-Mn distance of 2.7 Å. Substitution on ligand and the oxidation state of the metal ion have very little effect on the geometry around the metal ion. Different combinations of oxidation states *viz.*, Mn(II,III), Mn(III,III), Mn(III,IV) and Mn(IV,IV) are observed for the complexes. Except when there is lattice disorder, the crystal structure of the mixed-valent Mn complexes indicate trapped valences, with greater difference in geometry around the metal centers for Mn(II,III) compared to Mn(III,IV) compounds. Magnetic studies for these complexes show strong antiferromagnetic behavior and coupling values (J) ranging from $-82\ cm^{-1}$ for 16 to $-221\ cm^{-1}$ for 9 . Complexes with Schiff base ligands, 17 - 23, 26 and 29 which are bridged with alkoxy or phenoxy oxygen atom show longer Mn-Mn distance (3.3 Å). This increase in distance affects the magnetic interaction between the two metal centers with observed J values $< -16\ cm^{-1}$. There are only two examples 26 and 27 with the di-oxo core which show ferromagnetic interaction between the metal centers. EPR spectrum of the mixed-valence (III,IV) complexes shows hyperfine coupling with two in equivalent ^{55}Mn nuclei ($I = 5/2$) at $g = 2$ with $A_{1(Mn^{III})} = 2A_{2(Mn^{IV})}$. Typical values of A_1 and A_2 for diimine complexes are 167±3 and 79±3 G and does not vary substantially from complex to complex. The large difference in hyperfine constant indicates that the unpaired electron in the ground state is localized on the Mn^{III} center or transferred between the two

manganese atoms at a rate slower than $\|A_1|-|A_2\|$.

1.4.1(b) di(μ-oxo)-μ-acetato: (Fig. 1.5E)

Only five structurally characterized complexes are known in the literature and are given in Table 1.2. The first complex with this core, 33 was prepared by Wieghardt[101] by hydrolysis of $[L_2Mn_2(\mu\text{-}O)(\mu\text{-}OAc)_2](ClO_4)_2$, a (III,III) complex. The complex 33, a (III,IV) dimer has been structurally characterized and shows a Mn-Mn distance of 2.588 Å, which is lower than the value observed for di-μ-oxo dimers. It shows a strong antiferromagnetism (J = $-220cm^{-1}$) between the high spin Mn(III) and Mn(IV) ions. Later Armstrong *et al.* isolated two dimers, (III,IV) (34) and (IV,IV) (35) with a capped hexadentate ligand[102,103] and a (IV,IV) complex 37 with a tridentate ligand.[104] All the three complexes have comparable Mn-Mn distances with strong antiferromagnetism (J values are -125 and -124 cm^{-1} for 34 and 37 respectively). Similar observations are made for 36 with J = -114 cm^{-1}. EPR spectra for 34 and 36 show 16-line pattern similar to the μ-oxo dimer. There is no report of a (III,III) dimer with this core for manganese complexes.

1.4.1(c) (μ-oxo) di-(μ-acetato) and (μ-alkoxy or phenoxy) di-(μ-acetato): (Fig. 1.5G)

Table. 1.2 Di(μ-oxo)-μ-acetato dimanganese complexes.

Complex		O.S.	Mn--Mn (Å)	Mag (J in cm^{-1})	EPR (A in Gauss)	Optical nm(ε/$M^{-1}cm^{-1}$)	Ref
$[Mn_2O_2(OAc)(tacn)_2](BPh_4)_2$	(33)	III,IV	2.588(2)	J = -220	g = 2.00	628(345), 546(394) 440(sh)	101
$[Mn_2O_2(OAc)(tpen)](ClO_4)_2$	(34)	III,IV	2.591	g = 1.982 J = -125	g = 2.00 A = 80	800(sh), 650(440) 553(360)	102
$[Mn_2O_2(OAc)(tpen)](ClO_4)_3$	(35)	IV,IV	2.591(1)			630(sh), 590(395) 440(1570)	103
$[Mn_2O_2(OAc)(bpy)_2Cl_2]$	(36)	III,IV	2.667(2)	J = -114	g = 2.00 A = 77		97
$[Mn_2O_2(OAc)(bpea)_2](ClO_4)_3$	(37)	IV,IV	2.580(1)	g = 2.29 J = -124			104

This structural unit is found in ribonucleotide reductase and eudocatalase whereas isostructural unit with iron(III) is served in hemerythrin.[105,106] Wieghardt and co-workers isolated e first complex,[107] (Table. 1.3) a (III,III) dimer 38 with a identate cyclic ligand which completes the octahedron around the tal centers. Later another salt of this complex 41 and its idized form (III,IV) 43 were characterized by ystallography.[109,113] Two other complexes 39 and 44 with this re are known in the literature.[110,114] The sixth site in the se of complexes with bidentate ligands is occupied by water in , or an anion in 42. In all the complexes reported, Mn-Mn stance range from 3.0-3.3 Å, which is significantly larger than e 2.7 Å found in other oxo-dimers. Except 38 which shows rromagnetism (J = 9 cm^{-1}), all other (III,III) dimers show weak tiferromagnetism, J <-10cm^{-1}, in sharp contrast to the strong tiferromagnetism observed for iso-structural Fe(III) analogues. gnetic studies on 43 show strong antiferromagnetism with J = -40 $^{-1}$. Electronic spectrum of 39 shows some similarities with that *lactobacillus plantarum.*[110] Analogous compounds with -phenoxy)di-(μ-acetate) bridging units are known[150-120], in ich manganese is in (II,III) oxidation states (45 - 49). Mn-Mn stance is around 3.5 Å and shows weak antiferromagnetic teraction (J = -4.0 to -7.7 cm^{-1}).

Table. 1.2 Di(μ-oxo)-μ-acetato dimanganese complexes.

Complex	O.S.	Mn--Mn (Å)	Mag (J in cm^{-1})	EPR (A in Gauss)	Optical nm($\varepsilon/M^{-1}cm^{-1}$)	Ref
$[Mn_2O_2(OAc)(tacn)_2](BPh_4)_2$ (33)	III,IV	2.588(2)	J = -220	g = 2.00	628(345), 546(394) 440(sh)	101
$[Mn_2O_2(OAc)(tpen)](ClO_4)_2$ (34)	III,IV	2.591	g = 1.982 J = -125	g = 2.00 A = 80	800(sh), 650(440) 553(360)	102
$[Mn_2O_2(OAc)(tpen)](ClO_4)_3$ (35)	IV,IV	2.591(1)			630(sh), 590(395) 440(1570)	103
$[Mn_2O_2(OAc)(bpy)_2Cl_2]$ (36)	III,IV	2.667(2)	J = -114	g = 2.00 A = 77		97
$[Mn_2O_2(OAc)(bpea)_2](ClO_4)_3$ (37)	IV,IV	2.580(1)	g = 2.29 J = -124			104

This structural unit is found in ribonucleotide reductase and pseudocatalase whereas isostructural unit with iron(III) is observed in hemerythrin.[105,106] Wieghardt and co-workers isolated the first complex,[107] (Table. 1.3) a (III,III) dimer 38 with a tridentate cyclic ligand which completes the octahedron around the metal centers. Later another salt of this complex 41 and its oxidized form (III,IV) 43 were characterized by crystallography.[109,113] Two other complexes 39 and 44 with this core are known in the literature.[110,114] The sixth site in the case of complexes with bidentate ligands is occupied by water in 40, or an anion in 42. In all the complexes reported, Mn-Mn distance range from 3.0-3.3 Å, which is significantly larger than the 2.7 Å found in other oxo-dimers. Except 38 which shows ferromagnetism ($J = 9\ cm^{-1}$), all other (III,III) dimers show weak antiferromagnetism, $J < -10 cm^{-1}$, in sharp contrast to the strong antiferromagnetism observed for iso-structural Fe(III) analogues. Magnetic studies on 43 show strong antiferromagnetism with $J = -40\ cm^{-1}$. Electronic spectrum of 39 shows some similarities with that of *lactobacillus plantarum*.[110] Analogous compounds with (μ-phenoxy)di-(μ-acetate) bridging units are known[150-120], in which manganese is in (II,III) oxidation states (45 - 49). Mn-Mn distance is around 3.5 Å and shows weak antiferromagnetic interaction ($J = -4.0$ to $-7.7\ cm^{-1}$).

Table. 1.3 (μ-oxo) di-(μ-acetato) and (μ-alkoxy or phenoxy) di-(μ-acetato) dimanganese complexes.

Complex	O.S.	Mn--Mn (Å)	Mag J (cm^{-1})	Ref
$[Mn_2O(OAc)_2(tacn)_2](ClO_4)_2$ (38)	III,III	3.084	J = +9	107, 108
$[Mn_2O(O_2CR)_2(HB(Pz)_3)_2]$‡ (39)	III,III	3.159(1)	J = -0.2 to -0.7	110
$[Mn_2O(OAc)_2(bpy)_2(H_2O)_2](PF_6)_2$ (40)	III,III	3.132	g = 1.98 J = -3.4	111
$[Mn_2O(OAc)_2(tacn)_2](I_3)I$ (41)	III,III	3.096(2)		109
$[Mn_2O(OAc)_2(bpy)_2(H_2O)(S_2O_8)]$ (42)	III,III	3.145		112
$[Mn_2O(OAc)_2(tacn)_2](ClO_4)_3$ (43)	III,IV	3.23	g = 2.2 J = -40	113
$[Mn_2O(OAc)_2(tmip)_2](ClO_4)_2$ (44)	III,III	3.164(5)	J < -0.5	114
$[Mn_2(\mu\text{-}OAc)_2(bpmp)](ClO_4)_2$ (45)	II,III	3.447	J = -6.0	115.117
$[Mn_2(\mu\text{-}OAc)_2(bcmp)](ClO_4)_2$ (46)	II,III	3.422	J = -7.7	116,117
$[Mn_2(\mu\text{-}O_2CPh)_2(bpmp)](ClO_2)_2$ (47)	II,III	3.483	J = -6.3	118
$[Mn_2(\mu\text{-}OAc)_2(L\text{-}Im)](ClO_4)_2$ (48)	II,III	3.54	J = -4.5	119
$[Mn_2(\mu\text{-}OAc)_2(L\text{-}10)(N_3)]$ (49)	II,III	3.544	J = -4.0	120

‡ the structural data are for the acetate bridge while the magnetic data are also for other carboxylates.

Apart from the above mentioned dimers, some others bridging dimers are known in the literature.[121-126] Compound $[Mn_2O(5\text{-}NO_2saldien)_2]$,[121] shows Mn^{III}-O-Mn^{III} (Fig. 1.5A) core with Mn-Mn separation (3.490 Å) and has strong antiferromagnetism ($J = -120\ cm^{-1}$) between the metal ions. Other compounds with Mn-O-Mn core are from porphyrin ligated complexes,[122,123,126] $[Mn(Pcpy)]_2O$ has two manganese ions in 3+ oxidation state and in $[Mn(TPP)N_3]O$ Mn ions are in 4+ oxidation states. In these two complexes the Mn-Mn separation are 3.420 and 3.540 Å, respectively. There is only one peroxo- bridged dimer reported,[124] $[L_2Mn_2(\mu\text{-}O)_2(\mu\text{-}O_2)](ClO_4)_2$ (L = TACN) in which manganese is in 4+ oxidation state. $Mn\text{-}O_{peroxo}$ distance (1.820 Å) is comparable to $Mn\text{-}O_{oxo}$ (1.810 Å) distance. O-O distance of 1.460 Å is typical for peroxo group. Dimetallic core with tris(μ-O) bridge, (Fig. 1.5D) $[L'_2Mn_2^{IV}(\mu\text{-}O)_3](PF_6)_2$ was reported by Wieghardt *et al.*[108] Strong intra molecular antiferromagnetic coupling ($J = -390\ cm^{-1}$) was observed, because of short Mn-Mn distance (2.296 Å). Sarneski *et al.*[125] isolated another kind of bridged dimer, $[Mn_2^{IV}(O)_2(\mu\text{-}HPO_4)(bpy)_2(H_2PO_4)_2]$ (Fig. 1.5F) from $[Mn_2O_2(bpy)_4]^{3+}$ dimer upon acidification with phosphoric acid. It shows a Mn-Mn distance of 2.702 Å, typical of $Mn_2O_2^{3+/4+}$ core.

1.4.2 Trinuclear:

These are second generation complexes which show two distinct Mn-Mn distances, 2.7 and 3.3 Å. Possible geometries for which crystallographic data are available are shown in the Table. 1.4. Most of these metal complexes are bridged by oxide and acetate ions. The first kind (Fig 1.5H) which has $[Mn_3O]$ core forms an isosceles triangle with (μ_3-O) bridge at the center of the triangle.[127-131] Compounds 50 and 51 are the first ones synthesized by simple treatment of py- or Cl-py with $[Mn(OAc)_3(H_2O)_2]$. The starting material, $[Mn(OAc)_3(H_2O)_2]$ belongs to the class of basic acetates having a trinuclear geometry with a triply bridged oxide ion. Compound 50, a (II,III,III) trimer having an a average Mn-O bond length (1.941 Å) with antiferromagnetic interactions between the metal ions has been classified as a class-III system. It is not clear whether averaging due to crystal disorder can explain the equivalence of the Mn centers in the compound. On the other hand, compound 51 shows two distinct Mn-O bond distances showing that the two metal ions are not equal. Complex 52 prepared by oxidation of Mn(II) with $N\text{-}Bu_4MnO_4$ is iso-structural with 50 and 51. All Mn ions have high spin configuration with small exchange parameters, showing weak antiferromagnetism ($|J| < 11\ cm^{-1}$). Ground states are calculated for 52 and 53 as S = 3/2 and 1/2 respectively from variable field magnetization studies with supportive evidence from EPR.

Table. 1.4 Trinuclear manganese complexes.

Complex		O.S.	Mn--Mn (Å) min & max	Mag (J in cm^{-1})	Ground state	Ref
$[Mn_3O(OAc)_6(py)_3]$	(50)	Mn^{II},Mn_2^{III}	3.363(1)			127
$[Mn_3O(OAc)_6(3\text{-}Clpy)_3]$	(51)	Mn^{II},Mn_2^{III}				128
$[Mn_3O(OAc)_6(py)_3](py)$	(52)	Mn^{II},Mn_2^{III}	3.353(1)	g = 2.13 J = -5.1 J' = -8.3	S = 3/2	129, 130
$[Mn_3O(O_2CPh)_6(py)_2(H_2O)]$	(53)	Mn^{II},Mn_2^{III}	3.218(4) 3.418(5)	g = 2.11 J = -7.3 J' = -10.9	S = 1/2	129
$[Mn_3O_4(bpy)_4Cl_2]MnCl_4$	(54)	Mn_3^{IV}	2.681(3) 3.245(3)	J = -171 J' = -108		131
$[Mn_3O_4(bpy)_4(H_2O)_2](ClO_4)_4$	(55)	Mn_3^{IV}	2.679 3.263	J = -182 J' = -98	S = 1/2	132
$[Mn_3O_4(bpea)_3(OH)](ClO_4)_3$	(56)	Mn_3^{IV}		J = -76 J' = -11	S = 3/2	104
$[Mn_3(CH_3O)(MeOH)(L\text{-}4)_2(EtOH)](ClO_4)$	(57)	Mn_3^{III}	3.141(3) 3.686(4)	J = -19.2 J' = 0.0		133
$[Mn_3(\mu\text{-}O)_3(\mu\text{-}PO_4)(tacn)_3]Br_3$	(58)	Mn_3^{IV}	3.226(1)		S = 1/2	134

Table. 1.4 contd...

Complex	O.S.	Mn--Mn (Å) min & max	Mag (J in cm^{-1})	Ground state	Ref
α-[Mn_3(saladhp)$_2$(OAc)$_4$(MeOH)$_2$](59)	Mn^{II},Mn_2^{III}	3.551(1)	J = -7.09 J' = 0.0	S = 3/2	135
β-[Mn_3(saladhp)$_2$(OAc)$_4$(MeOH)$_2$](60)	Mn^{II},Mn_2^{III}	3.50	J = -6.7 J' = 0.0		136
α-[Mn_3(saladhp)$_2$(OAc)$_4$(H_2O)$_2$](61)	Mn^{II},Mn_2^{III}				
α-[Mn_3(salathm)$_2$(OAc)$_4$(MeOH)$_2$](62)	"	3.419 to 3.551	J = -4.0 to -7.1 J' = 0.0		137
α-[Mn_3(saladhp)$_2$(OAc)$_4$(HpyrO)$_2$](63)	"				
α-[Mn_3(saladhp)$_2$(OAc)$_2$(Hsal)$_2$(EeOH)$_2$](64)	"				

Complexes of the second category (Fig 1.5I) have $[Mn_3O_4]$ core.[104,131-133] 54, 55, and 56 have d^3 configuration while 57 has d^4 configuration for all the metal ions. 54, 55 and 56 have two distinct Mn-Mn distances 2.7 and 3.2 Å which are in close agreement with EXAFS values for OEC, whereas 57 shows longer Mn-Mn separation. This may be due to Jahn-Teller distortion of d^4 ions which increases $Mn-O_{oxo}$ bond distances. Magnetic studies reveal that they have moderate antiferromagnetic coupling. EPR spectra are reported for 54 and 55 and show 36-line pattern at g = 2.0.

Linear (Fig. 1.5J) and bent (Fig. 1.5K) geometries are observed for a few complexes (59 to 64). They are isolated by aerial oxidation of Mn^{II} in the presence of ligand. All complexes of this type have similar J values which show that spatial arrangement of the metal ions have little effect on magnetic properties.

1.4.3 Tetranuclear:

Tetranuclear model for water oxidation in PS-II led to the synthesis of many such complexes [138-161] over the last five years and are shown in the Table 1.5. Majority of these complexes contain bridging carboxylate and oxo groups. Several such complexes were reported from the group of Christou and Hendrickson. They were obtained by simple treatment of

Table. 1.5 Tetranuclear manganese complexes.

Complex		Structure[a]	O.S.	Mn--Mn (Å) min & max	Mag (J in cm^{-1})	Ground state	Ref
$[Mn_4O_6(tacn)_4]Br_{3.5}OH_{0.5}$	(65)	Ada	Mn_4^{IV}	3.21(1)			138
$[Mn_4(L-5)](ClO_4)_4$	(66)	Cub	Mn_4^{II}	3.321(1)			139
$(H_2Im)_2[Mn_4O_3Cl_6(HIm)(OAc)_3]$	(67)	Cub	Mn_3^{III},Mn^{IV}	2.818(4)	$J_1 = -30.3$	S = 1/2	141, 153
				3.323(5)	$J_2 = 11.1$		
$[Mn_4O_2(OAc)_7(bpy)_2](ClO_4)$	(68)	But	Mn_4^{III}	2.848(5)	$J_1 = -22.5$	S = 3	142, 143
				3.385(5)	$J_2 = -7.6$	S = 2	
$[Mn_4O_2(OAc)_6(bpy)_2]$	(69)	But	Mn_2^{II},Mn^{III}_2	2.779(1)	$J_1 = -3.12$		142, 143
				3.481(1)	$J_2 = -1.97$		
$[Mn_4(L-6)](ClO_4)_4$	(70)	Cub	Mn_4^{II}	3.33(1)			140
				3.45(1)			
$[Mn_4O_3Cl_4(OAc)_3(py)_3]$	(71)	Cub	Mn_3^{III},Mn^{IV}	2.815(2)	$J_1 = -26.8$	S = 9/2	144, 153
				3.272(2)	$J_2 = 12.1$		
$[Mn_4O(OAc)_3Cl(L-7)(MeOH)]$	(72)		Mn_2^{II},Mn_2^{III}	3.016(1)			145
				3.442(1)			
$[Mn_4O_2(O_2CPh_3)_6(OEt_2)_2]$	(73)	But	Mn_2^{II},Mn_2^{III}	2.770(4)	$J_1 = -5.6$	S = 2	146, 147
				3.265	$J_2 = -3.0$		

Table. 1.5 contd...

Complex		Structure	O.S.	Mn--Mn (Å) min & max	Mag (J in cm^{-1})	Ground state	Ref
$[MnO(tacn)]Br_4$	(74)	Ada	Mn_4^{IV}	3.22			108
$[Mn_4O(tpdp)_2(OAc)_2(H_2O)_2](CF_3SO_3)_4$	(75)	linear	Mn_2^{II},Mn_2^{III}	3.554(2) 3.699(2)	$J_1 = -45$ $J_2 = -6.0$		148
$[Mn_4O_2(tphpn)_2(H_2O)_2(CF_3SO_3)_2](CF_3SO_3)_3$	(76)	But	$Mn_2^{II},Mn^{III},Mn^{IV}$	2.724 3.874			149
$[Mn_4O_3Cl(OAc)_3(dbm)_3]$	(77)	Cub	Mn_3^{III},Mn^{IV}	2.792 3.252	$J_1 = -33.4$ $J_2 = 5.1$		150
$[Mn_4O_2(OAc)_6(dbm)_2(py)_2]$	(78)	But	Mn_4^{III}	2.875(1) 3.398(1)			150
$[(Mn_2O_2)_2(tphpn)_2](ClO_4)_4$	(79)	dd	Mn_2^{III},Mn_2^{IV}	2.654 3.971		S = 1	151
$[Mn_4O_3Cl_4(O_2CEt)_3(py)_3]$	(80)	Cub	Mn_3^{III},Mn^{IV}	2.814 3.271	$J_1 = -20.8$ $J_2 = 8.6$		153
$[Mn_4O_3Cl_7(OAc)_3]$	(81)	Cub	Mn_3^{III},Mn^{IV}	2.840 3.340	$J_1 = -46.6$ $J_2 = 19.3$	S = 9/2	154
$(NHC_5H_5)_3[Mn_4O_6(bpy)_6](ClO_4)_4$	(82)	dd	Mn_4^{IV}	2.7	$J_1 = -88$ $J_2 = -134$	S = 0	155

Table. 1.5 contd...

Complex	Structure	O.S.	Mn--Mn (Å) min & max	Mag (J in cm^{-1})	Ground state	Ref
$[Mn_4(L\text{-}8)_2(CH_3O)_4(CH_3OH)_8](ClO_4)_2$ (83)	But	Mn_4^{III}	3.127 3.485			156
$(NBu_4)[Mn_4O_2(OAc)_7(hqn)_2]$ (84)	But	Mn_4^{III}	2.82 3.414			157
$[Mn_4O_3Br(OAc)_3(dbm)_3]$ (85)	Cub	Mn_3^{III},Mn^{IV}	2.786(3) 3.285(4)	$J_1 = -28.8$ $J_2 = 6.8$	S = 9/2	158
$[Mn_4(\mu\text{-phth})_2(bpy)_8](ClO_4)_4$ (86)		Mn_4^{II}	5.16			160
$[Mn_4O_3Cl_4(O_2Ac)_3(HIm)_3]$ (87)	Cub	Mn_3^{III},Mn^{IV}	2.802(1) 3.260(1)			153
$[Mn_4O_2(L\text{-}9)_2](PF_6)_2$ (88)		Mn_4^{III}	2.906(3) 3.042(3)			171
$(NMe_4)[Mn_4O_2(O_2CPh)_7(hmp)_2]$ (89)	But	Mn_4^{III}	2.820 3.404			157
$[Mn_4O_3Cl_4(O_2CR)_3(py)_3]$ (90) R = 3,5-Cl_2-Ph	Cub	$Mn_3^{III}Mn^{IV}$	2.802 3.260	$J_1 = -27.1$ $J_2 = 11.1$	S = 9/2	159

[a] expanded abbreviation: But = butterfly; Cub = cubane; Ada = adamantane; dd = dimer of dimer

$Mn_3O(OAc)_6(py)_3$ with bpy and Me_4SiCl in different proportions. Abstraction of carboxylate group followed by rearrangement leads to tetranuclearity and the exact mechanism for the formation of this core is not clear. Observed oxidation states range from Mn_4^{II} (66,70 and 86) to Mn_4^{IV} (74 and 82) and complexes with more than 4+ oxidation are not known. Crystallographic studies reveal that the majority of these complexes have one of the four geometries: 'distorted cubane' (Fig. 1.5N), 'butterfly' (Fig. 1.5O and 1.5P), 'dimer of dimer' (Fig. 1.5Q and 1.5R) or 'adamantane' (Fig 1.5M). Cubic structures, except 66 and 70, which are formed by macrocyclic ligands, have $[Mn_4O_3X]^{6+}$ core (X = Cl for 67, 71, 77, 80, 81, 87, 90 and X = Br for 85) with Mn_3^{III},Mn^{IV} oxidation states. Magnetic studies indicate antiferromagnetic coupling between Mn(III) and Mn(IV) and ferromagnetic coupling between Mn(III) and Mn(III). Two Mn-Mn separations are seen, at 2.7 and 3.3 Å. Majority of the complexes with butterfly geometry have $[Mn_4O_2]^{n+}$ core (n = 6, 69 and 73; n = 8, 68, 78, 84 and 89). Like cubane structures these also have two Mn-Mn separations, one at 2.7 and the other at 3.3 Å. Two geometries are observed within the butterfly type, one with a planar and the other with bent structure as shown in the Fig 5O and 5P. Inner metal atoms in the planar geometry have penta coordination with distorted trigonal bipyramidal geometry, whereas, in the bent form an extra acetate bridges the two inner manganese atoms thereby completing their

octahedra. Magnetic studies show antiferromagnetism between the two types of metal atoms.

1.4.4 Polynuclear:

Though polynuclear complexes with nuclearity >4 with manganese have no known biological significance, some of these complexes were isolated while attempting to make di-, tri- and tetranuclear complexes.[162-169] These complexes show novel electronic and magnetic properties which are interesting to inorganic and theoretical chemists. Some of the newly synthesized complexes which have been characterized by crystallographic studies are shown in the Fig 1.6.

1.5 Scope of the present work:

As far as we know, under homogeneous conditions, none of the synthetic manganese complexes made to date have been found capable of oxidizing water and evolving O_2. On the other hand one report in the literature[170] shows a di-μ-oxo-dimer, $[Mn_2O_2(bpy)_4]^{3+}$ oxidizing water chemically in heterogeneous environment in the presence of the chemical oxidant, Ce(IV). In order to know the mechanism of water oxidation in this reaction, we carried out oxygen evolution studies with various di(μ-oxo) dimers. These

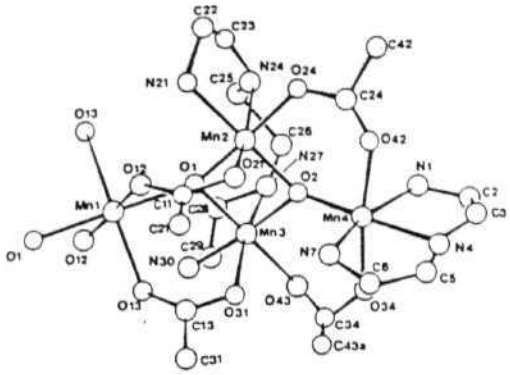

$[Mn_7(trien)_2(dien)_2O_4(OAc)_8](PF_6)_4 \cdot 2H_2O$

(Ref. 163)

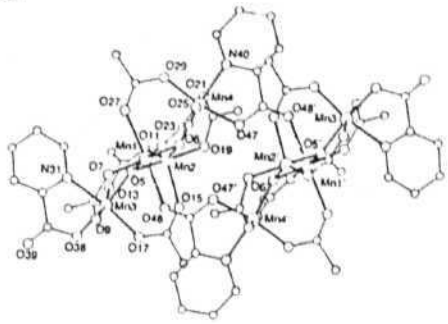

$Mn_8O_7(OAc)_{12}(pic)_4$ (Ref. 164)

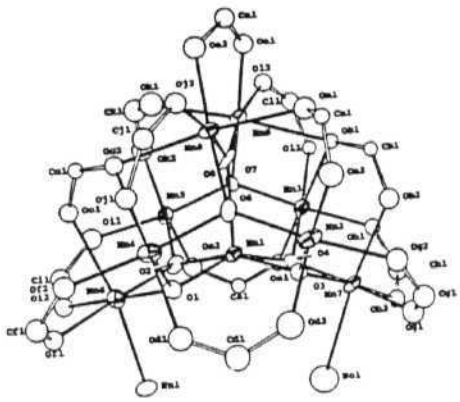

$Mn_9O_7(O_2CPh)_3(py)_2$ (Ref. 162)

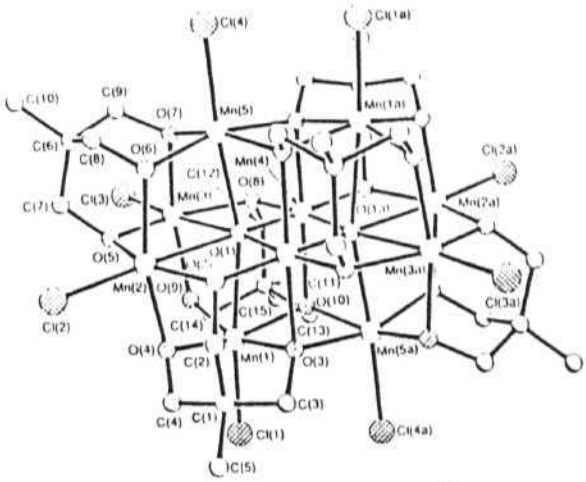

$[Mn_{10}O_2Cl_8\{(OCH_2)_3CMe\}_6]^{2-}$ (Ref. 169)

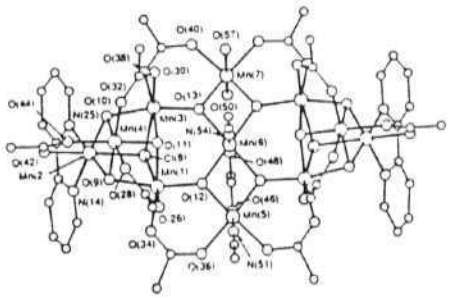

$[Mn_{11}O_{10}Cl_2(OAc)_{11}(bpy)_2(MeCN)_2(H_2O)_2]^{2+}$

(Ref. 165)

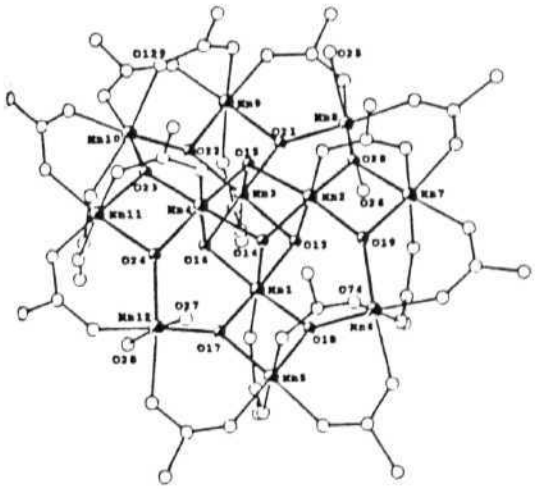

$Mn_{12}O_{12}(O_2CPh)_{16}(H_2O)_4$ (Ref. 168)

Fig. 1.6. Examples for the polynuclear manganese compounds

studies revealed the formation of permanganate ion in aqueous medium. It appears that a certain amount of dimer dissociates and forms permanganate apart from unknown manganese species and the mechanism is complicated.[172] As it is known from the literature that Ce(IV) acts as a good oxidizing agent, we planned to synthesize manganese complexes using Ce(IV) in order to know the unknown species formed during water oxidation. This approach led to the synthesis of a few interesting mono, di and tri nuclear complexes under various conditions which are characterized by X-ray crystallography. Interestingly, in some of these complexes water is coordinated to the manganese in trans fashion. There are only a few examples in literature with water coordination. The following chapters discuss the chemistry of these compounds.

CHAPTER 2.

SYNTHESIS, CRYSTAL STRUCTURE AND MAGNETIC PROPERTIES OF $[Mn_2O_2(OAc)(H_2O)_2(bpy)_2](ClO_4)_3.H_2O$ AND $[Mn_3O_4(H_2O)_2(phen)_4](NO_3)_4.2.5H_2O$.

2.1 Introduction:

Following the first preparation by Nyholm and Turco,[73] the mixed-valence dimer $[Mn_2O_2(bpy)_4]^{3+}$ and other related di(μ-oxo) dimeric complexes have been extensively studied. Introduction of the carboxylate group as a manganese bridging moiety in the above dimeric units has tremendously expanded the scope and type of compound that can be prepared from this system.[70] However, few compounds are known having coordinated water,[111,112] which is an important aspect to investigate in view of the possibility of water coordination to Mn during the oxidation cycle of PS-II. It has been recently shown that, $[Mn_2O_2(bpy)_4]^{3+}$ disproportionates in strongly acidic solution leading to the isolation of a tri-nuclear complex, $[Mn_3O_4(bpy)_4(H_2O)_2]^{4+}$.[132]

This chapter describes the synthesis, crystal structure and magnetic properties of an acetate bridged Mn(IV,IV) complex, $[Mn_2O_2(OAc)(H_2O)_2(bpy)_2](ClO_4)_3.H_2O$ (A) and synthesis and structure of a trinuclear Mn(IV,IV,IV) complex, $[Mn_3O_4(H_2O)_2(phen)_4](NO_3)_4.\ 2.5H_2O$ (B). We also present here a better method for the

preparation of the previously reported bpy analog of B, $[Mn_3O_4(OH_2)_2(bpy)_4](ClO_4)_4.5H_2O$ (C). All the preparations involve Ce(IV) oxidation of Mn^{2+}(aq) in presence of ligands. A has the smallest reported J value for a $Mn_2O_2^{3+/4+}$ core. Some general observations are made in this context regarding exchange coupling in high-valent dinuclear Mn complexes.

2.2 Experimental Section:

2.2.1 Materials. Manganese(II) acetate tetrahydrate, ammonium ceric nitrate, bpy and other chemicals are analytical grade and used as supplied. Manganese(II) perchlorate pentahydrate was purchased from Fluka. Acetonitrile and DMF were distilled and stored on molecular sieves as described in Vogel.[173]

2.2.2 Preparation of the compounds:

2.2.2(a) Preparation of ceric perchlorate solution. 20 g of ammonium ceric nitrate was dissolved in 100 ml water and added to 100 ml of NaOH solution (12 g). The white precipitate was filtered, washed with excess water and dried. 100 ml of conc. perchloric acid solution was added slowly to the white precipitate, the yellow solution formed was kept in a reagent bottle in the dark for further use.

2.2.2(b) **Preparation of $[Mn_2O_2(OAc)(H_2O)_2(bpy)_2](ClO_4)_3.H_2O$. (A)**

Bpy (600 mg, 3.80 mmol) was added to a solution of $Mn(OAc)_2.4H_2O$ (500 mg, 2.04 mmol) in 20 ml of water and 3 ml of acetic acid. After the dissolution of the ligand, a solution of ceric perchlorate (10 ml) was added. The resulting brown solution was filtered and set aside for a week to obtain 280 mg (yield 31.8 %)of well formed crystals of the dimer. Anal. % calcd. for $Mn_2C_{22}H_{25}N_4O_{19}Cl_3$: C, 30.52; H, 2.64; N, 6.47. Found: C, 29.96; H, 3.07; N, 6.15. Equivalent weight by iodometry, found (calc) 217(216.4).

2.2.2(c) **Preparation of $[Mn_3O_4(H_2O)_2(phen)_4](NO_3)_4.2.5H_2O$ (B)**

Phen (2.01 g, 10.16 mmol) was added to a solution of $Mn(OAc)_2.4H_2O$ (1.21 g, 4.94 mmol) in 20 ml of 1.6N HNO_3. Slow addition of aqueous ammonium ceric nitrate (3.3 g) resulted in a brown solution. The solution was filtered and kept at room temperature. In two days, a dark crystalline material deposited, which was filtered and washed with very dilute aq.HNO_3. The compound was recrystallised from 1.6N HNO_3 to obtain 1.25 g (yield 60%) of well shaped brown crystals of the trimer. Anal. % calcd for $C_{48}H_{41}Mn_3N_{12}O_{20.5}$: C, 44.23; H, 3.23; N, 13.14; Found: 44.23; H,3.36; N, 12.81. Equivalent weight by iodometry, found (calc) 226 (213.1).

2.2.2(d) **Preparation of $[Mn_3O_4(H_2O)_2(bpy)_4](ClO_4)_4.\ 5H_2O$. (C)**

$Mn(ClO_4)_2 \cdot 5H_2O$ (720 mg, 2.09 mmol) was added slowly to a solution of bpy (600 mg, 3.80 mmol) in 20 ml water and 10 ml ceric perchlorate solution with constant stirring. The resulting brown solution containing a small amount of precipitate was filtered and left for a few days at room temperature. The well formed dark crystals were filtered and dried (yield, 110 mg 23%). Anal. % calcd for $Mn_3C_{40}H_{46}N_8O_{27}Cl_4$: C, 34.88; H, 3.36; N, 8.10. Found: C, 35.7; H, 2.80; N, 7.83. Equivalent weight by iodometry, found (calc) 240±5 (229.6).

2.2.3 Analysis, Spectral and Magnetic measurements: I.R. spectra were obtained using KBr pellets on a Perkin-Elmer 297 infrared spectrometer. Electronic spectra were recorded using either a Shimadzu 200S double beam spectrometer or a Perkin-Elmer Lambda 3B UV-VIS spectrophotometer. C, H, N elemental analyses were performed on a Perkin- Elmer 240C elemental analyzer. Equivalent weights of the complexes were estimated by iodometry as described in Vogel.[174] Excess KI (10% solution in water) and 2 ml of 6N H_2SO_4 was added to the compound (50-80 mg) dissolved in 20 ml of water-acetonitrile mixture (2:1). Liberated iodine was titrated with 0.02 N sodium thiosulphate (standardised with KIO_3), using starch indicator.

EPR spectra were recorded for powder and frozen solution on a JEOL FE-3X spectrometer using DPPH as the internal standard. JEOL NM-7700 temperature controller was used for low temperature

measurements.

Room temperature magnetic data was obtained on a CAHN-3000 microbalance. Diamagnetic corrections were applied by using Pascal's constants.[175] Variable temperature magnetic susceptibility data were obtained on powdered polycrystalline samples with a Quantum Design MPMS SQUID susceptometer (Laboratoire de Chimie de Coordination du CNRS, Toulouse Cedex, France). Least-squares computer fittings of the magnetic susceptibility data was accomplished with an adapted version of the function-minimization program STEPT.[176]

2.2.4 X-ray crystallography:

2.2.4(a) $[Mn_2(O)_2(OAc)(H_2O)_2(bpy)_2](ClO_4)_3.H_2O$ (A).† (Laboratoire de Chimie de Coordination du CNRS, Toulouse, France).

A dark brown cubic crystal of A with approximate dimension 0.5 × 0.45 × 0.4 mm was sealed on a glass fiber and mounted on an Enraf-Nonius CAD-4 diffractometer. Cell constants were obtained from a least squares fit of 25 reflections in the 7 -13 θ MoKα range. Parameters of crystal and intensity measurements

---

† Identical compound has been reported recently by Czernuszewicz *et al.*[204] by oxidation of $Mn(OAc)_2$ with $KMnO_4$ in presence of ligand.

Table 2.1. Crystallographic Data for A.

chemical formula	$Mn_2C_{22}H_{25}N_4O_{19}Cl_3$	formula weight	865.69
a, Å	13.619(1)	space group	$P2_1/n$
b, Å	16.213(2)	temp, K	298
c, Å	16.266(1)	ρ_{calc}, g cm^{-3}	1.74
β, deg	113.08(1)	ρ_{obs}, g cm^{-3}	1.75
Z	4	V, $Å^3$	3304.1
μ, cm^{-1}	10.6	λ, Å	0.71073
crystal size, mm	0.5 × 0.45 × 0.4	radiation	MoKα
diffractometer	Enraf-Nonius CAD4		
data collected	7840		
data used			
($F > 6\sigma(F)$)	5159	no. of variables	496
R [a]	0.021	R_w [b]	0.024

[a] $R = (\sum \| |F_o| - |F_c| \|) / \sum |F_o|$

[b] $R_w = \{ [\sum w (|F_o| - |F_c|)^2] / \sum w F_o^2 \}^{1/2}$

are summarized in the Table 2.1. A total of 7480 reflections were recorded to a 2θ (MoKα) maximum of 60° by procedures described elsewhere and corrected for Lorenz and polarization effects.[177] Empirical absorption corrections were made.[178] 5159 reflections with $F > 6\sigma(F)$ were used in subsequent calculations. Compound A crystallises in the monoclinic system (space group $P2_1/n$). The structure was successfully solved and refined by full-matrix least-squares and Fourier techniques on a Digital microVAX 3400 computer using MOLEN,[177] SHELX76,[179] SHELXS86[180] and ORTEP[181] programs. The asymmetric unit contains one full molecule. One of the perchlorate anions was disordered and the statistical model offers two types of perchlorate anions equally distributed at two positions. All non-hydrogen atoms were refined by using anisotropic thermal parameters. Hydrogen atoms were included in the calculations coupled to their bonded atoms at a fixed distance of 0.95 Å with a mean isotropic temperature factor U = 0.065 $Å^2$. Atomic coordinates with equivalent isotropic thermal parameters, bond lengths and angles are given in Tables 2.2 to 2.4

2.2.5(b) $[Mn_3O_4(H_2O)_2(phen)_4](NO_3)_4.2.5H_2O$ (B). (Departement of Chemistry, Univ. of Wyoming, Laramie, U.S.A).

A brown rectangular prism with approximate dimension 0.20 X 0.38 X 0.50 mm was mounted on Siemens P4 diffractometer for data collection. Parameters of crystal and intensity measurements are summarized in the Table 2.5. A total of 7470 reflections were

Table 2.2. Fractional Atomic Coordinates and Isotropic or Equivalent Temperature Factors for A

Atom	x/a	y/b	z/c	U_{eq} [a]
Mn(1)	0.51251(2)	0.25089(2)	0.40419(2)	0.0307(5)
Mn(2)	0.64576(2)	0.22128(2)	0.32570(2)	0.0303(5)
Ow1	0.5385(1)	0.2547(1)	0.5329(1)	0.047(3)
H1(Ow1)	0.6090(7)	0.260(2)	0.577(1)	0.065
H2(Ow1)	0.498(1)	0.214(1)	0.548(1)	0.065
Ow2	0.6297(1)	0.1863(1)	0.2041(1)	0.047(3)
H1(Ow2)	0.664(2)	0.204(2)	0.167(1)	0.065
H2(Ow2)	0.574(1)	0.151(1)	0.168(1)	0.065
O(1)	0.6545(1)	0.25107(9)	0.43413(9)	0.031(2)
O(2)	0.5065(1)	0.24679(9)	0.29178(9)	0.031(2)
O(3)	0.5039(1)	0.13203(9)	0.4075(1)	0.041(3)
O(4)	0.6224(1)	0.10748(9)	0.3456(1)	0.041(3)
C(1)	0.5567(2)	0.0841(1)	0.3794(2)	0.040(4)
C(2)	0.5410(2)	-0.0067(1)	0.3850(2)	0.058(5)
N(1)	0.4996(1)	0.3738(1)	0.4013(1)	0.036(3)
C(3)	0.3989(2)	0.4040(1)	0.3674(2)	0.040(4)
C(4)	0.3826(2)	0.4882(2)	0.3569(2)	0.053(5)
C(5)	0.4688(3)	0.5402(2)	0.3820(2)	0.061(5)
C(6)	0.5710(2)	0.5090(2)	0.4189(2)	0.055(5)
C(7)	0.5842(2)	0.4251(2)	0.4277(2)	0.046(4)
N(2)	0.3517(1)	0.2634(1)	0.3647(1)	0.039(3)
C(8)	0.3158(2)	0.3418(2)	0.3467(2)	0.039(4)
C(9)	0.2073(2)	0.3586(2)	0.3121(2)	0.055(5)
C(10)	0.1374(2)	0.2948(2)	0.2977(2)	0.066(6)
C(11)	0.1733(2)	0.2151(2)	0.3163(2)	0.063(5)
C(12)	0.2830(2)	0.2002(2)	0.3506(2)	0.050(4)
N(3)	0.6880(1)	0.3327(1)	0.2973(1)	0.040(3)
C(13)	0.7950(2)	0.3480(2)	0.3335(2)	0.051(4)
C(14)	0.8315(2)	0.4239(2)	0.3225(2)	0.061(5)
C(15)	0.7616(2)	0.4826(2)	0.2757(2)	0.062(5)

Table 2.2. contd...

Atom	x/a	y/b	z/c	U_{eq} [a]
C(16)	0.6529(2)	0.4663(2)	0.2381(2)	0.060(5)
C(17)	0.6187(2)	0.3892(2)	0.2497(2)	0.054(5)
N(4)	0.6880(1)	0.3327(1)	0.2973(1)	0.040(3)
C(18)	0.8618(2)	0.2784(2)	0.3789(2)	0.050(4)
C(19)	0.9729(2)	0.2797(2)	0.4212(2)	0.051(4)
C(20)	1.0251(2)	0.2057(2)	0.4575(2)	0.056(5)
C(21)	0.9688(2)	0.1363(2)	0.4536(2)	0.066(6)
C(22)	0.8596(2)	0.1380(2)	0.4137(2)	0.054(5)
Cl(1)	0.33300(4)	0.26527(4)	0.62223(4)	0.049(1)
O(5)	0.2512(2)	0.2226(2)	0.6385(2)	0.095(5)
O(6)	0.3989(2)	0.2026(1)	0.6060(2)	0.102(5)
O(7)	0.2891(2)	0.3116(2)	0.5419(2)	0.090(5)
O(8)	0.3940(2)	0.3165(2)	0.6968(2)	0.099(6)
Cl(2)	0.31569(6)	0.47445(5)	0.10564(5)	0.064(1)
O(9)	0.3510(2)	0.3946(2)	0.1197(2)	0.115(7)
O(10)	0.3048(2)	0.5104(2)	0.0227(2)	0.091(5)
O(11)	0.2335(2)	0.4901(2)	0.1307(2)	0.113(6)
O(12)	0.4047(2)	0.5183(2)	0.1673(2)	0.124(8)
Cl(3)	0.38857(5)	0.06607(5)	0.10081(5)	0.058(1)
O(13)	0.3372(2)	0.0113(2)	0.0353(2)	0.128(7)
O(14)	0.4976(3)	0.0752(3)	0.1103(5)	0.110(1)
O(15)	0.3351(5)	0.1327(4)	0.0508(4)	0.110(1)
O(16)	0.3816(6)	0.0679(4)	0.1854(3)	0.100(1)
O(14')	0.4404(4)	0.1367(4)	0.0861(3)	0.080(1)
O(15')	0.3096(4)	0.0961(3)	0.1313(5)	0.100(1)
O(16')	0.4577(4)	0.0196(4)	0.1716(3)	0.090(1)
Ow3	0.2354(2)	0.2579(2)	0.1389(1)	0.064(4)
H1(Ow3)	0.264(2)	0.2076(7)	0.128(2)	0.080
H2(Ow3)	0.259(2)	0.3049(9)	0.117(2)	0.080

[a] U_{eq} = 1/3 trace u (u = diagonalized U matrix).

Table 2.3. Bond distances (Å) for A.

Mn(1)	- O(1)	1.800(1)	Mn(2)	- O(1)	1.787(2)
Mn(1)	- O(2)	1.799(2)	Mn(2)	- O(2)	1.804(1)
Mn(1)	- O(3)	1.933(2)	Mn(2)	- O(4)	1.921(2)
Mn(1)	- Ow(1)	1.982(2)	Mn(2)	- Ow(2)	1.985(2)
Mn(1)	- N(1)	1.999(2)	Mn(2)	- N(3)	2.004(2)
Mn(1)	- N(2)	2.037(2)	Mn(2)	- N(4)	2.049(2)
Mn(1)...Mn(2)		2.6401(5)	C(1)	- C(2)	1.496(3)
O(3)	- C(1)	1.260(3)	O(4)	- C(1)	1.277(3)
N(1)	- C(3)	1.354(3)	N(3)	- C(13)	1.364(3)
C(3)	- C(4)	1.382(3)	C(13)	- C(14)	1.364(4)
C(4)	- C(5)	1.371(4)	C(14)	- C(15)	1.351(4)
C(5)	- C(6)	1.379(4)	C(15)	- C(16)	1.388(4)
C(6)	- C(7)	1.372(3)	C(16)	- C(17)	1.372(4)
C(7)	- N(1)	1.347(3)	C(17)	- N(3)	1.326(3)
C(3)	- C(8)	1.453(3)	C(13)	- C(18)	1.457(4)
N(2)	- C(8)	1.352(3)	N(4)	- C(18)	1.357(4)
C(8)	- C(9)	1.386(3)	C(18)	- C(19)	1.395(3)
C(9)	- C(10)	1.363(4)	C(19)	- C(20)	1.402(4)
C(10)	- C(11)	1.373(5)	C(20)	- C(21)	1.349(5)
C(11)	- C(12)	1.396(3)	C(21)	- C(22)	1.370(4)
C(12)	- N(2)	1.344(3)	C(22)	- N(4)	1.338(3)
Cl(1)	- O(5)	1.421(3)	Cl(1)	- O(7)	1.421(2)
Cl(1)	- O(6)	1.446(3)	Cl(1)	- O(8)	1.435(3)
Cl(2)	- O(9)	1.369(3)	Cl(2)	- O(11)	1.357(3)
Cl(2)	- O(10)	1.423(3)	Cl(2)	- O(12)	1.424(3)
Cl(3)	- O(13)	1.352(3)			
Cl(3)	- O(14)	1.438(5)	Cl(3)	- O(14')	1.414(6)
Cl(3)	- O(15)	1.376(6)	Cl(3)	- O(15')	1.435(7)
Cl(3)	- O(16)	1.415(7)	Cl(3)	- O(16')	1.389(5)

Table 2.4. Bond angles (°) for A.

O(1)-	Mn(1)	-O(2)	83.76(6)	O(1)-	Mn(2)	-O(2)	83.99(6)
O(1)-	Mn(1)	-O(3)	93.70(7)	O(1)-	Mn(2)	-O(4)	92.55(7)
O(1)-	Mn(1)	-Ow(1)	89.22(7)	O(1)-	Mn(2)	-Ow(2)	177.50(7)
O(1)-	Mn(1)	-N(1)	94.58(7)	O(1)-	Mn(2)	-N(3)	94.02(8)
O(1)-	Mn(1)	-N(2)	173.66(8)	O(1)-	Mn(2)	-N(4)	89.52(7)
O(2)-	Mn(1)	-O(3)	90.73(7)	O(2)-	Mn(2)	-O(4)	92.77(7)
O(2)-	Mn(1)	-Ow(1)	172.97(6)	O(2)-	Mn(2)	-Ow(2)	93.94(7)
O(2)-	Mn(1)	-N(1)	92.54(8)	O(2)-	Mn(2)	-N(3)	94.92(7)
O(2)-	Mn(1)	-N(2)	93.90(7)	O(2)-	Mn(2)	-N(4)	171.60(8)
O(3)-	Mn(1)	-Ow(1)	89.35(8)	O(4)-	Mn(2)	-Ow(2)	86.13(7)
O(3)-	Mn(1)	-N(1)	171.38(8)	O(4)-	Mn(2)	-N(3)	170.37(9)
O(3)-	Mn(1)	-N(2)	92.22(7)	O(4)-	Mn(2)	-N(4)	92.85(8)
Ow(3)-	Mn(1)	-N(1)	88.38(8)	Ow(2)-	Mn(2)	-N(3)	87.55(8)
Ow(1)-	Mn(1)	-N(2)	93.12(7)	Ow(2)-	Mn(2)	-N(4)	92.67(8)
N(1)-	Mn(1)	-N(2)	79.61(8)	N(3)-	Mn(2)	-N(4)	80.18(8)
Mn(1)-	O(1)	-Mn(2)	94.79(5)	Mn(1)-	O(2)	-Mn(2)	94.24(5)
Mn(1)-	O(3)	-C(1)	123.7(2)	Mn(2)-	O(4)	-C(1)	123.2(2)
O(3)-	C(1)	-O(4)	124.7(2)	O(3)-	C(1)	-C(2)	118.0(3)
O(4)-	C(1)	-C(20)	117.3(2)				
Mn(1)-	N(1)	-C(7)	123.5(2)	Mn(2)-	N(3)	-C(17)	123.7(2)
Mn(1)-	N(1)	-C(3)	115.8(1)	Mn(2)-	N(3)	-C(13)	114.8(1)
C(7)-	N(1)	-C(3)	120.7(2)	C(17)-	N(3)	-C(13)	121.4(2)
N(1)-	C(3)	-C(4)	119.7(2)	N(3)-	C(13)	-C(14)	119.4(2)
C(3)-	C(4)	-C(5)	119.5(2)	C(13)-	C(14)	-C(15)	119.8(3)
C(4)-	C(5)	-C(6)	120.4(2)	C(14)-	C(15)	-C(16)	120.5(3)
C(5)-	C(6)	-C(7)	118.5(3)	C(15)-	C(16)	-C(17)	118.3(2)
C(6)-	C(7)	-N(1)	121.2(2)	C(16)-	C(17)-	N(3)	120.5(3)
N(1)-	C(3)	-C(8)	114.6(2)	N(3)-	C(13)	-C(18)	115.3(2)
C(4)-	C(3)	-C(8)	125.7(2)	C(14)-	C(13)	-C(18)	125.3(2)

Table 2.4 contd...

N(2)-	C(8)	-C(3)	114.8(2)	N(4)-	C(18)	-C(13)	114.9(2)
C(3)-	C(8)	-C(9)	124.5(2)	C(13)-	C(18)	-C(19)	125.4(3)
Mn(1)-	N(2)	-C(12)	124.6(2)	Mn(2)-	N(4)	-C(22)	124.4(2)
Mn(1)-	N(2)	-C(8)	114.5(1)	Mn(2)-	N(4)	-C(18)	113.7(2)
C(12)-	N(2)	-C(8)	120.7(2)	C(22)-	N(4)	-C(18)	121.4(2)
N(2)-	C(8)	-C(9)	120.6(2)	N(4)-	C(18)	-C(19)	119.6(2)
C(8)-	C(9)	-C(10)	118.9(3)	C(18)-	C(19)	-C(20)	117.9(3)
C(9)-	C(10)	-C(11)	120.8(2)	C(19)-	C(20)	-C(21)	120.6(2)
C(10)-	C(11)	-C(12)	118.9(3)	C(20)-	C(21)	-C(22)	119.8(3)
C(11)-	C(12)	-N(2)	120.1(3)	C(21)-	C(22)	-N(4)	120.6(3)
O(5)-	Cl(1)	-O(6)	106.3(1)	O(6)-	Cl(1)	-O(7)	105.7(2)
O(5)-	Cl(1)	-O(7)	110.6(1)	O(6)-	Cl(1)	-O(8)	111.4(1)
O(5)-	Cl(1)	-O(8)	111.1(2)	O(7)-	Cl(1)	-O(8)	111.5(2)
O(9)-	Cl(2)	-O(10)	116.4(2)	O(10)-	Cl(2)	-O(11)	114.6(2)
O(9)-	Cl(2)	-O(11)	113.8(2)	O(10)-	Cl(2)	-O(12)	102.0(2)
O(9)-	Cl(2)	-O(12)	102.0(2)	O(11)-	Cl(2)	-O(12)	105.7(2)
O(13)-	Cl(3)	-O(14)	110.2(3)	O(13)-	Cl(3)	-O(14')	122.4(2)
O(13)-	Cl(3)	-O(15)	93.4(3)	O(13)-	Cl(3)	-O(15')	105.6(2)
O(13)-	Cl(3)	-O(16)	124.6(3)	O(13)-	Cl(3)	-O(16')	105.7(3)
O(14)-	Cl(3)	-O(15)	105.5(4)	O(14')-	Cl(3)	-O(15')	106.0(3)
O(14)-	Cl(3)	-O(16)	110.6(4)	O(14')-	Cl(3)	-O(16')	111.0(3)
O(15)-	Cl(3)	-O(16)	109.6(4)	O(15')-	Cl(3)	-O(16')	104.7(4)

collected and the stability of the crystal was monitored by measuring the intensities of three check reflections for every 100 reflections. Out of 7470 total reflections, 4609 reflections with $F > 6.0\ \sigma(F)$ were used in subsequent calculations. The compound crystallises in the triclinic system. The structure was successfully solved in the space group $P\bar{1}$ by direct methods and refined by standard full-matrix least-square method using Siemens SHELXTL IRIS system. The asymmetric unit contains one trimeric cation, four nitrate anions and 2.5 water molecules. All non-hydrogen atoms were refined by using anisotropic thermal parameters. Hydrogen atoms were refined by a riding model with fixed isotropic temperature factors. Atomic coordinates, temperature factors, bond length and angles are given in Tables 2.6 to 2.9

2.3 Results and Discussion:

2.3.1 Synthesis. There are two aspects about the synthesis that merit some detailed mention: (i) the use of Ce^{4+} as an oxidising agent, and (ii) solution chemistry leading to the assembly of higher nuclearity species. While it is well known that oxidation of organic substrates by Ce^{4+} is often catalysed by Mn^{2+} salts,[182] the synthetic potential of ceric oxidation for the preparation of high valent manganese complexes has not been fully recognised until now. Our investigations in this direction were prompted by

Table 2.5. Crystallographic Data for B.

chemical formula	$C_{48}H_{41}Mn_3N_{12}O_{20.5}$	formula weight	1278.7
a, Å	10.700(2)	space group	$P\bar{1}$
b, Å	12.643(3)	temp, K	296
c, Å	20.509(4)	ρ_{calc}, g cm^{-3}	1.584
α, deg	78.37(3)	V, $Å^3$	2681.8(10)
β, deg	83.12(3)	Z	2
γ, deg	82.50(3)	λ, Å	0.71073
μ, cm^{-1}	7.86	radiation	MoKα
diffractometer	Siemens P4	crystal size, mm	0.2×0.38×0.5
monochromator	graphite	2θ range, deg	4 - 45
data used		data collected	7470
(F > 6.0 σ(F)	4609	no. of variables	754
max, min peak on final difference map,	e/$Å^3$ 0.68	F(000)	1304
R [a]	0.055	R_w [b]	0.076

[a] $R = (\sum \| |F_o| - |F_c| \|) / \sum |F_o|$

[b] $R_w = \{ [\sum w (|F_o| - |F_c|)^2] / \sum w F_o^2 \}^{1/2}$

Table 2.6. Fractional Atomic Coordinates and Isotropic or Equivalent Temperature Factors for B.

Atom	x/a	y/b	z/c	U_{eq} [a]
Mn(1)	0.3604	0.2663	0.2910	0.034(1)
O(1)	0.4802(4)	0.3759(3)	0.2295(2)	0.040(2)
O(2)	0.2219(4)	0.3332(3)	0.3274(2)	0.035(2)
N(1)	0.2762(5)	0.2118(4)	0.2240(3)	0.037(2)
N(2)	0.5152(5)	0.1702(4)	0.2521(3)	0.041(2)
N(3)	0.3239(5)	0.1306(4)	0.3639(3)	0.041(2)
N(4)	0.4563(5)	0.2937(5)	0.3639(3)	0.039(2)
Mn(2)	0.1494(1)	0.4717(1)	0.3059(1)	0.033(1)
O(3)	0.2919(4)	0.5393(3)	0.2878(2)	0.037(2)
O(4)	0.1684(4)	0.4767(3)	0.2164(2)	0.037(2)
O(1W)	-0.0172(4)	0.4078(4)	0.3274(2)	0.040(2)
N(5)	0.1452(5)	0.4960(5)	0.4034(3)	0.036(2)
N(6)	0.0345(5)	0.6193(4)	0.3012(3)	0.042(2)
Mn(3)	0.3289(1)	0.5118(1)	0.2043(1)	0.037(1)
O(2W)	0.5011(5)	0.5632(4)	0.1910(3)	0.057(2)
N(7)	0.2679(6)	0.6676(5)	0.1586(3)	0.046(2)
N(8)	0.3410(6)	0.4940(5)	0.1046(3)	0.048(2)
C(1)	0.1561(7)	0.2367(6)	0.2114(3)	0.045(3)
C(2)	0.1122(8)	0.2052(7)	0.1567(4)	0.057(3)
C(3)	0.1942(8)	0.1508(7)	0.1163(4)	0.059(3)
C(4)	0.3219(8)	0.1241(6)	0.1280(4)	0.050(3)
C(5)	0.4167(9)	0.0683(7)	0.0875(4)	0.066(4)
C(6)	0.5369(9)	0.0455(7)	0.1020(4)	0.067(4)
C(7)	0.5767(7)	0.0774(6)	0.1586(4)	0.050(3)
C(8)	0.7028(8)	0.0605(6)	0.1766(4)	0.059(3)
C(9)	0.7306(7)	0.0972(6)	0.2302(4)	0.055(3)
C(10)	0.6340(7)	0.1529(6)	0.2674(4)	0.046(3)
C(11)	0.4871(7)	0.1337(5)	0.1981(3)	0.042(3)
C(12)	0.3582(7)	0.1549(5)	0.1831(3)	0.039(3)

Table 2.6. contd...

Atom	x/a	y/b	z/c	U_{eq} [a]
C(13)	0.2556(7)	0.0504(6)	0.3628(4)	0.054(3)
C(14)	0.2273(8)	-0.0256(7)	0.4208(6)	0.073(4)
C(15)	0.2644(9)	-0.0193(7)	0.4790(5)	0.072(4)
C(16)	0.3346(8)	0.0647(7)	0.4832(4)	0.055(3)
C(17)	0.3763(9)	0.0829(8)	0.5425(4)	0.072(4)
C(18)	0.4431(9)	0.1650(9)	0.5427(4)	0.075(4)
C(19)	0.4750(7)	0.2406(7)	0.4824(4)	0.055(3)
C(20)	0.5401(9)	0.3302(8)	0.4785(5)	0.072(4)
C(21)	0.5613(8)	0.3976(8)	0.4194(5)	0.068(4)
C(22)	0.5165(7)	0.3788(6)	0.3614(4)	0.050(3)
C(23)	0.4361(7)	0.2234(6)	0.4235(3)	0.043(3)
C(24)	0.3652(7)	0.1370(6)	0.4243(3)	0.044(3)
C(25)	0.2009(6)	0.4318(6)	0.4533(3)	0.041(3)
C(26)	0.2069(7)	0.4648(7)	0.5137(4)	0.051(3)
C(27)	0.1521(7)	0.5644(7)	0.5229(4)	0.052(3)
C(28)	0.0906(7)	0.6342(6)	0.4717(4)	0.044(3)
C(29)	0.0247(8)	0.7380(7)	0.4766(5)	0.058(4)
C(30)	-0.0371(8)	0.7995(7)	0.4272(5)	0.064(4)
C(31)	-0.0382(8)	0.7626(6)	0.3653(4)	0.054(3)
C(32)	-0.1033(9)	0.8183(7)	0.3120(5)	0.072(4)
C(33)	-0.0982(8)	0.7747(7)	0.2559(5)	0.070(4)
C(34)	-0.0277(7)	0.6744(6)	0.2510(4)	0.053(3)
C(35)	0.0268(7)	0.6603(5)	0.3583(4)	0.042(3)
C(36)	0.0900(6)	0.5968(5)	0.4122(3)	0.033(2)
C(37)	0.2382(7)	0.7535(6)	0.1867(4)	0.051(3)
C(38)	0.1896(9)	0.8548(7)	0.1499(5)	0.072(4)
C(39)	0.1675(10)	0.8644(7)	0.0850(5)	0.075(4)
C(40)	0.2004(9)	0.7736(7)	0.0534(5)	0.066(4)
C(41)	0.1864(11)	0.7748(9)	-0.0142(5)	0.094(5)
C(42)	0.2244(12)	0.6856(9)	-0.0413(5)	0.097(5)

Table 2.6. contd...

Atom	x/a	y/b	z/c	U_{eq} [a]
C(43)	0.2760(9)	0.5861(8)	-0.0032(4)	0.072(4)
C(44)	0.3177(11)	0.4884(9)	-0.0276(4)	0.092(5)
C(45)	0.3704(11)	0.4011(8)	0.0129(4)	0.081(4)
C(46)	0.3835(9)	0.4063(7)	0.0806(4)	0.065(4)
C(47)	0.2892(7)	0.5831(6)	0.0639(4)	0.051(3)
C(48)	0.2513(7)	0.6759(6)	0.0930(4)	0.048(3)
N(9)	-0.1051(8)	0.1563(6)	0.3678(3)	0.057(3)
O(5)	-0.1146(7)	0.0655(5)	0.3602(3)	0.092(3)
O(6)	-0.2008(6)	0.2167(5)	0.3843(3)	0.080(3)
O(7)	0.0006(6)	0.1938(5)	0.3608(3)	0.072(3)
N(10)	0.2164(6)	0.5972(6)	0.7785(3)	0.056(3)
O(8)	0.1318(6)	0.6721(6)	0.7816(4)	0.094(3)
O(9)	0.3122(5)	0.5960(5)	0.8090(3)	0.073(3)
O(10)	o.2130(6)	0.5271(5)	0.7447(3)	0.074(3)
N(11)	0.8205(10)	0.8388(8)	0.0654(4)	0.115(6)
O(11)	0.7222(11)	0.8221(12)	0.0467(7)	0.245(10)
O(12)	0.8712(12)	0.9193(10)	0.0385(7)	0.225(9)
O(13)	0.8634(19)	0.7786(14)	0.1136(9)	0.398(18)
N(12)	0.4190(12)	0.8398(11)	0.2958(8)	0.382(29)
O(14)	0.3815(14)	0.7689(17)	0.3407(8)	0.495(33)
O(15)	0.5299(13)	0.8564(17)	0.2888(9)	0.368(15)
O(16)	0.3448(18)	0.8966(10)	0.2593(9)	0.385(16)
O(3W)	0.6594(8)	0.6304(6)	0.3413(4)	0.116(4)
O(4W)	0.5516(10)	0.7572(7)	0.1553(8)	0.222(8)
O(5W)	0.9799(73)	0.5342(77)	0.0670(34)	0.685(74)

[a] U_{eq} = 1/3 trace u (u = diagonalized U matrix)

Table 2.7. Bond distances (Å) for B.

Mn(1)	- O(1)	1.760(4)	Mn(1)	- O(2)	1.769(4)
Mn(1)	- N(1)	2.004(6)	Mn(1)	- N(2)	2.099(5)
Mn(1)	- N(3)	2.081(5)	Mn(1)	- N(4)	2.019(6)
O(1)	-Mn(3)	1.819(4)	O(2)	- Mn(2)	1.810(4)
N(1)	- C(1)	1.326(9)	N(1)	- C(12)	1.376(9)
N(2)	-C(10)	1.326(10)	N(2)	- C(11)	1.361(10)
N(3)	- C(13)	1.331(10)	N(3)	- C(24)	1.384(10)
N(4)	- C(22)	1.314(10)	N(4)	- C(23)	1.370(8)
Mn(2)	- O(3)	1.808(5)	Mn(2)	- O(4)	1.811(4)
Mn(2)	- O(1W)	2.017(5)	Mn(2)	- N(5)	2.079(6)
Mn(2)	- N(6)	2.089(5)	Mn(2)	- Mn(3)	2.675(1)
O(3)	- Mn(3)	1.804(5)	O(4)	- Mn(3)	1.806(5)
N(5)	- C(25)	1.320(8)	N(5)	- C(36)	1.370(8)
N(6)	- C(34)	1.320(9)	N(6)	- C(35)	1.363(10)
Mn(3)	- O(2W)	2.003(5)	Mn(3)	- N(7)	2.062(6)
Mn(3)	- N(8)	2.090(6)	N(7)	- C(37)	1.315(10)
N(7)	- C(48)	1.359(10)	N(8)	- C(46)	1.309(11)
N(8)	- C(47)	1.358(9)	C(1)	- C(2)	1.413(12)
C(2)	- C(3)	1.351(12)	C(3)	- C(4)	1.402(12)
C(4)	- C(5)	1.438(11)	C(4)	- C(12)	1.379(11)
C(5)	- C(6)	1.336(14)	C(6)	- C(7)	1.429(13)
C(7)	- C(8)	1.419(12)	C(7)	- C(11)	1.397(10)
C(8)	- C(9)	1.352(13)	C(9)	- C(10)	1.409(11)
C(11)	- C(12)	1.428(10)	C(13)	- C(14)	1.401(12)
C(14)	- C(15)	1.323(16)	C(15)	- C(16)	1.398(14)
C(16)	- C(17)	1.416(14)	C(16)	- C(24)	1.393(10)
C(17)	- C(18)	1.335(16)	C(18)	- C(19)	1.438(12)
C(19)	- C(20)	1.390(14)	C(19)	- C(23)	1.389(12)
C(20)	- C(21)	1.347(13)	C(21)	- C(22)	1.407(14)
C(23)	- C(24)	1.406(11)	C(25)	- C(26)	1.397(11)

Table 2.7. contd...

C(26)	- C(27)	1.357(12)	C(27)	- C(28)	1.398(10)
C(28)	- C(29)	1.422(11)	C(28)	- C(36)	1.396(11)
C(29)	- C(30)	1.333(12)	C(30)	- C(31)	1.439(14)
C(31)	- C(32)	1.385(12)	C(31)	- C(35)	1.413(10)
C(32)	- C(33)	1.365(15)	C(33)	- C(34)	1.404(11)
C(35)	- C(36)	1.414(9)	C(37)	- C(38)	1.417(11)
C(38)	- C(39)	1.358(15)	C(39)	- C(40)	1.414(14)
C(40)	- C(41)	1.411(14)	C(40)	- C(48)	1.417(11)
C(41)	- C(42)	1.350(16)	C(42)	- C(43)	1.422(13)
C(43)	- C(44)	1.424(14)	C(43)	- C(47)	1.393(12)
C(44)	- C(45)	1.343(13)	C(45)	- C(46)	1.426(13)
C(47)	- C(48)	1.413(11)	N(9)	- O(5)	1.208(11)
N(9)	- O(6)	1.249(10)	N(9)	- O(7)	1.264(10)
N(10)	- O(8)	1.227(9)	N(10)	- O(9)	1.260(10)
N(10)	- O(10)	1.237(11)	N(11)	- O(11)	1.219(18)
N(11)	- O(12)	1.217(16)	N(11)	- O(13)	1.217(19)
N(12)	- O(14)	1.219(22)	N(12)	- O(15)	1.218(20)
N(12)	- O(16)	1.218(22)			

Table 2.8. Bond angles (°) for B.

O(1)-	Mn(1)	-(92)	98.8(2)	O(1)-	Mn(1)	-N(1)	90.8(2)
O(2)-	Mn(1)	-N(1)	96.7(2)	O(1)-	Mn(1)	-N(2)	87.3(3)
O(2)-	Mn(1)	-N(2)	173.4(2)	N(1)-	Mn(1)	-N(2)	80.5(2)
O(1)-	Mn(1)	-N(3)	174.0(2)	O(2)-	Mn(1)	-N(3)	86.5(2)
N(1)	Mn(1)	-N(3)	91.6(2)	N(2)-	Mn(1)	-N(3)	87.7(2)
O(1)-	Mn(1)	-N(4)	96.6(2)	O(2)-	Mn(1)	-N(4)	88.9(2)
N(1)-	Mn(1)	-N(4)	170.0(2)	N(2)-	Mn(1)	-N(4)	93.1(2)
N(3)-	Mn(1)	-N(4)	80.5(2)	Mn(1)-	O(1)	-Mn(3)	130.4(2)
Mn(1)-	O(2)	-Mn(2)	130.4(2)	Mn(1)-	N(1)	-C(1)	126.0(5)
Mn(1)-	N(1)	-C(12)	114.1(5)	C(1)-	N(1)	-C(12)	119.4(6)
Mn(1)-	N(2)	-C(10)	129.5(5)	Mn(1)-	N(2)	-C(11)	111.6(4)
C(10)-	N(2)	-C(11)	118.4(6)	Mn(1)-	N(3)	-C(13)	130.0(5)
Mn(1)-	N(3)	-C(24)	111.5(5)	C(13)-	N(3)	-C(24)	117.9(6)
Mn(1)-	N(4)	-C(22)	126.0(5)	Mn(1)-	N(4)	-C(23)	113.4(5)
C(22)-	N(4)	-C(23)	119.8(7)	O(2)-	Mn(2)	-O(3)	98.5(2)
O(2)-	Mn(2)	-O(4)	95.4(2)	O(3)-	Mn(2)	-O(4)	82.8(2)
O(2)-	Mn(2)	-O(1W)	85.8(2)	O(3)-	Mn(2)	-O(1W)	175.3(2)
O(4)-	Mn(2)	-O(1W)	98.7(2)	O(2)-	Mn(2)	-N(5)	92.2(2)
O(3)-	Mn(2)	-N(5)	86.9(2)	O(4)-	Mn(2)	-N(5)	168.0(2)
O(1W)-	Mn(2)	-N(5)	91.1(2)	O(2)-	Mn(2)	-N(6)	166.0(2)
O(3)-	Mn(2)	-N(6)	91.9(2)	O(4)-	Mn(2)	-N(6)	95.1(2)
O(1W)-	Mn(2)	-N(6)	83.5(2)	N(5)-	Mn(2)	-N(6)	79.0(2)
O(2)-	Mn(2)	-Mn(3)	90.2(1)	O(3)-	Mn(2)	-Mn(3)	42.2(1)
O(4)-	Mn(2)	-Mn(3)	42.2(1)	O(1W)-	Mn(2)	-Mn(3)	140.2(1)
N(5)-	Mn(2)	-Mn(3)	128.7(2)	N(6)-	Mn(2)	-Mn(3)	103.8(2)
Mn(2)-	O(3)	-Mn(3)	95.6(2)	Mn(2)-	O(4)	-Mn(3)	95.4(2)
Mn(2)-	N(5)	-C(25)	127.5(5)	Mn(2)-	N(5)	-C(36)	113.4(4)
C(25)-	N(5)	-C(36)	118.6(6)	Mn(2)-	N(6)	-C(34)	128.1(5)
Mn(2)-	N(6)	-C(35)	113.0(4)	C(34)-	N(6)	-C(35)	118.9(6)
O(1)-	Mn(3)	-Mn(2)	89.9(1)	O(1)-	Mn(3)	-O(3)	95.7(2)

Table 2.8. contd...

Mn(2)-	Mn(3)	-O(3)	42.3(1)	O(1)-	Mn(3)	-O(4)	97.7(2)
Mn(2)-	Mn(3)	-O(4)	42.4(1)	O(3)-	Mn(3)	-O(4)	83.0(2)
O(1)-	Mn(3)	-O(2W)	86.7(2)	Mn(2)-	Mn(3)	-O(2W)	136.7(2)
O(3)-	Mn(3)	-O(2W)	95.2(2)	O(4)-	Mn(3)	-O(2W)	175.4(2)
O(1)-	Mn(3)	-N(7)	167.8(2)	Mn(2)-	Mn(3)	-N(7)	102.3(2)
O(3)-	Mn(3)	-N(7)	94.2(2)	O(4)-	Mn(3)	-N(7)	90.5(2)
O(2W)-	Mn(3)	-N(7)	85.4(2)	O(1)-	Mn(3)	-N(8)	91.9(2)
Mn(2)-	Mn(3)	-N(8)	131.8(2)	O(3)-	Mn(3)	-N(8)	170.2(2)
O(4)-	Mn(3)	-N(8)	89.8(2)	O(2W)-	Mn(3)	-N(8)	91.4(2)
N(7)-	Mn(3)	-N(8)	79.1(2)	Mn(3)-	N(7)	-C(37)	127.4(5)
Mn(3)-	N(7)	-C(48)	113.1(5)	C(37)-	N(7)	-C(48)	119.4(6)
Mn(3)-	N(8)	-C(46)	127.0(5)	Mn(3)-	N(8)	-C(47)	113.1(5)
C(46)-	N(8)	-C(47)	119.8(7)	N(1)-	C(1)	-C(2)	120.5(7)
C(1)-	C(2)	-C(3)	119.5(8)	C(2)-	C(3)	-C(4)	121.2(8)
C(3)-	C(4)	-C(5)	125.5(8)	C(3)-	C(4)	-C(12)	116.5(7)
C(5)-	C(4)	-C(12)	118.1(7)	C(4)-	C(5)	-C(6)	122.0(9)
C(5)-	C(6)	-C(7)	120.8(8)	C(6)-	C(7)	-C(8)	125.0(7)
C(6)-	C(7)	-C(11)	118.4(7)	C(8)-	C(7)	-C(11)	116.6(8)
C(7)-	C(8)	-C(9)	120.0(7)	C(8)-	C(9)	-C(10)	119.6(7)
N(2)-	C(10)	-C(9)	122.1(8)	N(2)-	C(11)	-C(7)	123.3(7)
N(2)-	C(11)	-C(12)	116.4(6)	C(7)-	C(11)	-C(12)	120.3(7)
N(1)-	C(12)	-C(4)	122.8(7)	N(1)-	C(12)	-C(11)	116.6(7)
C(4)-	C(12)	-C(11)	120.4(6)	N(3)-	C(13)	-C(14)	120.9(8)
C(13)-	C(14)	-C(15)	121.7(9)	C(14)-	C(15)	-C(16)	119.7(8)
C(15)-	C(16)	-C(17)	125.3(8)	C(15)-	C(16)	-C(24)	117.5(8)
C(17)-	C(16)	-C(24)	171.1(8)	C(16)-	C(17)	-C(18)	122.0(8)
C(17)-	C(18)	-C(19)	121.5(9)	C(18)-	C(19)	-C(20)	125.2(9)
C(18)-	C(19)	-C(23)	117.3(8)	C(20)-	C(19)	-C(23)	117.4(7)
C(19)-	C(20)	-C(21)	120.0(10)	C(20)-	C(21)	-C(22)	120.5(9)
N(4)-	C(22)	-C(21)	120.3(7)	N(4)-	C(23)	-C(19)	121.9(7)

Table 2.8. contd...

N(4)-	C(23)	-C(24)	117.5(7)	C(19)-	C(23)	-C(24)	120.4(6)
N(3)-	C(24)	-C(16)	122.2(7)	N(3)-	C(24)	-C(23)	116.2(6)
C(16)-	C(24)	-C(23)	121.5(7)	N(5)-	C(25)	-C(26)	121.8(7)
C(25)-	C(26)	-C(27)	119.9(7)	C(26)-	C(27)	-C(28)	120.1(8)
C(27)-	C(28)	-C(29)	125.1(8)	C(27)-	C(28)	-C(36)	117.1(7)
C(29)-	C(28)	-C(36)	117.7(7)	C(28)-	C(29)	-C(30)	122.8(9)
C(29)-	C(30)	-C(31)	120.3(8)	C(30)-	C(31)	-C(32)	124.8(7)
C(30)-	C(31)	-C(35)	118.6(7)	C(32)-	C(31)	-C(35)	116.5(8)
C(31)-	C(32)	-C(33)	119.6(8)	C(32)-	C(33)	-C(34)	121.2(8)
N(6)-	C(34)	-C(33)	120.4(8)	N(6)-	C(35)	-C(31)	123.2(7)
N(6)-	C(35)	-C(36)	117.4(6)	C(31)-	C(35)	-C(36)	119.3(7)
N(5)-	C(36)	-C(28)	122.5(6)	N(5)-	C(36)	-C(35)	116.3(6)
C(28)-	C(36)	-C(35)	121.2(6)	N(7)-	C(37)	-C(38)	121.4(8)
C(37)-	C(38)	-C(39)	120.5(9)	C(38)-	C(39)	-C(40)	119.1(8)
C(39)-	C(40)	-C(41)	124.3(8)	C(39)-	C(40)	-C(48)	117.1(8)
C(41)-	C(40)	-C(48)	118.6(9)	C(40)-	C(41)	-C(42)	120.7(9)
C(41)-	C(42)	-C(43)	122.3(9)	C(42)-	C(43)	-C(44)	125.9(9)
C(42)-	C(43)	-C(47)	117.8(9)	C(44)-	C(43)	-C(47)	116.2(8)
C(43)-	C(44)	-C(45)	120.1(9)	C(44)-	C(45)	-C(46)	119.9(9)
N(8)-	C(46)	-C(45)	120.9(7)	N(8)-	C(47)	-C(43)	123.1(7)
N(8)-	C(47)	-C(48)	116.1(7)	C(43)-	C(47)	-C(48)	120.8(7)
N(7)-	C(48)	-C(40)	122.5(7)	N(7)-	C(48)	-C(47)	117.7(6)
C(40)-	C(48)	-C(47)	119.7(7)	O(5)-	N(9)	-O(6)	120.6(8)
O(5)-	N(9)	-O(7)	122.2(7)	O(6)-	N(9)	-O(7)	117.2(7)
O(8)-	N(10)	-O(9)	117.5(8)	O(8)-	N(10)	-O(10)	122.7(7)
O(9)-	N(10)	-O(10)	119.8(7)	O(11)-	N(11)	-O(12)	119.9(12)
O(11)-	N(11)	-O(13)	119.8(14)	O(12)-	N(11)	-O(13)	120.1(15)
O(14)-	N(12)	-O(15)	120.0(16)	O(14)-	N(12)	-O(16)	120.0(15)
O(15)-	N(12)	-O(16)	119.9(16)				

Table 2.9. Anisotropic Thermal parameters[a] for B.

Atom	U_{11}	U_{22}	U_{33}	U_{12}	U_{13}	U_{23}
Mn(1)	0.031(1)	0.038(1)	0.034(1)	-0.002(1)	-0.004(1)	-0.012(1)
O(1)	0.030(3)	0.047(3)	0.039(3)	-0.005(2)	0.003(2)	-0.004(2)
O(2)	0.031(3)	0.038(3)	0.037(3)	-0.003(2)	0.001(2)	-0.012(2)
N(1)	0.036(4)	0.042(3)	0.036(3)	-0.001(3)	-0.006(3)	-0.016(3)
N(2)	0.034(4)	0.042(3)	0.046(4)	0.005(3)	-0.008(3)	-0.011(3)
N(3)	0.039(4)	0.039(3)	0.044(4)	0.000(3)	0.000(3)	-0.007(3)
N(4)	0.033(3)	0.050(4)	0.038(4)	0.002(3)	-0.007(3)	-0.015(3)
Mn(2)	0.030(1)	0.037(1)	0.032(1)	-0.002(1)	-0.004(1)	-0.010(1)
O(3)	0.034(3)	0.039(3)	0.039(3)	-0.006(2)	-0.004(2)	-0.013(2)
O(4)	0.032(3)	0.044(3)	0.037(3)	-0.003(2)	-0.008(2)	-0.012(2)
O(1W)	0.027(3)	0.051(3)	0.046(3)	-0.011(2)	0.002(2)	-0.017(2)
N(5)	0.030(3)	0.047(4)	0.034(3)	-0.006(3)	0.003(3)	-0.016(3)
N(6)	0.031(3)	0.041(3)	0.054(4)	-0.004(3)	-0.005(3)	-0.011(3)
Mn(3)	0.037(1)	0.039(1)	0.035(1)	-0.006(1)	0.001(1)	-0.007(1)
O(2W)	0.037(3)	0.060(3)	0.072(4)	-0.015(3)	0.005(3)	-0.010(3)
N(7)	0.041(4)	0.048(4)	0.047(4)	-0.011(3)	-0.002(3)	-0.004(3)
N(8)	0.056(4)	0.049(4)	0.037(3)	-0.005(3)	0.004(3)	-0.010(3)
C(1)	0.042(5)	0.050(4)	0.046(4)	-0.006(4)	-0.003(4)	-0.020(4)
C(2)	0.044(5)	0.074(6)	0.061(5)	-0.004(4)	-0.013(4)	-0.026(5)
C(3)	0.062(6)	0.069(6)	0.055(5)	-0.004(5)	-0.020(4)	-0.029(4)
C(4)	0.055(5)	0.051(5)	0.049(5)	0.003(4)	-0.012(4)	-0.019(4)
C(5)	0.072(7)	0.077(6)	0.055(5)	0.013(5)	-0.013(5)	-0.039(5)
C(6)	0.069(7)	0.072(6)	0.065(6)	0.011(5)	-0.003(5)	-0.036(5)
C(7)	0.048(5)	0.053(5)	0.046(5)	0.015(4)	-0.002(4)	-0.018(4)
C(8)	0.051(6)	0.060(5)	0.061(5)	0.014(4)	0.005(4)	-0.021(4)
C(9)	0.032(5)	0.062(5)	0.066(5)	0.009(4)	0.001(4)	-0.015(4)
C(10)	0.040(5)	0.045(4)	0.055(5)	0.001(4)	-0.015(4)	-0.008(4)
C(11)	0.045(5)	0.036(4)	0.045(4)	0.004(3)	-0.006(4)	-0.010(3)

Table 2.9. contd...

Atom	U_{11}	U_{22}	U_{33}	U_{12}	U_{13}	U_{23}
C(12)	0.041(5)	0.037(4)	0.041(4)	0.001(3)	-0.009(3)	-0.014(3)
C(13)	0.048(5)	0.039(4)	0.073(6)	-0.011(4)	0.000(4)	-0.003(4)
C(14)	0.054(6)	0.047(5)	0.109(8)	-0.011(4)	0.001(6)	0.003(5)
C(15)	0.064(6)	0.059(6)	0.075(7)	0.006(5)	0.010(5)	0.014(5)
C(16)	0.044(5)	0.061(6)	0.047(5)	0.014(4)	0.006(4)	-0.002(4)
C(17)	0.066(7)	0.094(8)	0.043(5)	0.017(6)	0.001(5)	-0.001(5)
C(18)	0.068(7)	0.119(9)	0.033(5)	0.030(6)	-0.018(5)	-0.020(5)
C(19)	0.034(5)	0.082(6)	0.049(5)	0.017(4)	-0.10(4)	-0.023(5)
C(20)	0.063(6)	0.096(8)	0.067(6)	0.009(6)	-0.029(5)	-0.039(6)
C(21)	0.042(5)	0.087(7)	0.086(7)	-0.011(5)	-0.014(5)	-0.038(6)
C(22)	0.041(5)	0.060(5)	0.058(5)	-0.013(4)	-0.008(4)	-0.027(4)
C(23)	0.034(4)	0.053(5)	0.039(4)	0.015(4)	-0.011(3)	-0.013(4)
C(24)	0.039(4)	0.046(4)	0.039(4)	0.017(4)	0.001(4)	-0.007(4)
C(25)	0.033(4)	0.055(5)	0.034(4)	0.001(4)	-0.001(3)	-0.010(4)
C(26)	0.037(5)	0.077(6)	0.041(5)	-0.007(4)	-0.008(4)	-0.015(4)
C(27)	0.034(4)	0.089(6)	0.042(5)	-0.017(4)	0.010(4)	-0.032(4)
C(28)	0.037(4)	0.052(5)	0.048(5)	-0.017(4)	0.006(4)	-0.022(4)
C(29)	0.058(6)	0.057(5)	0.065(6)	-0.014(5)	0.014(5)	-0.033(5)
C(30)	0.061(6)	0.055(5)	0.083(7)	-0.011(5)	0.019(5)	-0.039(5)
C(31)	0.050(5)	0.042(5)	0.066(6)	-0.005(4)	0.004(4)	-0.008(4)
C(32)	0.074(7)	0.041(5)	0.096(8)	0.013(5)	-0.006(6)	-0.012(5)
C(33)	0.061(6)	0.056(6)	0.086(7)	0.009(5)	-0.017(5)	0.000(5)
C(34)	0.044(5)	0.055(5)	0.055(5)	0.002(4)	-0.017(4)	0.005(4)
C(35)	0.035(4)	0.037(4)	0.056(5)	-0.002(3)	0.005(4)	-0.019(4)
C(36)	0.023(4)	0.038(4)	0.039(4)	-0.009(3)	0.006(3)	-0.014(3)
C(37)	0.059(5)	0.040(5)	0.053(5)	-0.004(4)	-0.005(4)	-0.009(4)
C(38)	0.082(7)	0.046(5)	0.087(7)	-0.009(5)	-0.002(6)	-0.012(5)
C(39)	0.095(8)	0.046(5)	0.076(7)	0.000(5)	-0.014(6)	0.006(5)

Table 2.9. contd...

Atom	U_{11}	U_{22}	U_{33}	U_{12}	U_{13}	U_{23}
C(40)	0.068(6)	0.060(6)	0.065(6)	-0.003(5)	-0.005(5)	0.000(5)
C(41)	0.127(10)	0.083(8)	0.059(7)	0.018(7)	-0.027(6)	0.007(6)
C(42)	0.151(11)	0.085(8)	0.050(6)	-0.001(7)	-0.035(6)	0.005(6)
C(43)	0.091(7)	0.076(6)	0.044(5)	0.000(5)	-0.002(5)	-0.009(5)
C(44)	0.153(11)	0.092(8)	0.033(5)	-0.011(7)	-0.006(6)	-0.019(5)
C(45)	0.0126(9)	0.070(6)	0.044(5)	0.000(6)	0.006(5)	-0.014(5)
C(46)	0.084(7)	0.058(6)	0.046(5)	-0.008(5)	0.010(5)	-0.006(4)
C(47)	0.056(5)	0.057(5)	0.038(5)	-0.006(4)	-0.002(4)	-0.005(4)
C(48)	0.053(5)	0.047(5)	0.041(5)	-0.009(4)	-0.002(4)	0.001(4)
N(9)	0.066(5)	0.054(5)	0.049(4)	-0.013(4)	-0.008(4)	0.000(3)
O(5)	0.128(6)	0.053(4)	0.104(5)	-0.024(4)	-0.023(4)	-0.020(4)
O(6)	0.055(4)	0.082(5)	0.098(5)	-0.009(4)	0.005(4)	-0.014(4)
O(7)	0.046(4)	0.067(4)	0.098(5)	-0.012(3)	0.002(3)	-0.006(3)
N(10)	0.037(4)	0.080(5)	0.047(4)	0.006(4)	-0.006(3)	-0.013(4)
O(8)	0.049(4)	0.123(6)	0.126(6)	0.028(4)	-0.029(4)	-0.071(5)
O(9)	0.047(4)	0.106(5)	0.073(4)	0.007(3)	-0.026(3)	-0.032(4)
O(10)	0.065(4)	0.078(4)	0.092(5)	0.012(3)	-0.029(3)	-0.044(4)
N(11)	0.099(8)	0.181(12)	0.077(7)	-0.046(8)	-0.026(6)	-0.024(7)
O(11)	0.224(17)	0.320(19)	0.207(15)	-0.071(15)	-0.032(12)	-0.054(13)
O(12)	0.199(14)	0.188(12)	0.284(17)	-0.086(11)	-0.034(12)	0.014(11)
O(13)	0.509(37)	0.459(30)	0.219(18)	-0.198(28)	-0.195(22)	0.142(19)
N(12)	0.576(56)	0.254(30)	0.411(50)	0.228(32)	-0.342(46)	-0.288(35)
O(14)	0.218(19)	0.955(79)	0.502(43)	0.038(32)	-0.129(24)	-0.593(51)
O(15)	0.276(22)	0.474(30)	0.248(18)	-0.074(20)	-0.013(15)	0.192(19)
O(16)	0.627(35)	0.169(12)	0.449(27)	0.113(16)	-0.447(28)	-0.137(14)
O(3W)	0.143(7)	0.113(6)	0.091(5)	-0.007(5)	-0.027(5)	-0.016(4)
O(4W)	0.129(8)	0.072(6)	0.434(20)	-0.040(5)	0.089(10)	-0.021(8)
O(5W)	0.522(90)	0.86(15)	0.70(10)	-0.56(10)	-0.03(11)	0.07(14)

[a] $-2\pi^2(h^2a^{*2}U_{11} + \ldots\ldots + 2hka^*b^*U_{12})$

the observation of formation of MnO_4^- species during oxygen evolution experiments using Mn(III,IV) bipyridyl complexes in $(NH_4)Ce(NO_3)_6$.[172] The only other instance of the use of Ce^{4+} for the preparation of high valent Mn complex is the conversion of anionic Mn(IV) complex of an amide group ligand to the corresponding Mn(V) complex.[183] Ce^{4+} is a one-electron oxidising agent and its potential depends on the anions present.[184] For example in perchloric acid solution the potential for Ce^{4+}/Ce^{3+} is 1.7 V, and it is reduced to 1.4 V in sulphuric acid solution due to the preferential complexing of the Ce^{4+} ion with the sulphate. Ce^{4+} oxidation are done at low pH (< 2.0) and directly lead to the formation of A, B and C starting from Mn(II) salts and ligands. In the case of bpy, acetate bridged (IV,IV) complex A is obtained in the presence of acetate while trinuclear complex C is obtained in the absence of acetate. C has been previously obtained by reacting $Mn_2O_2(bpy)_4^{3+}$ with nitric acid.[132] In the case of phen, both in presence and absence of acetate the trinuclear complex B is obtained. Attempts to do the oxidation using ceric perchlorate was not successful in this case, due to the crystallisation of phenH(ClO_4). It may be noted that the HPO_4^{2-} bridged (IV,IV) complex analogous to A but having $H_2PO_4^-$ instead of water as terminal ligand has been prepared earlier, again starting from $Mn_2O_2(bpy)_4^{3+}$.[125]

Coming to the second point, *viz.* solution chemistry, the picture is complicated by the several disproportionation

equilibria present in aqueous solution. The possible reactions are summarised in Scheme-1, in which the main (or perhaps, the only) role of Ce^{4+} is to maintain an adequate supply of MnL_n^{3+}. The initial species formed by one electron transfer to Ce^{4+} is proposed to be $MnL_2(OH)(H_2O)^{2+}$, where L = bpy or phen. This species has been suggested to be the only one existing in dilute (mM) solution at low pH.[185] Scheme-1 is constructed on the assumption that the entire chemistry in concentrated solution follows from the disproportionation of the hydroxo Mn(III) species, and subsequent aggregation. While the low yields generally obtained for the isolated compounds in the Scheme-1 are consistent with this pathway, the role of electron transfer involving Ce^{4+} as an alternative to step 3 and 9 can not be ruled out. However the involvement of Ce^{4+} in the formation of the Mn(IV,IV) species (step 5) is less likely because, the tendency of Mn(III) species to disproportionate will preclude the formation of the Mn(III,III) species by direct aggregation of the Mn(III) hydroxo species. It may be pointed out that Calvin and co-workers[85] propose that the formation of $L_2Mn_2^{III}O_2^{2+}$ species by dimerisation of $LMn(H_2O)_2^{3+}$ (where L is an N_4-macrocycle) is the first step in assembling the Mn_2O_2 core. They have not considered the disproportionation pathway.

The term "spontaneous self assembly"[85] has often been used to characterise the formation of higher nuclearity Mn compounds. It is probably not appropriate in the present context

$$Mn^{2+}(aq) \xrightarrow[Ce^{4+}]{2L} [MnL_2(H_2O)_2]^{3+} \rightleftharpoons [MnL_2(OH)(H_2O)]^{2+} + H^+ \quad \ldots 1$$

$$[MnL_2(OH)(H_2O)]^{2+} \xrightarrow{2X^-} [MnL_2X_2]^+ \quad \ldots 2$$

(L = phen, X = Cl; Chapt: IV)

$$2[MnL_2(OH)(H_2O)]^{2+} \xrightarrow{H^+} [MnL_2(OH)(H_2O)]^{3+} + [MnL_2(H_2O)_2]^{2+} \quad \ldots 3$$

$$[MnL_2(OH)(H_2O)]^{2+} + [MnL_2(OH)(H_2O)]^{3+} \longrightarrow [Mn_2O_2L_4]^{3+} + 2H^+ + 2H_2O \quad \ldots 4$$

(L = phen, Chapt: V)

$$2[Mn_2O_2L_4]^{3+} \xrightarrow{H^+} [Mn_2O_2L_4]^{4+} + [Mn_2O(OH)L_4]^{3+} \text{ or } [Mn_2(OH)_2L_4]^{4+} \quad \ldots 5$$

$$[Mn_2O_2L_4]^{4+} + OAc^- \xrightarrow{2H_2O} [Mn_2O_2(OAc)(H_2O)_2L_2]^{3+} + 2L \quad \ldots 6$$

(L = bpy: A)

$$[Mn_2O(OH)L_4]^{3+} \text{ or } [Mn_2(OH)_2L_4]^{4+} + 2OAc^- \xrightarrow{H_2O} [Mn_2O(OAc)_2(H_2O)_2L_2]^{2+} \quad \ldots 7$$

(L = bpy; Chapt: III)

$$[Mn_2O_2L_4]^{4+} + [MnL_2(OH)(H_2O)]^{2+} \xrightarrow{2H_2O} [Mn_3O_4L_4(H_2O)_2]^{3+} + 3H^+ + 2L \quad \ldots 8$$

(III, IV, IV)

$$[Mn_3O_4L_4(H_2O)_2]^{3+} + [MnL_2(OH)(H_2O)]^{2+} \xrightarrow{H^+} [Mn_3O_4L_4(H_2O)_2]^{4+} + [MnL_2(OH)(H_2O)]^{2} \quad \ldots 9$$

(L = phen: B; L = bpy: C)

$$[Mn_3O_4L_4(H_2O)_2]^{3+} + OAc^- \xrightarrow[3H^+]{H_2O} [Mn_2O_2(OAc)(H_2O)_2L_2]^{3+} + [MnL_2(OH)(H_2O)]^{2+} \quad \ldots 10$$

SCHEME-1

since the aggregation takes place in concentrated solution and is mainly driven by proton coupled electron transfer reactions. What is intriguing is the crystallisation of only one isomer where several are actually possible (Scheme-2). All the three structurally characterised $Mn_2O_2L_4^{3+/4+}$ complexes (where L is a bidentate ligand)[74,76] have the 'C_2' structure in the crystal lattice (see Scheme-2 for an explanation of the symmetry label). All the known $Mn_2O_2(OAc)L_2A_2^{2+/3+}$ (where A is a monodentate ligand)[97] also have the 'C_2' structure. If one assumes that same isomers prevail in solution, it follows that the $Mn_2O_2(OAc)$ core is formed from the Mn_2O_2 core by the minimum rearrangement of the terminal ligands. However, a more reasonable explanation based on the kinetics of initial formation and the thermodynamics of crystallisation can be given as follows: Since both reactants in step 4 (Scheme-1) are present as racemic mixtures, there will be (nearly) equal probability for the formation of ΛΛ ('C_2'), ΛΔ ('S_2'), ΔΛ ('S_2') and ΔΔ ('C_2'). Centrosymmetric lattices can be formed containing the two 'C_2' or the two 'S_2' molecules. Due to the expected substitutional lablity at the Mn(III) site, any small difference in the stabilities of the two lattices can result in the exclusive crystallisation of the more stable isomer. It appears that the 'C_2' molecules form a more stable lattice than 'S_2' molecules with the present set of ligands.

2.3.2 Structure. The crystal structure of the cation is A shown in

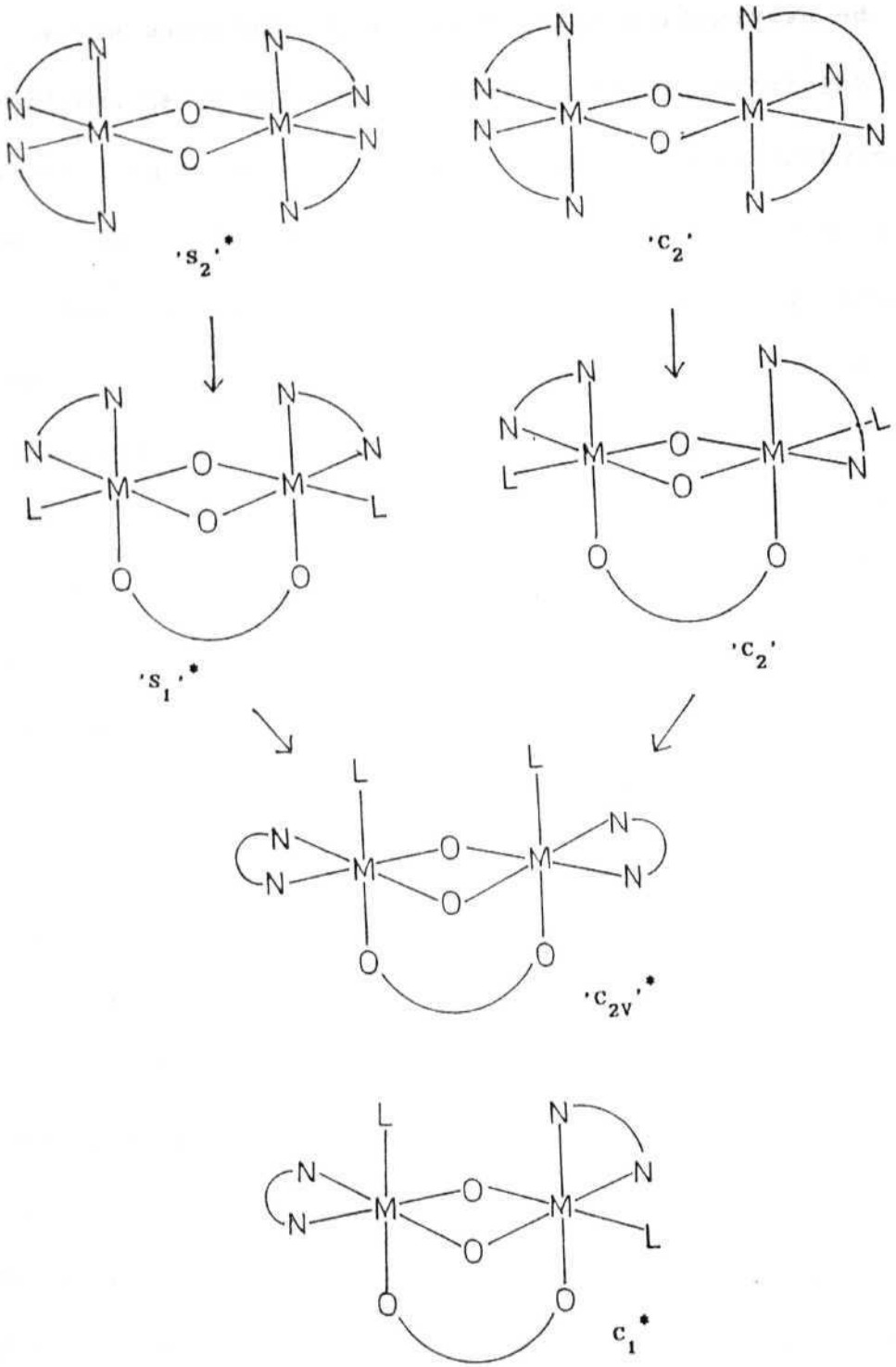

SCHEME-2

The point group symbols given in quotes actually refers to pseudo-symmetry since the two halves of the molecules have unequal metric parameters. Starred structures are not isolated in the solid state.

the Fig. 2.1. It is the third example of the species containing a $[Mn_2(\mu\text{-}O)_2(\mu\text{-}O_2CCH_3)]^{3+}$ core.[103,104] Two other examples (35 and 37) and the one electron reduced core $[Mn_2(\mu\text{-}O)_2(\mu\text{-}O_2CCH_3)]^{2+}$ (33, 34 and 36) have been observed previously.[97,101,102] An important feature of the present complex is that it is the first example with water coordination for this core. The complex molecule defining the asymmetric unit is composed of one binuclear complex cation, three perchlorate anions and one water molecule of crystallisation. The central unit of the complex cation consists of two Mn(IV) centers bridged by the two μ-oxo and one μ-acetato anions. Bond distances and angles are listed in the Table 2.3 and 2.4. The Mn - Mn distance (2.640(1) Å) is lower than the values (2.676(2) - 2.748(2) Å) found for the di(μ-oxo) (IV,IV) dimers,[76,81,83,88,95,98,100] whereas the value is at the higher side compared to the two known complexes (2.591 Å in 35 and 2.580 Å in 37) of the similar core prepared by Armstrong *et al.*[103,104] The average Mn1-L distance is equal to the average Mn2-L distance (1.925 Å), which clearly establish that the two manganese atoms are virtually identical. Similar observations are found for the two other Mn(IV,IV) dimers. On the other hand one electron reduced dimeric species show two distinct manganese centers because of the Jahn-Teller distortion at one of the Manganese ions (Mn^{3+}). $Mn\text{-}O_{oxo}$ bond distance(1.797 Å) in A is comparable to those in other Mn(IV,IV) dimers (1.770-1.819 Å). Equatorial Mn-N distances (2.042 Å) are longer than the axial Mn-N distance (2.001 Å) and a

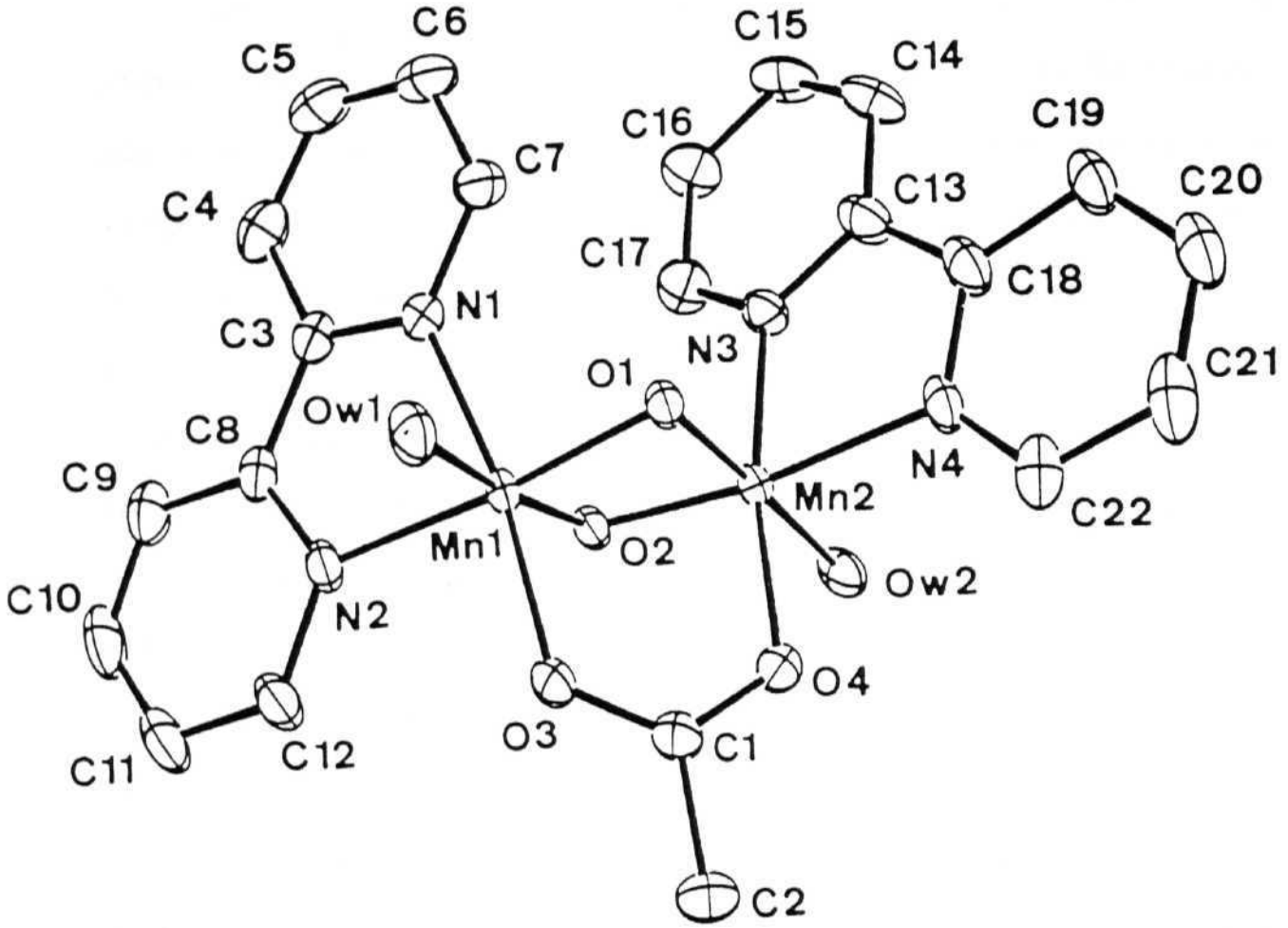

Fig 2.1. ORTEP view of the cation A.

similar observation is found for most of the (IV,IV) dimers, reflecting the trans influence of the bridged oxygen atoms on the equatorial nitrogen atoms. Two Mn-O (water) distances (1.982 Å and 1.985 Å) are within the bonding distance and are fully protonated. Due to the presence of acetate bridge, the four membered Mn_2O_2 ring is not planar (dihedral angle between Mn(1)O(1)O(2) and Mn(2)O(1)O(2) least square planes is 161.7^{o} and a similar value 161.3^{o} is observed for $[MnO(OAc)(tpen)]^{3+}$.[103] On the other hand di-μ-oxo dimeric complexes show planar geometry. This clearly indicates that the presence of acetate distorts the Mn_2O_2 plane. Deviation of manganese atoms from their least-square coordination planes are less than 0.046 Å.

The perchlorate anions containing Cl(1) and Cl(2) are not disordered and exhibit usual bond lengths and angles. On the other hand, a statistical disorder affords two types of perchlorate anions equally distributed among the Cl(3), O(13), O(14), O(15), O(16) and Cl(3), O(13), O(14'), O(15'), O(16') positions. The crystallisation water molecules, the three perchlorate anions and the two manganese coordinated water molecules participate in a three dimensional hydrogen bonding network (Fig. 2.2) including the following six contacts: Ow1 - H1(Ow1) .. Ow3i, Ow1 - H2(Ow1) .. O6, Ow2 - H1(Ow2) .. O5ii, Ow2 - H2(Ow2) .. O14 (or Ow2 - H2(Ow2) .. O14', Ow3 - H2(Ow3) .. O9, and Ow3 - H1(Ow3) .. O15 (or Ow3 - H1(Ow3) .. O15').

The structure of B (Fig. 2.3) is made up of a trinuclear

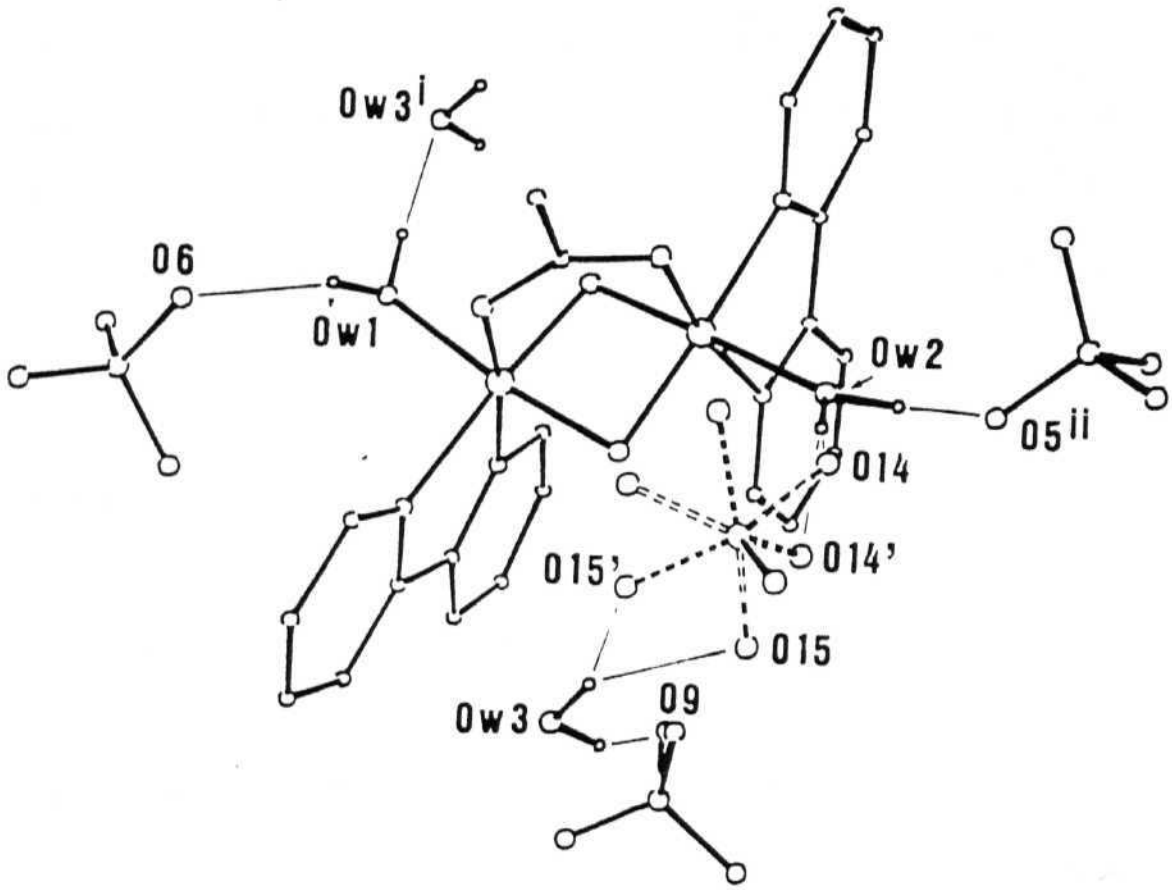

Fig 2.2. Molecular structure of A showing the three dimensional hydrogen bonding.

cation, $[Mn_3O_4(OH_2)_2(phen)_4]^{4+}$ with nitrate as a counter ion. The Mn atoms of the cation occupy the corners of an isosceles triangle. Two single oxo-bridges relate Mn1 to Mn2 and Mn3, while Mn2 and Mn3 are linked by a double oxo-bridge. Two Mn-Mn distances are observed at 2.675 Å and 3.249 Å. Mn2-Mn3 separation of 2.675 Å is characteristic of a $(\mu\text{-O})_2Mn_2$ group. The other Mn-Mn separation for Mn1-Mn2 and Mn1-Mn3 are at equal distances (3.249 Å) and are bridged by single μ_2-oxo groups. The two Mn-Mn distances are in good agreement with the values observed for PS-II by EXAFS studies.[53,54] Further the structural parameters of our complex are close to the values observed for the bpy analog (55) prepared by Sarenski[132] and its substituted Cl^- complex (54) of Girerd.[131] On the other hand, these values are lower compared (3.141 and 3.686 Å) with the complex (57) prepared by Mikuriya.[133] This may be attributed to the Jahn-Teller distortion observed at the d^4 site in the latter complex which has all the metal ions with Mn(III) oxidation state. The single bridge O1 and O2 are in the plane (Mn(1), Mn(2) and Mn(3)) of the triangle, (similar observation is made in two other examples 54 and 55, while 56 shows a deviation of one of the manganese atoms from the plane, Fig. 2.4) while the double bridge O3 and O4 atoms form a segment perpendicular to it. The Oh coordination around manganese is completed by four phen N-atoms for Mn1 and by two phen N-atoms and one H_2O molecule for Mn2 and Mn3. Average Mn-N and $Mn\text{-}O_{oxo}$ distances (2.065 Å and 1.798 Å) and oxidation state analysis demonstrate that the cluster

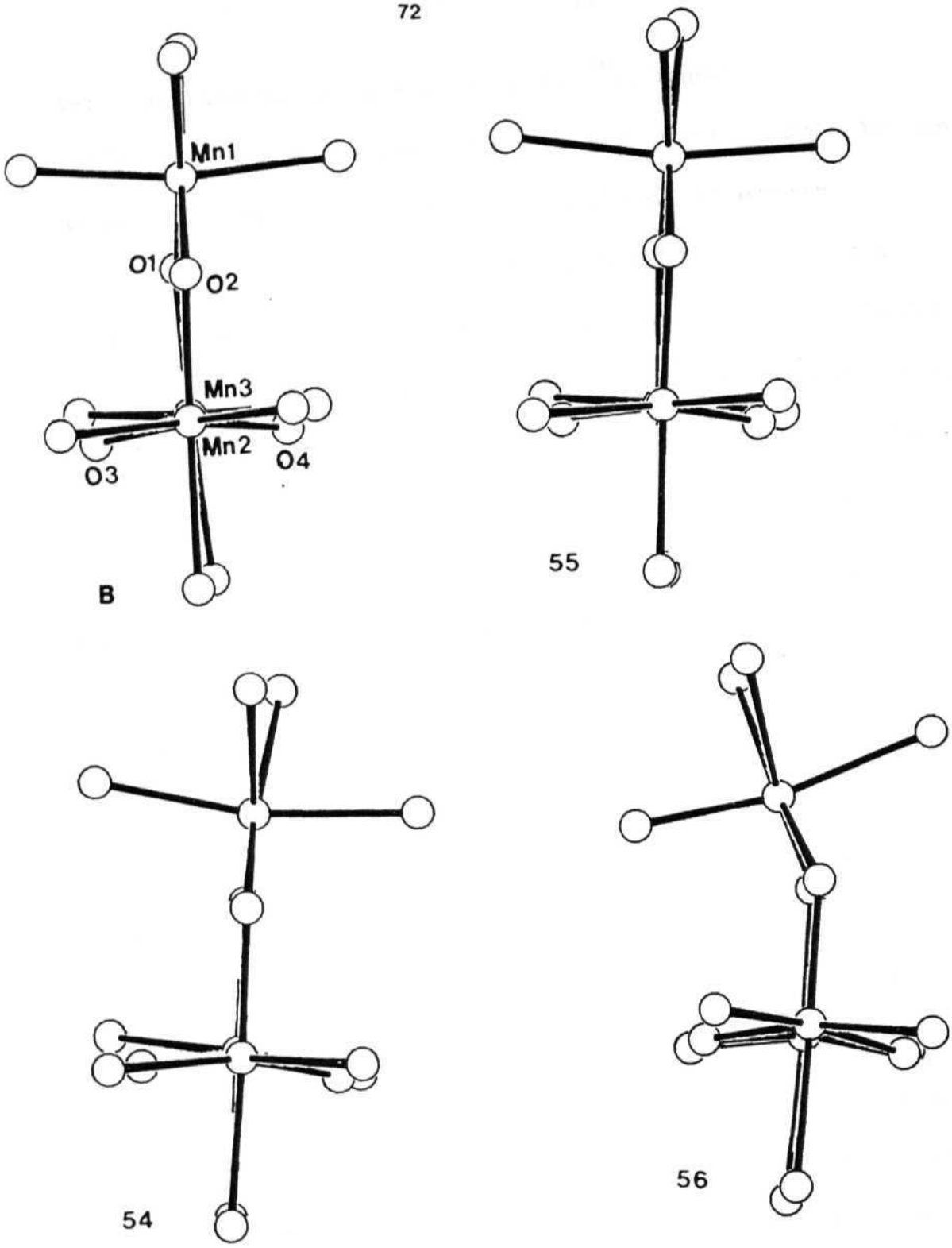

Fig 2.4. Side view of the $[Mn_3O_4]$ units along Mn1,Mn2,Mn3 plane (atoms directly coordinated to manganese are shown)

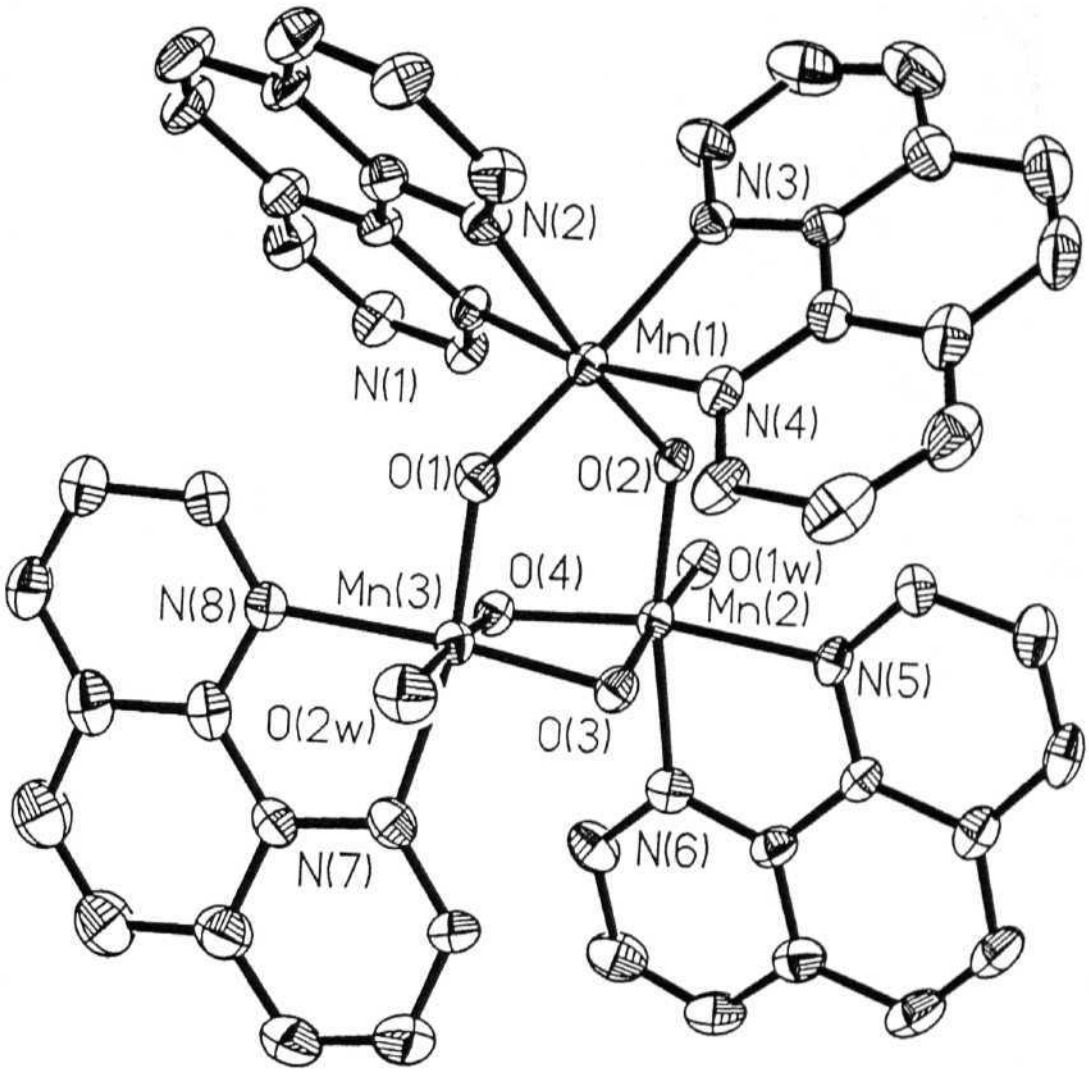

Fig 2.3. ORTEP view of the cation B.

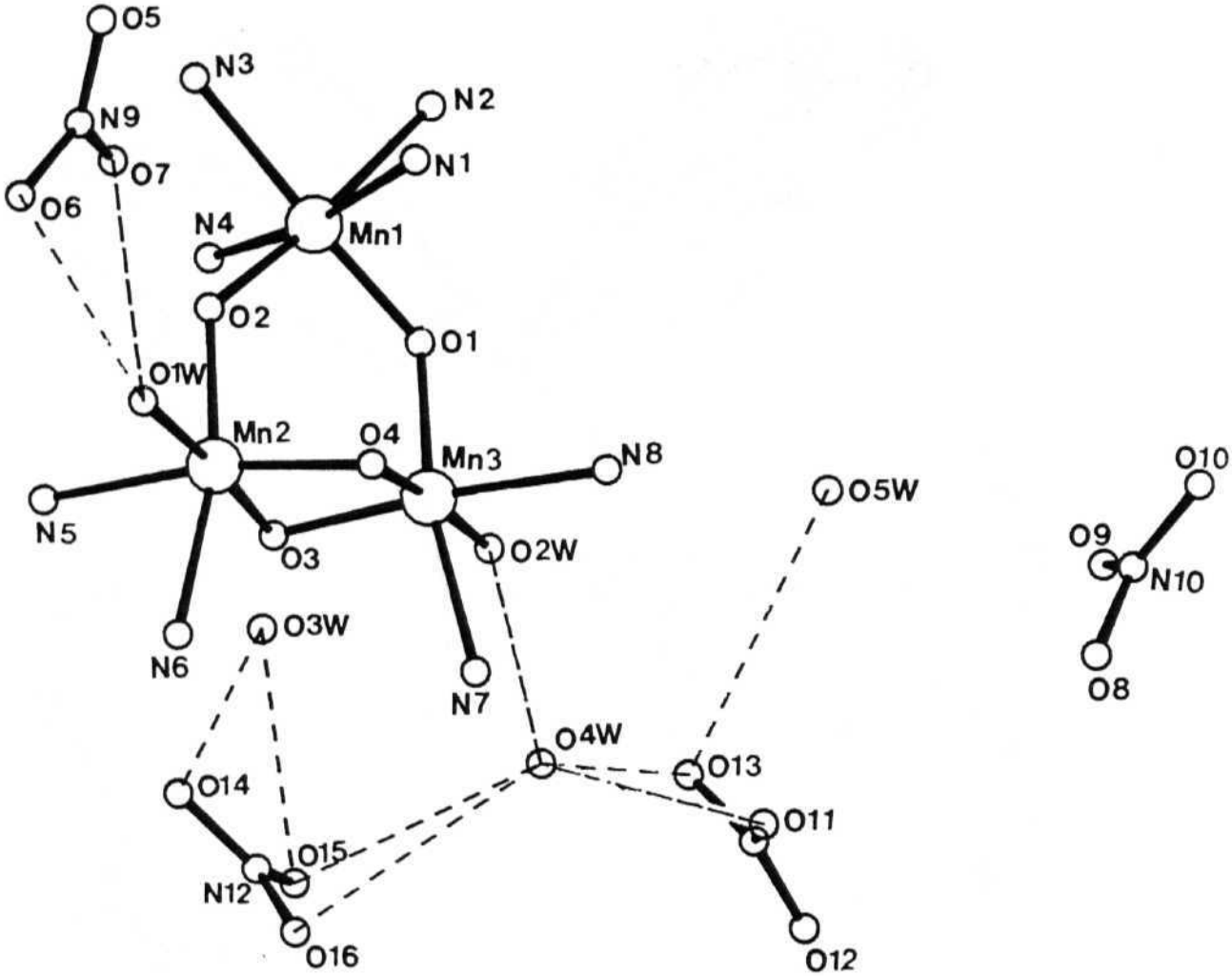

Fig 2.5. Hydrogen bonding net work in B. (ring carbon atoms are excluded)

contains three Mn(IV) ions. Apart from the bpy complex (55) This is the second example to contain water in the coordination sphere of Mn(IV) dimer. The state of protonation is clear from the long (2.01 Å) Mn-OH_2 bond lengths. Lattice water molecules and anions (NO_3^-) are stabilised by hydrogen bonding, which are participating with the coordinated water molecules (Fig. 2.5). Strong hydrogen bondings (<3.0 Å) are observed between O1w...O7 (2.641 Å), O2w...O4w (2.524 Å) and O4w...O11 (2.765 Å). Whereas other hydrogen bondings are relatively weaker (3 to 3.5 Å), this hydrogen bonding network is continued to other symmetry related molecule *via* O5w, which is at a special position.

2.3.4 Infrared Spectra. Asymmetric and symmetric vibrations of carboxylate O-C-O group were located at 1580 and 1395 cm^{-1} respectively for A. These values are comparable to the values reported earlier for $[Mn_2O_2(OAc)]^{2+/3+}$ core. IR spectra can be used to distinguish A and C. Compound C does not show any band at 1395 whereas a very weak signal appeared at 1580 cm^{-1} (which may be from bpy). Presence of these bands can not be seen in B because of the overlap of nitrate bands in this region. There is also a diffence between the spectra in the Mn-O_{oxo} stretching region which are characteristic of $[Mn_2O_2]$ core. A strong broad band at 1100 cm^{-1} for A and C, and a band at around 1380 cm^{-1} for B are observed for perchlorate and nitrate respectively.

2.3.5 Solution Chemistry. The Mn (IV, IV) complex (A) is sparingly soluble in water. Dilute aqueous solutions are deep brown in colour and are fairly stable. It also dissolves readily in solvents such as DMF, CH_3CN and picolenes to afford brown solutions. These solutions however decolorise slowly depositing brown solids, probably MnO_2 (solvate). The electronic spectrum of the aqueous solution shows a broad shoulder at 490 nm. In DMF, CH_3CN and acetate buffer (pH = 4.5) a band was observed at 610 nm and a very weak absorption at nearly 750 nm (Fig. 2.6). Bands at 640, 530 and 417 nm reported for (IV,IV) complexes are and assigned to the Mn^{4+} center and specifically to charge transfer transitions from the oxo-group to the metal $d\pi^*$ orbital. When the complex is dissolved in bpy/bpyHNO$_3$ buffer (pH 4.5), the spectrum gradually changes to that of the mixed valent $[Mn_2(O)_2(bpy)_4]^{3+}$. Based on the extinction coefficient (ε) of the intervalence absorption band, (IVTA) it is clear that nearly 80 % of the Mn is present as the Mn (III, IV) complex (Fig. 2.7).

The Mn(IV,IV,IV) complex B, is soluble in highly polar solvents, like H_2O, DMF and DMSO and is insoluble in less polar solvents like DCM, $CHCl_3$ and CH_3CN. Solutions are deep-brown in colour and are not stable for a long time, depositing brown precipitate. Electronic spectra in water (Fig. 2.8) and acetate buffer (pH 4.5) show a broad band at 610 nm (Fig. 2.9(a)). Buffer solution of this complex in presence of excess phen ligand shows the disappearance of 610 nm band, and slowly generates the

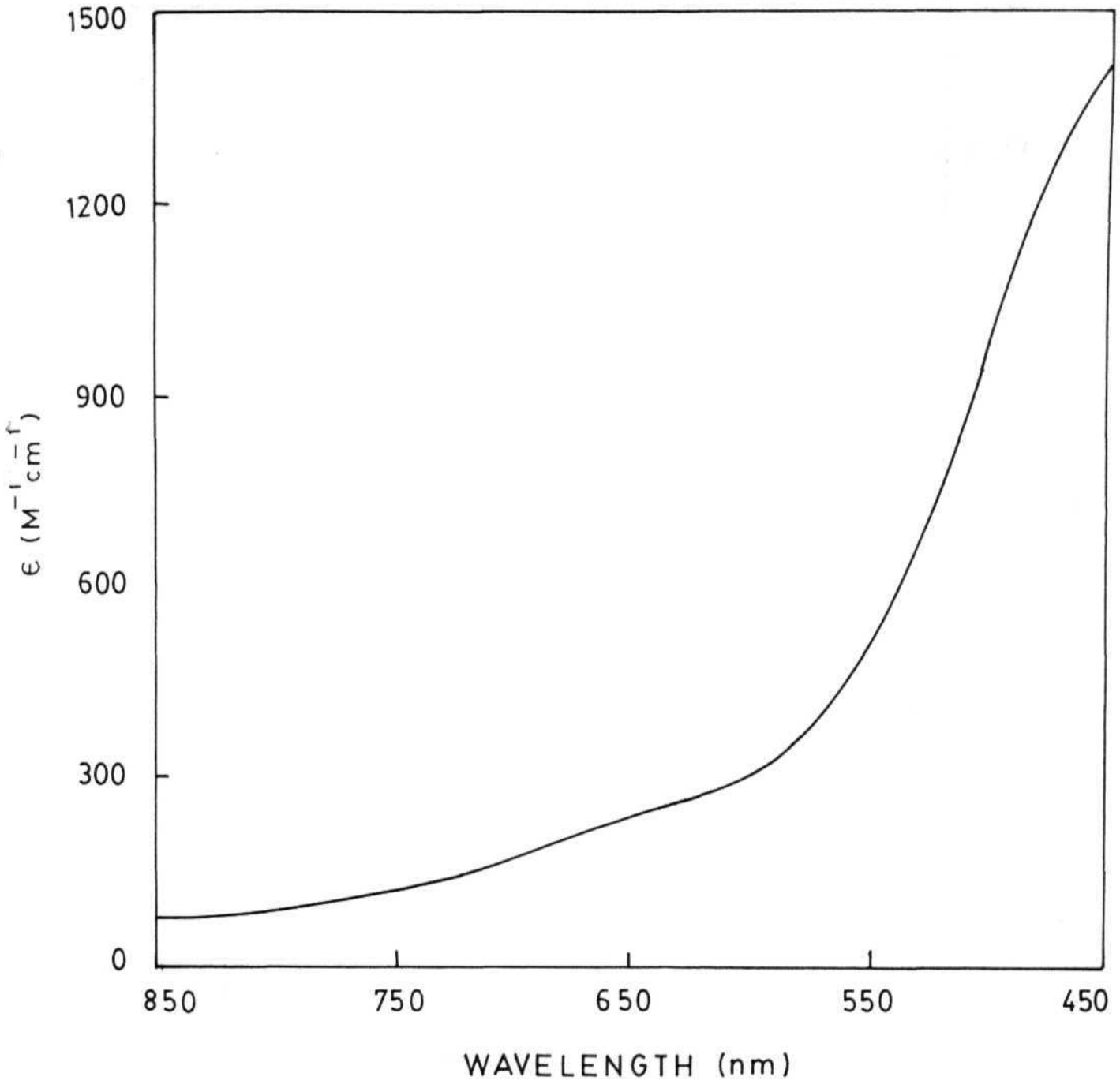

Fig 2.6(a). Electronic spectrum of A in CH_3CN.

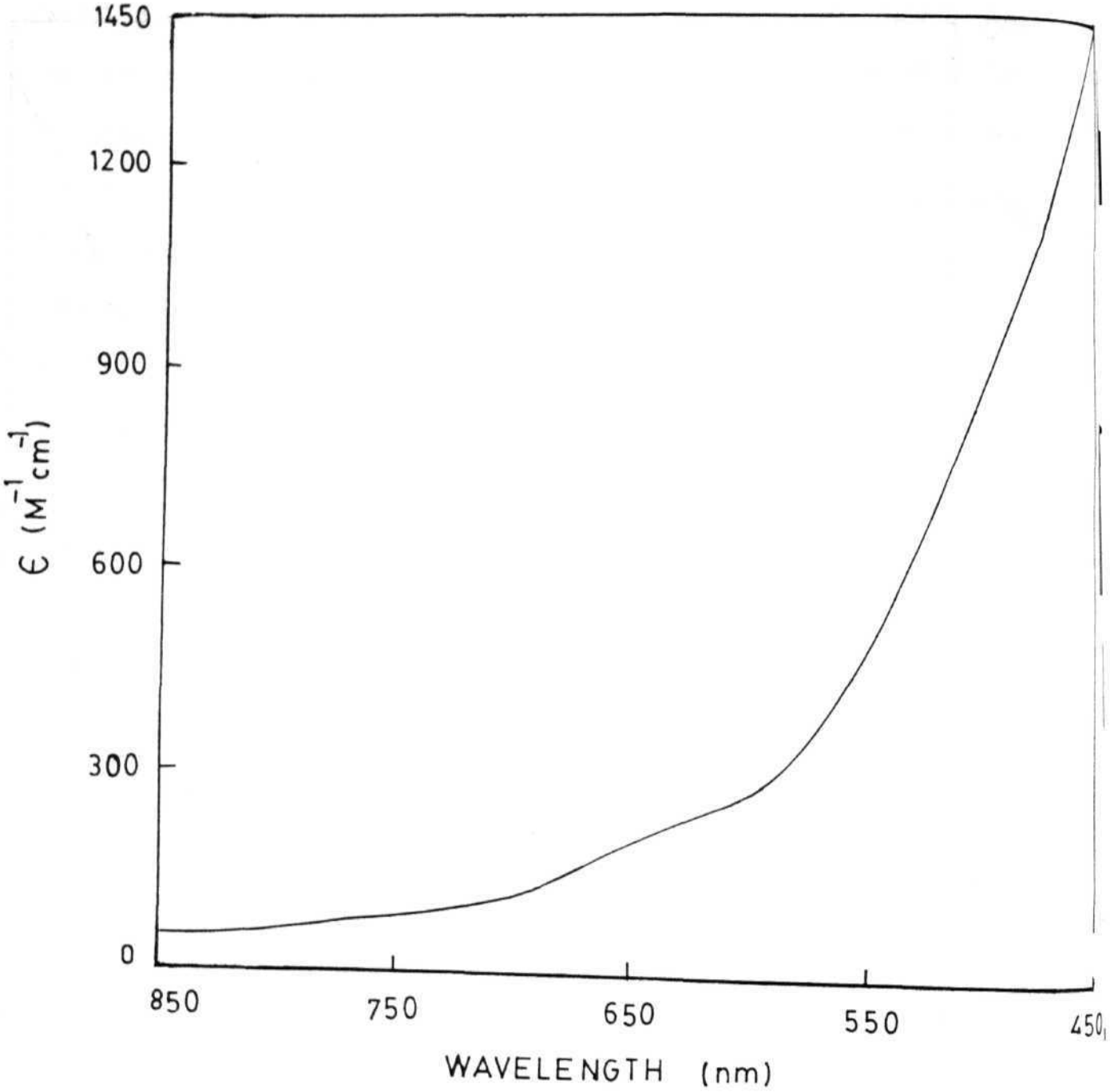

Fig 2.6(b). Electronic spectrum of A in acetate buffer pH = 4.5.

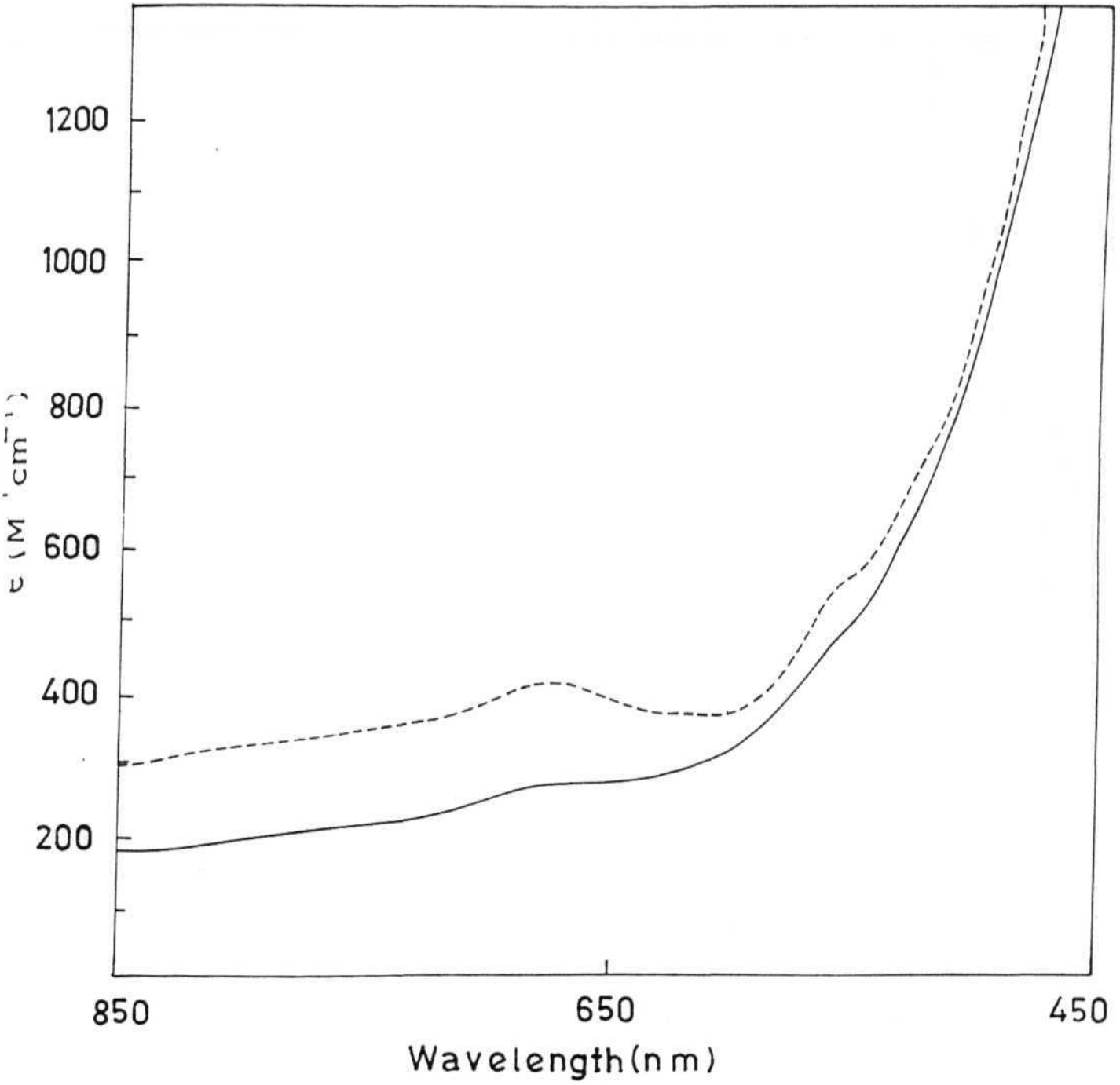

Fig 2.7. Electronic spectrum of A in ligand buffer at pH = 4.5

(——— : freshly prepared solution; -----: after 72 hours).

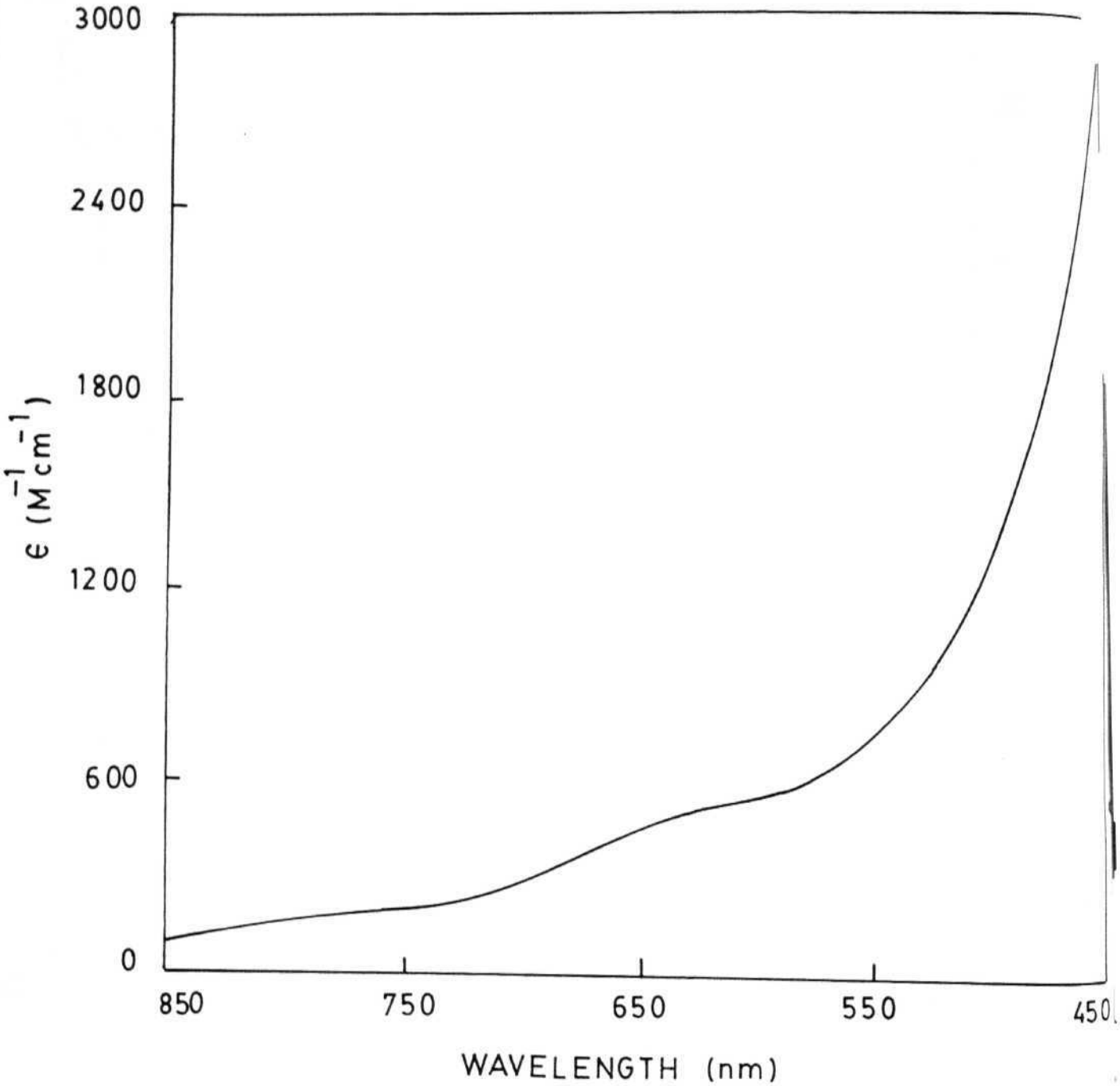

Fig 2.8. Electronic spectrum of B in water.

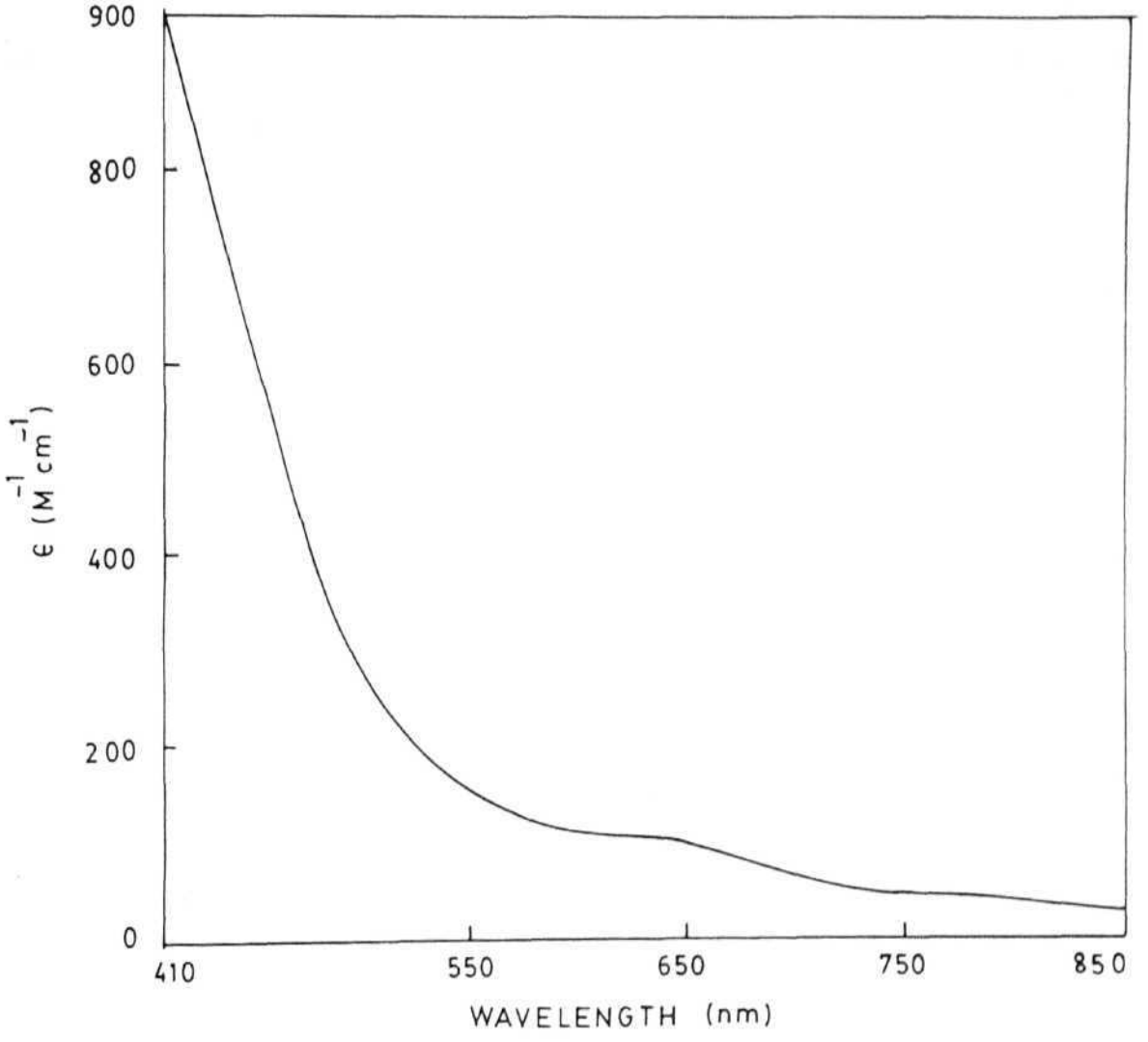

Fig 2.9(a). Electronic spectrum of B in acetate buffer.(pH = 4.5)

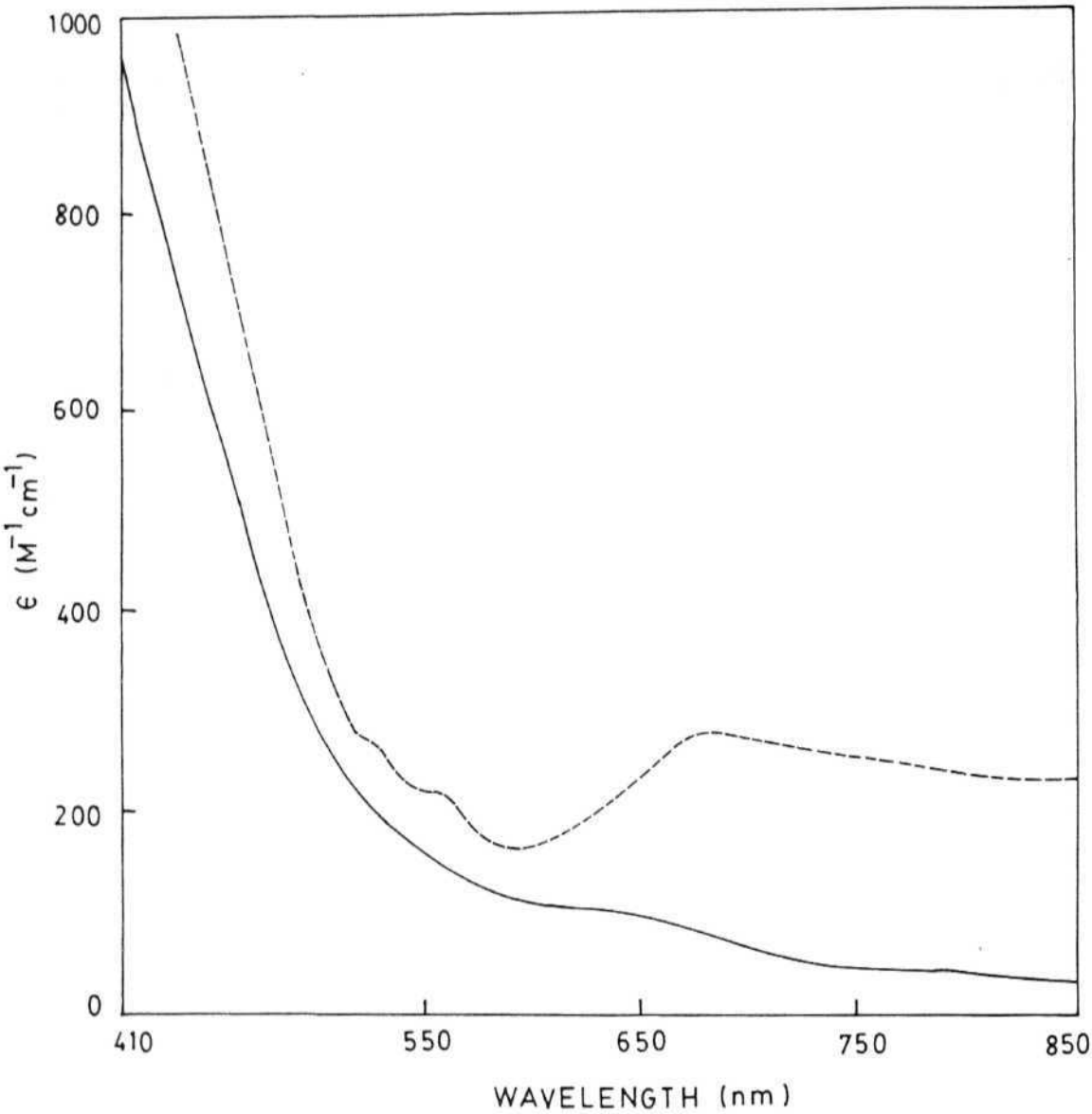

Fig 2.9(b). Electronic spectrum of B in ligand buffer at pH = 4.5

(——— : initial, -----: after 68 hours).

(III,IV) bands (Fig. 2.9(b)) similar to the reported $[Mn_2O_2(phen)_4]^{3+}$ complex.

2.3.6 EPR and Magnetic properties. X-band powder EPR spectrum of A at room temperature exhibits a strong $g \cong 2$ centered resonance with an ill-defined six-line resonance structure. On lowering the temperature, the main $g \cong 2$ resonance broadens and additional low field lines appears (Fig. 2.10). Single crystal spectra clearly show the ^{55}Mn hyperfine splitting at 300K for a randomly oriented sample at $g \cong 2$ with weak signals at lower fields. At lower temperature (120 K) hyperfine resolution reduces due to overlap with additional lines which appear at lower and higher fields (Fig. 2.11).

The energy level scheme along with Boltzman factors for the spin states are as follows:

$$(J = -45\ cm^{-1},\ \mathcal{H} = -2JS_1S_2,\ S_1 = S_2 = 3/2)$$

		Energy (cm^{-1})	Boltzman factors 300 K	120 K
12J	S = 3	540	0.11	0.00
6J	S = 2	270	0.28	0.09
2J	S = 1	90	0.40	0.46
0	S = 0	0	0.20	0.45

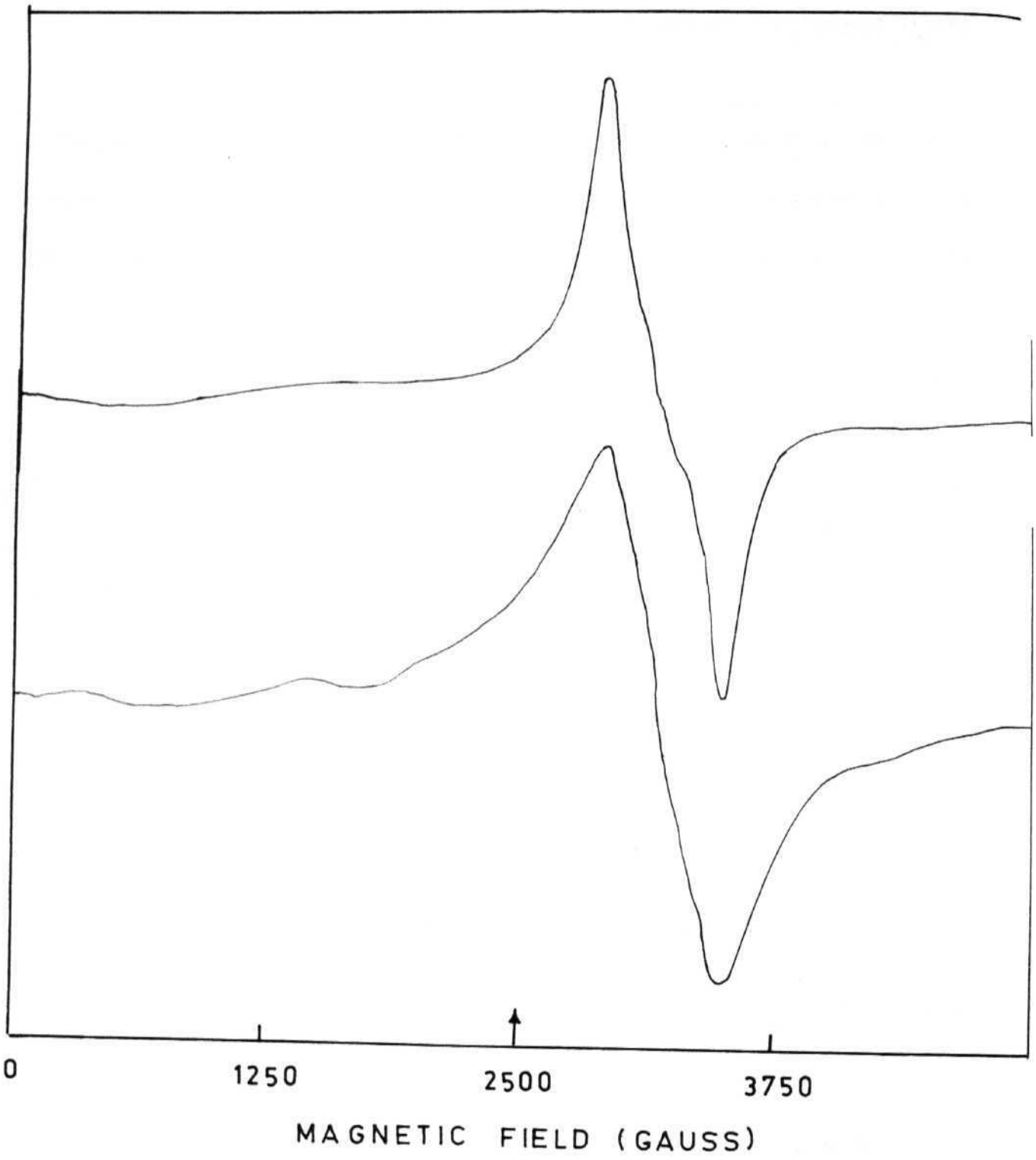

Fig 2.10. Powder EPR spectra of A (a) at 298 K, ν = 9.218 GHz (b) at 150 K, ν = 9.215 GHz.

This means that at 120 K the triplet is the only paramagnetic state with appreciable population. The EPR spectrum is complicated by the presence of a sextet at $g \cong 2$, while a 11 line pattern with half the spacing is expected for an exchange coupled dinuclear complex. A tentative interpretation is as follows: The six line pattern arises from mononuclear (Mn^{4+} or Mn^{2+}) impurity, while the 120 K spectrum is a superposition of the middle sextet and the $\Delta M_s = \pm 1$ transition of the triplet state of the two magnetically in equivalent dinuclear complexes in the crystal unit cell. The loss of resolution in the middle sextet at low temperature is due to its overlap with the broad signal from the triplet state molecules. More detailed measurements, preferably at Q-band and using monomer free crystal will be needed to extract the spin Hamiltonian parameters of the dimer.

The glass EPR spectrum of the freshly prepared DMF solution (Fig. 2.12(a)) clearly shows the formation of the Mn(III,IV) and Mn(II) species. On the other hand freshly prepared frozen spectrum in CH_3CN shows the Mn(II) signals without any Mn(III,IV) formation. The solutions are unstable and decompose slowly and give six-line pattern of Mn(II) after some time. The solution reactions are therefore quite complex. It appears that solvent molecules are able to displace the coordinated H_2O or the bridging acetate and the resulting substituted complex decomposes gradually to MnO_2, Mn(III,IV) and Mn(II) species oxidising water

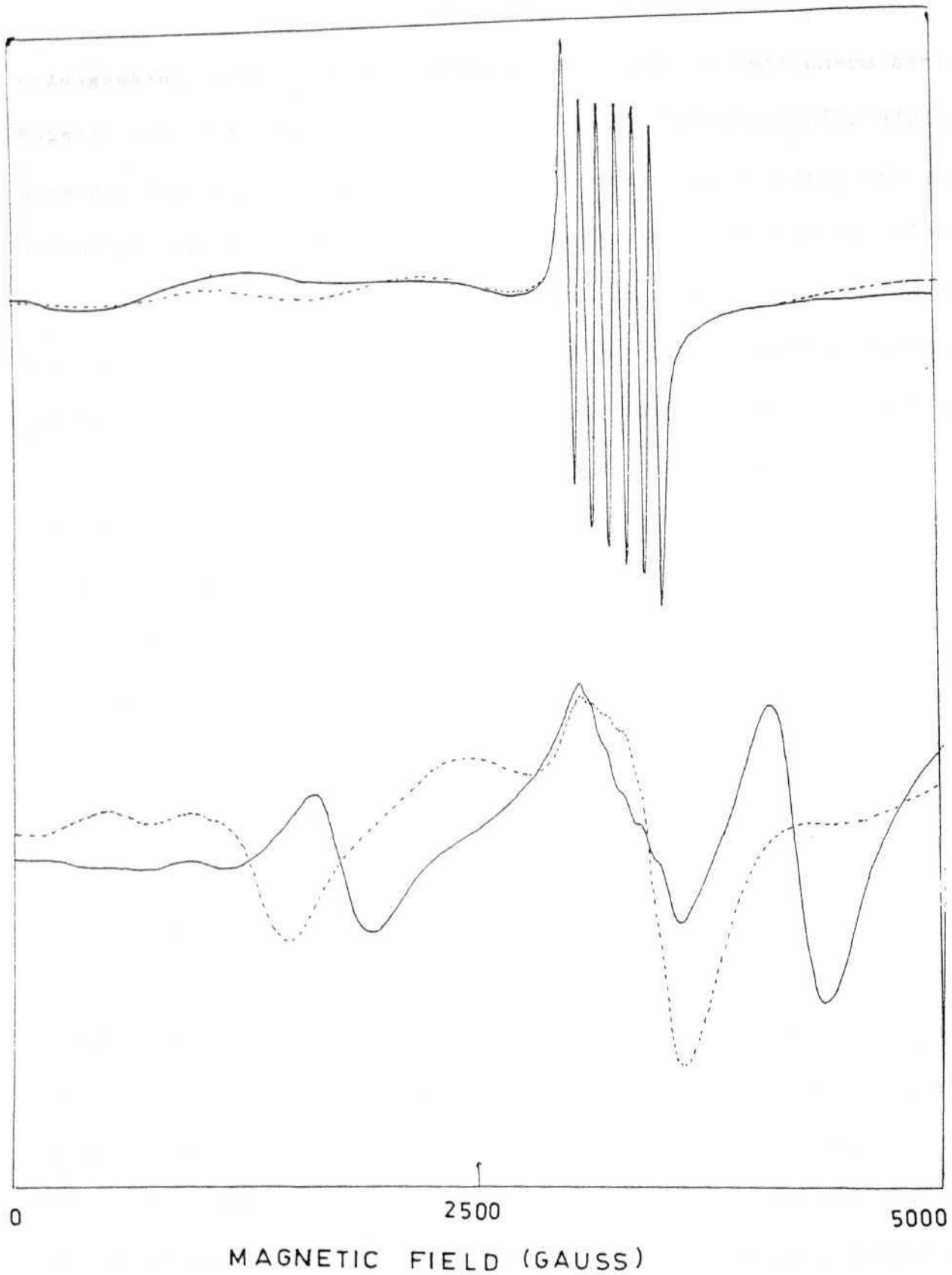

Fig 2.11. Single crystal EPR spectra of A at random orientations (a) at 298 K, ν = 9.223 GHz (b) at 120 K, ν = 9.234 GHz.

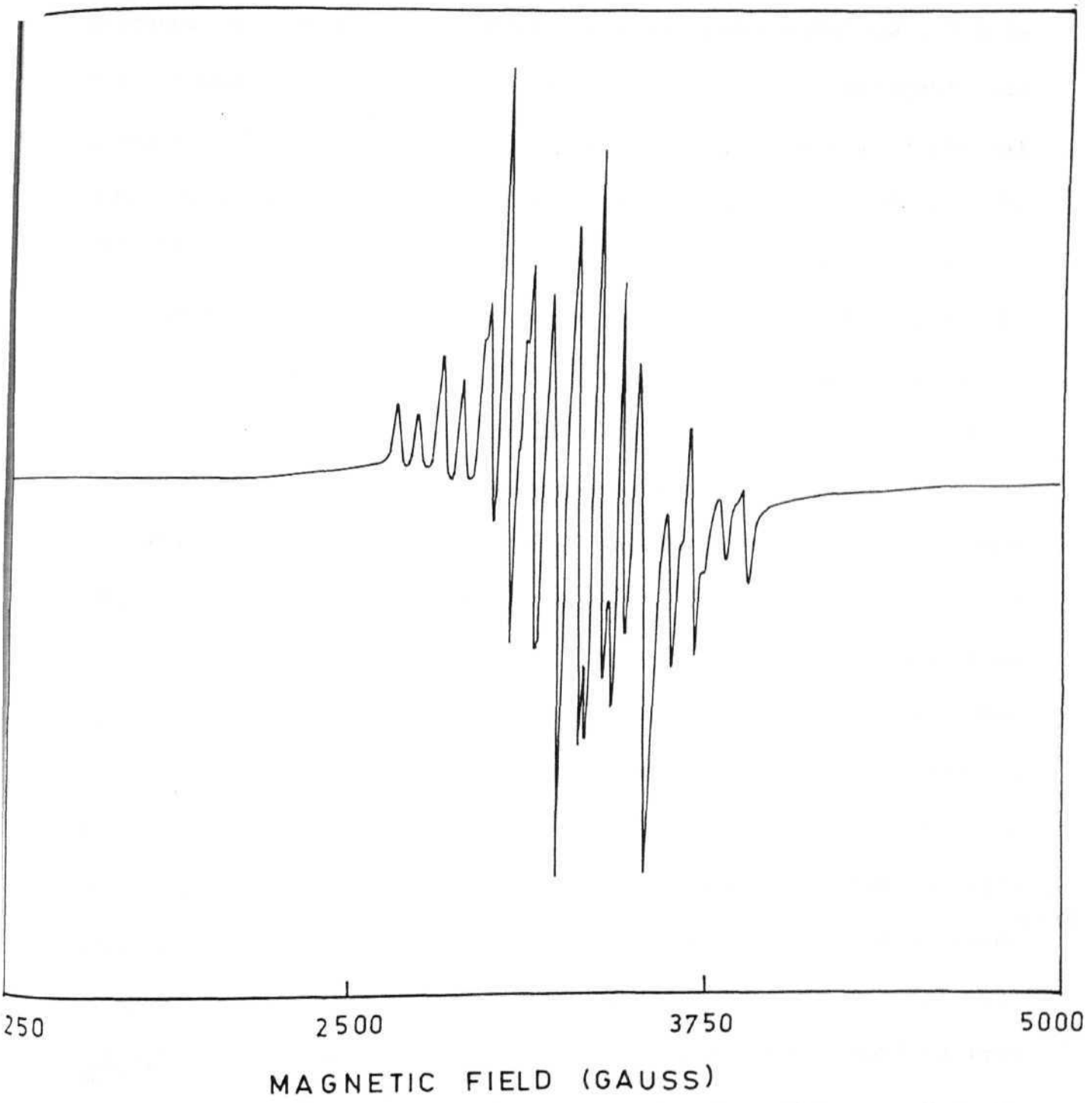

Fig 2.12(a). Frozen EPR spectrum of A in DMF at 163 K. (ν = 9.207 GHz)

or solvent.

Powder EPR spectrum of B at 300 K shows a strong signal at $g \cong 2$ and additional low-field lines were observed on lowering the temperature (Fig. 2.13). DMF glass spectrum shows the formation of small amount of (III,IV) along with Mn(II) signals (Fig. 2.12(b)). In water-glycerol mixture compound B does not show 35-line spectra as reported for the bipyridine complex.[131,132] This may be because of change in the ground state as expected in the case of $[Mn_3O_4(bpea)_3(OH)]^{3+}$ (56) or the temperature is too high to isolate the ground spin state.

The temperature dependence of the magnetic susceptibility and effective magnetic moment per manganese of the Mn(IV,IV) complex A are shown in the Fig. 2.14. μ_{eff}/Mn decreases from 3.51 BM at 300 K to 0.92 BM at 10 K, indicating an antiferromagnetic coupling of the S = 3/2 spin system of the two Mn(IV) ions. However, the 3.51 (BM) room temperature values, close to the S = 3/2 spin-only value (3.87) clearly indicate that the antifferomagnetic interactions operating in this compound are lower than that measured for other binuclear Mn(IV,IV) complexes (see Table 2.10). The data were fitted by employing the expression derived from the isotropic spin-exchange Hamiltonian $H = -2JS_1S_2$ ($S_1 = S_2 = 3/2$) and the Van Vleck equation.[186] Least-squre refinement afforded an excellent fit with $J = -44.6$ cm^{-1}, par = 0.58%, TIP = 3.6×10^{-6} and $g = 1.976$, where par is the mole percent of the paramagnetic impurity assumed to be a Mn(III)

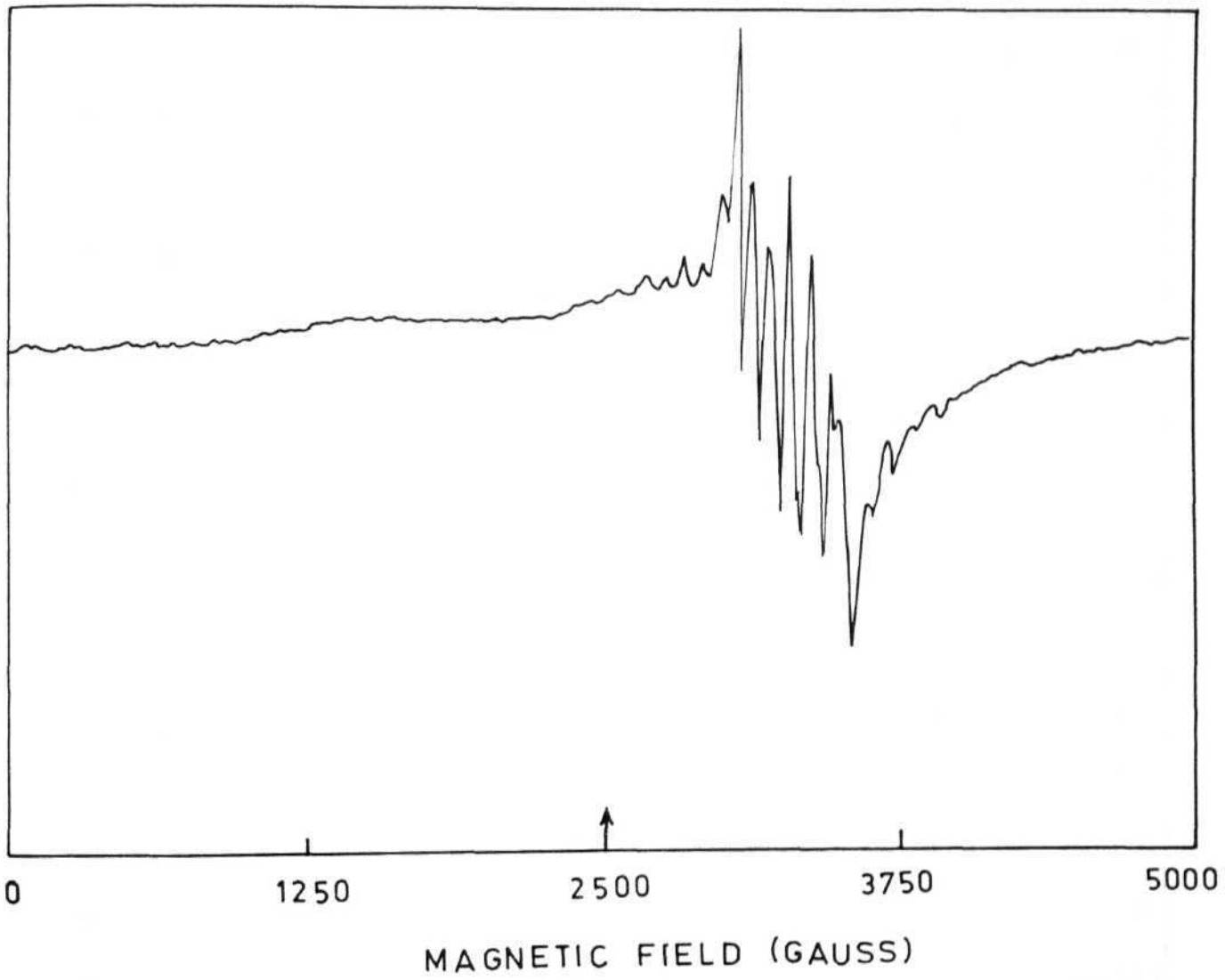

Fig 2.12(b). Frozen EPR spectrum of B in DMF at 153 K. (ν = 9.212 GHz)

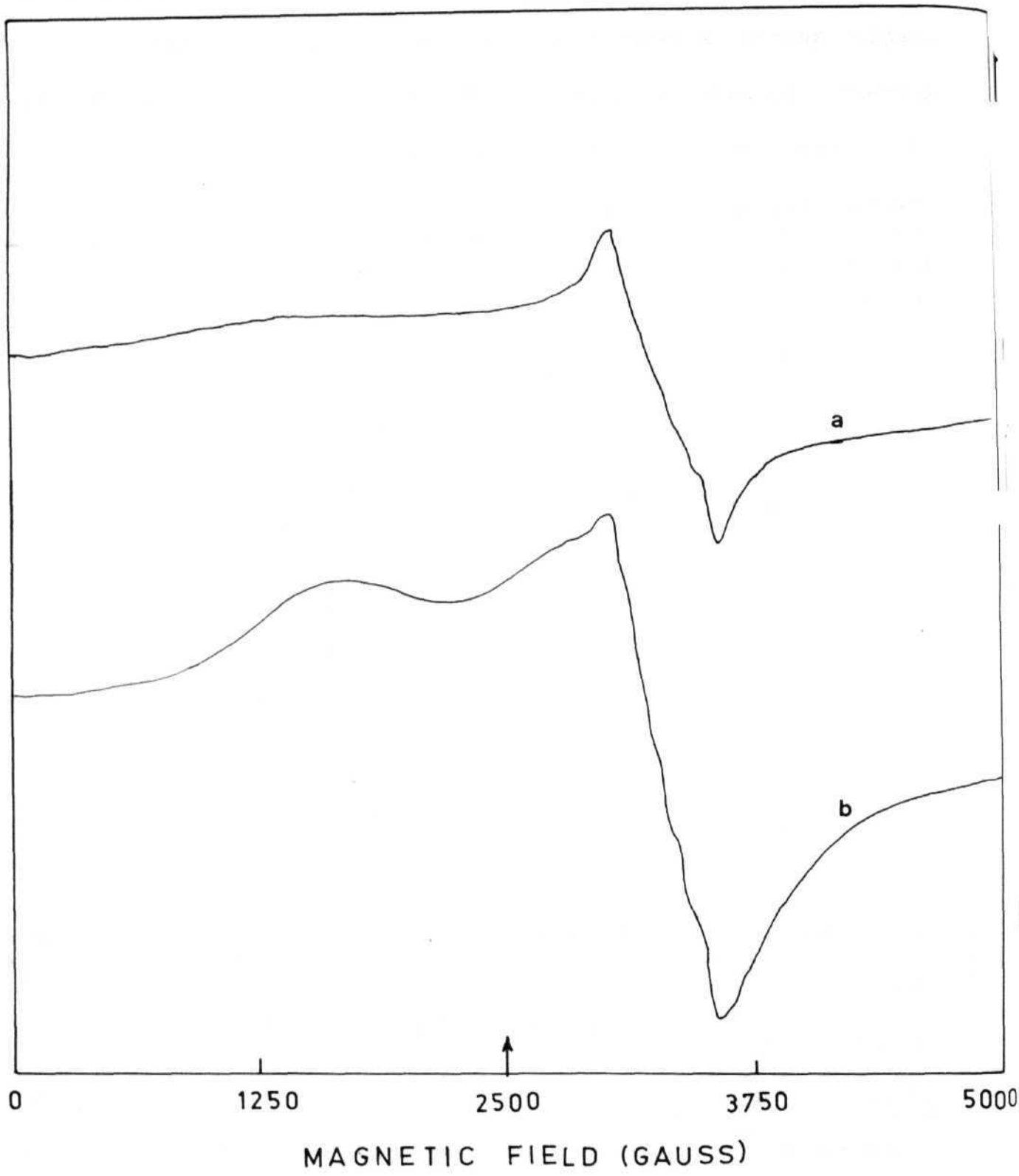

Fig 2.13. Powder EPR spectra of B (a) at 298 K, ν = 9.228 GHz (b) at 147 K, ν = 9.230 GHz.

monomer and TIP is the temperature independent paramagnetism. This result confirms that the present complex has the smallest‡ antiferromagnetic interaction determined for the (IV,IV) complexes. Magnetic interactions and structural parameters for $Mn^{IV}(\mu\text{-}O)_2Mn^{IV}$ dimers are given in the Table 2.10.

Recently, it was reported[104] that exchange integral J for the structurally characterized species containing $Mn^{IV}(\mu\text{-}O)_2Mn^{IV}$ core does not correlate with $Mn\text{-}O_{oxo}$ and / or Mn-Mn distances and / or Mn-O-Mn angles and this additional example seems to confirm the lack of correlation (Table 2.10) between J and structural parameters, which are supposed to better reflect the direct $d_{xy}\text{-}d_{xy}$ orbital overlap (x and y axes coincident with the $Mn\text{-}O_{oxo}$ bonds).

Low J value for the present complex A is probably related to the deviation of the $Mn_2(\mu\text{-}O)_2$ ring from planarity. Di-μ-oxo complexes show dihedral angle (α) of 180° between μ-O(1)Mn(1)-μ-O(2) and μ-O(1)Mn(2)-μ-O(2) reflecting the perfect planarity. Presence of additional bridging unit (μ-OAc) or μ-HPO_4 deviates α from 180° thereby effecting the direct $d_{xy}\text{-}d_{xy}$ orbital overlap. Compounds with $\alpha = 180^o$ shows higher J values compared

---

‡ Magnetic studies on $[Mn_2O_2(HPO_4)(bpy)_2(H_2PO_4)_2]$[125] has been reported very recently,[203] and it shows the lowest J ($-39.5\ cm^{-1}$).

Table 2.10. Selected structural and magnetic properties for Mn(IV,IV) dimers.

compound		Mn-O$_{oxo}$ (Å)	Mn..Mn (Å)	Mn-O-Mn (deg)	α(°)	J(cm^{-1})	g	ref.
$[Mn_2O_2(phen)_2]^{4+}$	(3)	1.801	2.748	99.5	180.0	-144.0	1.96	76
$[Mn_2O_2(pic)_2]$	(28)	1.813	2.747	98.1	180.0	-86.5	1.83	98
$[Mn_2O_2(bispicen)_2]^{4+}$	(5)	1.811	2.676	95.2	180.0	-122.5	1.95	81
$[Mn_2O_2(dmepa)_2]^{4+}$	(10)	1.780	2.750	101.5	180.0	-131.0	-	83
$[Mn_2O_2(bispictn)_2]^{4+}$	(30)	1.803	2.719	97.8	180.0	-105.5	1.83	100
$[Mn_2O_2(salpn)_2]^{4+}$	(16)	1.819	2.728	97.2	180.0	-82.0	1.79	88
$[Mn_2O_2(HPO_4)(bpy)_2(H_2PO_4)_2]$		1.810	2.702	96.5	164.5	-39.5	1.89	125, 203
$[Mn_2O_2(OAc)(tpen)]^{3+}$	(35)	1.798	2.591	92.2	161.3	-	-	103
$[Mn_2O_2(OAc)(bpea)]^{3+}$	(37)	1.799	2.580	91.6	164.8	-124.0	2.29	104
$[Mn_2O_2(OAc)(bpy)_2(H_2O)_2]^{3+}$		1.797	2.640	94.5	161.7	-44.6	1.98	this work

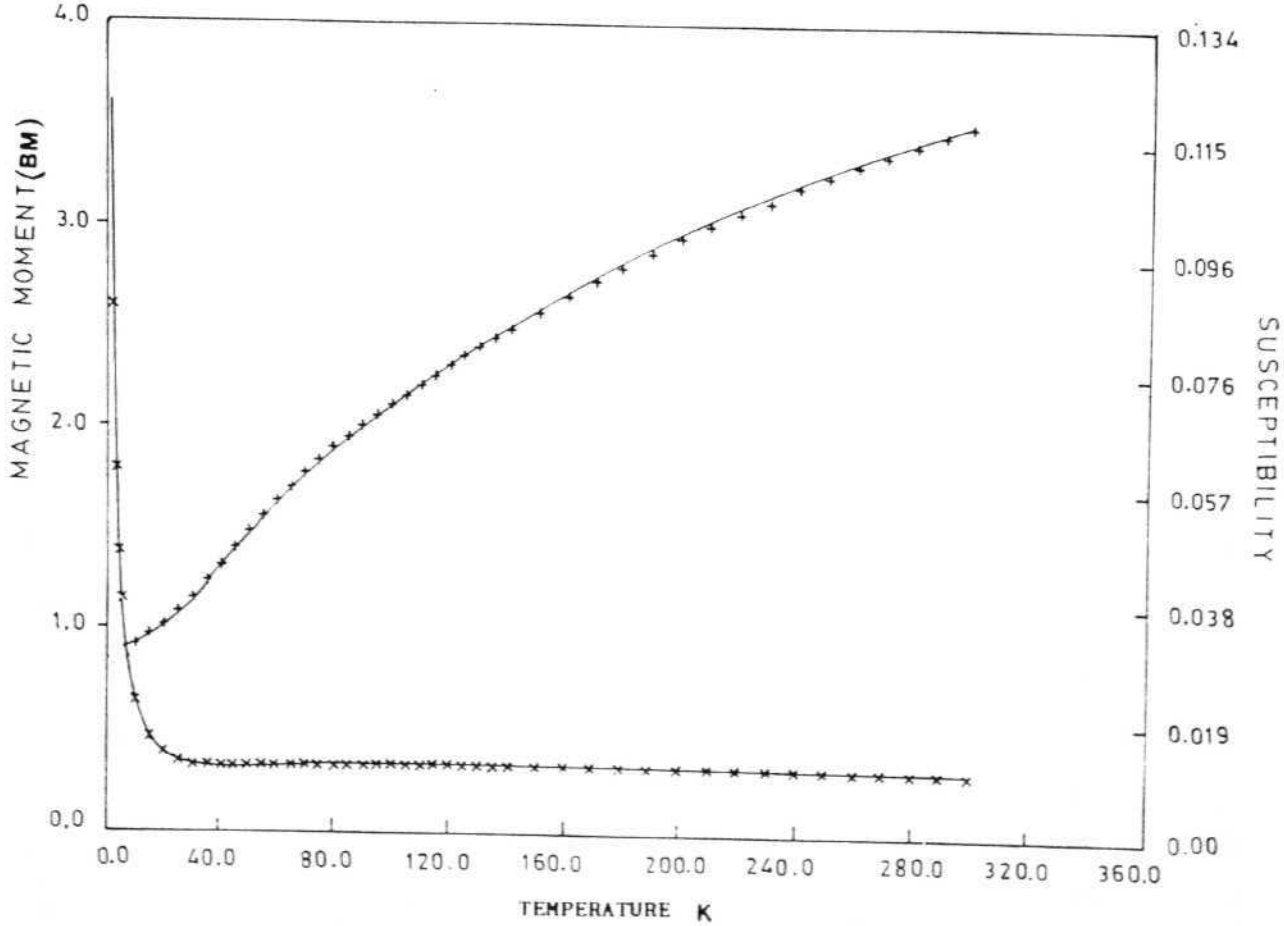

Fig 2.14. Variable-temperature magnetic susceptibility data for A. The solid line results from a least-squares fit of the data to the theoretical magnetic susceptibility calculated as mentioned in the text.

with the present complex. Only one example is known in the literature with an additional acetate bridge, and shows higher J ($-124\ cm^{-1}$) value. Present understanding with insufficient number of examples may not provide a good correlation based on dihedral angles.

Compound B, shows a room temperature magnetic moment value of 3.75 BM and is comparable to the values reported to the other Mn(IV,IV,IV) complexes. The lower value from the expected spin-only value indicates the presence of strong antifferomagnetic interactions. Ground state in this type of complexes are often varied by a small change in the structural parameters which in turn effects the interaction between the metal ions. Further characterisation will require variable temperature magnetic susceptibility studies.

We conclude this chapter with some general comments on the magneto structural correlations in dinuclear manganese complexes (Fig. 2.15).

(i). $d^4 - d^3$ (Mn^{III}, Mn^{IV}) and $d^3 - d^3$ (Mn^{IV}, Mn^{IV}) systems have the largest couplings (mostly $|J| \geq 100\ cm^{-1}$) while $d^4 - d^4$ (Mn^{III}, Mn^{III}), $d^5 - d^4$ (Mn^{II}, Mn^{III}) and $d^5 - d^5$ (Mn^{II}, Mn^{II}) have much smaller couplings (mostly $|J| \leq 20\ cm^{-1}$).

(ii). The majority of the $d^3 - d^4$ and $d^3 - d^3$ systems have dioxo bridging leading to short Mn - Mn distances (2.65 ± .1 Å). While most of the $d^4 - d^4$, $d^5 - d^4$ and $d^5 - d^5$ systems have other

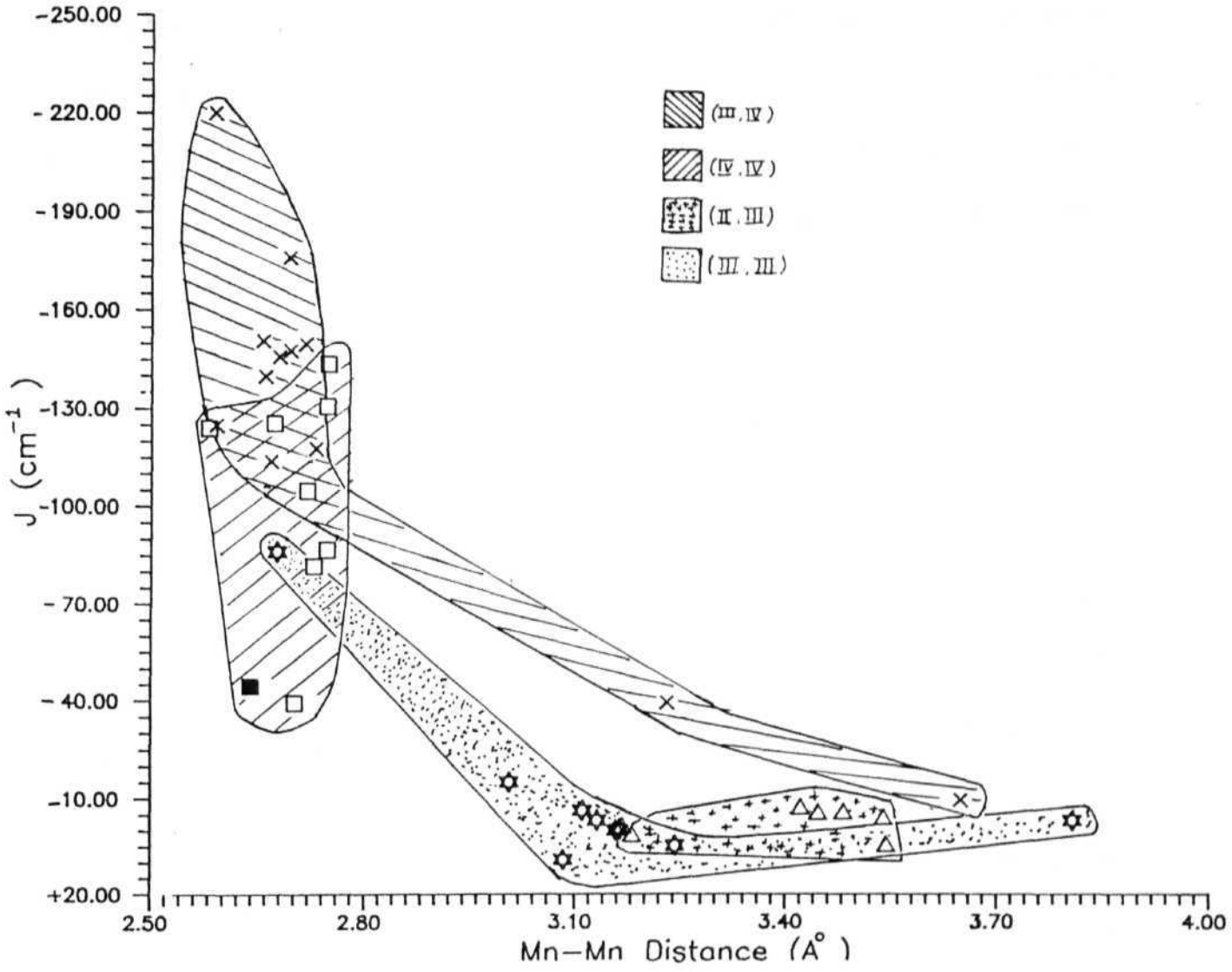

Fig 2.15. J *vs* Mn-Mn distance (Å) in manganese dimers. ($\mathcal{H} = -2JS_1S_2$)

types of bridges leading to longer Mn - Mn distance (mostly 3.12 ± .1 Å).

(iii). The few non-dioxo bridged d^3 - d^4 systems having large Mn - Mn separations have small couplings ($|J|$ as low as 5 cm^{-1}).

(iv). Within a short range of Mn -Mn distances (2.55 to 2.76 Å) the $|J|$ value varies from 40 cm^{-1} to 145 cm^{-1} for d^3 - d^3 complexes, and from 115 to 220 cm^{-1} for d^3 - d^4 complexes.

(v). The only (weakly) ferromagnetic examples known are having d^4 - d^4 configuration.

There have been sporadic attempts in the literature to consider orbital pathways for exchange in these systems. Hendrickson *et al.*[207] considered the difference between (d^5, d^4) and (d^3, d^4) systems and conclude that there are more ferromagnetic pathways in the former case involving nearly orthogonal e_g - t_{2g} overlap. They also consider the Mn-O-Mn angles and the differences between Mn-L distances for the two sites, but surprisingly do not take into account the Mn-Mn separations which are quite different for the two sets of mixed valent complexes. Wieghardt *et al.*[205,206] have studied a series of Mn_2^{III} systems having d^3, d^4 and d^5 ions and conclude that the crossed interaction (d_z2 - d_{xz}) is the most important contribution in trigonally distorted complexes having $[Mn_2O(OAc)_2]$ core.

While a general understanding is presently possible for the $M_2O(OAc)_2$ systems, what is perhaps most puzzling is the observation of (iv) above. Detailed calculation taking into

account the core geometry, oxidation states as well as terminal ligands which influence d- levels at the individual sites are needed to analyse this problem. This is outside the scope of the present thesis. Suffice it to say that the Mn(IV,IV) complex described in this chapter along with another such recently characterised complex[203] has considerably extended the range of J values in these dioxobridged d^3-d^3 systems without enlarging the range of Mn-Mn distances.

CHAPTER 3

SYNTHESIS AND STRUCTURAL CHARACTERISATION OF (μ-oxo)-di-(μ-acetato) MANGANESE(III,III) DIMERS: $[Mn_2O(OAc)_2(H_2O)(NO_3)(bpy)_2](ClO_4).CH_3COOH$ and $[Mn_2O(OAc)_2(H_2O)_2(bpy)_2](ClO_4)_2$.

3.1. Introduction:

A number of manganese complexes in their higher valences are proposed as synthetic models for manganese containing metal proteins.[46,47] Our approach in synthesising such models with ceric oxidation, yielded (IV,IV) dimeric and (IV,IV,IV) trimeric complexes which were described in the previous chapter. The present chapter deals with (μ-oxo)bis-(μ-carboxylato) dimanganese(III) complexes which are characterised by X-ray crystallography. This bridging unit constitutes another class of manganese complexes which have biological importance. These units are proposed for the active sites in ribonucleotide reductase and pseudocatalase.[47] Similar structural units with diiron(III) occur in haemerythrin.[105,106] A few examples are found recently in the literature with other transition metals with interesting electronic and magnetic properties.[187-192]

Only few model compounds are known for $[Mn_2^{III}(O)(OAc)_2]^{2+}$ core.[107-114] Where the earlier compounds are reported for tridentate cyclic ligands, later compounds with

bidentate ligands expanded the scope of the dimetal core. Complexes with the bidentate ligand, bpy leave the sixth coordination site free, which can be bound by a monodentate ligand. Complexes coordinated with H_2O and $S_2O_8^{2-}$ are reported[111,112] where coordination of water and bonding of smaller anions have relevance to oxygen evolution at PS-II.[193]

This chapter describes the isolation and characterization of $[Mn_2(O)(OAc)_2(bpy)_2(H_2O)(NO_3)](ClO_4).CH_3COOH$ (D) and $[Mn_2(O)(OAc)_2(H_2O)_2(bpy)_2](ClO_4)_2$ (E). Both are obtained as perchlorate salts. E has been previously characterized as a PF_6^- salt.[111] Compound D was also isolated as a PF_6 salt (D1).

3.2. Experimental Section:

3.2.1. Materials: All the chemicals are analytical grade and are used as purchased. Purification of solvents and other procedures are described in the Section 2.2.1.

3.2.2. Preparation of Compounds:

3.2.2a. $[Mn_2(O)(OAc)_2(H_2O)(NO_3)(bpy)_2](ClO_4).CH_3COOH$. (D) Bpy (1.6 g, 10 mmol) was added to a solution of $Mn(OAc)_2.4H_2O$ (1.2 g, 4.9 mmol) in 30 ml of water, glacial-acetic acid mixture (1:2). The resulting yellow solution was cooled and 10 ml of aqueous ammonium

ceric nitrate (2.7 g, 4.9 mmol) was added slowly with constant stirring. The solution turned to brown. Saturated aqueous $NaClO_4$ was then added. The solution was filtered and kept for slow evaporation. Dark brown crystals deposited after a few days, which were filtered and dried.(1.65 g, 85% yield). Anal, calc for $C_{26}H_{28}N_5O_{15}ClMn_2$; C, 39.23; H, 3.54; N, 8.82; Found: C, 38.61; H, 3.31; and N, 9.34. Equivalent weight by iodometry, found (calc): 387 (397.7).

3.2.2b. $[Mn_2(O)(OAc)_2(H_2O)_2(bpy)_2](ClO_4)_2$. (E) This compound was found as a minor product in the above preparation. This was established by X-ray study on some other crystal in the same batch of preparation. Anal, calc: for $C_{24}H_{26}N_4O_{15}Cl_2Mn_2$, C, 36.43; H, 3.31; N, 7.08. Equivalent weight, calc (395.6).

3.2.2c. $[Mn_2(O)(OAc)_2(H_2O)(NO_3)(bpy_2)](PF_6)$. (D1) Compound prepared by similar procedure employed for D. To the brown solution obtained after Ce(IV) addition, aqueous NH_4PF_6 was added. The present complex crystallises out after few days. Anal, calc for $C_{24}H_{24}N_5O_9PF_6Mn_2$: C, 36.89; H, 3.10; N, 8.96; Found: C, 36.33; H, 3.16; N, 8.75.

3.2.3. Analysis, Spectral and physical Measurements: I.R., Optical and EPR spectra are recorded as described in the section 2.2.3.

3.2.4. X-Ray crystallography:

3.2.4a. $[Mn_2(O)(OAc)_2(H_2O)(NO_3)(bpy)_2](ClO_4).CH_3COOH$. D

The diffraction data were collected at room temperature on an Enraf-Nonius CAD-4 Kappa geometry automated diffractrometer using MoKα radiation (data collected at RSIC, IIT, Madras). Parameters of crystal and intensity measurements are given in the Table 3.1. A total of 4456 reflections were collected, out of which 4322 reflections with $F > 6\sigma(F)$ were used for the subsequent calculations. The structure was solved in the triclinic space group $P\bar{1}$. The atomic positions of manganese atom and part of the ring were obtained on an initial direct methods computation using the SHELX-86 crystallographic programme package.[180] Subsequently the structure was solved by full-matrix least-squares method and Fourier technique using SHELX-76 programme.[179] All the non-hydrogen atoms were refined anisotropically and hydrogen atoms were picked up from the Fourier map and refined isotropically. Structure was brought to a final agreement factor R = 6.0%. Atomic coordinates, bond lengths and angles and thermal parameters are given in the Tables 3.2 to 3.5

3.2.4b. $[Mn_2(O)(OAc)_2(H_2O)_2(bpy)_2](ClO_4)_2$. E

Brown crystals of dimension 0.4 × 0.15 × 0.05 mm, mounted on an Enraf-Nonius CAD-4

Table 3.1. Crystallographic Data for D.

Formula	$C_{26}H_{28}N_5O_{15}ClMn_2$	formula weight	795.62
a, Å	10.083(3)	space group	$P\bar{1}$
b, Å	10.888(2)	temp, K	298
c, Å	16.642(2)	ρ_{calc}, g cm^{-3}	1.59
α, deg	80.915(2)	ρ_{obs}, g cm^{-3}	1.61
β, deg	72.807(4)	V, Å^3	1662.1
γ, deg	72.789(4)	Z	2
μ, cm^{-1}	7.42	λ, Å	0.71073
diffractometer	Enraf Nonius CAD-4	radiation	MoKα
monochromator	graphite	no. of variables	618
data collected	5524	data used ($F > 6\sigma(F)$)	4322
R^a = 0.060		$R_w{}^b$	0.062

[a] $R = (\sum\| |F_o| - |F_c| \|) / \sum |F_o|$

[b] $R_w = \{ [\sum w (|F_o| - |F_c|)^2] / \sum w F_o^2 \}^{1/2}$

Table 3.2. Fractional atomic coordinates and isotropic or equivalent temperature factors for D.[a]

Atom	x/a	y/b	z/c	U_{eq}[b]
Mn1	0.1946(1)	0.3386(9)	0.6880(5)	0.027
Mn2	0.3786(1)	0.3061(9)	0.8162(6)	0.030
C1	-0.0882(2)	-0.1757(2)	0.7702(1)	0.052(1)
O1	0.2727(4)	0.4041(4)	0.7486(3)	0.031(2)
O2	0.0304(8)	0.7298(7)	0.7314(5)	0.096(3)
O3	-0.2149(9)	-0.2058(9)	0.7665(6)	0.115(3)
O4	-0.0882(10)	-0.1742(5)	0.8527(5)	0.123(3)
O5	-0.0826(8)	-0.0553(6)	0.7259(5)	0.093(2)
C25	1.2963(12)	0.9000(11)	0.6743(8)	0.112(3)
C26	1.4083(17)	0.7886(16)	0.7079(11)	0.152(3)
O14	0.5036(12)	0.2728(10)	0.3563(7)	0.163(3)
O15	1.4172(17)	0.7671(16)	0.7702(11)	0.273(3)
N5	0.6479(7)	0.4420(7)	0.7758(4)	0.060(2)
O6	0.7336(9)	0.3373(8)	0.7780(6)	0.113(3)
O7	0.3128(7)	0.4616(7)	0.2353(4)	0.047(2)
O8	0.5251(6)	0.4417(6)	0.7735(4)	0.068(2)
N1	0.2516(5)	0.4615(5)	0.5829(3)	0.029(2)
N2	0.1177(5)	0.2816(5)	0.6011(3)	0.315(2)
N3	0.2736(6)	0.4288(5)	0.9110(3)	0.037(2)
N4	0.4845(6)	0.2186(5)	0.9080(3)	0.037(2)
O13	-0.0137(5)	0.4888(5)	0.7198(3)	0.048(2)
H13'	-0.07897	0.46836	0.78208	0.028
H13"	-0.07415	0.49969	0.67413	0.028
C11	0.1411(6)	0.1670(6)	0.8435(4)	0.035(2)
C12	0.0481(9)	0.0794(8)	0.8923(5)	0.062(3)
O9	0.2328(5)	0.1839(5)	0.8718(3)	0.049(2)
O10	0.1148(5)	0.2178(5)	0.7734(3)	0.043(2)
C13	0.4944(7)	0.1455(6)	0.6712(4)	0.034(2)

Table 3.2 contd...

Atom	x/a	y/b	z/c	U_{eq} [a]
C14	0.6201(8)	0.0426(7)	0.6281(5)	0.052(2)
O11	0.3923(5)	0.1914(4)	0.6399(3)	0.044(2)
O12	0.5054(5)	0.1792(4)	0.7383(3)	0.044(2)
C1	0.3122(7)	0.5547(6)	0.5823(4)	0.038(2)
C2	0.3494(8)	0.6338(6)	0.5093(4)	0.046(2)
C3	0.3202(8)	0.6137(7)	0.4375(4)	0.051(2)
C4	0.2573(8)	0.5179(7)	0.4385(4)	0.045(2)
C5	0.2229(6)	0.4422(5)	0.5122(4)	0.030(2)
C6	0.1526(6)	0.3378(5)	0.5213(4)	0.033(2)
C7	0.1205(8)	0.2975(7)	0.4562(4)	0.048(2)
C8	0.0515(8)	0.2015(7)	0.4724(5)	0.055(2)
C9	0.0140(8)	0.1467(7)	0.5537(5)	0.051(2)
C10	0.0495(7)	0.1893(6)	0.6163(4)	0.043(2)
C15	0.1743(8)	0.5395(7)	0.9035(4)	0.050(2)
C16	0.1022(1)	0.6193(8)	0.9695(5)	0.075(3)
C17	0.1406(1)	0.5761(1)	0.0492(1)	0.081(3)
C18	0.2460(1)	0.4603(1)	1.0547(1)	0.065(3)
C19	0.3118(1)	0.3895(1)	0.9847(1)	0.042(2)
C20	0.4300(1)	0.2719(1)	0.9828(1)	0.041(2)
C21	0.4862(1)	0.2189(1)	1.0506(1)	0.055(2)
C22	0.6012(1)	0.1099(1)	1.0406(1)	0.058(2)
C23	0.6583(1)	0.0575(1)	0.9645(1)	0.044(2)
C24	0.5964(7)	0.1131(7)	0.8986(4)	0.054(2)

[a] Water hydrogen atoms and ring hydrogen atoms are fixed and refined isotropically

[b] $U(eq) = (1/3)(U_{11}a^2a^{*2} + U_{22}b^2b^{*2} + U_{33}c^2c^{*2} + U_{12}a^*b^*ab\cos\gamma + U_{13}a^*c^*ac\cos\beta + U_{23}b^*c^*bc\cos\alpha)$

Table 3.3. Bond distances (Å) for D.

O2 ---C1	1.390(7)	O3 ---C1	1.429(10)
O4 ---C1	1.376(9)	O5 ---C1	1.407(7)
C25 ---C26	1.551(19)	O14 ---C26	1.300(7)
O15 ---C26	1.051(26)	C11 ---O9	1.223(8)
C11 ---O12	1.277(6)	C11 ---C12	1.511(6)
C13 ---O10	1.274(9)	C13 ---O11	1.229(8)
C13 ---C14	1.501(8)	N5 ---O6	1.213(10)
N5 ---O7	1.198(9)	N5 ---O8	1.251(10)
Mn2 ---Mn1	3.137(2)	Mn1 ---O1	1.782(5)
Mn1 ---N1	2.074(4)	Mn1 ---N2	2.076(6)
O11 ---Mn1	2.180(4)	O12 ---Mn1	1.938(4)
O13 ---Mn1	2.224(4)	O8 ---Mn2	2.281(6)
N3 ---Mn2	2.057(5)	Mn2 ---N4	2.069(6)
Mn2 ---O1	1.790(4)	Mn2 ---O9	2.180(5)
Mn2 ---O10	1.941(4)	C1 ---N1	1.328(7)
C2 ---C1	1.397(9)	C3 ---C2	1.378(12)
C4 ---C3	1.367(12)	C5 ---C4	1.383(8)
C5 ---N1	1.352(7)	C6 ---C5	1.472(10)
C6 ---N2	1.362(5)	C7 ---C6	1.384(11)
C8 ---C7	1.371(12)	C9 ---C8	1.381(10)
C10 ---C9	1.380(12)	N2 ---C10	1.332(8)
C15 ---N3	1.335(7)	C15 ---C16	1.397(11)
C17 ---C16	1.458(14)	C18 ---C17	1.399(12)
C19 ---C18	1.384(10)	N3 ---C19	1.360(7)
C20 ---C19	1.466(8)	N4 ---C20	1.351(6)
C21 ---C20	1.381(10)	C22 ---C21	1.386(10)
C23 ---C22	1.366(11)	C24 ---C23	1.389(8)
N4 ---C24	1.341(8)		

Table 3.4. Bond angles (^{o}) for D.

O3	-C1	-O2	108.0(5)	O4	-C1	-O2	109.4(5)
O4	-C1	-O3	110.4(6)	O5	-C1	-O2	109.2(4)
O5	-C1	-O3	109.0(5)	O5	-C1	-O4	110.7(5)
C23	-C24	-N4	121.3(3)	O15	-C26	-C25	127.7(15)
O8	-N5	-O6	116.1(9)	N2	-Mn1	-N1	78.5(2)
O1	-Mn1	-N1	92.2(2)	O1	-Mn1	-N2	170.6(2)
O11	-Mn1	-N1	89.7(2)	O11	-Mn1	-N2	85.2(2)
O11	-Mn1	-O1	94.0(2)	O12	-Mn1	-N1	167.8(2)
O12	-Mn1	-N2	89.8(2)	O12	-Mn1	-O1	99.5(2)
O12	-Mn1	-O11	92.6(2)	O13	-Mn1	-N1	85.8(2)
O13	-Mn1	-N2	87.4(2)	O13	-Mn1	-O1	92.9(2)
O13	-Mn1	-O11	172.0(2)	O13	-Mn1	-O12	90.4(2)
N3	-Mn2	-O8	83.5(2)	N4	-Mn2	-O8	89.5(2)
N4	-Mn2	-N3	78.8(2)	O1	-Mn2	-O8	87.9(2)
O1	-Mn2	-N3	91.5(2)	O1	-Mn2	-N4	170.1(2)
O9	-Mn2	-O8	173.3(2)	O9	-Mn2	-N3	90.5(2)
O9	-Mn2	-N4	86.5(2)	O9	-Mn2	-O1	95.1(2)
O10	-Mn2	-O8	93.3(2)	O10	-Mn2	-N3	169.2(2)
O10	-Mn2	-N4	90.9(2)	O10	-Mn2	-O1	98.7(2)
O10	-Mn2	-O9	92.1(2)	C1	-N1	-Mn1	124.0(3)
C5	-N1	-Mn1	115.6(3)	C5	-N1	-C1	120.4(4)
C6	-N2	-Mn1	115.2(3)	C10	-N2	-Mn1	125.0(3)
C10	-N2	-C6	119.5(4)	C15	-N3	-Mn2	124.3(3)
C19	-N3	-Mn2	115.1(2)	C19	-N3	-C15	120.6(4)
C20	-N4	-C24	119.7(3)	Mn2	-O1	-Mn1	122.9(0)
O11	-C13	-O10	125.4(0)	C14	-C13	-O10	115.2(0)
C14	-C13	-O11	119.4(0)	C2	-C1	-N1	121.5(7)
C3	-C2	-C1	118.0(8)	C4	-C3	-C2	120.3(6)
C5	-C4	-C3	119.3(7)	C4	-C5	-N1	120.5(6)
C6	-C5	-N1	115.3(4)	C6	-C5	-C4	124.2(7)
C5	-C6	-N2	114.9(5)	C7	-C6	-N2	120.4(6)

Table 3.4. contd...

C7	-C6	-C5	124.7(5)	C8	-C7	-C6	119.7(6)
C9	-C8	-C7	119.6(8)	C10	-C9	-C8	118.5(8)
C9	-C10	-N2	122.3(5)	O12	-C11	-O9	125.4(5)
C12	-C11	-O9	120.2(4)	C12	-C11	-O12	114.5(5)
C16	-C15	-N3	123.2(7)	C17	-C16	-C15	116.3(7)
C18	-C17	-C16	119.1(8)	C19	-C18	-C17	119.5(8)
C18	-C19	-N3	121.3(6)	C21	-C20	-N4	121.2(5)
C22	-C21	-C20	118.7(7)	C23	-C22	-C21	120.0(7)
C22	-C23	-C24	118.9(6)				

Table 3.5. Anisotropic thermal parameters for D.[a]

Atom	U11	U22	U33	U23	U13	U12
Mn1	0.0325(5)	0.0284(4)	0.0204(4)	0.0035(3)	-0.0106(3)	-0.0097(3)
Mn2	0.0312(5)	0.0347(5)	0.0241(4)	-0.0005(3)	-0.0117(3)	-0.0048(3)
Cl	0.0677(11)	0.0398(9)	0.0497(10)	-0.0019(7)	-0.0200(9)	-0.0071(8)
O1	0.0379(17)	0.0318(17)	0.0265(18)	0.0014(14)	-0.0159(15)	-0.0086(15)
O2	0.1023(26)	0.0746(25)	0.1126(27)	-0.0281(24)	-0.0023(20)	-0.0022(20)
O3	0.0968(26)	0.1155(27)	0.1336(27)	0.0129(26)	-0.0369(25)	-0.0486(24)
O4	0.1576(28)	0.1250(28)	0.0873(26)	-0.0193(25)	-0.0534(25)	-0.0024(20)
O5	0.1023(26)	0.0627(24)	0.1142(26)	0.0230(23)	-0.0365(24)	-0.0275(22)
C25	0.1064(29)	0.0987(29)	0.1321(29)	-0.0109(28)	-0.0260(28)	-0.0249(28)
C26	0.1475(29)	0.1599(30)	0.1474(30)	-0.0094(29)	-0.0505(29)	-0.0505(29)
O14	0.1560(29)	0.1519(29)	0.1813(29)	-0.0345(28)	-0.0569(28)	-0.0246(28)
O15	0.2750(30)	0.2846(30)	0.2583(30)	-0.0163(30)	-0.0870(30)	-0.0767(30)
N5	0.0488(23)	0.0861(26)	0.0443(23)	-0.0003(20)	-0.0157(21)	-0.0151(22)
O6	0.0890(26)	0.1229(27)	0.1278(27)	0.0089(26)	-0.0240(25)	-0.0303(25)
O7	0.0469(22)	0.0582(23)	0.0363(23)	0.0014(21)	-0.0130(20)	-0.0427(20)
O8	0.0482(21)	0.0813(23)	0.0745(23)	0.0152(21)	-0.0227(20)	-0.0345(19)
N1	0.0351(20)	0.0285(19)	0.0243(19)	0.0023(16)	-0.0077(17)	-0.0071(17)
N2	0.0343(19)	0.0314(19)	0.0288(19)	-0.0004(17)	-0.0123(16)	-0.0085(17)
N3	0.0418(21)	0.0432(21)	0.0250(19)	-0.0034(18)	-0.0143(18)	-0.0006(17)
N4	0.0358(20)	0.0432(22)	0.0318(20)	-0.0012(18)	-0.0147(18)	-0.0025(18)
O13	0.0363(20)	0.0527(21)	0.0541(21)	-0.0091(18)	-0.0089(18)	-0.0021(18)
C11	0.0368(21)	0.0362(21)	0.0307(21)	0.0045(19)	-0.0049(19)	-0.0113(19)
C12	0.0638(25)	0.0674(25)	0.0549(26)	0.0197(24)	-0.0127(23)	-0.0349(23)
O9	0.0519(20)	0.0549(20)	0.0409(19)	0.0186(17)	-0.0241(18)	-0.0241(17)
O10	0.0503(19)	0.0478(19)	0.0325(18)	0.0138(16)	-0.0182(16)	-0.0261(17)
C13	0.0342(22)	0.0355(22)	0.0321(22)	0.0004(19)	-0.0078(20)	-0.0087(19)
C14	0.0495(24)	0.0534(25)	0.0531(25)	-0.0150(23)	-0.0120(23)	0.0007(23)
O11	0.0469(20)	0.0429(19)	0.0415(19)	-0.0156(16)	-0.0189(17)	0.0012(17)

Table 3.5. contd...

Atom	U11	U22	U33	U23	U13	U12
O12	0.0441(20)	0.0499(20)	0.0388(19)	-0.0114(17)	-0.0189(16)	0.0070(17)
C1	0.0438(22)	0.0334(21)	0.0372(22)	0.0010(19)	-0.0095(20)	-0.0141(19)
C2	0.0574(24)	0.0404(21)	0.0430(23)	0.0011(21)	-0.0059(21)	-0.0171(21)
C3	0.0668(25)	0.0460(23)	0.0392(23)	0.0074(21)	-0.0015(22)	-0.0167(22)
C4	0.0618(24)	0.0480(23)	0.0265(21)	0.0063(20)	-0.0601(21)	-0.0158(21)
C5	0.0322(21)	0.0337(21)	0.0255(20)	-0.0018(18)	-0.0050(18)	-0.0036(18)
C6	0.0384(22)	0.0326(21)	0.0275(21)	-0.0029(18)	-0.0106(19)	-0.0019(19)
C7	0.0574(23)	0.0516(23)	0.0360(22)	-0.0072(21)	-0.0199(21)	-0.0100(21)
C8	0.0619(24)	0.0543(24)	0.0503(24)	-0.0126(22)	-0.0229(22)	-0.0164(22)
C9	0.0558(23)	0.0456(23)	0.0532(23)	-0.0075(21)	-0.0214(21)	-0.0188(21)
C10	0.0468(22)	0.0395(22)	0.0433(22)	0.0003(20)	-0.0198(20)	-0.0135(19)
C15	0.0554(24)	0.0498(24)	0.0454(23)	-0.0094(21)	-0.0183(21)	0.0075(22)
C16	0.0883(26)	0.0790(26)	0.0567(25)	-0.0191(24)	-0.0306(24)	0.0187(25)
C17	0.0965(27)	0.0862(27)	0.0608(25)	-0.0230(25)	-0.0324(25)	0.0159(26)
C18	0.0816(26)	0.0703(25)	0.0441(24)	-0.0141(23)	-0.0259(23)	0.0102(25)
C19	0.0493(23)	0.0475(23)	0.0288(21)	-0.0035(20)	-0.0173(19)	-0.0010(20)
C20	0.0431(22)	0.0469(23)	0.0339(22)	0.0001(20)	-0.0168(20)	-0.0055(20)
C21	0.0587(24)	0.0662(25)	0.0403(23)	0.0016(22)	-0.0263(21)	-0.0022(23)
C22	0.0585(24)	0.0672(24)	0.0496(23)	0.0080(22)	-0.0313(21)	-0.0045(23)
C24	0.0410(23)	0.0458(24)	0.0458(24)	0.0004(21)	-0.0157(21)	-0.0017(21)
C23	0.0505(23)	0.0567(24)	0.0533(24)	0.0047(22)	-0.0260(21)	-0.0049(22)

[a] The Temperature factor expression used

$$\exp\left[-2\pi^2\left(U_{11}h^2a^{*2} + U_{22}k^2b^{*2} + U_{33}l^2c^{*2} + 2U_{12}hka^*b^*\cos\gamma^* + 2U_{13}hla^*c^*\cos\beta^* + 2U_{23}klb^*c^*\cos\alpha^*\right)\right]$$

diffractrometer. Intensity data were collected at room temperature using MoKα radiation. Parameters of crystal and intensity measurements are given in the Table 3.6. A total of 5404 reflections were collected and corrected for Lorentz and polarisation effects. Empirical absorption corrections were made. The compound crystallises in monoclinic system and space group could be C2/c or Cc based on systematic absences. The structure was succesfully refined in C2/c. Initial positions of the heavy atoms were found by a combination of Patterson and direct methods using SHELX-86 programme.[180] Subsequently the structure was completed by difference Fourier and refined using full-matrix least-squares methods (SHELX-76).[179] Of the total 5404 reflections only 3301 reflections with $F > 5\ \sigma(F)$ were used for refinement. All the non-hydrogen atoms were refined anisotropically and hydrogen atoms are included by riding model and refined isotropically. The structure was refined to a final agreement factor R = 4.8%. Atomic coordinates, bond lengths and angles and thermal parameters are given in the Tables 3.7 to 3.10.

3.3. Results and Discussions:

3.3.1. Synthesis. Aqueous chemistry of high-valent manganese involves multiple redox equilibria. Isolation of different complexes with a variety of nuclearities by slight variation of

Table 3.6. Crystallographic Data for E.

Formula	$C_{24}H_{26}N_4O_{15}Cl_2Mn_2$	formula weight	719.2
a, Å	34.035(7)	space group	C2/c
b, Å	8.664(2)	temp, K	298
c, Å	21.616(4)	ρ_{calc}, g cm^{-3}	1.55
β, deg	105.29(2)	V, $Å^3$	6148(2)
crystal size mm	0.4×0.15×0.05	Z	8
μ, cm^{-1}	7.42	λ, Å	0.71073
diffractometer	Enraf Nonius CAD-4	radiation	MoKα
monochromator	graphite	F(000)	3215.88
unique data	5404	data used ($F > 5\sigma(F)$)	3301
R^a = 0.048		$R_w{}^b$	0.045

[a] $R = (\sum\| |F_o| - |F_c| \|) / \sum |F_o|$

[b] $R_w = \{ [\sum w (|F_o| - |F_c|)^2] / \sum w F_o^2 \}^{1/2}$

$w^{-1} = \sigma^2 |F_o| + g |F_o|^2$; $g = 0.005$

Table 3.7. Fractional Coordinates[a] and isotropic or equivalent temperature factors for E.

Atom	x	y	z	Ueq[b]
Mn1	0.6496(0)	0.5327(1)	0.4799(0)	0.033(0)
Mn2	0.6167(0)	0.4121(1)	0.5937(0)	0.034(0)
O2	0.6449(1)	0.3615(5)	0.3960(2)	0.052(2)
O3	0.6701(1)	0.3140(5)	0.6737(2)	0.056(2)
O6	0.6583(1)	0.7231(4)	0.5476(2)	0.050(2)
O1	0.6438(1)	0.3842(4)	0.5345(2)	0.035(1)
O4	0.5923(1)	0.5792(4)	0.4455(2)	0.042(1)
O5	0.5650(1)	0.5081(4)	0.5245(2)	0.044(1)
O7	0.6353(1)	0.6157(4)	0.6249(2)	0.048(1)
C21	0.5622(1)	0.5532(6)	0.4691(3)	0.036(2)
C22	0.5209(2)	0.5856(8)	0.4245(3)	0.056(2)
C23	0.6601(2)	0.8708(6)	0.6409(3)	0.055(2)
C24	0.6509(2)	0.7272(6)	0.6012(3)	0.039(2)
N1	0.7113(1)	0.4986(5)	0.5017(2)	0.033(2)
N2	0.6663(1)	0.6818(5)	0.4165(2)	0.036(2)
C1	0.7319(2)	0.4075(6)	0.5482(3)	0.042(2)
C8	0.6409(2)	0.7736(7)	0.3745(3)	0.045(2)
C9	0.7058(2)	0.6732(6)	0.4145(2)	0.035(2)
C5	0.7197(2)	0.7544(7)	0.3702(3)	0.048(2)
C6	0.6939(2)	0.8487(7)	0.3280(3)	0.055(2)
C3	0.7932(2)	0.4528(7)	0.5193(3)	0.053(2)
C4	0.7728(2)	0.5487(7)	0.4718(3)	0.046(2)
C2	0.7734(2)	0.3811(7)	0.5593(3)	0.050(2)
C10	0.7312(2)	0.5701(6)	0.4633(2)	0.035(2)
C7	0.6534(2)	0.8590(7)	0.3296(3)	0.052(2)

Table 3.7. contd...

Atom	x	y	z	Ueq
N3	0.5859(1)	0.4024(5)	0.6646(2)	0.037(2)
N4	0.5897(1)	0.1967(5)	0.5786(2)	0.033(1)
C15	0.5495(2)	0.0102(7)	0.6143(3)	0.049(2)
C14	0.5512(2)	0.2357(7)	0.7210(3)	0.044(2)
C17	0.5702(2)	-0.0331(7)	0.5190(3)	0.058(2)
C11	0.5848(2)	0.5148(7)	0.7056(3)	0.054(2)
C19	0.5694(1)	0.1505(6)	0.6205(2)	0.032(2)
C16	0.5505(2)	-0.0811(7)	0.5628(3)	0.060(2)
C18	0.5898(2)	0.1073(6)	0.5288(3)	0.044(2)
C20	0.5687(1)	0.2635(6)	0.6713(2)	0.033(2)
C13	0.5513(2)	0.3520(8)	0.7636(3)	0.052(2)
C12	0.5676(2)	0.4945(8)	0.7560(3)	0.057(2)
C11	0.4437(0)	0.1001(2)	0.1583(1)	0.062(1)
O1Cl	0.0620(2)	0.3785(6)	0.7800(2)	0.103(3)
O2Cl	0.0404(1)	0.5492(5)	0.8474(2)	0.079(2)
O3Cl	0.0964(2)	0.3927(6)	0.8859(2)	0.095(2)
O4Cl	0.0325(2)	0.2865(6)	0.8580(3)	0.140(3)
C12	0.2224(1)	0.1408(2)	0.7868(1)	0.071(1)
OACl	0.2568(2)	0.1204(7)	0.8375(3)	0.107(3)
OBCl	0.2255(2)	0.0906(10)	0.7291(3)	0.158(4)
OCCl	0.1889(2)	0.0783(10)	0.7992(3)	0.157(4)
ODCl	0.2146(4)	0.2989(9)	0.7853(5)	0.296(8)

[a] ring hydrogen and methyl hydrogen atoms were fixed and refined with common thermal paremeters 0.06(6), 0.113(9) respectively.

[b] $U(eq) = (1/3)(U_{11}a^2a^{*2} + U_{22}b^2b^{*2} + U_{33}c^2c^{*2} + U_{12}a^*b^*ab\cos\gamma + U_{13}a^*c^*ac\cos\beta + U_{23}b^*c^*bc\cos\alpha)$

Table 3.8. Bond distances (Å) for E.

Mn2	...Mn1	3.139			
O2	---Mn1	2.316 (4)	O6	---Mn1	2.173 (4)
O1	---Mn1	1.793 (3)	O4	---Mn1	1.939 (3)
N1	---Mn1	2.046 (4)	N2	---Mn1	2.069 (5)
O3	---Mn2	2.314 (4)	O1	---Mn2	1.780 (4)
O5	---Mn2	2.153 (3)	O7	---Mn2	1.934 (4)
N3	---Mn2	2.075 (5)	N4	---Mn2	2.067 (4)
C21	---O5	1.241 (7)	Mn2	---O7	1.934 (4)
C24	---O7	1.274 (7)	O4	---C21	1.279 (7)
O5	---C21	1.241 (7)	C22	---C21	1.505 (6)
C21	---C22	1.505 (6)	C24	---C23	1.496 (8)
O6	---C24	1.250 (7)	O7	---C24	1.274 (7)
C23	---C24	1.496 (8)	C1	---N1	1.324 (6)
C10	---N1	1.353 (7)	C8	---N2	1.337 (6)
C9	---N2	1.358 (7)	N1	---C1	1.324 (6)
C2	---C1	1.388 (8)	N2	---C8	1.337 (6)
C7	---C8	1.374 (9)	N2	---C9	1.358 (7)
C5	---C9	1.368 (8)	C10	---C9	1.476 (7)
C9	---C5	1.368 (8)	C6	---C5	1.359 (8)
C5	---C6	1.359 (8)	C7	---C6	1.393 (9)
C4	---C3	1.359 (8)	C2	---C3	1.379 (9)
C3	---C4	1.359 (8)	C10	---C4	1.392 (7)
C1	---C2	1.388 (8)	C3	---C2	1.379 (9)
N1	---C10	1.353 (7)	C4	---C10	1.392 (7)
C8	---C7	1.374 (9)	C6	---C7	1.393 (9)
C11	---N3	1.325 (7)	C20	---N3	1.361 (7)
C19	---N4	1.338 (7)	C18	---N4	1.328 (7)
C19	---C15	1.379 (7)	C16	---C15	1.371 (9)
C20	---C14	1.380 (8)	C13	---C14	1.365 (9)
C16	---C17	1.363 (0)	C18	---C17	1.376 (8)

Table 3.8. contd...

N3 ---C11	1.325 (7)	C12 ---C11	1.375 (9)
N4 ---C19	1.338 (7)	C15 ---C19	1.379 (7)
C20 ---C19	1.476 (7)	C15 ---C16	1.371 (9)
C17 ---C16	1.363 (0)	N4 ---C18	1.328 (7)
C17 ---C18	1.376 (8)	N3 ---C20	1.361 (7)
C14 ---C20	1.380 (8)	C19 ---C20	1.476 (7)
C14 ---C13	1.365 (9)	C12 ---C13	1.381 (9)
C11 ---C12	1.375 (9)	C13 ---C12	1.381 (9)
OAC1---C12	1.390 (5)	OBC1---C12	1.351 (7)
OCC1---C12	1.350 (7)	ODC1---C12	1.393 (8)
O1C1---C11	1.410 (6)	O2C1---C11	1.420 (5)
O3C1---C11	1.447 (5)	O4C1---C11	1.376 (7)

Table 3.9. Bond angles (^{o}) for E.

O6	-Mn1	-O2	169.4 (2)	O1	-Mn1	-O2	93.4 (2)
O1	-Mn1	-O6	96.9 (2)	O4	-Mn1	-O2	88.8 (1)
O4	-Mn1	-O6	92.6 (1)	O4	-Mn1	-O1	97.2 (2)
N1	-Mn1	-O2	86.7 (2)	N1	-Mn1	-O6	90.3 (2)
N1	-Mn1	-O1	91.7 (2)	N1	-Mn1	-O4	170.2 (2)
N2	-Mn1	-O2	81.7 (2)	N2	-Mn1	-O6	87.8 (2)
N2	-Mn1	-O1	169.1 (2)	N2	-Mn1	-O4	92.3 (2)
N2	-Mn1	-N1	78.4 (2)	O1	-Mn2	-O3	92.0 (2)
O5	-Mn2	-O3	175.9 (2)	O5	-Mn2	-O1	92.1 (1)
O7	-Mn2	-O3	87.4 (1)	O7	-Mn2	-O1	101.1 (2)
O7	-Mn2	-O5	91.3 (1)	N3	-Mn2	-O3	83.3 (2)
N3	-Mn2	-O1	169.8 (2)	N3	-Mn2	-O5	92.8 (1)
N3	-Mn2	-O7	87.8 (2)	N4	-Mn2	-O3	90.8 (1)
N4	-Mn2	-O1	93.2 (2)	N4	-Mn2	-O5	89.5 (1)
N4	-Mn2	-O7	165.7 (2)	N4	-Mn2	-N3	77.8 (2)
C24	-O6	-Mn1	128.5 (4)	Mn2	-O1	-Mn1	123.0 (2)
C21	-O5	-Mn2	129.2 (3)	C24	-O7	-Mn2	133.2 (4)
O5	-C21	-O4	125.2 (4)	C22	-C21	-O4	114.9 (5)
C22	-C21	-O5	119.9 (5)	O7	-C24	-O6	124.0 (5)
C23	-C24	-O6	119.5 (5)	C23	-C24	-O7	116.6 (5)
C1	-N1	-Mn1	124.6 (4)	C10	-N1	-Mn1	116.3 (3)
C10	-N1	-C1	119.1 (4)	C8	-N2	-Mn1	125.4 (4)
C9	-N2	-Mn1	115.7 (3)	C9	-N2	-C8	118.6 (5)
C2	-C1	-N1	122.8 (6)	C7	-C8	-N2	122.3 (5)
C5	-C9	-N2	121.4 (4)	C10	-C9	-N2	114.1 (5)
C10	-C9	-C5	124.5 (5)	C6	-C5	-C9	119.9 (6)
C7	-C6	-C5	119.3 (6)	C2	-C3	-C4	120.8 (5)
C10	-C4	-C3	118.7 (6)	C3	-C2	-C1	117.5 (5)
C9	-C10	-N1	114.9 (4)	C4	-C10	-N1	121.1 (4)
C4	-C10	-C9	124.0 (5)	C6	-C7	-C8	118.4 (5)

Table 3.9. contd...

C11 -N3 -Mn2	125.0 (4)	C20 -N3 -Mn2	115.4 (3)
C20 -N3 -C11	119.4 (5)	C19 -N4 -Mn2	116.8 (3)
C18 -N4 -Mn2	124.0 (4)	C18 -N4 -C19	119.1 (4)
C16 -C15 -C19	118.2 (6)	C20 -C14 -H14	120.9 (6)
C13 -C14 -C20	118.1 (5)	C18 -C17 -C16	118.1 (6)
C12 -C11 -N3	121.9 (6)	C15 -C19 -N4	121.7 (5)
C20 -C19 -N4	114.6 (4)	C20 -C19 -C15	123.7 (5)
C17 -C16 -C15	120.5 (6)	C17 -C18 -N4	122.4 (6)
C14 -C20 -N3	121.5 (5)	C19 -C20 -N3	114.7 (5)
C19 -C20 -C14	123.9 (5)	C12 -C13 -C14	120.6 (6)
C13 -C12 -C11	118.4 (6)		
O2C1-C11 -O1C1	110.7 (3)	O3C1-C11- O1C1	106.1 (3)
O3C1-C11 -O2C1	107.2 (3)	O4C1-C11 -O1C1	112.7 (4)
O4C1-C11 -O2C1	111.4 (4)	O4C1-C11 -O3C1	108.3 (3)
OBC1-C12 -OAC1	115.6 (4)	OCC1-C12 -OAC1	111.8 (4)
OCC1-C12 -OBC1	109.3 (4)	ODC1-C12 -OAC1	105.0 (5)
ODC1-C12 -OBC1	110.9 (6)	ODC1-C12 -OCC1	103.5 (7)

Table 3.10. Anisotropic Thermal Parameters of E.[a]

ATOM	U11	U22	U33	U23	U13	U12
Mn1	0.026(0)	0.036(0)	0.037(0)	0.005(0)	0.014(0)	-0.003(0)
Mn2	0.035(0)	0.032(0)	0.033(0)	0.002(0)	0.015(0)	-0.005(0)
O2	0.049(2)	0.051(3)	0.053(3)	-0.011(2)	0.017(2)	-0.008(2)
O3	0.054(3)	0.061(3)	0.046(2)	0.004(2)	-0.001(2)	-0.004(2)
O6	0.058(3)	0.036(2)	0.058(3)	-0.007(2)	0.035(2)	-0.011(2)
O1	0.033(2)	0.032(2)	0.039(2)	0.004(2)	0.017(2)	-0.002(2)
O4	0.025(2)	0.052(2)	0.047(2)	0.014(2)	0.016(2)	-0.001(2)
O5	0.035(2)	0.059(3)	0.037(2)	0.014(2)	0.016(2)	0.008(2)
O7	0.065(3)	0.034(2)	0.042(2)	-0.001(2)	0.023(2)	-0.015(2)
C21	0.028(3)	0.033(3)	0.044(3)	0.002(3)	0.012(2)	-0.001(2)
C22	0.028(3)	0.084(5)	0.053(4)	0.017(4)	0.014(3)	0.002(3)
C23	0.063(4)	0.039(4)	0.061(4)	-0.012(3)	0.024(3)	-0.011(3)
C24	0.032(3)	0.033(3)	0.049(4)	-0.004(3)	0.012(3)	-0.003(2)
N1	0.028(2)	0.035(3)	0.035(3)	-0.001(2)	0.011(2)	-0.001(2)
N2	0.032(2)	0.038(3)	0.038(3)	0.001(2)	0.015(2)	-0.009(2)
C1	0.037(3)	0.037(3)	0.049(3)	0.001(3)	0.012(3)	-0.001(3)
C8	0.043(3)	0.049(4)	0.039(3)	0.009(3)	0.005(3)	-0.004(3)
C9	0.038(3)	0.028(3)	0.039(3)	-0.009(3)	0.018(3)	-0.009(2)
C5	0.048(3)	0.044(4)	0.051(4)	-0.005(3)	0.026(3)	-0.009(3)
C6	0.068(4)	0.050(4)	0.046(4)	0.006(3)	0.030(3)	-0.017(3)
C3	0.032(3)	0.061(4)	0.063(4)	-0.006(4)	0.013(3)	0.004(3)
C4	0.034(3)	0.047(4)	0.056(4)	-0.009(3)	0.021(3)	-0.007(3)
C2	0.037(3)	0.054(4)	0.053(4)	-0.003(3)	0.006(3)	0.006(3)
C10	0.032(3)	0.031(3)	0.041(3)	-0.010(3)	0.016(2)	-0.006(2)
C7	0.057(4)	0.052(4)	0.044(4)	0.011(3)	0.016(3)	-0.002(3)
N3	0.041(2)	0.036(3)	0.034(2)	-0.003(2)	0.015(2)	-0.003(2)
N4	0.034(2)	0.031(3)	0.033(2)	-0.002(2)	0.012(2)	-0.004(2)

Table 3.10. contd...

ATOM	U11	U22	U33	U23	U13	U12
C15	0.052(3)	0.036(4)	0.059(4)	0.001(3)	0.026(3)	-0.007(3)
C14	0.038(3)	0.054(4)	0.039(3)	0.004(3)	0.016(3)	-0.001(3)
C17	0.072(4)	0.047(4)	0.050(4)	-0.020(3)	0.020(3)	-0.008(3)
C11	0.066(4)	0.048(4)	0.049(4)	-0.010(3)	0.028(3)	-0.014(3)
C19	0.027(3)	0.032(3)	0.036(3)	0.001(2)	0.008(2)	0.001(2)
C16	0.068(4)	0.041(4)	0.070(4)	-0.014(3)	0.028(3)	-0.018(3)
C18	0.048(3)	0.040(4)	0.041(3)	-0.004(3)	0.016(3)	-0.007(3)
C20	0.028(3)	0.035(3)	0.034(3)	0.006(2)	0.009(2)	0.002(2)
C13	0.053(4)	0.068(4)	0.037(3)	-0.000(3)	0.023(3)	-0.000(3)
C12	0.067(4)	0.057(4)	0.046(4)	-0.015(3)	0.026(3)	-0.003(3)
Cl1	0.074(1)	0.047(1)	0.060(1)	0.010(1)	0.022(1)	0.016(1)
O1Cl	0.167(5)	0.074(4)	0.060(3)	-0.005(3)	0.037(3)	0.018(3)
O2Cl	0.087(3)	0.055(3)	0.091(3)	0.016(3)	0.037(3)	0.027(3)
O3Cl	0.093(4)	0.100(4)	0.083(4)	0.017(3)	0.012(3)	0.045(3)
O4Cl	0.155(6)	0.066(4)	0.199(7)	0.027(4)	0.098(5)	-0.021(4)
Cl2	0.082(1)	0.069(1)	0.057(1)	0.002(1)	0.019(1)	-0.001(1)
OACl	0.087(4)	0.141(5)	0.073(3)	0.016(4)	-0.026(3)	-0.005(4)
OBCl	0.085(4)	0.292(10)	0.096(4)	-0.099(6)	0.043(3)	-0.008(5)
OCCl	0.073(4)	0.281(10)	0.115(5)	0.051(6)	0.045(4)	-0.027(5)
ODCl	0.520(2)	0.073(6)	0.212(9)	-0.011(6)	-0.096(10)	0.072(9)

[a] The Temperature factor expression used

$$\exp\,[-2\pi^2\,(U_{11}h^2a^{*2} + U_{22}k^2b^{*2} + U_{33}l^2c^{*2} + 2U_{12}hka^*b^*\cos\gamma^* + 2U_{13}hla^*c^*\cos\beta^* + 2U_{23}klb^*c^*\cos\alpha^*)]$$

condition (pH and ligand) are observed. In the presence of excess acetic acid (acetate), the present complexes are isolated by Ce(IV) oxidation. Two complexes are isolated under the similar conditions. The two compounds, unsymmetrical D and symmetrical E are involved in an equilibrium in solution.

$$\underset{(E)}{[Mn_2(O)(OAc)_2(bpy)_2(H_2O)_2]^{2+}} \underset{H_2O}{\overset{NO_3^-}{\rightleftharpoons}} \underset{(D)}{[Mn_2(O)(OAc)_2(bpy)_2(H_2O)(NO_3)]^{+}}$$

Slight shift in equilibrium towards right aided by solubility differences will lead to preferential crystallisation of D over E. While the perchlorate salt D contains predominantly aquo-nitrato complex with a small amount of diaquo complex E, the PF_6^- salt (D1) is a pure aquo-nitrato complex. This is seen from the C,H,N analysis data for the two complexes.

Formation of the present core, $[Mn_2(O)(OAc)_2]^{2+}$ can be explained by the reaction scheme shown in Section 2.3.1. Initial oxidation of Mn(II) by Ce(IV) generates short lived Mn(III) hydroxo species, which undergoes self assembly assisted by disproportionation. Presence of excess acetate may be one of the requirements for the formation of this core, because previously known complexes are also prepared in the presence of excess acetate[109-112] or starting with Mn(III) acetate *via* disproportionation.[114]

In the earlier preparation of the diaquo complex, addition of $KMnO_4^-$ followed by aqueous NH_4PF_6 solution resulted in the formation of PF_6 salt. Absence of any coordinating anion stabilised the di aquo complex while Christou *et al.* observed the formation of an anion ($S_2O_8^{2-}$) coordinated unsymmetrical complex.[112]

Substitutional lability of Mn(III) by anions may have relevance to the water oxidation center (WOC) of PS-II. It was observed previously that oxygen evolution capacity was affected by nitrate substitution in place of chloride ion.[193] There is no experimental proof till today for the presence of this dimetallic manganese(III) core in PS-II. Participation of this core in the manganese aggregate at PS-II can not be ruled out, particularly at lower S-states (S_{-1}, S_0 and S_1).

3.3.2 Structure. Molecular structure of D and E are shown in the Fig. 3.1 and 3.2. Both complexes are bridged by two acetates and an oxide ion. Each metal center has a distorted octahedral environment. In D the other three coordination sites are occupied by two N-atoms of the ligand on each metal center and a water oxygen and nitrate oxygen on different metal ions. On the otherhand, two N-atoms of ligand and a O-atom of the water molecule complete the octahedron environment around each metal ion in E. Mn-Mn distances of 3.137 and 3.139 Å for D and E are close

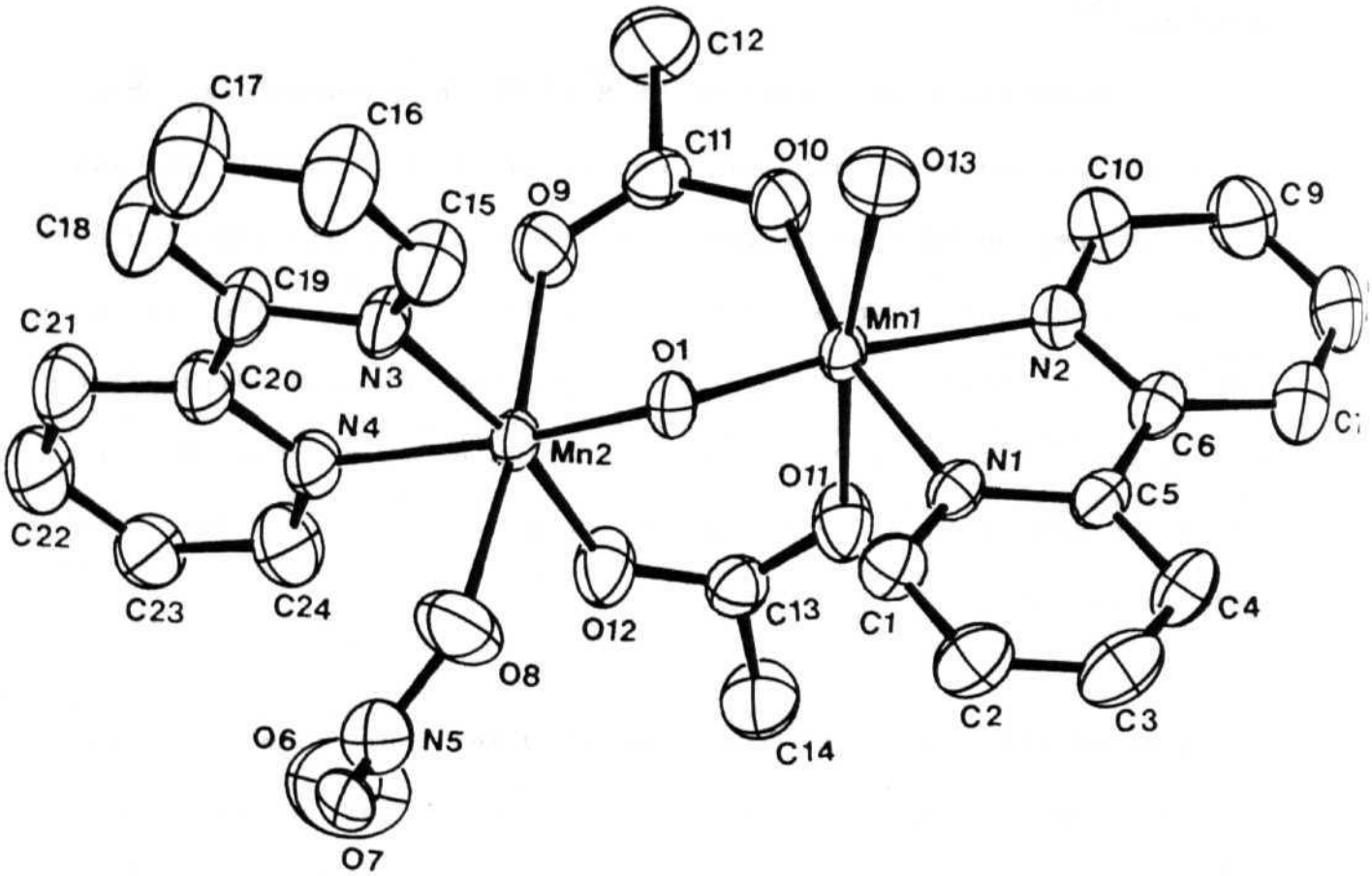

Fig 3.1. ORTEP view of the cation D.

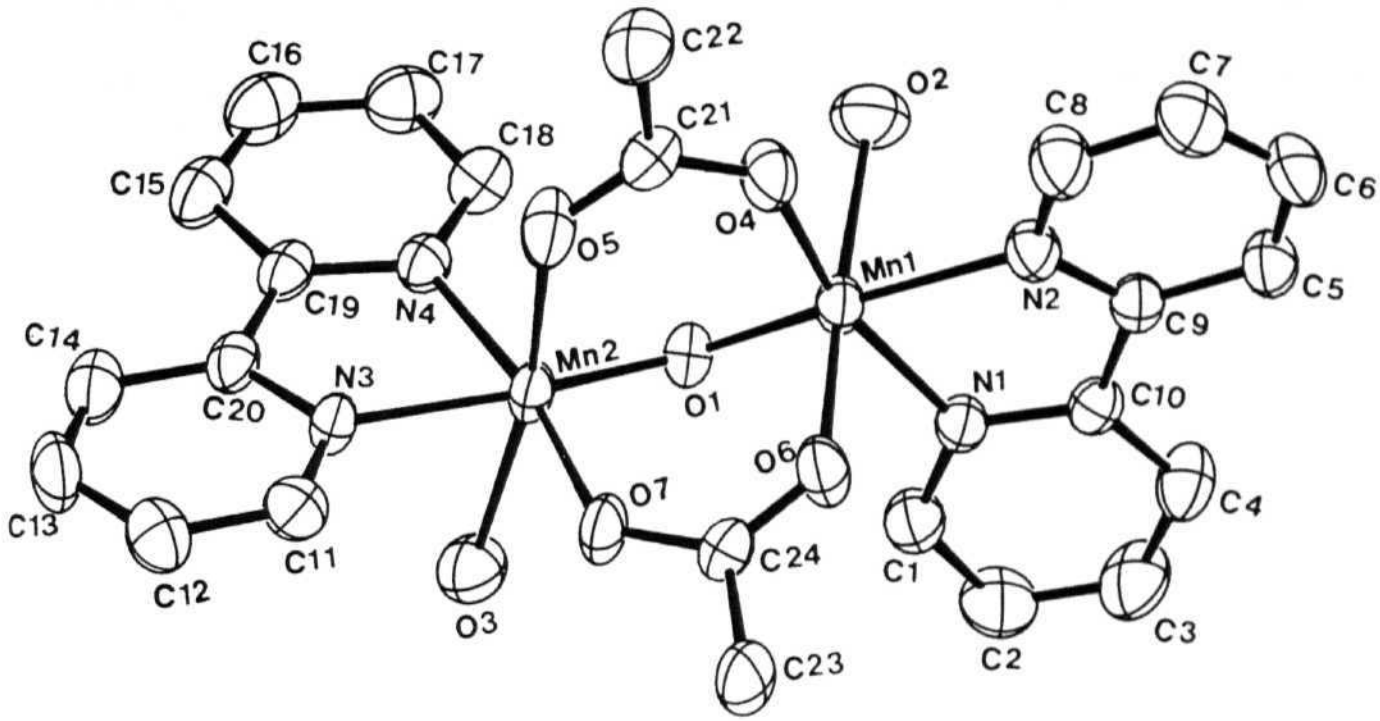

Fig 3.2. ORTEP view of the cation E.

to the reported values of other complexes. This is so with $Mn-O_{oxo}$ bond distances as well, 1.786 and 1.787 Å. Each metal ion has d^4 configuration, established by equivalent weight estimation and was further confirmed by crystallography. Each metal undergoes a Jahn-Teller distortion along *trans*-$O(H_2O,NO_3)$-Mn-O(OAc) bond, which is expected for d^4 metal ions. Comparison of H_2O, NO_3^- structural data for D and E, with known complexes are given in the Table 3.11. A closer look at the table shows that there are two types of distortions possible for $[Mn_2(O)(OAc)_2]^{2+}$ core and are shown schematically in the following figure with a dashed line.

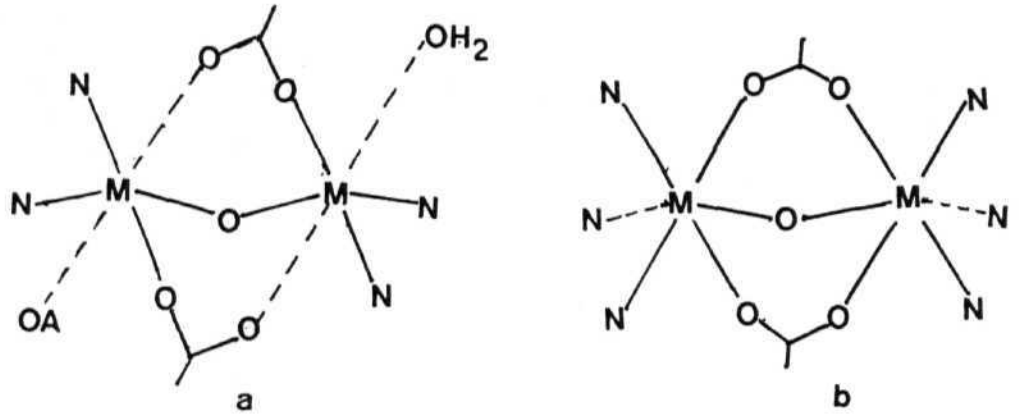

Fig 3.3. Jahn-Teller distortion in $[Mn_2O(OAc)_2]^{2+/3+}$ core (dashed line shows the distortion bond which is elongated (a) or shortened (b)).

The first kind (a) of distortion is an axial elongation of bonds along *trans*-$O(H_2O,NO_3)$-Mn-O(OAc). Because of this effect, two kinds of Mn-O(OAc) bonds are observed in D, one with a longer bond length at 2.180 Å and the other with a shorter bond at 1.939 Å. Similar observation was also made in 2 (2.163 and 1.936 Å).

Table 3.11 Comparative structural data for $[Mn_2O(OAc)_2]^{2+/3+}$ core.

Complex		Mn-O$_{oxo}$ (Å)	Mn-N (Å)	Mn-O(OAc) (Å)	Mn-OH$_2$ (Å)	Mn-O$_A$ (Å)	Mn-Mn (Å)	Mn-O-Mn (deg)	Ref
$[Mn_2O(OAc)_2(H_2O)(NO_3)(bpy)_2](ClO_4)$	(D)	1.786	2.069	1.939	2.224	2.281	3.137	122.9	
				2.180					present work
$[Mn_2O(OAc)_2(H_2O)_2(bpy)_2](ClO_4)_2$	(E)	1.787	2.064	1.936	2.315		3.139	123.0	
				2.163					
$[Mn_2O(OAc)_2(H_2O)_2(bpy)_2](PF_6)_2$	40	1.783	2.058	1.938	2.312		3.132	122.9	111
				2.158					
$[Mn_2O(OAc)_2(H_2O)(S_2O_8)(bpy)_2]$	42	1.773	2.080	1.941	2.176	2.231	3.145	125.1	112
				2.149					
$[Mn_2O(OAc)_2(L)_2](ClO_4)_2$	38	1.80	2.06	1.995			3.084	117.9	107,
			2.35						108
$[Mn_2O(OAc)_2(L)_2](I_3)I$	41	1.788	2.066	2.063			3.096	119.9	109
			2.183						
$[Mn_2O(OAc)_2(TMIP)_2](ClO_4)_2$	44	1.789	2.07	1.979			3.164	124.4	114
			2.244	2.135					
$[Mn_2O(OAc)_2\{HB(pz)_3\}_2].CH_3CN$	39a	1.790	2.079	2.001			3.175	125.0	110
			2.232	2.133					
$[Mn_2O(OAc)_2\{HB(pz)_3\}_2].4CH_3CN$	39b	1.773	2.057	2.066			3.159	125.1	110
			2.174						

L = TACN; L1 = N,N',N''-trimethyl-1,4,7-triazacyclononane; A = NO_3^- for D and $S_2O_8^{2-}$ for 42

This kind of distortion was found in earlier reported bidentate complexes also.[111,112] On the other hand, complexes with tridentate ligands except $[Mn_2O(OAc)_2(tmip)_2](ClO_4)_2$ (44) and to some extent $[Mn_2O(OAc)\{HB(pz)_3\}_2].CH_3CN$ (39a) shows the second kind (b) of distortion. In this the Mn-N bond, trans to the $Mn-O_{oxo}$ bond shortens. This can be seen from the Table 3.11. The shortening of the Mn-N bond with respect to the $Mn-N_{cis}$ bonds can be explained by empty dz^2 orbitals. The short $Mn-O_{oxo}$ bond raises the energy of the dz^2 orbital directed along the $Mn-O_{oxo}$ bond vector. This highest lying d-orbital is empty in high spin, d^4 Mn(III), resulting in a shortened trans Mn-N bond. Whatever be the kind of distortion, the major electronic consequences are expected to be the same for the two types of distortions.[109]

In both the complexes, D and E perchlorate anions are in general positions with relatively high thermal parameters. In D, the perchlorate anion is hydrogen bonded with the coordinated water molecule (Fig. 3.4) and solvent acetic acid molecule with coordinated nitrate ion. Bond lengths of solvent acid molecule in D, C=O (1.05 Å) and C-OH (1.30 Å) clearly show the presence of acetic acid. In E, both the perchlorate anions are hydrogen bonded (Fig. 3.5) with the coordinated water molecules (bond distances are < 3.5 Å).

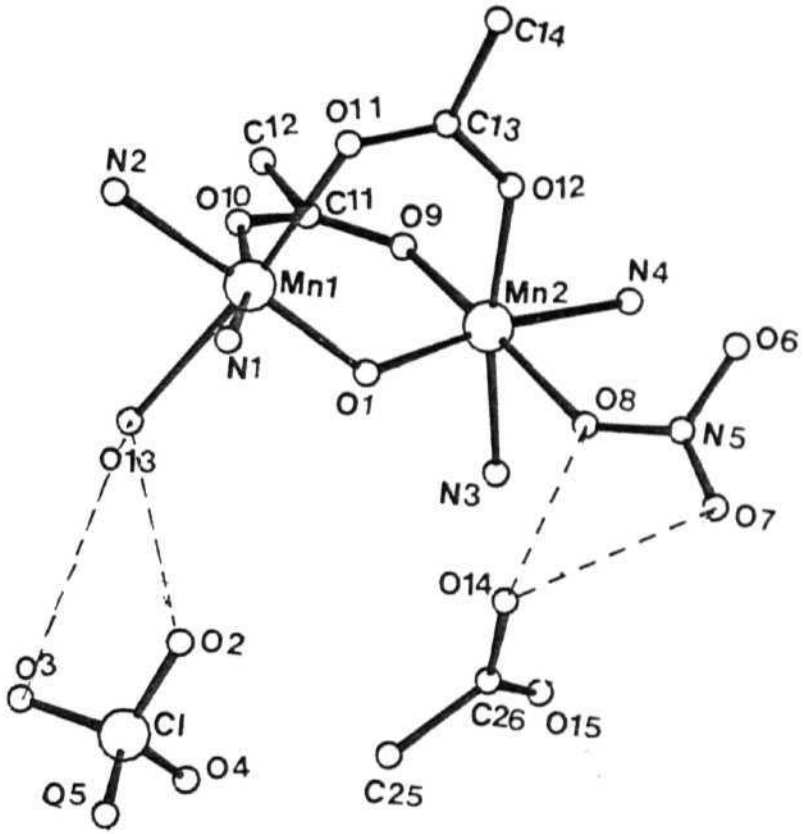

Fig 3.4. Hydrogen bonding net work in D (ring carbon atoms are excluded).

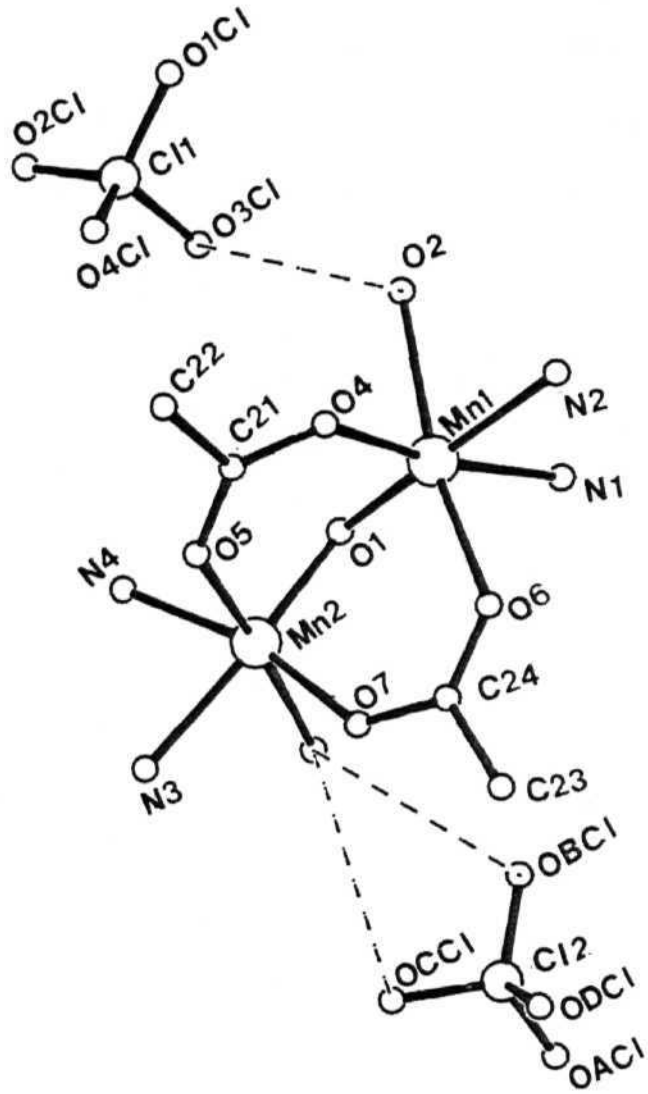

Fig 3.5. Hydrogen bonding net work in E (ring carbon atoms are excluded).

3.3.3. Infrared spectra. Characteristic bands of bridged acetate, ν_{as} (CO_2) 1580, $\nu_s(CO_2)$ 1400 cm^{-1} are observed for D and D.PF_6. A broad band around 3400 cm^{-1} is assigned to the ν_{OH} vibration. Ligand and anion bands are observed within the expected range. Presence of lattice acid molecule in D was observed with a doublet around 1740 cm^{-1} which is absent in D1.

3.3.4. Solution chemistry. Compounds are soluble in polar solvents and are not stable for a long time, depositing brown precipitates. Freshly prepared solutions of CH_3CN and H_2O does not show any bands in electronic spectra. Optical spectrum in acetate buffer (pH = 4.5) shows a band at 610 nm, which disappears slowly in the presence of excess ligand generating the well known Mn(III,IV) spectra (Fig. 3.6). This shows that the present compound undergoes disproportionation, which is observed for other higher valent complexes as described in the previous chapter.

3.3.5. EPR and Magnetic Properties. Assuming that there is only a small amount of E in D, room temperature magnetic data shows a magnetic moment value, 6.61 BM which is lower than the expected spin only value. This indicates that at room temperature there is antiferromagnetic interaction between the two metal centers. Previously known complexes with the dimetal manganese(III) core have weaker antiferromagnetic interactions. This can be explained

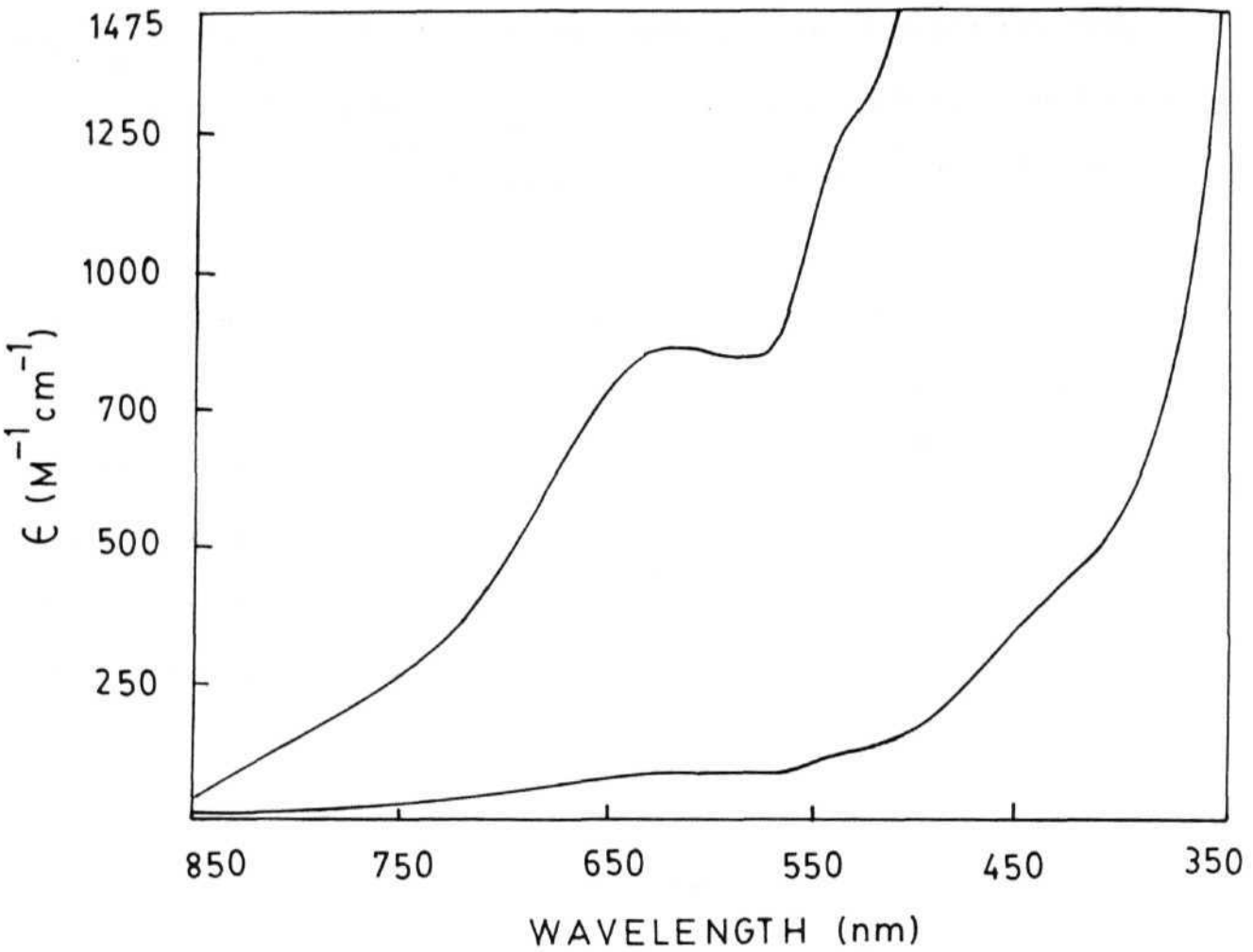

Fig 3.6(a) Electronic spectrum of D in acetate buffer (pH = 4.5).

(% of E neglected in ε calculation)

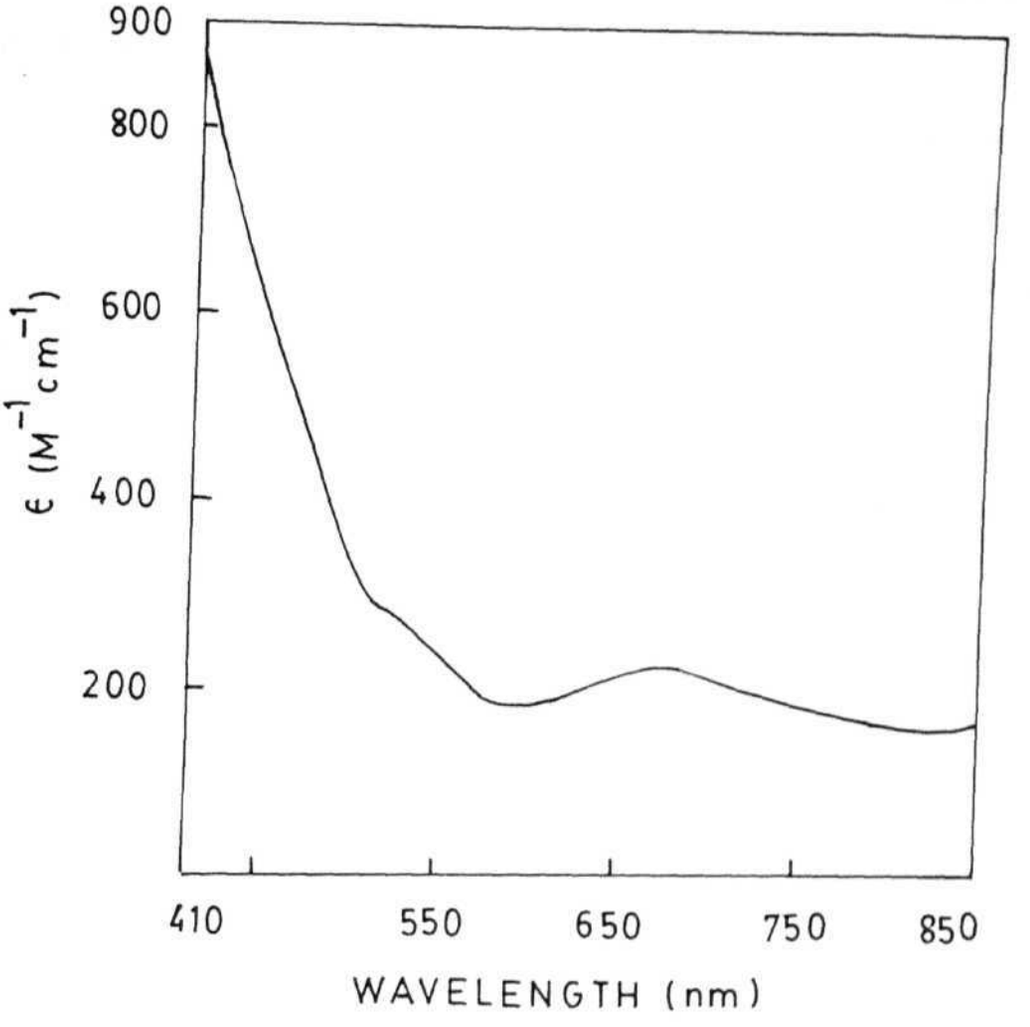

Fig 3.6(b) Electronic spectrum of D in ligand buffer (pH = 4.5).

(% of E neglected in ε calculation)

by longer Mn-Mn separation and decreased dx^2-y^2 interaction pathway. Detailed magnetic studies may provide further information in this direction.

Single crystal EPR spectra at 298 K and 150 K does not show any signal. Powder samples at higher amplitudes show a weak signal centered at $g \cong 2.0$ with Mn(II) signals. Since Mn(III) dimeric units are known to be EPR silent in the normal detection mode, weaker signal in the present case may be from Mn(II) or Mn(III,IV) impurity. Frozen solution spectrum in DMF shows Mn(II) signals with weak Mn(III,IV) signals (Fig. 3.7) as expected due to disproportionation of Mn(III) ions in solution generating small amounts of Mn(III,IV) species.

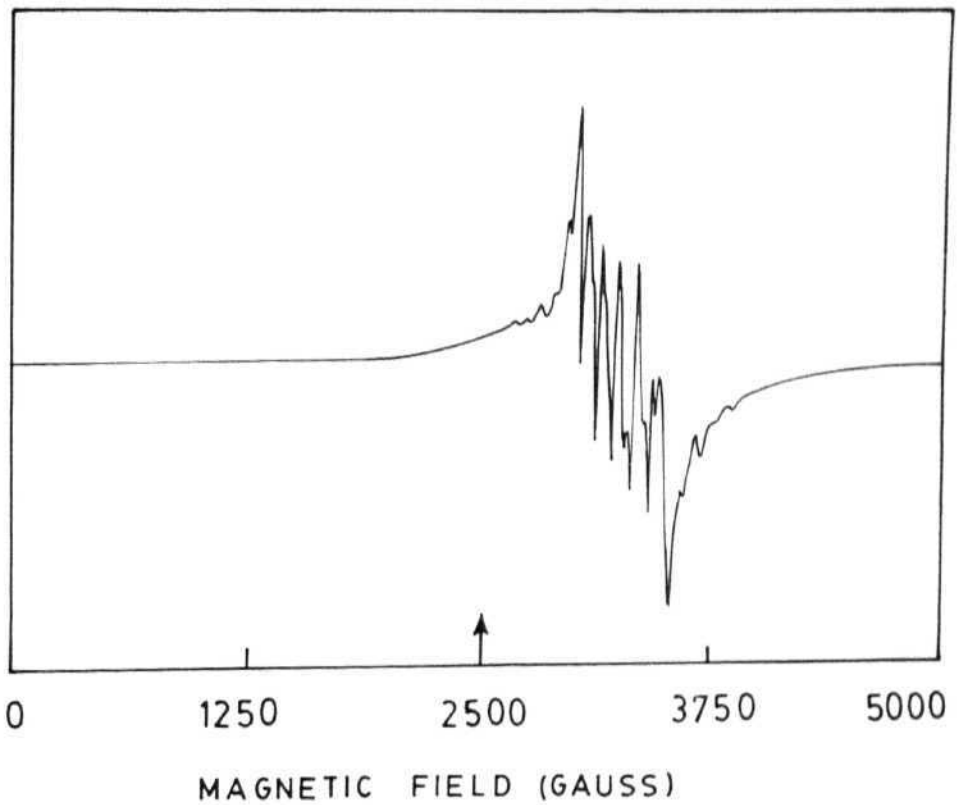

Fig 3.7. Frozen solution EPR spectrum of D1 in DMF at 147 K. (ν = 9.207 GHz)

CHAPTER 4.

SYNTHESIS AND STRUCTURAL CHARACTERISATION OF Mn(III) MONOMERS: $[Mn(phen)_2Cl_2](NO_3).2.5CH_3COOH$ and $[Mn(phen)(H_2O)Cl_3]$.

4.1. Introduction:

It is known that Mn(II) gets oxidised to Mn(III), but oxidation products are not known clearly. It can be a simple Mn(III) species or a mixture of oxidation states. Especially in aqueous solutions Mn(III) is quite unstable and disproportionates to give different products.

There are a few cationic compounds with neutral ligands; most of the reported chemistry involves anionic ligands with generally more electronegative donors such as O and F. However there is extensive chemistry with macrocyclic ligands.

Mononuclear Mn^{III} complexes with bpy and phen are rare. Early attempts by Nyholm and Turco[73] to synthesise $Mn(bpy)_3^{3+}$ led to the isolation of the di-μ-oxo dimer $Mn_2O_2(bpy)_4^{3+}$, which was later characterised by Cooper and Calvin.[77]

The present chapter describes the synthesis of two monomeric Mn^{III} complexes with phen ligand which are characterised by X-ray crystallography. Compound F $[Mn(phen)_2Cl_2](NO_3).2.5CH_3COOH$ was prepared by Ce(IV) oxidation whereas G $[Mn(phen)(H_2O)Cl_3]$ was synthesised by nitric acid oxidation. G was earlier prepared by

Goodwin and Sylva[78] by the reduction of MnO_4^- with HCl in the presence of ligand and it has been earlier used as precursor for Mn(III,IV)[77] and Mn(IV,IV)[76] complexes. The present preparation is simple and straightforward and gives crystalline material.

4.2. Experimental Section:

4.2.1. Materials: All the chemicals are analytical grade and are used as received. Solvent and other purification procedures are described in Section 2.2.1.

4.2.2. Preparation of Compounds:

4.2.2a. $[Mn(phen)_2Cl_2](NO_3).2.5CH_3COOH$: (F) To a solution of $Mn(OAc)_2.4H_2O$ (1.25 g, 5 mmol) in 8 ml of water, 20 ml of glacial acetic acid was added, followed by phen (2.0 g, 10 mmol). The resulting yellow solution was cooled and a saturated solution of $(NH_4)_2Ce(NO_3)_6$ (3.3 g, 6.0 mmol) was added with constant stirring. The colour of the solution changes to dark brown and to this a saturated solution of KCl (1.0 g, 13.4 mmol) was added. It was filtered and the filtrate kept in a desiccator for over one week. Brown-red crystals were deposited, which were filtered and dried. Yield: 1.6 g (44.9%) based on total available manganese. Anal. calcd for $C_{29}H_{26}N_5Cl_2O_8Mn$: C, 49.9; H, 3.75; N, 10.0, obs: C,

49.9; H, 3.35; N, 10.9. Acetic acid, estimated by titration with NaOH, calcd(obs) 21.5(21.7). Equivalent weight by iodometry; found (calcd) 636(698.5).

4.2.2b. $Mn(phen)(H_2O)Cl_3$: (G) 1.0 g (5.05 mmol) of phen ligand was dissolved in 20 ml of 50% HNO_3 solution and $MnCl_2.4H_2O$ was added (1.0 g, 5.05 mmol). The solution immediately turned light-brown and it was kept in a desiccator for a few days. Brown-red crystals were deposited which were filtered and washed with dil.HNO_3 solution and dried. Yield: 0.69 g (38%) based on total manganese. Anal, calcd for $C_{12}H_{10}N_2OCl_3Mn$, C, 40.1; H, 2.80; N, 7.79; obs: C, 39.95; H, 2.81; and N, 7.83. Equivalent weight by iodometry; found(calcd) 370(359.5).

4.2.3. Analysis, spectral and magnetic measurements: All the physical measurements were carried out as described in the Section 2.2.3.

4.2.4. X-ray Crystallography:

4.2.4a. $[Mn(phen)_2Cl_2](NO_3)$. $2.5CH_3COOH$ (F). Data was collected at room temperature on a Nicolet R3m/v diffractrometer using graphite monochromated MoKα radiation. Crystallographic data and data collection parameters are given in the Table 4.1. The compound

Table 4.1. Crystallographic Data for F.

formula	$MnC_{29}H_{26}N_5Cl_2O_8$	formula weight	698.42
a, Å	15.362(8)	space group	C2/c
b, Å	13.411(9)	ρ_{calcd} g cm^{-3}	1.75
c, Å	13.132(6)	λ Å	0.71073
β, deg	100.79(4)	2θ range:	$2 - 52^{o}$
V, $Å^3$	2657(2)	Z	4
diffractometer: Nicolet R3m/v		data collected	2774
data used ($F > 5\sigma(F)$)	1159	monochromator	graphite
μ, cm^{-1}	6.92	T, K	298
F(000)	1407.97	no of variables	179
R^a	0.093	$R_w{}^b$	0.082

[a] $R = (\sum\|F_o|-|F_c\|) / \sum|F_o|$

[b] $R_w = \{ [\sum w (|F_o|-|F_c|)^2] / \sum w F_o^2 \}^{1/2}$

$w^{-1} = \sigma^2 |F_o| + g |F_o|^2$; $g = 0.0001$

crystallises in monoclinic system and space group could be C2/c or Cc based on systematic absences of hkl reflections. The structure was refined in C2/c. A combination of heavy atom and direct methods (SHELXS-86)[180] followed by difference Fourier and full matrix-least squares method (SHELX-76)[179] were used. Of the total 2774 reflections only 1159 reflections with $F > 5\sigma(F)$ were used for the structure refinement. All the non-hydrogen atoms of the cation were readily found in the Fourier map and refined anisotropically. The ring hydrogens were fixed and their common isotropic thermal parameters were refined. The nitrate ion in the special position and solvent acetic acid molecules which were located in channels formed by the aromatic rings of the symmetry related cations, were in severe disorder. At this stage the difference Fourier map showed four major peaks which were assigned as oxygen atoms and refined anisotropically. The final difference map showed a residual electron density (peak value 1.6 $e^-/Å^3$) along the two fold axis corresponding to the disordered nitrate anion. Atomic coordinates, bond lengths and angles and thermal parameters are given in the Tables 4.2 to 4.4.

4.2.4b. $Mn(phen)(H_2O)Cl_3$: (G) Data for a brown-red crystal of dimension 0.4 × 0.2 × 0.08 mm were collected at room temperature on an Enraf-Nonius CAD-4 diffractrometer using MoKα radiation. Parameters of the crystal and intensity measurements are given in

Table 4.2. Fractional Coordinates and Isotropic or Equivalent Thermal Parameters for F.[a]

ATOM	x	y	z	$U_{(eq)}$ [b]
Mn	0.0000(0)	0.3368(2)	0.2500(0)	0.039(1)
Cl	0.1088(2)	0.4507(2)	0.2621(2)	0.053(1)
N(1)	-0.0954(6)	0.2260(6)	0.2183(6)	0.044(2)
N(2)	-0.0137(6)	0.3174(6)	0.0790(5)	0.041(2)
C(1)	-0.1354(8)	0.1809(9)	0.2868(8)	0.061(3)
C(2)	-0.1998(8)	0.1100(9)	0.2608(8)	0.067(3)
C(3)	-0.2280(8)	0.0851(9)	0.1574(8)	0.060(3)
C(4)	-0.1896(7)	0.1327(8)	0.0832(8)	0.049(3)
C(5)	-0.2179(8)	0.1136(8)	-0.0265(8)	0.055(3)
C(6)	-0.1763(8)	0.1605(9)	-0.0965(7)	0.056(3)
C(7)	-0.1073(8)	0.2312(8)	-0.0647(7)	0.046(3)
C(8)	-0.0666(8)	0.2869(9)	-0.1330(8)	0.058(3)
C(9)	-0.0004(9)	0.3539(9)	-0.0954(8)	0.063(3)
C(10)	0.0240(7)	0.3667(8)	0.0117(8)	0.048(3)
C(11)	-0.1225(7)	0.2012(7)	0.1153(7)	0.039(3)
C(12)	-0.0785(7)	0.2519(8)	0.0417(7)	0.041(3)
O(1)*	0.335(2)	0.334(2)	0.132(1)	0.317(4)
O(2)*	0.244(2)	0.318(2)	0.011(2)	0.370(4)
O(3)*	0.479(2)	0.464(2)	0.142(2)	0.474(4)
O(4)*	0.403(2)	0.404(2)	0.022(2)	0.479(4)

[a] Ring hydrogen atoms are fixed and refined with a common thermal parameter 0.086(6).

[b] $U(eq) = (1/3)(U_{11}a^2a^{*2} + U_{22}b^2b^{*2} + U_{33}c^2c^{*2} + U_{12}a^*b^*ab\cos\gamma + U_{13}a^*c^*ac\cos\beta + U_{23}b^*c^*bc\cos\alpha)$

* atoms blonging to disordered acetic acid.

Table 4.3. Bond Lengths (Å) and Angles (°) for F.[a]

Cl---	Mn		2.248(3)	N(1)-	Mn-	Cl	171.6(2)
N(1)---	Mn		2.073(9)	N(2)-	Mn-	Cl	94.6(2)
N(2)---	Mn		2.231(7)	N(2)-	Mn-	N(1)	77.6(3)
C(1)---	N(1)		1.327(12)	Cl-	Mn-	Cl'	94.4(2)
C(11)---	N(1)		1.380(10)	N(1)-	Mn-	Cl'	89.1(3)
C(10)---	N(2)		1.321(11)	N(2)-	Mn-	Cl'	94.5(3)
C(12)---	N(2)		1.349(12)	C(1)-	N(1)-	Mn	126.2(7)
C(2)---	C(1)		1.368(15)	C(11)-	N(1)-	Mn	116.3(6)
C(3)---	C(2)		1.387(13)	C(11)-	N(1)-	C(1)	117.5(10)
C(4)---	C(3)		1.385(13)	N(1)-	Mn-	N(1)'	88.4(5)
C(5)---	C(4)		1.448(13)	C(10)-	N(2)-	Mn	130.1(7)
C(11)---	C(4)		1.386(13)	C(12)-	N(2)-	Mn	111.4(6)
C(6)---	C(5)		1.367(14)	C(12)-	N(2)-	C(10)	118.0(9)
C(7)---	C(6)		1.426(14)	C(2)-	C(1)-	N(1)	123.5(10)
C(8)---	C(7)		1.400(14)	C(3)-	C(2)-	C(1)	119.4(10)
C(9)---	C(8)		1.377(15)	C(4)-	C(3)-	C(2)	118.7(11)
C(10)---	C(9)		1.397(13)	C(5)-	C(4)-	C(3)	122.0(11)
C(12)---	C(11)		1.448(13)	C(11)-	C(4)-	C(3)	118.9(10)
C(7)---	C(12)		1.412(12)	C(11)-	C(4)-	C(5)	119.2(9)
C(8)-	C(7)-	C(6)	124.3(10)	C(6)-	C(5)-	C(4)	119.8(11)
C(12)-	C(7)-	C(8)	115.7(11)	C(7)-	C(6)-	C(5)	121.6(10)
C(10)-	C(9)-	C(8)	118.9(10)	C(12)-	C(7)-	C(6)	119.9(9)
C(4)-	C(11)-	N(1)	121.9(9)	C(9)-	C(8)-	C(7)	120.4(10)
C(12)-	C(11)-	C(4)	121.5(9)	C(9)-	C(10)-	N(2)	122.9(11)
C(11)-	C(12)-	N(2)	118.0(9)	C(12)-	C(11)-	N(1)	116.6(9)
C(7)-	C(12)-	N(2)	124.1(9)				

[a] The ' denotes atoms related by the two-fold axis passing through the Mn atom.

Table 4.4. Anisotropic Thermal Parameters for F.[a]

ATOM	U11	U22	U33	U23	U13	U12
Mn	0.040(2)	0.042(1)	0.035(1)	0.000(0)	0.011(1)	0.000(0)
Cl	0.050(2)	0.052(2)	0.054(2)	0.003(1)	0.010(1)	-0.006(2)
N(1)	0.048(4)	0.041(4)	0.040(4)	0.002(3)	0.013(4)	-0.005(4)
N(2)	0.036(4)	0.049(4)	0.037(3)	-0.002(3)	0.006(3)	-0.003(4)
C(1)	0.076(5)	0.060(5)	0.046(4)	0.003(4)	0.024(4)	-0.004(5)
C(2)	0.072(5)	0.068(5)	0.058(5)	0.007(4)	0.015(4)	-0.027(5)
C(3)	0.046(5)	0.060(5)	0.070(5)	-0.012(4)	0.007(4)	-0.015(5)
C(4)	0.044(5)	0.047(5)	0.056(4)	-0.003(4)	0.022(4)	0.000(4)
C(5)	0.046(5)	0.061(5)	0.052(4)	-0.006(4)	-0.009(4)	-0.013(4)
C(6)	0.060(5)	0.060(5)	0.042(4)	-0.007(4)	-0.002(4)	-0.003(5)
C(7)	0.056(5)	0.042(4)	0.039(4)	-0.001(4)	0.012(4)	0.006(4)
C(8)	0.065(5)	0.067(5)	0.040(4)	0.009(4)	0.013(4)	0.011(5)
C(9)	0.070(5)	0.072(5)	0.045(4)	0.008(4)	0.018(4)	-0.001(5)
C(10)	0.045(5)	0.046(6)	0.052(4)	0.008(4)	0.017(4)	-0.004(4)
C(11)	0.034(4)	0.044(4)	0.035(4)	-0.007(4)	-0.001(4)	0.001(4)
C(12)	0.038(6)	0.046(4)	0.036(4)	0.004(4)	0.009(4)	0.009(4)
O(1)	0.376(6)	0.377(6)	0.194(6)	0.103(6)	0.091(6)	0.225(6)
O(2)	0.388(6)	0.378(6)	0.347(6)	0.034(6)	0.156(6)	-0.027(6)
O(3)	0.347(6)	0.372(6)	0.677(6)	-0.184(6)	0.055(6)	0.250(6)
O(4)	0.682(6)	0.344(6)	0.334(6)	-0.122(6)	-0.082(6)	0.368(6)

[a] The temperature factor expression used is

$$\exp\left[-2\pi^2(U_{11}h^2a^{*2} + U_{22}k^2b^{*2} + U_{33}l^2c^{*2} + 2U_{12}hka^*b^*\cos\gamma^* + 2U_{13}hla^*c^*\cos\beta^* + 2U_{23}klb^*c^*\cos\alpha^*)\right]$$

the Table 4.5. The complex crystallises in the triclinic system, and space group could be P1 or $P\bar{1}$. Structure was refined in $P\bar{1}$. A combination of heavy atom and direct methods (SHELXS-86)[180] followed by difference Fourier and full matrix-least squares method (SHELX-76)[179] were used.Out of 2466 total reflections only 2098 reflections with $F > 5\sigma(F)$ were used for refinement. All the non-hydrogen atoms were found on the Fourier map and refined anisotropically. Hydrogen atoms were included by riding model on an adjacent atom and refined with common temperature factors. Atomic coordinates, bond lengths and angles and temperature factors are given in Tables 4.6 to 4.9.

4.3. Results and Discussions:

4.3.1. Synthesis: Compounds F and G are formed by Ce(IV) and nitric acid oxidations respectively. From the studies described in the previous chapters it is clear that Ce(IV) oxidises Mn^{II} to Mn^{III}, which in turn undergoes disproportionation leading to the formation of higher nuclearity complexes. Nitric acid oxidation leading to G has been achieved by reducing the Mn^{II}/Mn^{III} oxidation potential in the presence of the ligand and chloride ions. Since the reaction was carried out in aerobic conditions, aerial oxidation can not be ruled out. Compound G was earlier prepared by Goodwin and Sylva by reduction of MnO_4^- by HCl in the

Table 4.5. Crystallographic Data for G.

chemical formula	$C_{12}H_{10}N_2OCl_3Mn$	formula weight	359.5
a, Å	6.722(1)	space group	$P\bar{1}$
b, Å	10.201(1)	temp, K	296
c, Å	10.510(1)	ρ_{calc}, g cm^{-3}	1.79
α, deg	80.69(1)	V, $Å^3$	666.9(2)
β, deg	79.59(1)	Z	2
γ, deg	71.21(1)	λ, Å	0.71073
μ, cm^{-1}	7.42	radiation	MoKα
diffractometer	Enraf Nonius CAD-4	crystal size, mm	0.27×0.2×0.1
monochromator	graphite	F(000)	179.99
data used		data collected	2466
(F > 5.0 σ(F))	2098	no. of variables	180
R^a	0.027	$R_w{}^b$	0.030

[a] $R = (\sum\| |F_o| - |F_c| \|) / \sum |F_o|$

[b] $R_w = \{ [\sum w (|F_o| - |F_c|)^2] / \sum w F_o^2 \}^{1/2}$

$w^{-1} = \sigma^2 |F_o| + g |F_o|^2$; g = 0.00008

Table 4.6. Fractional Atomic Coordinates and Equivalent Isotropic Temperature Factors for G.[a]

Atom	x/a	y/b	z/c	Ueq[b]
Mn	0.2124(1)	0.1969(0)	0.1581(0)	0.025(0)
Cl1	0.1909(1)	-0.0155(1)	0.1476(1)	0.044(0)
Cl2	-0.1822(1)	0.3038(1)	0.2194(1)	0.036(0)
Cl3	0.2296(1)	0.2548(1)	-0.0560(1)	0.043(0)
N1	0.2340(3)	0.1576(2)	0.3559(2)	0.025(1)
N2	0.2507(3)	0.3814(2)	0.1905(2)	0.024(1)
O1	0.5772(3)	0.1127(2)	0.1421(2)	0.036(1)
H1O1	0.644(7)	0.744(5)	0.061(3)	0.13(1)
H2O1	0.678(6)	0.164(4)	0.106(4)	0.13(1)
C1	0.2281(4)	0.0428(3)	0.4357(3)	0.031(1)
C2	0.2294(4)	0.0340(3)	0.5696(3)	0.037(1)
C3	0.2385(4)	0.1453(3)	0.6216(3)	0.039(1)
C4	0.2477(4)	0.2686(3)	0.5400(2)	0.031(1)
C5	0.2552(4)	0.3919(3)	0.5849(3)	0.039(1)
C6	0.2639(4)	0.5061(3)	0.5003(3)	0.038(1)
C7	0.2693(4)	0.5065(3)	0.3635(3)	0.031(1)
C8	0.2825(4)	0.6201(3)	0.2693(3)	0.038(1)
C9	0.2775(4)	0.6123(3)	0.1435(3)	0.039(1)
C10	0.2591(4)	0.4920(3)	0.1049(3)	0.033(1)
C11	0.2475(3)	0.2686(2)	0.4066(2)	0.024(1)
C12	0.2567(3)	0.3884(2)	0.3180(2)	0.024(1)

[a] Water hydrogen atoms are refined isotropically. Ring hydrogen atoms are fixed and refined with a common thermal parameter 0.047(3).

[b] $U(eq) = (1/3)(U_{11}a^2a^{*2} + U_{22}b^2b^{*2} + U_{33}c^2c^{*2} + U_{12}a^*b^*ab\cos\gamma + U_{13}a^*c^*ac\cos\beta + U_{23}b^*c^*bc\cos\alpha)$

Table 4.7. Bond distances (Å) for G.

Mn ---Cl1	2.239(1)	Mn ---Cl2	2.528(1)
Mn ---Cl3	2.223(1)	Mn ---N2	2.067(2)
Mn ---N1	2.075(2)	Mn ---O1	2.306(2)
N2 ---C12	1.362(3)	C11 ---C12	1.423(3)
C7 ---C12	1.398(3)	N1 ---C11	1.361(3)
C4 ---C11	1.402(3)	N2 ---C10	1.335(3)
C9 ---C10	1.402(4)	N1 ---C1	1.332(3)
C1 ---C2	1.397(4)	C2 ---C3	1.359(4)
C3 ---C4	1.415(4)	C4 ---C5	1.432(4)
C5 ---C6	1.357(4)	C6 ---C7	1.432(4)
C7 ---C8	1.412(4)	C8 ---C9	1.344(4)

Table 4.8. Bond angles (^{o}) for G.

Cl2 -Mn -Cl1	94.7(0)	Cl3 -Mn -Cl1	93.7(0)
Cl3 -Mn -Cl2	98.4(0)	N2 -Mn -Cl1	172.2(1)
N2 -Mn -Cl2	87.9(1)	N2 -Mn -Cl3	93.2(1)
N1 -Mn -Cl1	93.0(1)	N1 -Mn -Cl2	87.2(1)
N1 -Mn -Cl3	170.9(1)	N1 -Mn -N2	79.8(1)
O1 -Mn -Cl1	91.3(1)	O1 -Mn -Cl2	168.3(1)
O1 -Mn -Cl3	91.3(1)	O1 -Mn -N2	85.0(1)
O1 -Mn -N1	82.4(1)		
C10 -N2 -Mn	128.3(2)	C10 -N2 -C12	118.4(2)
C1 -N1 -Mn	128.4(2)	C1 -N1 -C11	118.6(2)
C11 -N1 -Mn	113.0(2)	C12 -N2 -Mn	113.2(2)
C4 -C11 -N1	122.5(2)	C12 -C11 -N1	116.9(2)
C4 -C11 -C12	120.5(2)	C7 -C12 -C11	119.9(2)
C7 -C12 -N2	123.1(2)	C11 -C12 -N2	117.0(2)
C2 -C1 -N1	122.3(2)	C3 -C2 -C1	119.5(3)
C3 -C4 -C11	117.0(2)	C4 -C3 -C2	120.0(2)
C5 -C4 -C11	118.6(2)	C5 -C6 -C7	121.2(2)
C5 -C4 -C3	124.4(2)	C4 -C5 -C6	120.9(2)
C6 -C7 -C12	118.8(2)	C7 -C8 -C9	120.0(2)
C8 -C7 -C6	124.5(2)	C8 -C7 -C12	116.7(2)
C8 -C9 -C10	120.5(3)	C9 -C10 -N2	121.3(2)

Table 4.9. Anisotropic Thermal Parameters for G.[a]

ATOM	U11	U22	U33	U23	U13	U12
Mn	0.0319(2)	0.0231(2)	0.0165(2)	-0.0034(2)	-0.0043(2)	-0.0073(2)
Cl1	0.0595(5)	0.0299(4)	0.0375(4)	-0.0121(3)	0.0009(3)	-0.0180(3)
Cl2	0.0294(3)	0.0364(4)	0.0371(4)	-0.0090(3)	-0.0054(3)	-0.0066(3)
Cl3	0.0542(4)	0.0491(4)	0.0178(3)	-0.0026(3)	-0.0091(3)	-0.0127(3)
N1	0.024(1)	0.024(1)	0.021(1)	-0.0015(8)	-0.0029(8)	-0.0053(8)
N2	0.026(1)	0.022(1)	0.019(1)	-0.0010(9)	-0.0039(8)	-0.0048(8)
O1	0.032(1)	0.041(1)	0.029(1)	-0.0084(8)	-0.0021(8)	-0.0069(8)
C1	0.030(1)	0.030(1)	0.028(1)	0.004(1)	-0.005(1)	-0.010(1)
C2	0.036(1)	0.042(2)	0.026(1)	0.009(1)	-0.005(1)	-0.011(1)
C3	0.035(1)	0.056(2)	0.019(1)	0.00391)	-0.006(1)	-0.012(1)
C4	0.023(1)	0.043(1)	0.022(1)	-0.005(1)	-0.004(1)	-0.007(1)
C5	0.031(1)	0.053(2)	0.027(1)	-0.015(1)	-0.005(1)	-0.010(1)
C6	0.028(1)	0.043(2)	0.038(2)	-0.019(1)	-0.005(1)	-0.009(1)
C7	0.022(1)	0.029(1)	0.037(1)	-0.010(1)	-0.003(1)	-0.005(1)
C8	0.035(1)	0.026(1)	0.049(2)	-0.007(1)	-0.008(1)	-0.008(1)
C9	0.043(2)	0.025(1)	0.043(2)	0.006(1)	-0.008(1)	-0.009(1)
C10	0.036(1)	0.028(1)	0.029(1)	0.004(1)	-0.005(1)	-0.008(1)
C11	0.021(1)	0.027(1)	0.019(1)	-0.003(1)	-0.002(1)	-0.004(1)
C12	0.021(1)	0.026(1)	0.021(1)	-0.005(1)	-0.0032(9)	-0.0038(9)

[a] The Temperature factor expression used

$$\exp\left[-2\pi^2 \left(U_{11}h^2a^{*2} + U_{22}k^2b^{*2} + U_{33}l^2c^{*2} + 2U_{12}hka^*b^*\cos\gamma^* + 2U_{13}hla^*c^*\cos\beta^* + 2U_{23}klb^*c^*\cos\alpha^*\right)\right]$$

presence of ligand.[78] The present procedure is a more straightforward method which gives good crystalline material.

Stabilization of monomeric Mn^{III} species was achieved by the presence of chlorides. It is known from earlier studies of Christou[150,153,159] that chloride can abstract bridged acetate and oxide groups. At higher concentration of chloride, they isolated $[Mn(bpy)Cl_3]_n$ which has a polymeric network.[194] Wieghardt *et al.* also observed the dissociation of Mn(III,III) dimers in the presence of chlorides.[108]

From the previous observations and from our experimental results, it is clear that manganese(III) monomers can be formed either by the simple substitution of chlorides at the initially formed manganese(III) aquo-hydroxo species or the dissociation of the initially formed Mn(III,III) dimers (see Scheme-1 in Section 2.3.1).

4.3.2. Structure: Molecular structures of F and G are shown in the Fig. 4.1 and 4.2. Both the complexes have distorted octahedral geometry and expected Jahn-Teller distortion was observed along N(2)-Mn-N(2)' in F and Cl2-Mn-OH_2 in G. The manganese atom in F lies on a two-fold axis. Four ligand N-atom and two Cl^- completes the six coordination around the metal center, axial Mn-N(2) bond being 0.16 Å longer than the equatorial Mn-N(1) bond. This may be contrasted with the nearly equal equatorial (2.27 Å) and axial

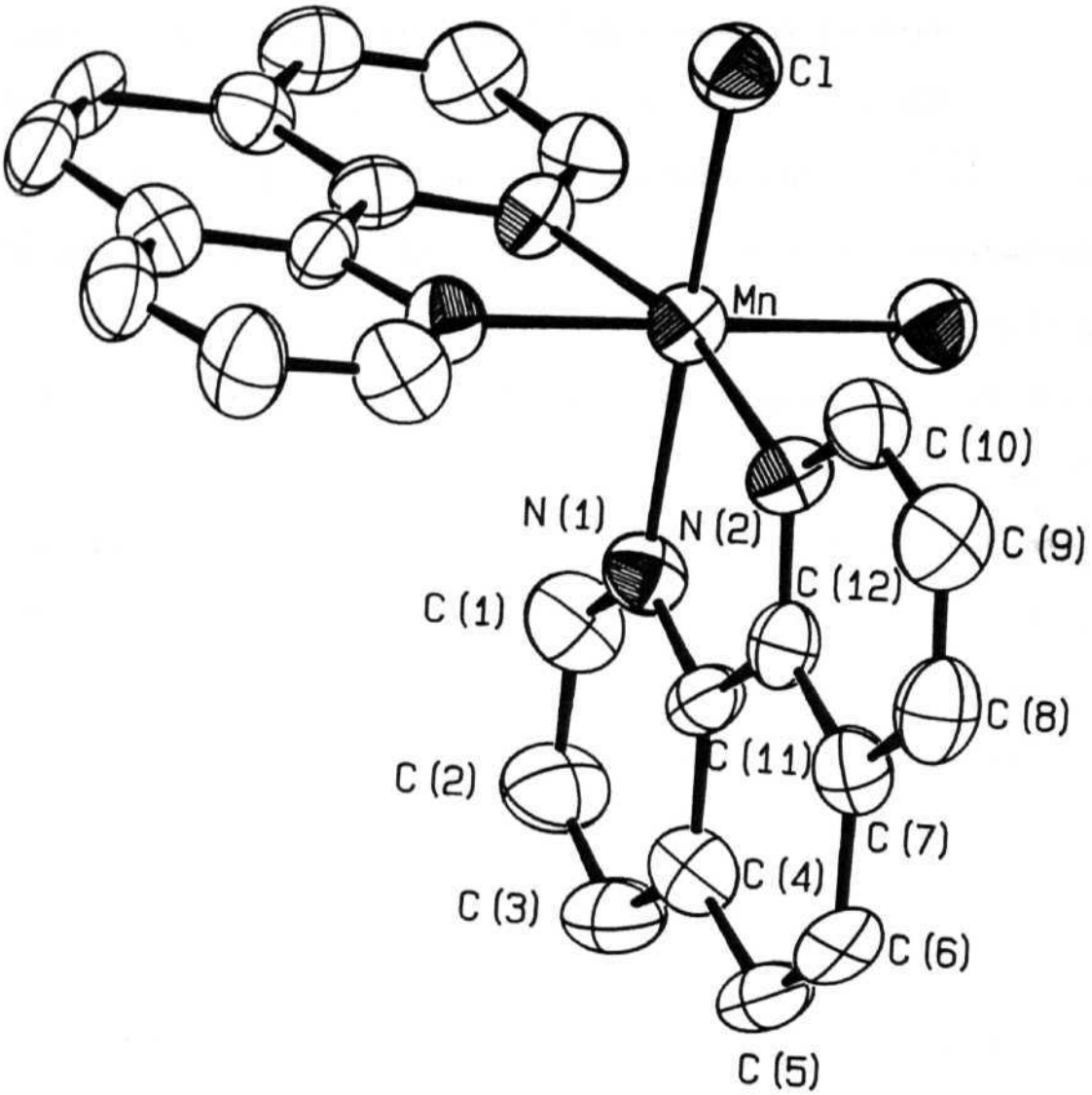

Fig. 4.1. ORTEP view of the cation of F.

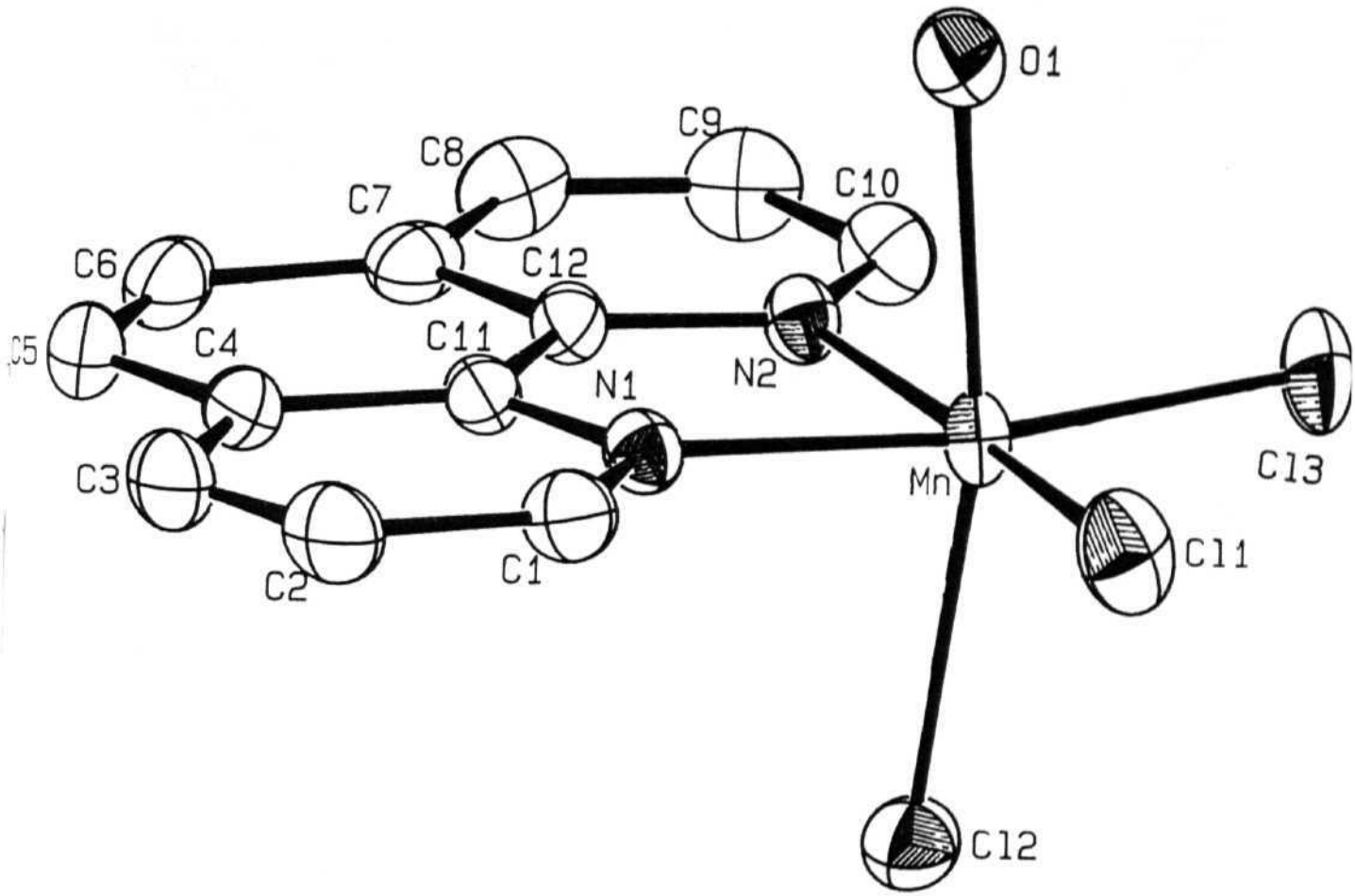

Fig. 4.2. ORTEP view of G.

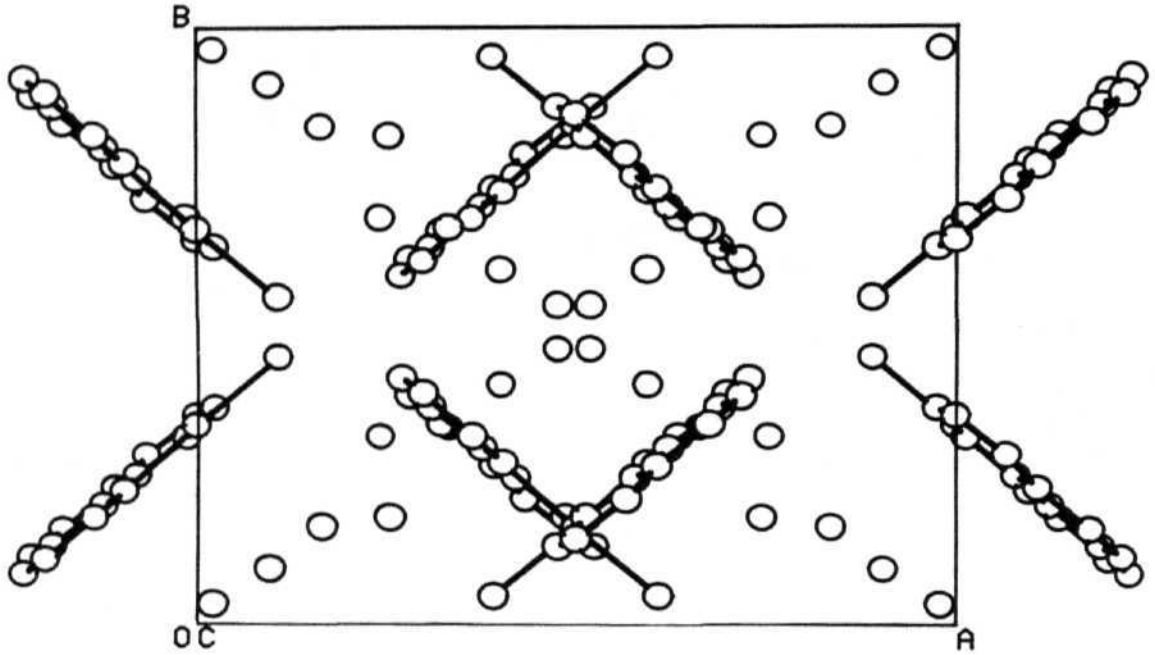

Fig. 4.3. Unit cell packing diagram of F.

(2.34 Å) Mn-N bonds seen in the Mn(II) complex *cis*-$Mn(bpy)_2Cl_2$.[195] Further, Cl-Mn-Cl angle (100.7°) in $Mn(bpy)_2Cl_2$ shows greater deviation from orthogonality in spite of longer Mn-Cl bonds (2.44 Å). This is a consequence of the greater electrostatic repulsions between the *cis*-Cl ions in the Mn(II) complex which has lesser internal charge compensation compared to the Mn(III) complex. It is true for G also which has a smaller Cl-Mn-Cl angle (93.7°) between the equatorial chloride ions. This observation also has a bearing on the non-occurrence of structures like *cis*-CuL_2Cl_2.[196] Fig. 4.3 shows the close packing arrangement of the cations with the disordered nitrate and solvent acetic acid molecules in the channels between the aromatic rings of the ligand.

In the compound G, octahedral geometry was completed by two N-atoms of the ligand and three Cl^- ions, the sixth coordination site was completed by water coordination. It has a severe axial distortion and a deviation of 0.3 Å was observed between axial Mn-Cl and equatorial Mn-Cl bonds. There are only four structurally characterised mononuclear Mn(III) complexes known in the literature with water coordination.[197-201] The present complex shows the longest Mn-OH_2 (2.306 Å) compared with the reported complexes in the literature. The geometric data on the aquo complexes are collected in Table 4.10 .

Lattice was stabilised by hydrogen bonding (Fig. 4.4) between Cl2 and H_2O bound to the neighboring molecule along the b-axis

Table 4.10. $Mn-OH_2$ bond distances (Å) in Mn(III) complexes.[a]

complex	$Mn-OH_2$ (Å)	ref
$[Mn(TTP)(H_2O)]^+$	2.105	197
$[Mn(mal)_2(H_2O)_2]^-$	2.299;2.276	198,199
$[Mn(F)_4(H_2O)_2]^-$	2.260	200
$[Mn(acac)(H_2O)_2]^+$	2.240;2.270	201
$Mn(phen)(H_2O)Cl_3$	2.306	present work

[a] in all the complexes H_2O coordinated in axial position

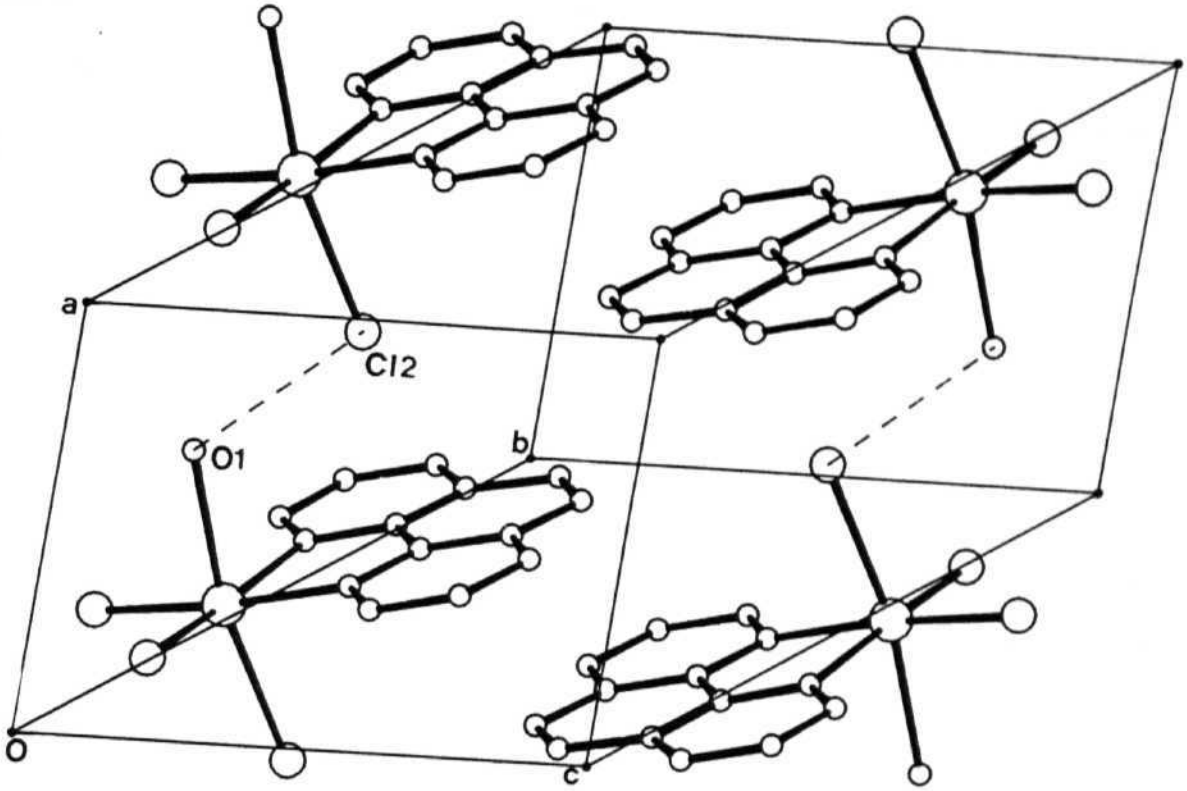

Fig. 4.4. Unit cell packing diagram of G.

(O1....Cl2, 3.178 Å).

4.3.3. Solution chemistry: Compound F is soluble in polar solvents, like H_2O, DMF, CH_3CN and ligand buffers. Optical spectrum (Fig. 4.5) in ligand buffer (pH = 4.5) shows the near quantitative conversion of Mn(III) to Mn(III,IV) according to the following equation:

$$3Mn(III) \longrightarrow Mn_2(III,IV) + Mn(II)$$

A similar spectrum was observed in water. This is expected because the solvated acetic acid molecules decreases the pH of the solution, thereby stabilising the Mn(III,IV) species formed (Fig. 4.6). In a mixture of CH_3CN and water solution, a Mn(III,IV) μ-oxo dimeric complex was precipitated by the addition of aqueous sodium perchlorate solution. A freshly prepared solution of F in CH_3CN shows (Fig. 4.7) a band at 526 nm assigned to the d-d transition,[202] $^5E_g \rightarrow {}^5T_{2g}$ in Oh symmetry. No bands are observed in DMF solution in the visible region.

Optical spectra of G are recorded in ligand buffer and water. The compound is not stable in DMF, and slowly reduces to Mn(II). On the other hand, it is not soluble in CH_3CN and DCM. In ligand buffer it converts into Mn(III,IV) (Fig. 4.8(a)) while the absence of ligand leads to the deposition of a brown precipitate. In water, optical spectrum show two bands at 765 and 625 nm; (Fig. 4.8(b)) these bands are also observed for higher valent compounds,

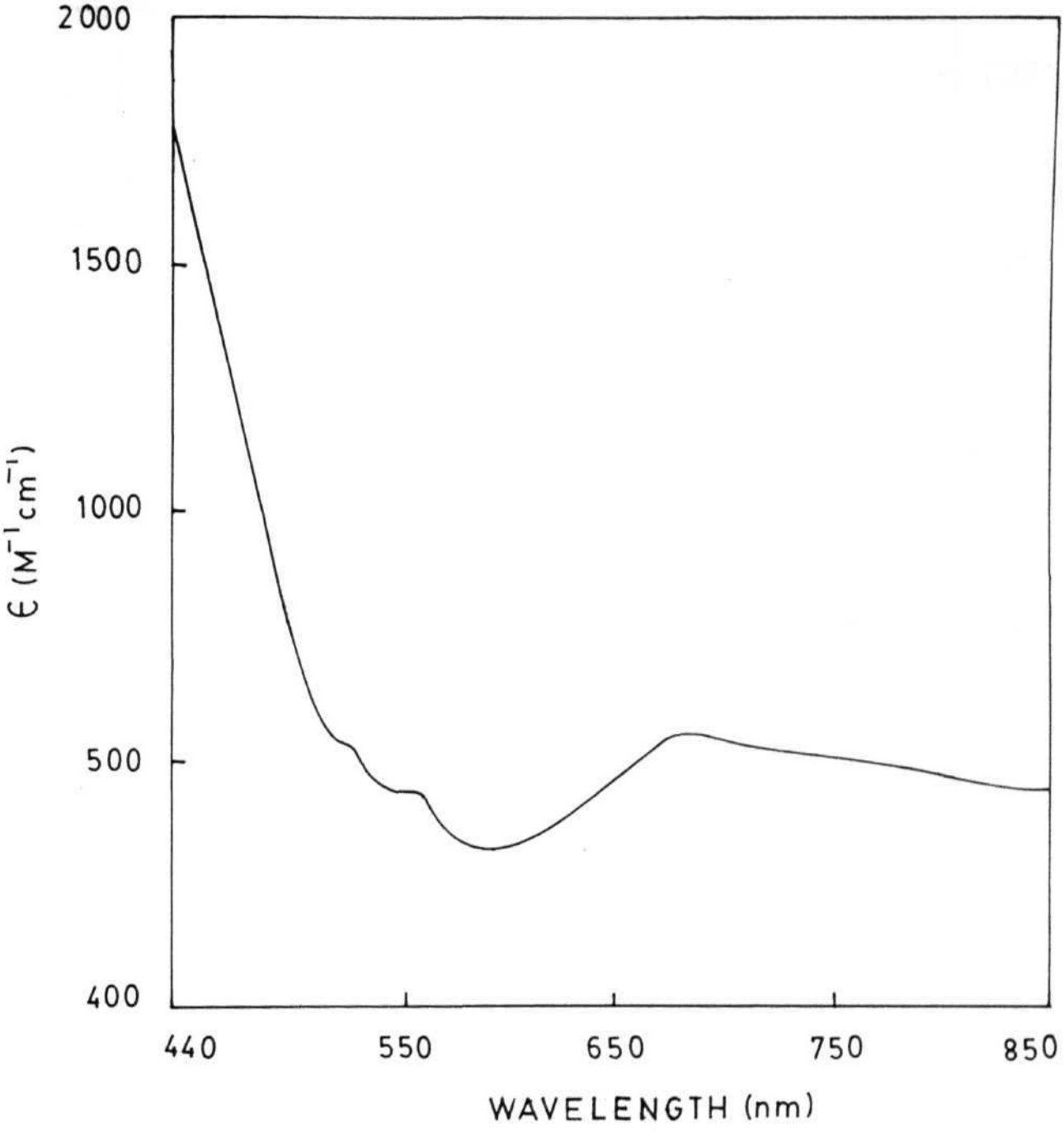

Fig. 4.5. Electronic spectrum of F in ligand buffer. (pH = 4.5)

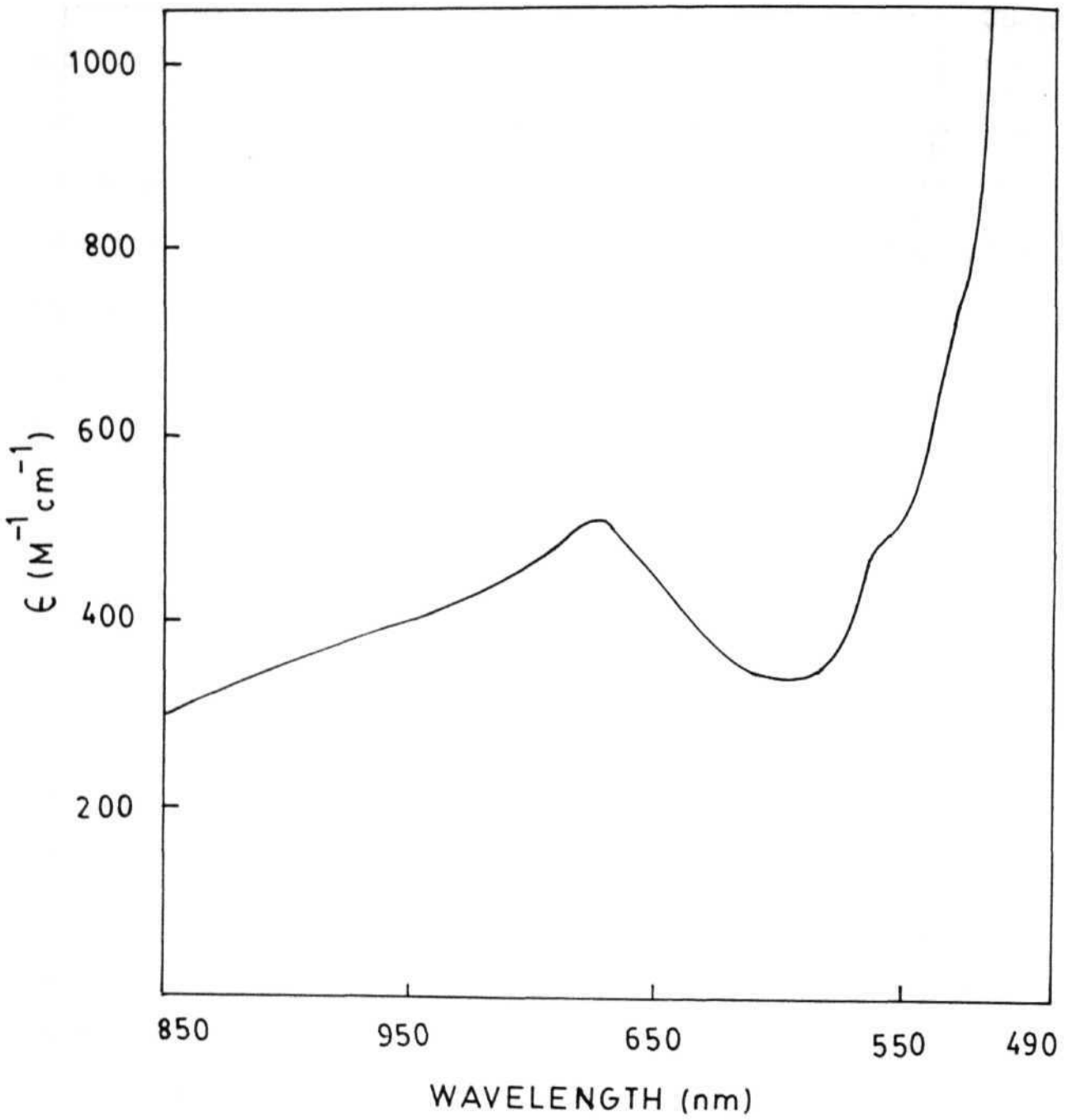

Fig. 4.6(a). Electronic spectrum of F in H_2O.

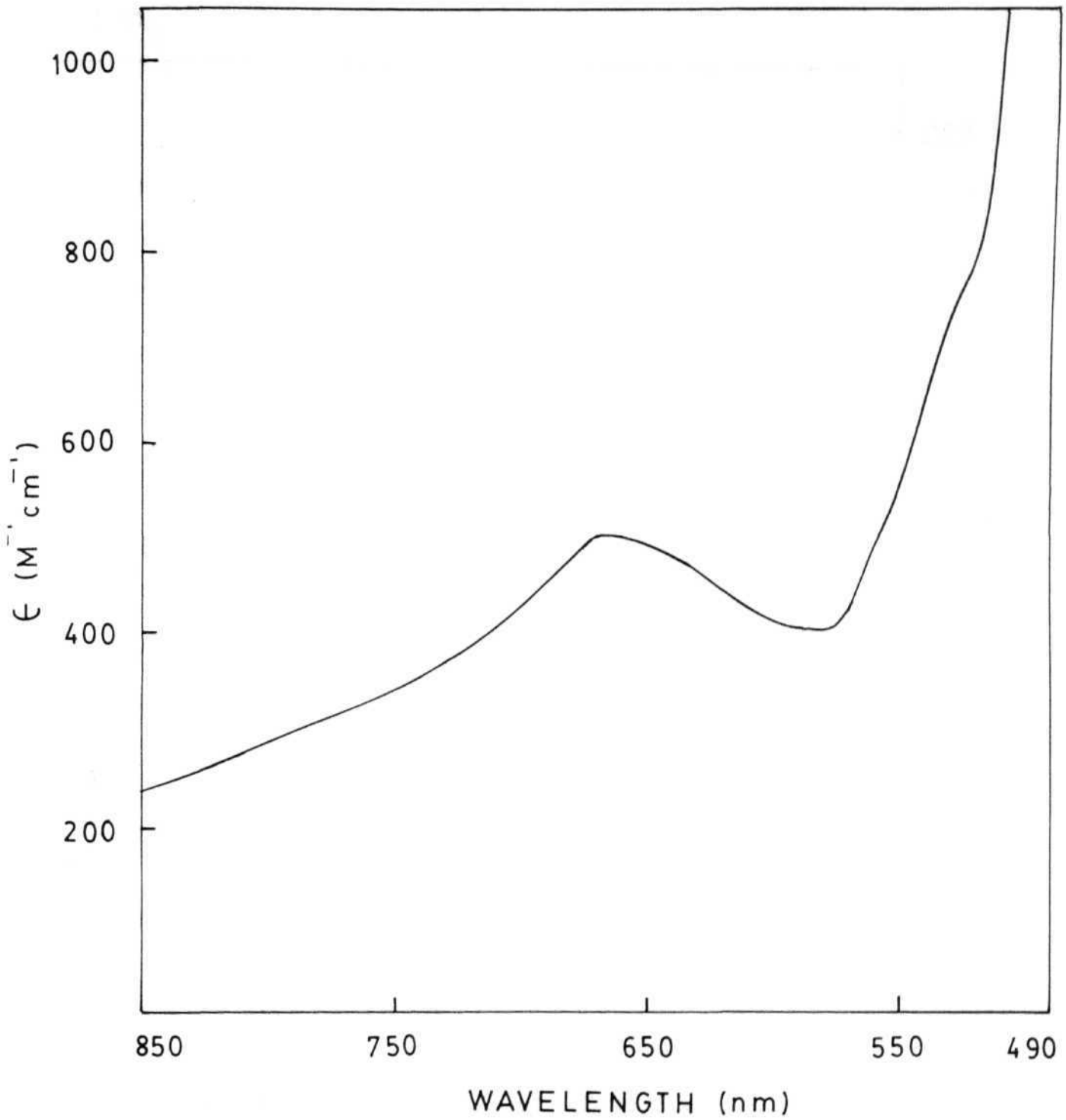

Fig. 4.6(b). Electronic spectrum of F in acetate buffer. (pH = 4.5)

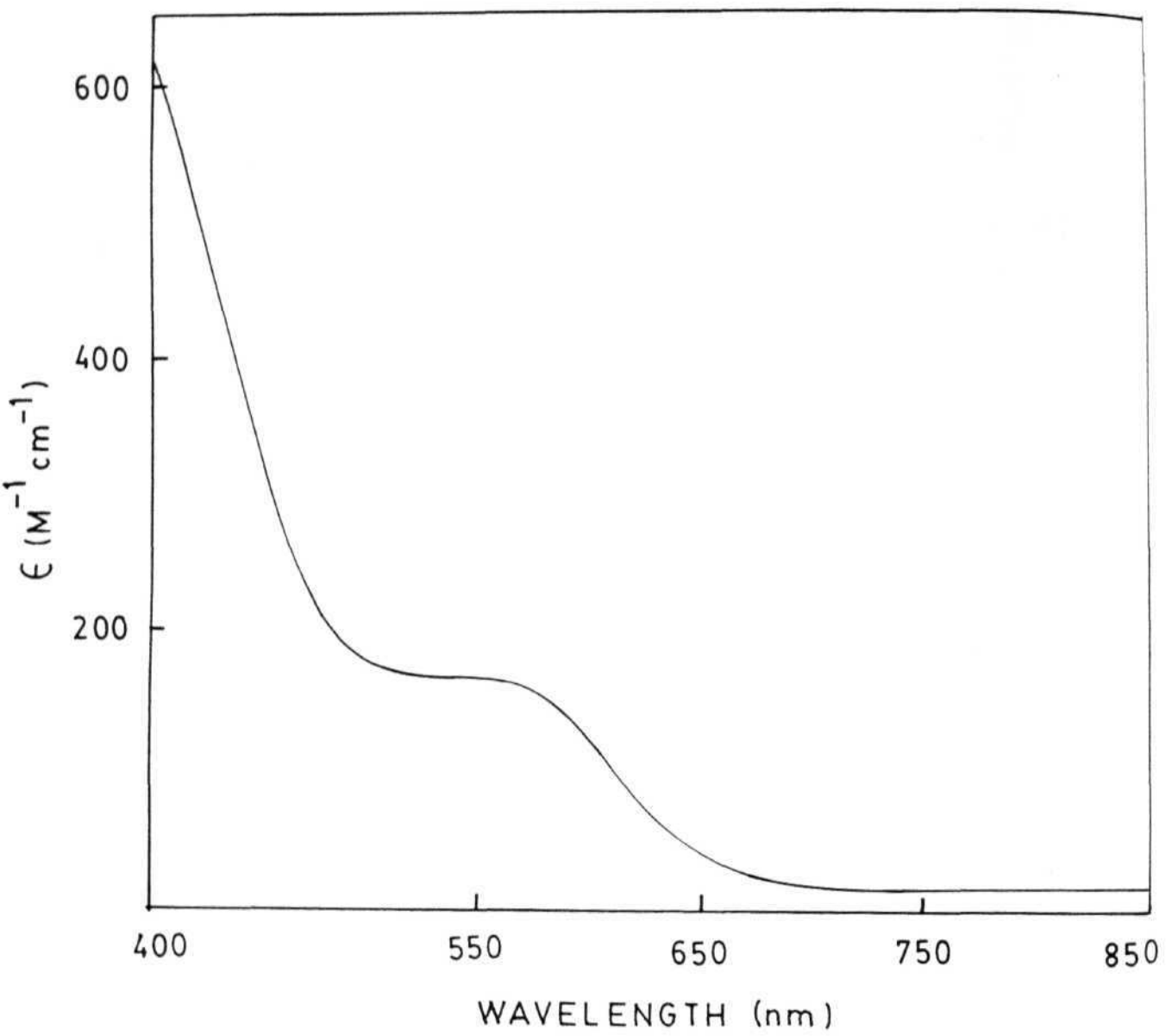

Fig. 4.7. Electronic spectrum of F in CH_3CN.

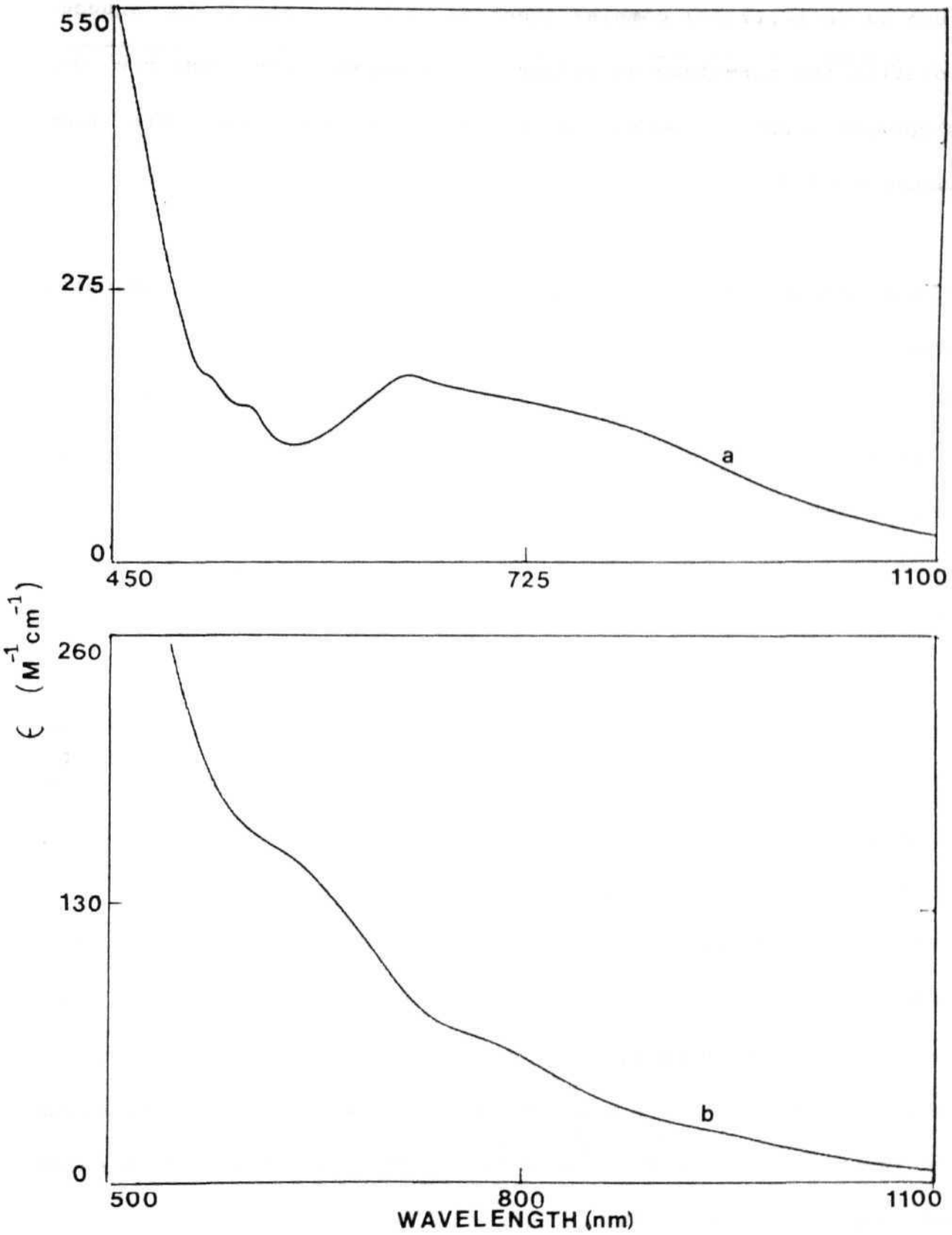

Fig. 4.8. Electronic spectra of G (a) in ligand buffer, (pH = 4.5) (b) in H_2O.

such as Mn(IV,IV,IV) complex (Section 2.3.5). Since in aqueous solution the formation of polymeric complexes are possible *via* disproportionation, we can not be sure that these bands are from manganese(III) monomers.

4.3.4. EPR and Magnetic properties: Room temperature magnetic moment for F has a value of 5.07 BM (μ_{eff}) consistent with the high spin d^4 (S = 2) system. EPR of powder samples at room temperature and low temperature shows a band at g = 2.0 with two additional bands at lower field (Fig. 4.9). Frozen solution spectrum in DMF shows resolved bands with 16-lines at g = 2, along with two low field lines (Fig. 4.10). Solutions are not stable; these signals disappear on keeping the solutions and six line pattern of the reduced Mn(II) results. The 16-line spectrum arises from the Mn(III,IV) species formed by disproportionation. The instability is associated with the presence of Cl^-. This was further demonstrated by adding Cl^- to $Mn_2O_2(phen)_4^{3+}$ solution in DMF which resulted in the low field lines (assigned to the quartet state) in addition to 16-line pattern. This solution also decomposes upon keeping, leading to the Mn(II) signals. It is possible that the mixed valence complexes contain Cl^- in bridging or terminal position which affects the doublet-quartet separation and solution stabilities.

Powder spectra of G shows a broad signal at g = 2.0 with a

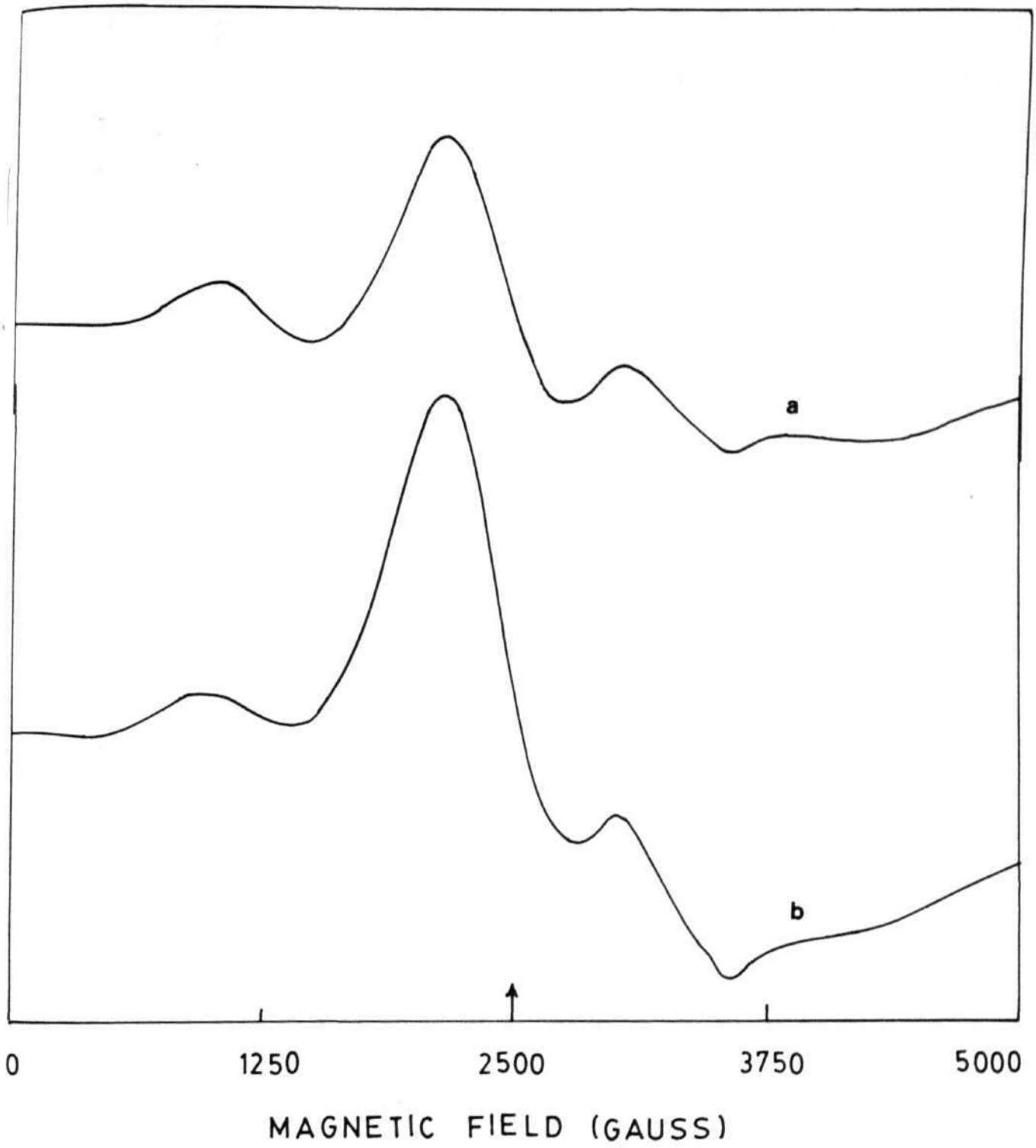

Fig. 4.9. Powder EPR spectra of F (a) at 298 K, ν = 9.235 GHz (b) at 157 K, ν = 9.233 GHz.

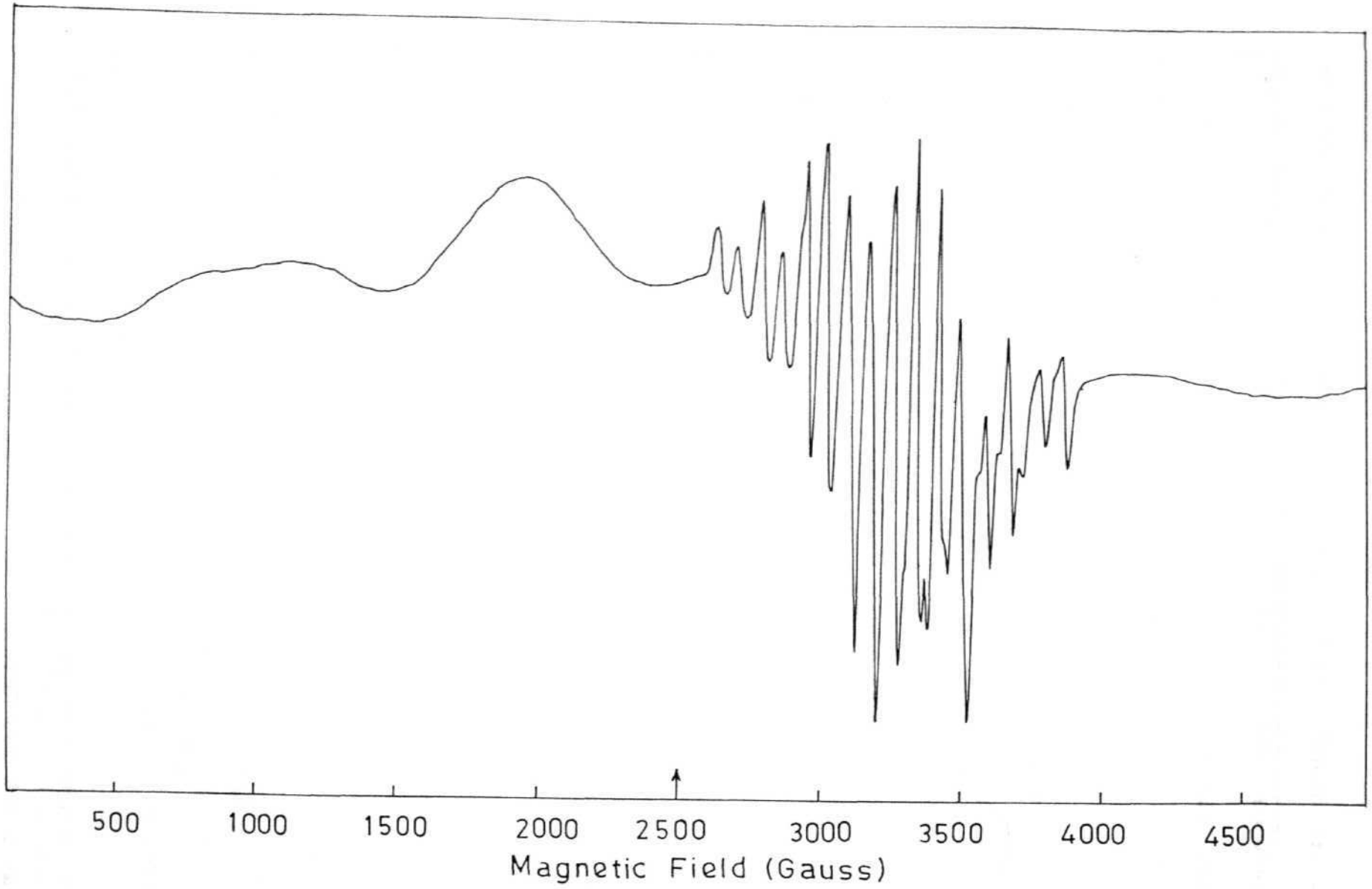

Fig. 4.10. Frozen EPR spectrum of F in DMF at 147 K. (ν = 9.205 GHz)

low intensity signal at g = 5.86; there is little variation of these signals with temperature (Fig. 4.11). In DMF solution, EPR spectrum shows a six line pattern, indicating the reduction to Mn(II).

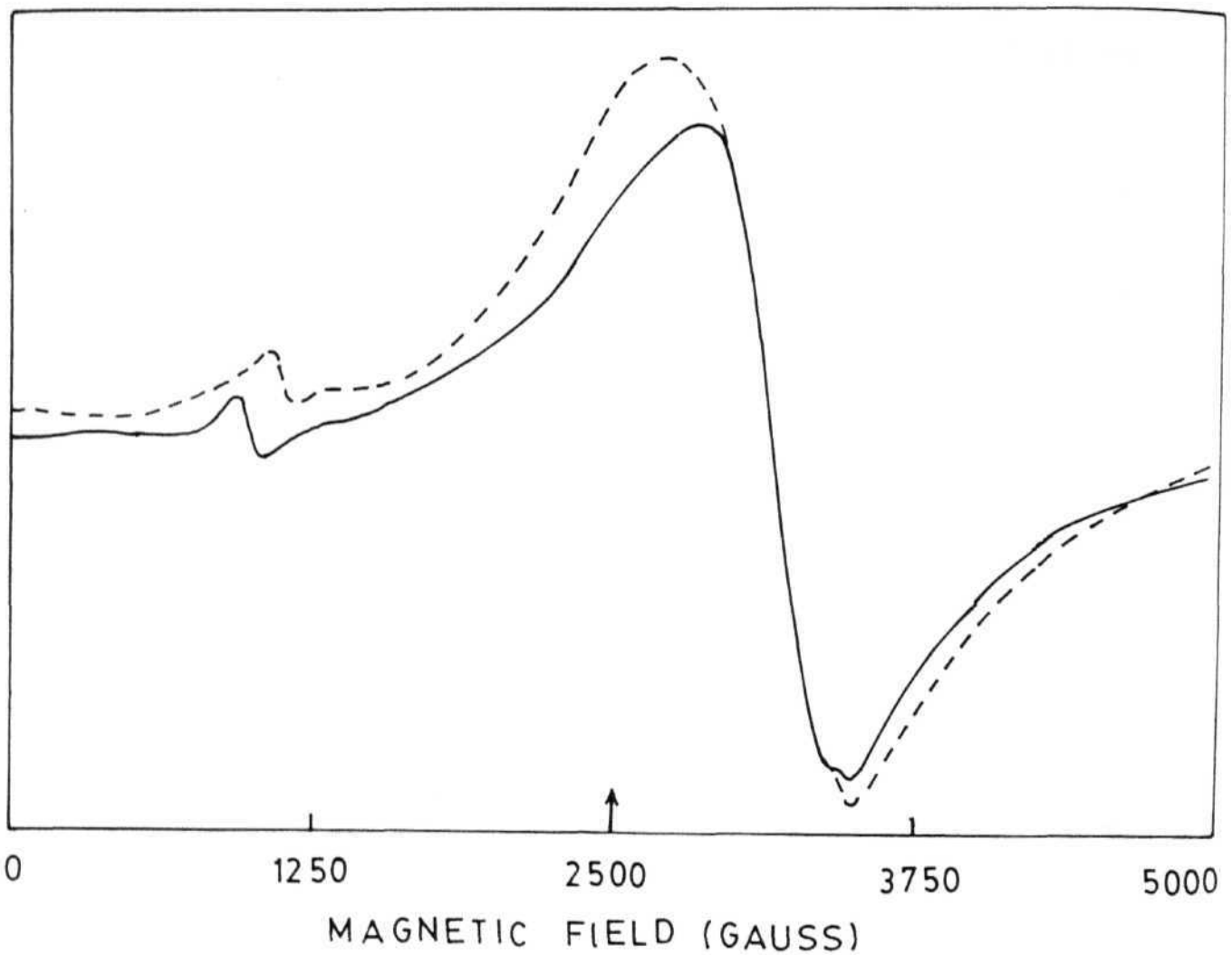

Fig. 4.11. Powder EPR spectra of G, ——— : 298 K (ν = 9.226 GHz); -----: 149 K (ν = 9.226 GHz).

CHAPTER 5.

SYNTHESIS AND STRUCTURAL CHARACTERISATION OF $[Mn_2O_2(OAc)(H_2O)_2(bpy)_2](ClO_4)_2.HNO_3$ AND PRELIMINARY INVESTIGATION ON A FEW OTHER SYSTEMS.

5.1 Introduction:

In our continuous efforts to synthesise polynuclear manganese complexes, we carried out reactions under various conditions and isolated mono-, di- and tri- nuclear compounds which are described in the previous chapters.

The present chapter describes the synthesis and structural characterization of $[Mn_2O_2(OAc)(H_2O)_2(bpy)_2](ClO_4)_2.HNO_3$ (H), $[Mn_2O_2(phen)_4](ClO_4)_3.0.5CH_3COOH.H_2O$ (I) and preliminary investigation on complexes which have been tentatively assigned formulae as $[Mn_2O_2(bpy)_2(Br)_2(H_2O)_2]Br$ (J) and $[Mn_2O_2(HPO_4)(phen)_2(H_2PO_4)_2].4H_2O$ (K) based on experimental evidence. Compound H was isolated by simple disproportionation of Mn(III) under acidic condition in presence of ligand while I and J were prepared by Ce(IV) oxidation.

5.2. Experimental Section:

5.2.1. Materials: All the chemicals are analytical grade and are used as purchased. Purification of solvents and other procedures

are described in the section 2.2.1.

5.2.2 Preparation of the compounds:

5.2.2(a) Preparation of $[Mn_2O_2(OAc)(H_2O)_2(bpy)_2](ClO_4)_2.HNO_3$. (H)
740 mg of 'manganic acetate' was dissolved in 10 ml of 1.6 N HNO_3 containing 485 mg (3.1 mmol) of bpy and the resulting green solution was treated with $NaClO_4$(aq). Dark green crystals were deposited, yield 400 mg (63% based on bpy). Anal, % calcd for $C_{22}H_{24}N_5O_{17}Cl_2Mn_2$: C, 32.57; H, 2.98; N, 8.63; Found: C, 32.68; H, 2.86; N, 8.87. Equivalent weight by iodometry; found (calcd) 265±10 (270.4). (iodometry and CHN analysis varied slightly for different preparations indicating the varying amounts of HNO_3 trapped in the crystal)

5.2.2(b) Preparation of $[Mn_2O_2(phen)_4](ClO_4)_3$ $0.5CH_3COOH.H_2O$. (I)
$Mn(OAc)_2.4H_2O$ (1.25 g, 5 mmol) was dissolved in 30 ml water-glacial acetic acid mixture (1:1) and 2.0 g (10 mmol) of 1,10-phenanthroline was added. The resulting yellow solution was cooled and 5 ml of aqueous ammonium ceric nitrate (3.3 g, 6.0 mmol) was added slowly with constant stirring. Saturated solution of $NaClO_4$ (0.5 g, 5 mmol) was added to the resulting green solution and filtered. Upon keeping for few a days, dark green crystals were deposited which were filtered and dried, yield: 1.7 g (53% based

on total manganese). Anal., calcd for $C_{49}H_{37}N_8O_{16}Cl_3Mn_2$: C, 46.52; H, 2.95; N, 8.85; Found: C, 47.1; H, 2.66; N, 8.96. Equivalent weight by iodometry; found (calcd) 418±5 (421.7).

5.2.2(c) Preparation of $[Mn_2O_2(bpy)_2(Br)_2(H_2O)_2]Br$. (J) To 600 mg of bpy in 15 ml of water, acetic acid (1:1) mixture, $Mn(OAc)_2.4H_2O$ (.5 g, 2 mmol) was added. To the resulting yellow solution 5 ml of aqueous ammonium ceric nitrate (1.3 g, 2.5 mmol) was added with stirring, after which the solution changed to brown colour. Saturated solution of KBr (nearly 0.3 g) was added and the solution was filtered. The filtrate upon keeping for a few days deposited brown crystals which were filtered and dried, (yield ≅ 400 mg) (crystals are not stable and slowly collapses). Anal, calcd for $C_{20}H_{20}N_4O_4Br_3Mn_2$: C, 32.91; H, 2.76; N, 7.67; Found: C, 32.56; H, 2.71; N, 7.12. Equivalent weight by iodometry; found (calcd) 225±5 (243).

5.2.2(d) Preparation of $[Mn_2O_2(HPO_4)(phen)_2(H_2PO_4)_2].4H_2O$: (K) This complex crystallises out by dissolving 100 mg of $[Mn_3O_4(H_2O)_2(phen)_4](NO_3)_4.2.5H_2O$ (B) in 5 ml of 10 N phosphoric acid. Anal, calcd for $C_{24}H_{27}N_4O_{18}P_3Mn_2$: C, 33.4; H, 3.1; N, 6.49; Found: C, 32.9; H, 2.70; N. 6.50.

5.2.3 Analysis, spectral and magnetic measurements: All the

spectral, analytical and magnetic measurements are carried out as described in section 2.2.3.

5.2.4 X-ray crystallography

5.2.4a. $[Mn_2O_2(OAc)(H_2O)_2(bpy)_2](ClO_4)_2.HNO_3$. (H) The diffraction data were collected on a dark brown crystal with approximate dimension 0.4 × 0.2 × 0.05 mm at room temperature on an Enraf-Nonius CAD-4 Kappa geometry automated diffractrometer using MoKα radiation . Parameters of crystal and intensity measurements are given in the Table 5.1. The compound crystallises in monoclinic system. The space group could be Cc or C2/c based on systematic absences of hkl reflections. The structure was solved in the lower space group Cc, but attempts to refine in this group led to severe correlations between the two halves of the molecule related by (pseudo) two-fold axis and therefore C2/c was adopted for refinement. A combination of heavy atom and direct methods (SHELXS-86)[180] followed by difference Fourier and full matrix-least squares method (SHELX-76)[179] were used. Of the total 2780 reflections only 1597 reflections with ($F > 5\sigma(F)$) were used for the structure refinement. All the non-hydrogen atoms of the cation and the perchlorate anion were readily found in the Fourier map and refined anisotropically. The ring hydrogen atoms were fixed with their common isotropic thermal parameters which was

refined. The lattice nitric acid was in disordered and the disorder could not be modelled. Atomic parameters, bond lengths and angles and thermal parameters are given in the Tables 5.2 to 5.5.

5.2.4b $[Mn_2O_2(phen)_4](ClO_4)_3.0.5HOAc.H_2O$: (I) A dark green crystal was mounted on Siemens P4 diffractometer and data were collected for 3704 reflections at room temperature using MoKα radiation. Compound crystallises in monoclinic system, a = 9.744 Å, b = 23.994 Å, c = 21.858 Å, β = 93.12°, V = 5110.35 Å^3, Z = 4. Space group could be Cc or C2/c based on systematic absences of hkl reflections. A combination of heavy atom and direct methods (SHELXS-86)[180] was used to locate the initial positions of the atom. This has given a reasonable picture of the cation and anions. Half the molecule constitutes the asymmetric unit and another half is related by a pseudo two-fold axis passing through the Mn_2O_2 ring. Attempts to refine the structure using full matrix least-squares method (SHELX-76)[179] in C2/c and Cc space groups were not successful; severe correlations were observed between the two halves. This may be because of the disorder of the molecule, which is possible because of the pseudo two-fold axis relating the two halves. Suitable model may provide a good refinement but we have not pursued it mainly because the cation is already characterised in other systems.[76]

Table 5.1. Crystallographic Data for H.

formula	$Mn_2C_{22}H_{24}N_5Cl_2O_{17}$	formula weight	811.23
a, Å	21.115(4)	space group	C2/c
b, Å	11.495(2)	ρ_{calcd} g cm^{-3}	1.706
c, Å	15.500(4)	λ Å	0.71073
β, deg	122.94(2)	data collected:	2780
V, $Å^3$	3157.28	data used ($F > 5\sigma(F)$)	1597
crystal size mm	0.4×0.2×0.05		
diffractometer: Enarf Nonius CAD-4			
monochromator	graphite	no of parameters	224
Z	4	T, K	298
μ, cm^{-1}	9.78	F(000)	1643.94
R^a	0.072	$R_w{}^b$ =	0.073

[a] $R = (\sum\|F_o|-|F_c\|) / \sum|F_o|$

[b] $R_w = \{ [\sum w (|F_o|-|F_c|)^2] / \sum w F_o{}^2 \}^{1/2}$

$w^{-1} = \sigma^2 |F_o| + g |F_o|^2$; $g = 0.00045$

Table 5.2. Fractional coordinates and equivalent or isotropic thermal parameters for H.[a]

Atom	x	y	z	U(eq)[b]
Mn	0.4473(1)	0.2018(1)	0.7714(1)	0.073(1)
O1	0.4518(3)	0.1831(4)	0.6605(4)	0.071(3)
N1	0.4266(3)	0.0354(5)	0.7791(4)	0.049(3)
N2	0.3318(4)	0.2028(8)	0.6845(5)	0.090(4)
O2	0.4500(4)	0.2265(5)	0.8991(5)	0.098(4)
H1O2	0.400(2)	0.217(6)	0.887(6)	0.09(2)
H2O2	0.443(4)	0.297(4)	0.927(6)	0.09(2)
C1	0.4813(4)	-0.0419(6)	0.8391(5)	0.060(4)
C2	0.4625(6)	-0.1580(7)	0.8387(7)	0.081(5)
C9	0.3549(5)	0.0010(7)	0.7221(6)	0.062(4)
C10	0.3013(5)	0.0971(10)	0.6662(7)	0.083(5)
C7	0.2093(11)	0.2825(17)	0.5765(14)	0.176(13)
C8	0.2885(8)	0.2983(11)	0.6428(10)	0.135(8)
C4	0.3347(5)	-0.1140(9)	0.7193(7)	0.084(5)
C5	0.2227(6)	0.0817(13)	0.6011(8)	0.114(6)
C3	0.3895(7)	-0.1931(8)	0.7785(8)	0.095(6)
C6	0.1804(9)	0.1799(21)	0.5608(14)	0.178(12)
Cl	0.1926(2)	-0.3768(3)	0.5710(3)	0.124(2)
O1Cl	0.2638(5)	-0.4014(12)	0.6528(11)	0.253(9)
O2Cl	0.1325(4)	-0.4355(8)	0.5700(7)	0.152(5)
O3Cl	0.1803(7)	-0.2619(11)	0.5778(14)	0.324(15)
O4Cl	0.1857(11)	-0.4115(16)	0.4867(12)	0.382(16)
O3	0.4535(5)	0.3684(5)	0.7636(7)	0.165(6)
C1AC	0.5000(0)	0.4192(12)	0.7500(0)	0.204(18)
C2AC	0.5000(0)	0.5515(13)	0.7500(0)	0.434(40)

Table 5.2 contd...

Atom	x	y	z	U(eq)[b]
N1T	-0.0230(8)	-0.0096(17)	0.4856(13)	0.042(2)
O2T	0.0686(14)	-0.0631(21)	0.5484(18)	0.067(4)
O3T	-0.0131(26)	0.0091(37)	0.5540(34)	0.137(9)
O4T	-0.0250(10)	-0.0993(19)	0.4770(14)	0.073(3)

[a] Disordered HNO_3 and water hydrogen atoms are refined isotropically. Ring hydrogen atoms are fixed and refined with a common thermal parameter 0.13(1).

[b] $U(eq) = (1/3)(U_{11}a^2a^{*2} + U_{22}b^2b^{*2} + U_{33}c^2c^{*2} + U_{12}a^*b^*ab\cos\gamma + U_{13}a^*c^*ac\cos\beta + U_{23}b^*c^*bc\cos\alpha)$

Table 5.3. Bond lengths (Å) for H.[a]

O1	-- Mn	1.786(5)	O1'	-- Mn	1.805(7)
O2	-- Mn	1.968(6)	O3	-- Mn	1.927(6)
N1	-- Mn	1.979(5)	N2	-- Mn	2.045(8)
N1	-- C1	1.349(9)	N1	-- C9	1.332(9)
N2	-- C10	1.332(11)	N2	-- C8	1.348(11)
C1	-- C2	1.391(10)	C2	-- C3	1.360(13)
C3	-- C4	1.361(12)	C4	-- C9	1.383(11)
C9	-- C10	1.477(12)	C5	-- C10	1.409(13)
C5	-- C6	1.361(20)	C6	-- C7	1.288(23)
C7	-- C8	1.421(21)	O3	-- C1Ac	1.254(8)
C1Ac	-- C2Ac	1.521(19)	O1Cl	-- Cl	1.369(10)
O2Cl	-- Cl	1.432(8)	O3Cl	-- Cl	1.361(12)
O4Cl	-- Cl	1.296(11)	Mn	-- Mn	2.647(2)

[a] The ' denotes atom related by the (pseudo) two-fold axis passing, perpendicular to the Mn_2O_2 plane.

Table 5.4. Bond angles (°) for H.[a]

O1	- Mn	-O1'	83.3(3)	O1	- Mn	-O2	175.7(3)
O1	- Mn	-O3	91.0(3)	O1	- Mn	-N1	94.0(2)
O1	- Mn	-N2	92.0(3)	O2	- Mn	-O3	87.4(3)
O2	- Mn	-N1	88.1(2)	O2	- Mn	-N2	92.0(3)
O3	- Mn	-N1	171.3(3)	O3	- Mn	-N2	92.9(4)
N1	- C1	-C2	119.7(7)	C1	- C2	-C3	120.1(8)
C2	- C3	-C4	119.7(8)	C3	- C4	-C9	118.9(8)
C4	- C9	-N1	121.7(8)	C9	-C10	-N2	115.4(8)
N1	- C9	-C10	113.5(8)	C9	- N1	-C1	119.9(7)
N2	-C10	-C5	120.8(10)	C6	- C5	-C10	116.6(14)
C5	- C6	-C7	123.2(18)	C6	- C7	-C8	120.2(15)
C7	- C8	-N2	117.9(13)	C9	- N1	-Mn	117.1(5)
C8	- N2	-Mn	125.1(9)	C10	- N2	-Mn	113.6(6)
C8	- N2	-C10	121.2(10)	O2Cl	-- Cl	--O1Cl	115.6(8)
O3	- C1Ac	-C2Ac	117.8(7)	O3Cl	-- Cl	--O1Cl	106.8(9)
O4Cl	-- Cl	--O3Cl	117.1(12)	O3Cl	-- Cl	--O2Cl	104.6(7)
O4Cl	-- Cl	--O1Cl	109.6(11)	O4Cl	-- Cl	--O2Cl	103.4(8)

[a] The ' denotes atom related by (pseudo) two-fold axis passing, perpendicular to the Mn_2O_2 plane.

Table 5.5. Anisotropic thermal parameters for H.[a]

ATOM	U11	U22	U33	U23	U13	U12
Mn	0.079(1)	0.039(1)	0.075(1)	0.007(1)	0.051(1)	0.006(1)
O1	0.068(4)	0.049(3)	0.069(4)	0.020(3)	0.039(3)	0.023(3)
N1	0.037(4)	0.044(3)	0.043(4)	0.004(3)	0.013(3)	-0.004(3)
N2	0.077(5)	0.099(6)	0.070(5)	0.036(5)	0.049(4)	0.048(5)
O2	0.109(5)	0.067(4)	0.089(5)	-0.023(4)	0.072(4)	-0.018(4)
C1	0.059(5)	0.045(5)	0.045(5)	0.007(4)	0.015(4)	0.001(4)
C2	0.086(7)	0.046(5)	0.070(6)	0.014(4)	0.034(5)	0.004(5)
C9	0.052(5)	0.070(6)	0.043(5)	0.005(4)	0.023(4)	0.002(5)
C10	0.059(7)	0.102(8)	0.067(6)	0.017(6)	0.041(5)	0.015(6)
C7	0.151(18)	0.210(19)	0.128(13)	0.100(15)	0.105(14)	0.141(16)
C8	0.125(11)	0.121(9)	0.124(9)	0.065(8)	0.088(9)	0.084(9)
C4	0.065(6)	0.088(7)	0.07(6)	-0.017(6)	0.031(5)	-0.028(6)
C5	0.056(7)	0.172(12)	0.082(7)	0.031(8)	0.034(6)	0.024(8)
C3	0.100(8)	0.056(5)	0.090(7)	-0.016(6)	0.053(7)	-0.025(6)
C6	0.076(10)	0.294(26)	0.127(12)	0.095(18)	0.061(9)	0.086(16)
Cl	0.095(2)	0.142(3)	0.099(2)	-0.040(2)	0.058(2)	-0.040(2)
O1Cl	0.075(7)	0.235(14)	0.282(15)	-0.036(11)	-0.024(8)	-0.026(8)
O2Cl	0.094(6)	0.136(7)	0.168(8)	-0.006(6)	0.067(6)	-0.035(5)
O3Cl	0.161(11)	0.134(9)	0.540(28)	-0.127(14)	0.205(15)	-0.076(9)
O4Cl	0.447(25)	0.408(23)	0.221(14)	-0.116(15)	0.272(17)	-0.117(19)
O3	0.207(9)	0.036(4)	0.215(9)	0.013(4)	0.180(8)	0.019(4)
C1Ac	0.264(26)	0.032(8)	0.263(25)	0.000(0)	0.220(23)	0.000(0)
C2Ac	0.583(58)	0.026(8)	0.622(57)	0.000(0)	0.563(53)	0.000(0)

[a] The Temperature factor expression used

$$\exp\left[-2\pi^2 \left(U_{11}h^2a^{*2} + U_{22}k^2b^{*2} + U_{33}l^2c^{*2} + 2U_{12}hka^*b^*\cos\gamma^* + 2U_{13}hla^*c^*\cos\beta^* + 2U_{23}klb^*c^*\cos\alpha^*\right)\right]$$

5.3 Results and Discussion:

5.3.1 Synthesis. From the preceding chapters it is clear that simple one electron oxidation of Mn(II) by Ce(IV) leads to the formation of unstable Mn(III)aquo-hydroxo species (see Scheme-1, section 2.3.1), which undergo disproportionation giving polynuclear manganese complexes. Formation of the present complexes can also be explained in the same line. Compound **H**, a (III,IV) dimer formed by simple disproportionation of $Mn^{III}(OAc)_3$ in the presence of ligand and it crystallises out as a perchlorate salt by the addition of $NaClO_4$(aq). An analogous one electron oxidised product **A** was prepared by Ce(IV) oxidation in perchloric acid (Section 2.2.2).

Compound I is a well known (III,IV) μ-oxo dimer which prepared earlier by $KMnO_4$ oxidation or from disproportionation of $Mn(OAc)_3$ in acetate buffer (pH = 4.5). The present method uses Ce(IV) as the oxidising agent and the product crystallises in a different space group.

Compound J, based on preliminary experimental data, is assigned the molecular formula, $[Mn_2O_2(bpy)_2(Br)_2(H_2O)_2]Br$. This can have different possible isomers which are shown in the Fig 5.1. From earlier experimental evidences of Christou[150,153,194] and our isolation of **F** it is clear that halides have preference in

coordination over bridging oxide and acetate ions. Formation of this complex can be explained by simple substitution of acetate bridge in Mn(III,IV) dimer.

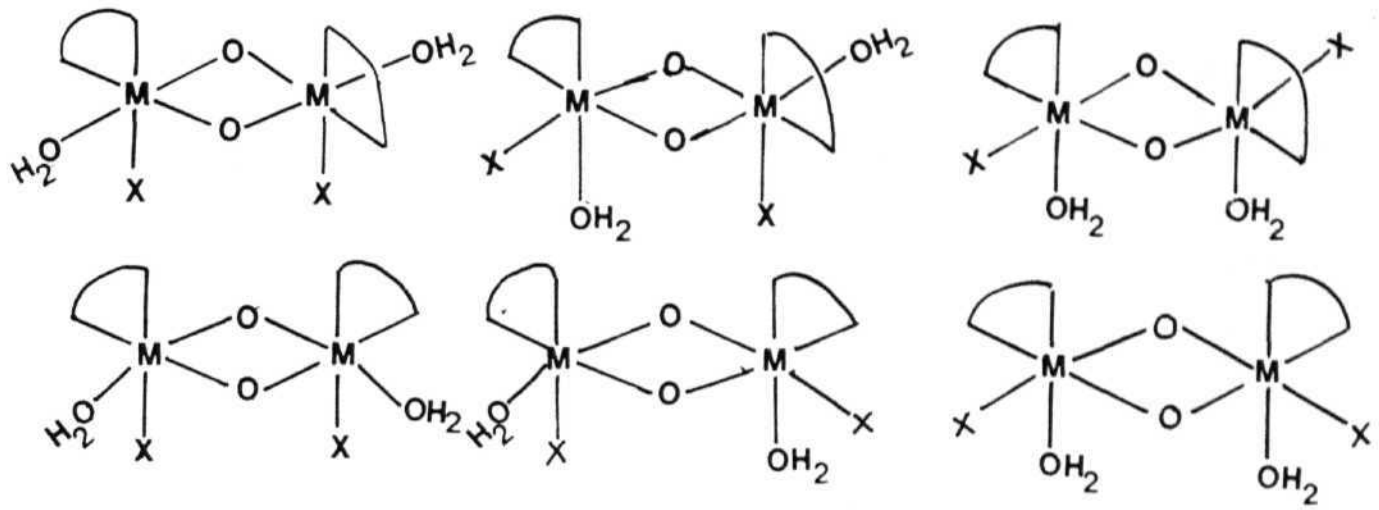

Fig. 5.1. Possible isomers of J.

Formation of K can be explained from the Fig.5.2. Simple substitution of the the third manganese center by bridging phosphate gives the compound. Depending on the concentration of the bridging units, the equilibrium will shift towards one particular direction. All the three structural cores are reported with bpy ligand. We isolated and structurally characterised the tri-nuclear core (see chapter-II) with phen ligand.

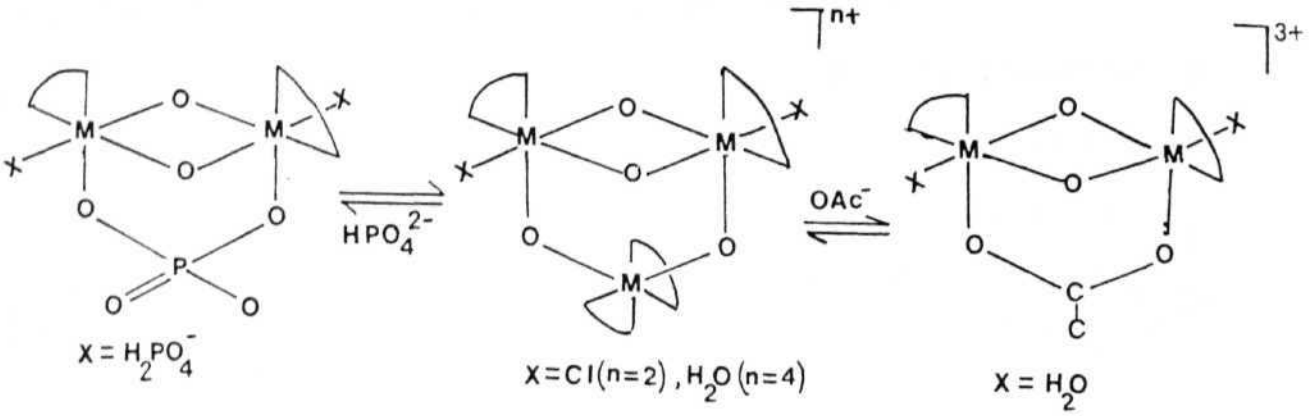

Fig. 5.2. Schematic representation for the formation of acetate and phosphate bridged Mn(IV,IV) dimers from trinuclear Mn_3O_4 core.

5.3.2 Structure. The molecular structure of **II** is shown in the Fig. 5.3. Each manganese is in octahedron environment with $Mn_2O_2(OAc)^{2+}$ core. Two ligand N-atoms and one water O-atom completes the six coordination around each metal. Mn-Mn distance (2.647 Å) is comparable with known $Mn_2O_2(OAc)^{2+/3+}$ cores. Unfortunately, the disorder about an imposed two-fold axis does not allow us to distinguish between the Mn(III) and Mn(IV) centers in the crystal. Such disorder is commonly observed in the crystal structures of Mn(III,IV) complexes.[76,101,113] The acetate is bound more strongly in this complex compared to $[Mn_2O_2(OAc)(bpy)_2Cl_2]$.[97] The Jahn-Teller distortion can be described as either a 'tetragonal' compression along N 1 -Mn-O 3 or as a 'tetragonal'

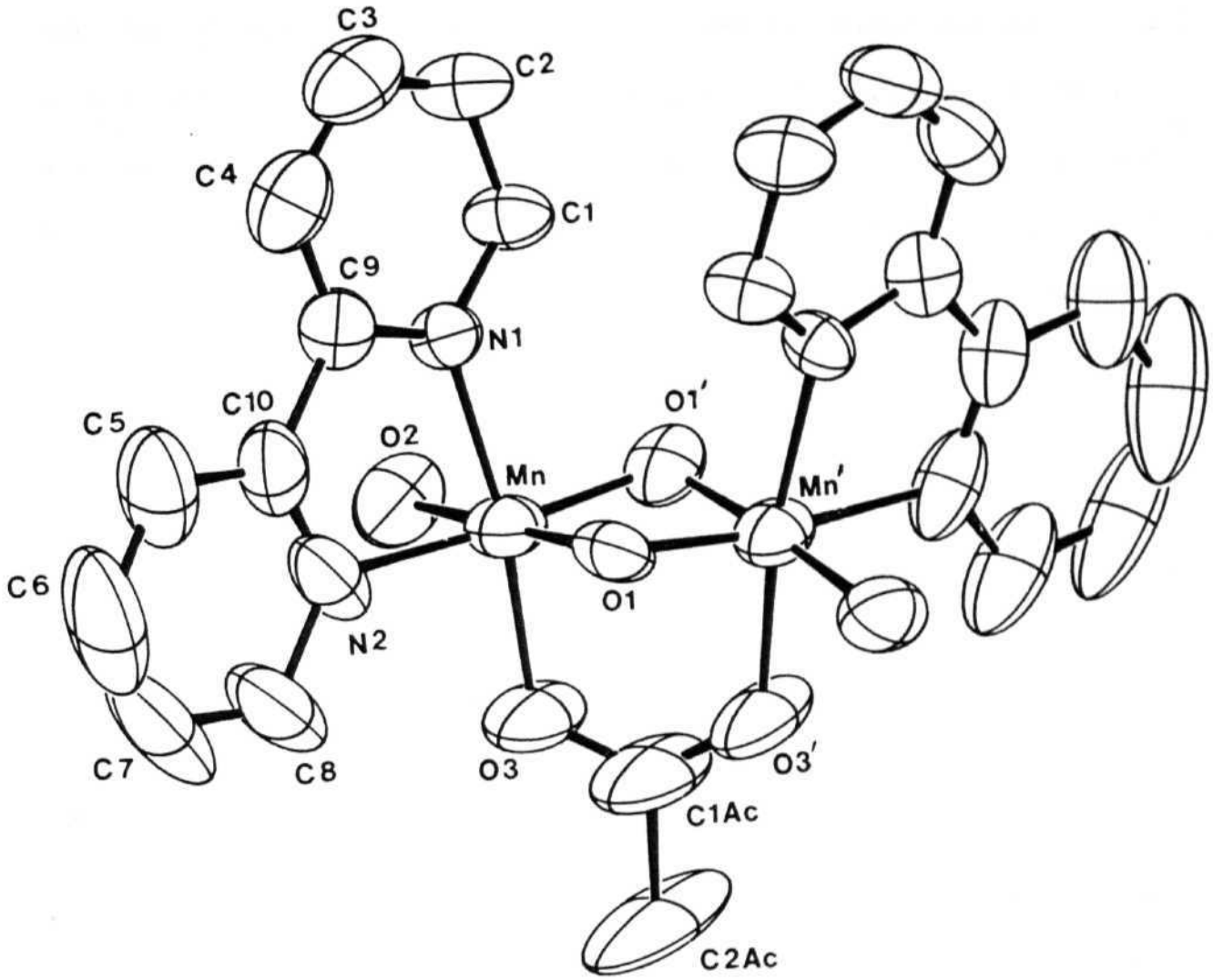

Fig. 5.3. ORTEP diagram of the cation of II.

elongation along N 2 -Mn-O 1′ direction. Surprisingly, the metal-ligand bond distances are similar to that in the corresponding Mn(IV,IV) compound A (see Table 2.3, Chapter 2). The (IV,IV) formulation for the present complex is not consistent with the equivalent weight, nor it is consistent with the optical and EPR data. The bond shortening arises from a combination of different factors, *viz.*, averaging due to disorder and the particular nature of Jahn-Teller distortion at the Mn(III) center. In this context, one may note that the Mn(III)-Cl distance is actually shorter than Mn(IV)-Cl distance in $[Mn_2O_2(OAc)(bpy)_2Cl_2]$.[97]

5.3.3 Solution Chemistry. Compound H is soluble in polar solvents and solutions are not stable, depositing a brown precipitate over a period of several days. Electronic spectrum in water shows (Fig. 5.4) weak shoulders at 790 and 770 nm and a weak band at 720nm. There is rising absorption from 600 nm downwards. The absorption at 790 nm probably arises from the intervalence transfer band (IVTA). These IVTA bands are known to be sensitive to the nature of solvent and deviations in structural geometries. In ligand buffer (pH = 4.5), it generates a spectrum similar to the reported Mn(III,IV) di(μ-oxo) dimers.

Compound I was reported previously by Cooper and Calvin and spectral features are similar.

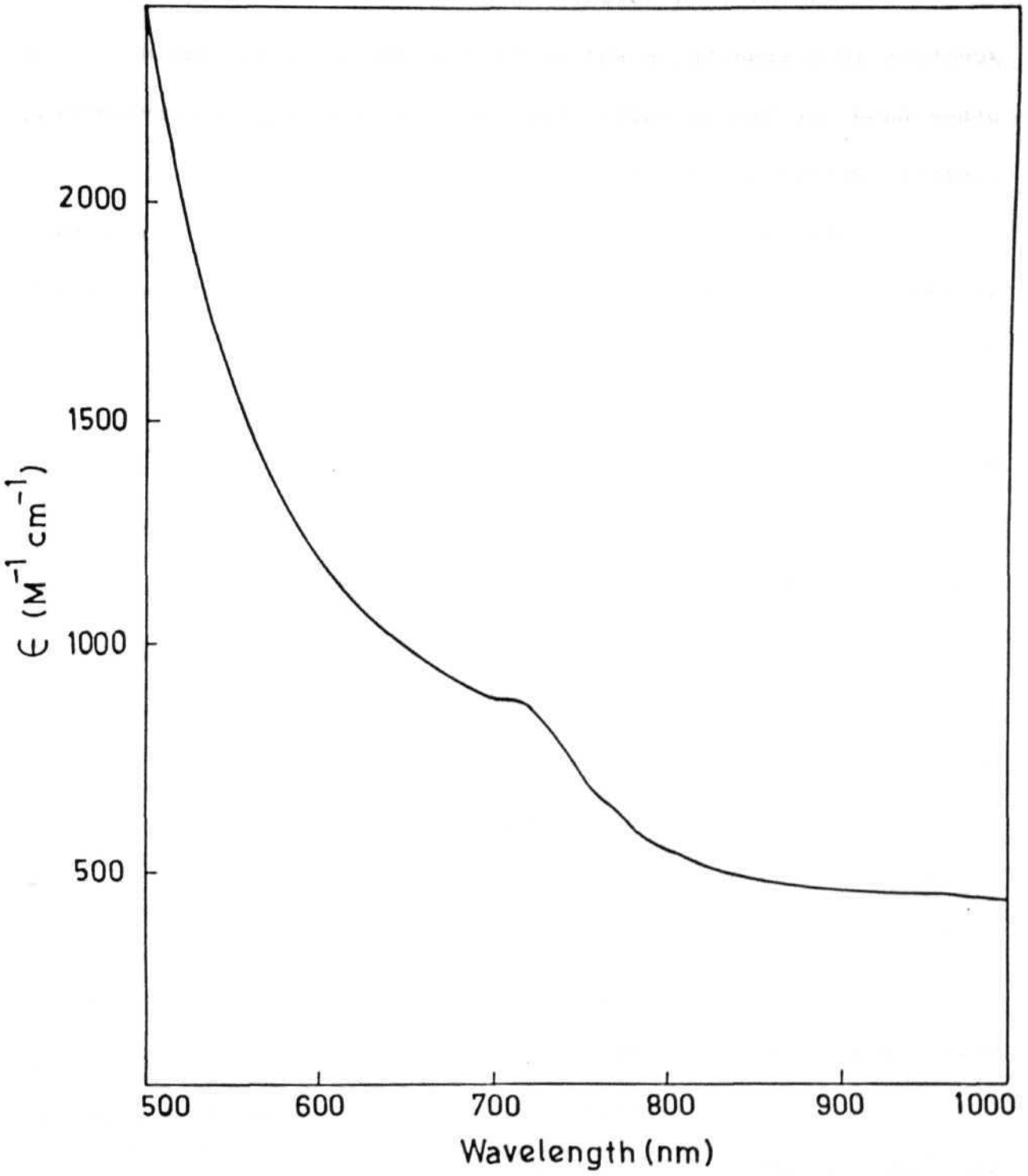

Fig. 5.4. Electronic spectrum of H in H_2O.

Compound J is soluble in polar solvents and electronic spectrum in acetonitrile and water does not show any bands. On the other hand, in ligand buffer (pH = 4.5) it converts slowly to the reported Mn(III,IV) dimer.

Compound K does not dissolve in any of the common solvents. In conc. phosphoric acid it gives a pink solution which decomposes slowly and becomes colourless.

5.3.4 EPR and Magnetic Properties. Powder EPR spectrum for H at room and low temperature (157 K) shows a signal at $g \cong 2.0$ with low field lines (Fig. 5.5). Single crystal spectra at random orientations show small anisotropy for $g \cong 2.0$ signal and larger anisotropy for low field lines (Fig. 5.6). Powder spectrum shows a $g \cong 2$ line with weak signal at low field. Frozen solution in DMF at 157K shows 16-line pattern (Fig. 5.7) which is expected for strongly coupled Mn(III,IV) complexes having a $S = 1/2$ ground state.

Powder spectrum for J at room and low temperature shows a weak signal at $g \cong 2.0$. Frozen solution spectrum in DMF shows Mn(II) signals and weak Mn(III,IV) signals. This may be because of the unstable nature of the complex.

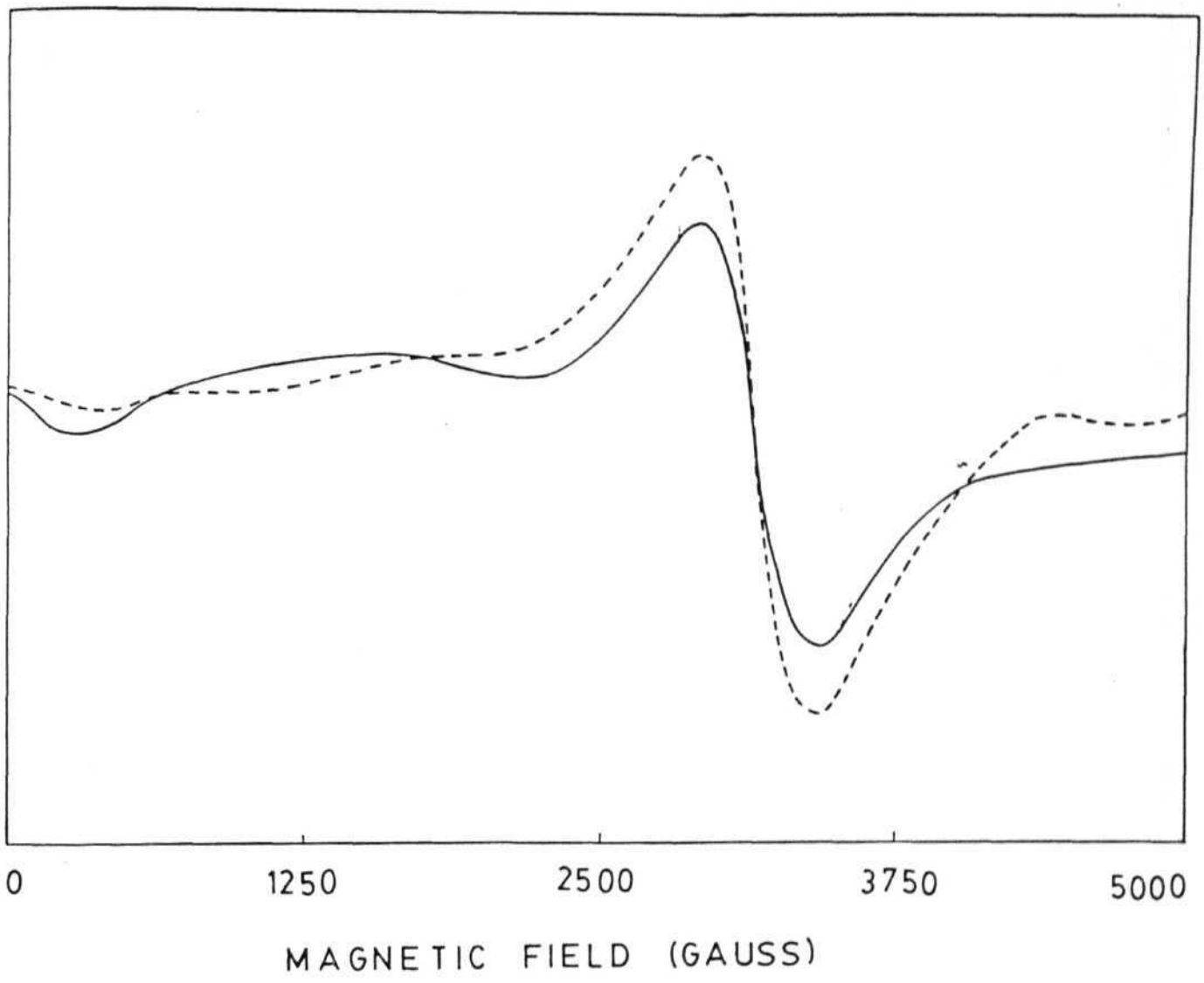

Fig. 5.5. Powder EPR spectra of H. (——— : 298 K, ----: 157 K; ν = 9.22 GHz)

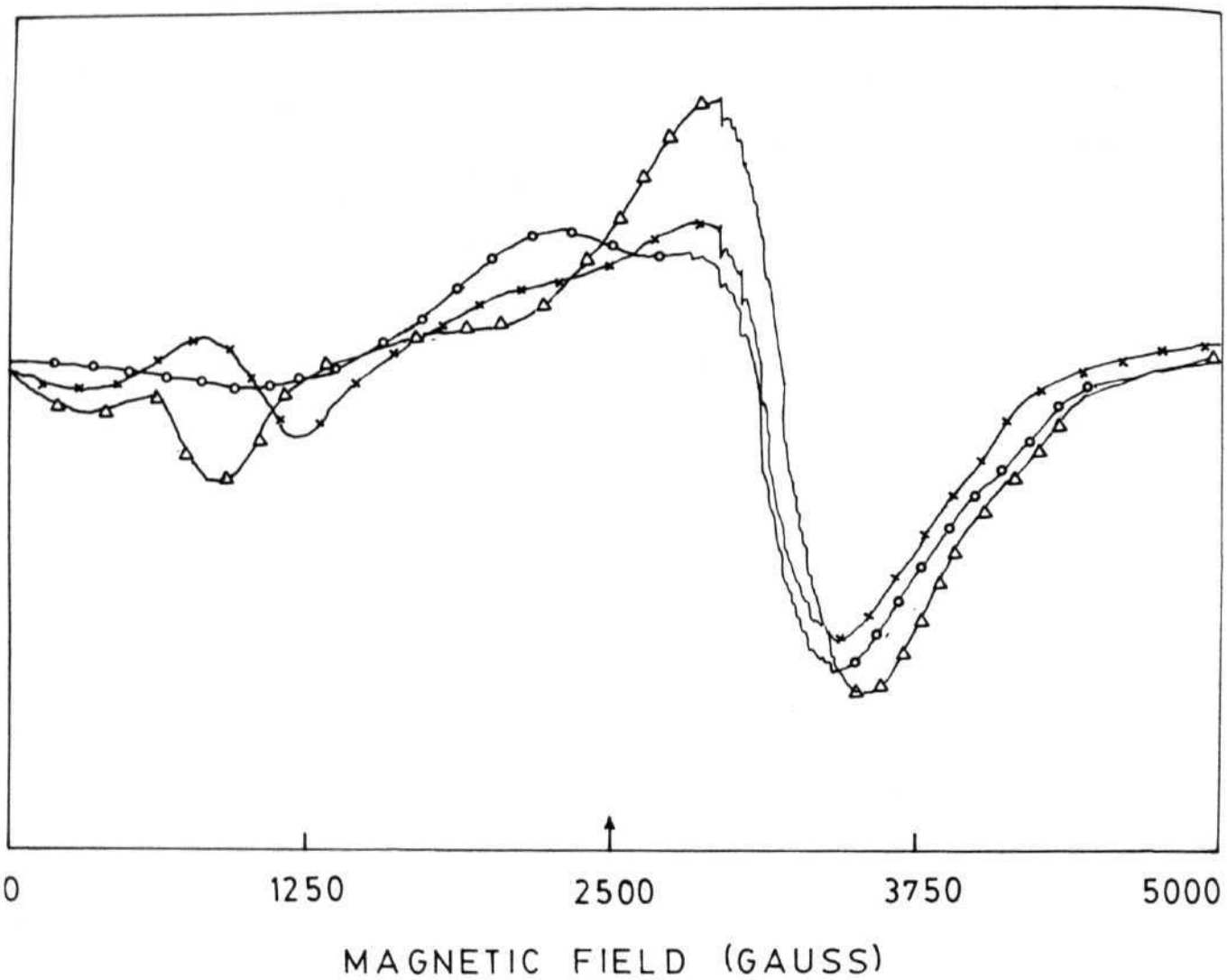

Fig. 5.6. Single crystal EPR spectra of H at random orientations.

(157 K; ν = 9.230 GHz)

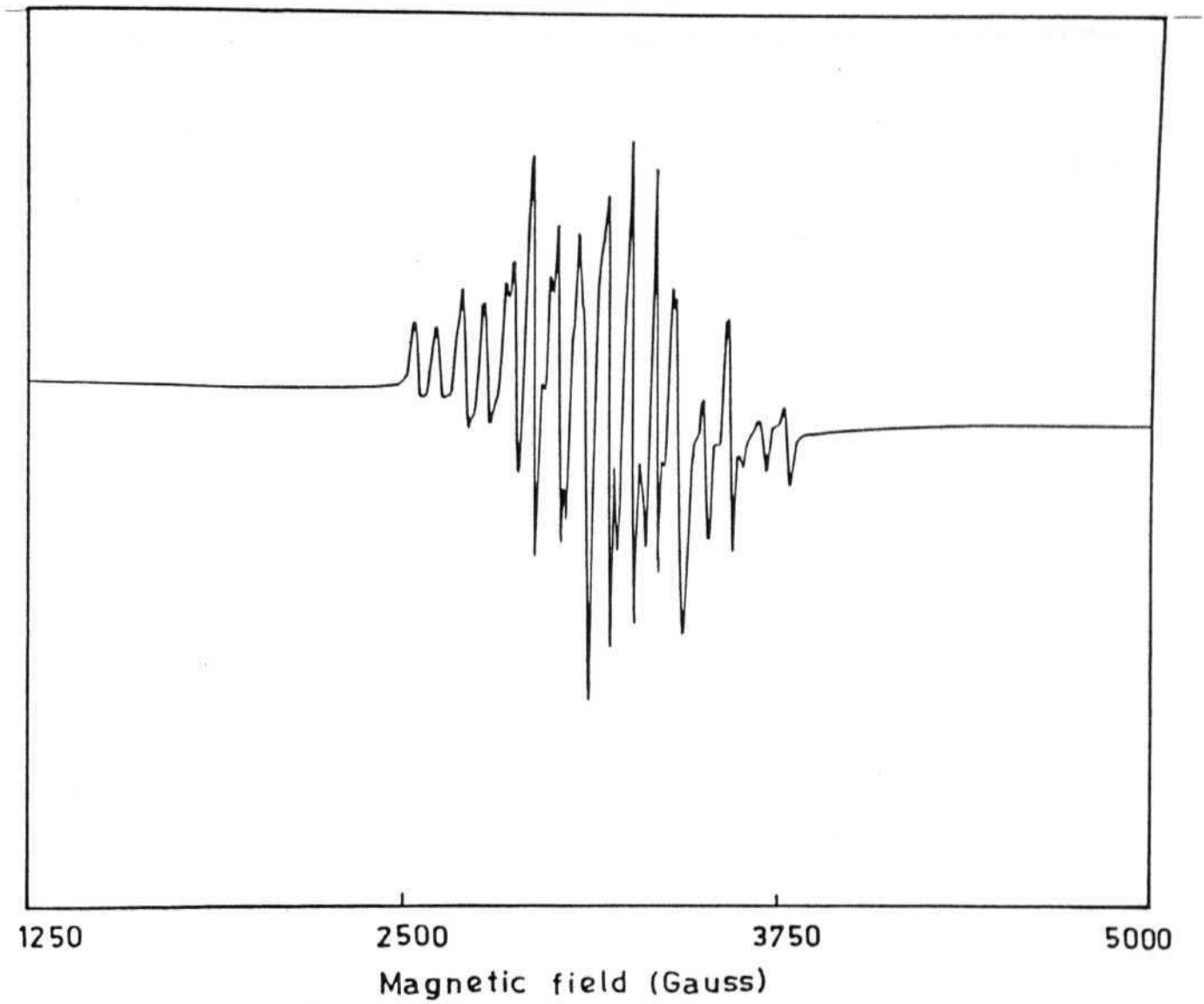

Fig. 5.7. Frozen EPR spectrum of H in DMF at 157 K. (ν = 9.195 GHz)

SUMMARY AND CONCLUSIONS

1. Ce(IV) is a good oxidising agent for synthesis of high-valent manganese complexes.

2. Formation of different cores ($Mn_2O_2(OAc)$, $Mn_2O(OAc)_2$ and Mn_3O_4) and nuclearity (mono, di and tri) shows that the aqueous chemistry of manganese is quite complex and variation of ligand (bpy or phen), acid ($HClO_4$, HNO_3, HOAc and H_3PO_4) and anion (ClO_4^-, PF_6^-, Cl^- and Br^-) resulted in the formation of different complexes.

3. Reactions in aqueous media are successful in preparing aquo-bound complexes. However, water coordination on the two metal centers in di- and tri- nuclear complexes are found to be in trans position. Formation of only one type of isomer (trans) is probably because of thermodynamic and kinetic factors responsible for preferential formation of one isomer over the other possible isomers.

4. In perchloric acid media, presence of acetate resulted in the formation of $[Mn_2O_2(OAc)(H_2O)_2(bpy)_2](ClO_4)_3.H_2O$ compound while in the absence of acetate $[Mn_3O_4(H_2O)_2(bpy)_4](ClO_4)_4.5H_2O$ was obtained. This is true with bpy ligand; attempts with phen ligand were not successful because of precipitation of $phenHClO_4$. On the other hand, in HNO_3 medium, even in the presence of acetate, only $[Mn_3O_4(H_2O)_2(phen)_4](NO_3)_4.2.5H_2O$ is formed. Reactions with bpy in HNO_3 are failed to

crystallise out probably because of high solubilities of the species present in solution. These results show, the reactivities of bpy and phen are different and variation of acid and bridging units will lead to the formation of different complexes.

5. Variable temperature magnetic susceptibility study on $[Mn_2O_2(OAc)(H_2O)_2(bpy)_2](ClO_4)_3.H_2O$ shows relatively weak antiferromagnetic interactions ($J = -44.6\ cm^{-1}$; $\mathcal{H} = -2JS_1S_2$) compared with the other known Mn(IV,IV) dimers.

6. Oxidation of manganese in acetic acid medium resulted in the formation of two compounds, $[Mn_2O(OAc)_2(H_2O)(NO_3)(bpy)_2]ClO_4.CH_3COOH$ and $[Mn_2O(OAc)_2(H_2O)_2(bpy)_2](ClO_4)_2$ from the same reaction mixture. Formation of the first compound as the major product shows the substitutional lability of the Mn(III) sites. Change of anion from ClO_4^- to PF_6^- results in the exclusive formation of first compound as PF_6^- salt. Unsymmetrical environment in the first compound effects the $Mn-OH_2$ distance and shows a smaller $Mn-OH_2$ distance (2.224 Å) compared with the value (2.315 Å) in the symmetrical environment of the second compound. Jahn-Teller distortions observed in both the complexes along *trans*-O_A-Mn-OAc bonds (O_A is the NO_3^- oxygen or water oxygen for the first compound and it is only water oxygen for the second compound).

7. Presence of Cl^- resulted in the formation of Mn(III) monomers $[Mn(phen)_2Cl_2](NO_3).2.5CH_3COOH$ and $[Mn(phen)(H_2O)Cl_3]$. Both

the compounds show a Jahn-Teller distortion by axial elongation. the second compound shows the longest $Mn-OH_2$ bond (2.306 Å) of all the known Mn(III)-aquo bound monomers.

8. $Mn(OAc)_3$ in aqueous solutions leads to the formation of Mn(III,IV) complex, $[Mn_2O_2(OAc)(H_2O)_2(bpy)_2](ClO_4)_2.HNO_3$. Observed structural deviation may be because of symmetry related disorder or particular type of Jahn-Teller distortion at the Mn(III) site.

9. Comparison of exchange parameter (J) with Mn-Mn distances shows a poor correlation for (III,IV) and (IV,IV) complexes. Detailed EHMO calculations will provide a better understanding of exchange interactions.

10. In general low yields of the present complexes shows that, characterisation of unisolated species in solution will provide further understanding of high-valent manganese chemistry in aqueous solution.

11. Formation of $[Mn_2O_2(HPO_4)(bpy)_2(H_2PO_4)_2].4H_2O$ and $[Mn_2O_2(H_2O)_2-(Br)_2(bpy)_2]Br$ are interesting and further structural studies on these complexes will help in understanding the reactions of aqueous solutions.

12. Though trans coordinated water complexes of manganese are not favorable for peroxo bridge formation (which is a key step in water oxidation reaction at WOC), the present complexes are interesting because of (i) uncommonly observed water coordination to high valent manganese (ii) possibility of

making magneto-structural correlations for dinuclear manganese complexes and (iii) possibility of using these complexes for chemical and photochemical oxidation of water, which aspect needs to be investigated in detail.

REFERENCES:

1. Hay, R. W. Bio-Inorganic Chemistry., Ellis Horwood Ltd: England, 1987.
2. Eichhorn, G. L. Inorganic Bio-Chemistry., Elsevier: New York, 1975; Vol. 1 and 2.
3. Cotton, F. A. and Wilkinson, G. Advanced Inorganic Chemistry., John Wiley: 5th Ed.; London, 1988.
4. "Bio-inorganic Chemistry - State of the Art" (series of articles) J. Chem. Edu., 1985, 62, 916.
5. Chiswell, B.; Mckenzie, E. D. and Lindoy, F. L. in Comprehensive Coordination Chemistry., Pergmon Press: 1987, Vol.4
6. Hughes, M. N. in Comprehensive Coordination Chemistry., Pergmon Press: 1987, Vol. 6.
7. Mann, S.; Frankel, R. B. and Blakemore, R. P. Nature (London), 1984, 310, 405.
8. Neilands, J. B. Struct. Bond. (Berlin), 1984, 58, 1.
9. Klotz, I. M. and Kurtz. Jr, D. M. Acc. Chem. Res. 1984, 17, 16.
10. Gnengerich, F. P. and Macdonald, T. L. Acc. Chem. Res. 1984, 17, 9.
11. Spiro, T. G. and Saltman, P. Struct. Bond. (Berlin), 1969, 6, 116.

12. Suslick, K. S. and Reinert, T. J. J. Chem. Edu. 1985, 62, 974.

13. Basolo, F.; Hoffman, B. M. and Ibers, J. A. Acc. Chem. Res. 1975, 8, 384.

14. Collman, J. P. Acc. Chem. Res. 1977, 10, 265.

15. Almog, J.; Baldwin, J. E.; Dyer, R. L. and Peters, M. J. Am. Chem. Soc. 1975, 97, 226.

16. Almog, J.; Baldwin, J. E. and Huff, J. J. Am. Chem. Soc. 1975, 97, 227.

17. Stenkamp, R. E.; Sieker, L. C. and Jensen, L. H. J. Am. Chem. Soc. 1984, 106, 618.

18. Elam, W. T.; Stern, E. A.; McCallum, J. D. and Loehr, J. S. J. Am. Chem. Soc. 1983, 105, 1919.

19. Shiemke, A. K.; Loehr, T. M. and Loehr, J. S. J. Am. Chem. Soc. 1986, 108, 2437.

20. Reem, R. C. and Solomon, E. I. J. Am. Chem. Soc. 1987, 109, 1216.

21. Armstrong, W. H.; Spool, A.; Papaefthymiou, G. C.; Frankel, R. B. and Lippard, S. J. J. Am. Chem. Soc. 1984, 106, 3653.

22. Spool, A.; Williams, I. D. and Lippard, S. J. Inorg. Chem. 1985, 24, 2156.

23. Wieghardt, K.; Tolksdorf, I. and Herrmann, W. Inorg. Chem. 1985, 24, 1230.

24. Groves, J. T. and Olson, J. R. Inorg. Chem. 1985, 24, 2717 and references there in.

25. Bertini, I.; Canti, G.; Luchinat, C. and Mani, F. J. Am. Chem. Soc. 1981, 103, 7784.

26. Bertini, I.; Canti, G. and Luchinat, C. J. Am. Chem. Soc. 1982, 104, 4943.

27. Bertini, I.; Gerber, M.; Lanini, G.; Luchinat, C.; Maret, W.; Rawer, S. and Zeppezauer, M. J. Am. Chem. Soc. 1984, 106, 1826.

28. Bertini, I.; Luchinat, C. and Scozzafava, A. Struct. Bond. (Berlin). 1982, 48, 45.

29. Rosenberg, R. C.; Root, C. A.; Bernstein, P. K. and Gray, H. B. J. Am. Chem. Soc. 1975, 97, 2092.

30. Shulman, R. G.; Navon, G.; Wiluda, B. J.; Douglas, D. C. and Yamane, T. Proc. Natl. Acad. Sci. (U.S.A), 1966, 56, 39.

31. Kushmir, T. and Navon, G. J. Mag. Reson. 1984, 56, 373.

32. Bertini, I.; Briganti, F.; Luchinat, C.; Mancini, M. and Spina, G. J. Mag. Reson. 1985, 62,

33. Solomon, E. I.; Penfield, K. W. and Wilcox, D. E. Struct. Bond. (Berlin), 1983, 53, 1.

34. McMillin, D. R. J. Chem. Edu. 1985, 62, 997.

35. Sykes, A. G. Chem. Soc. Rev. 1985, 14, 283.

36. Valentine, J. S. and deFreitas, M. D. J. Chem. Edu. 1985, 62,

990.

37. Solomon, E. I.; Hare, J. W.; Dooley, D. M.; Dawson, J. H.; Stephens, P. J. and Gray, H. B. J. Am. Chem. Soc. 1980, 102, 168.

38. Blair, D. F.; Campbell, G. W.; Schoonover, J. R.; Chan, S. I.; Gray, H. B.; Malmstrom, B. G.; Pecht, I.; Sawnson, B. I.; Woodruff, W. H.; English, A. M.; Fry, H. A.; Lum, V. and Norton, K. A. J. Am. Chem. Soc. 1985, 107, 5755.

39. Hay, R. W. Coord. Chem. Rev. 1981, 35, 85 and 1982, 41, 191.

40. Burgmayer, S. J. N. and Stiefel E. I. J. Chem. Edu. 1985, 62, 943.

41. Frank, P.; Carlson, R. M. K. and Hodgson, K. O. Inorg. Chem. 1986, 25, 470.

42. Tracey, A. S.; Gresser, M. J. and Parkinson, K. M. Inorg. Chem. 1987, 26, 627.

43. Barret, J.; Brien, P. O. and deJesus, J. P. Polyhedron. 1985, 4, 1.

44. Broderick, W. E. and Legg, J. I. Inorg. Chem. 1985, 24, 3724.

45. Thomson, A. J. Nature. (London), 1982, 298, 602.

46. Livorness, J. and Smith, T. D. Struct. Bond. (Berlin), 1982, 48, 1.

47. Wieghardt, K. Angew. Chem. Int. Ed. Engl. 1989, 28, 1153.

48. Battscheffsky, M., Ed.; Current Research in Photosynthesis,

Kluwer, Academic Publisher: Netherland, 1990, Vol. 1.

49. Renger, G. Angew. Chem. Int. Ed. Engl. 1987, 26, 643.

50. Govindjee.; Kambara, T. and Coleman, W. Photochem. Photobiol. 1985, 42, 187.

51. Renger, G. and Govindjee. Photosynth. Res. 1985, 6, 33.

52. George, G. N.; Prince, R. C. and Cramer, S. P. Science. 1989, 243, 789.

53. Gulies, R. D.; Zimmermann, J. L.; McDermott, A. E.; Yachandra, V. K.; Cole, J. L.; Dexheimer, S. L.; Britt, R. D.; Wieghardt, K.; Bossek, U.; Sauer, K. and Klein, M. P. Biochemistry. 1990, 29, 471.

54. Gulies, R. D.; Yachandra, V. K.; McDermott, A. E.; Cole, J. L.; Dexheimer, S. L.; Britt, R. D.; Bossek, U.; Sauer, K. and Klein, M. P. Biochemistry. 1990, 29, 486.

55. Penner-Hahn, J. E.; Fronko, R. M.; Pecoraro, V. L.; Yocum, C. F.; Betts, S. D. and Bowlby, N. R. J. Am. Chem. Soc. 1990, 112, 2549.

56. Kusunoki, M.; Ono, T.; Matsushita, T.; Oyanagi, H. and Inoue, Y. J. Biochem. 1990, 108, 560.

57. Yachandra, V. K.; Derose, V. J.; Latimer, M. J.; Mukerji, I.; Sauer, K. and Klein, M. P. Photochem. Photobiol. 1991, 53S, 98S.

58. Kim, D. H.; Britt, R. D.; Klein, M. P. and Sauer, K. J. Am.

Chem. Soc. 1990, 112, 9389.

59. Sivaraja, M.; Philo, J. S.; Lary, J. and Dismukes, G. C. J. Am. Chem. Soc. 1989, 111, 3221.

60. Radmer, R. and Cheniac, G. M. Topics. Photosynth. 1977, 2, 304 and 348.

61. Murata, N.; Miyaga, M.; Omata, T.; Matsunami, H. and Kuwabara, T. Biochim. Biophys. Acta. 1984, 765, 363.

62. Kok, B.; Forbush, B. and McGloin, M. Photochem. Photobiol. 1970, 11, 457.

63 (a)Dismukes, G. C. and Siderer, Y. Proc. Natl. Acad. Sci. USA. 1981, 78, 274.

(b)Dismukes, G. C.; Ferris, K. and Watnick, P. Photobiochem. Photobiophys. 1982, 3, 243.

64. Hansson, O. and Andreasson, L. E. Biochim. Biophys. Acta. 1982, 697, 261.

65. Cooper, S. R.; Dismukes, G. C.; Klein. M. P. and Calvin, M. J. Am. Chem. Soc. 1978, 100, 7248.

66. Dexheimer, S. L.; Sauer, K. and Klein, M. P. In Current Research In Photosynthesis Battschaffsky, M., Ed.; Kluwer, Academic Publisher: Netherland, 1990; Vol. 1, pp 761.

67. Brudwig, G. W. and Crabtree, R. H. Proc. Natl. Acad. Sci. (U.S.A), 1986, 83, 4586.

68. Vincent, J. B. and Christou, G. Inorg. Chim .Acta. 1987, 136,

L41.

69. Kambara, T. and Govindjee. Proc. Natl. Acad. Sci.(U.S.A) 1985, 82, 6119.

70. Christou, G. Acc. Chem. Res. 1989, 22, 328.

71. Pecoraro, V. Photochem. Photobiol. 1988, 48, 249.

72. Young, C. G. Coord. Chem. Rev. 1989, 96, 89.

73. Nyholm, R. S. and Turco, A. Chem. Ind. (London) 1960, 74.

74. Plaksin, P. M.; Stoufer, R. C.; Mathew, M. and Palenik, G. J. J. Am. Chem. Soc. 1972, 94, 2121.

75. Uson, R.; Riera, V. and Laguna, M. Transition. Met. Chem. 1975-76, 1, 21.

76. Stebler, M.; Ludi, A. and Burgi, H. B. Inorg. Chem. 1986, 25, 4743.

77. Cooper, S. R. and Calvin, M. J. Am. Chem. Soc. 1977, 99, 6623.

78. Goodwin, H. A. and Sylva, R. N. Aust. J. Chem. 1967, 20, 629.

79. Collins, M. A.; Hodgson, D. J.; Michelsen, K. and Towle, D. K. J. Chem. Soc. Chem. Commun. 1987, 1659.

80. Goodson, P. A.; Oki, A. R.; Glerup, J. and Hodgson, D. J. J. Am. Chem. Soc. 1990, 112, 6248.

81. Goodson, P. A.; Glerup, J.; Hodgson, D. J.; Michelsen, K. and Pedersen, E. Inorg. Chem. 1990, 29, 503.

82. Towle, D. K.; Botsford, C. A. and Hodgson, D. J. Inorg. Chim. Acta. 1988, 141, 167.

83. Oki, A. R.; Glerup, J. and Hodgson, D. J. Inorg. Chem. 1990, 29, 2435.

84. Hagan, K. S.; Armstrong, W. H. and Hope, H. Inorg. Chem. 1988, 27, 967.

85. Brewer, K, J.; Calvin, M.; Lumpkin, R. S.; Otvos, J. W. and Spreer, L. O. Inorg. Chem. 1989, 28, 4446.

86. Suzuki, M.; Senda, H.; Kobayashi, Y.; Oshio, H. and Uehara, A. Chem. Lett. 1988, 1763.

87. Goodson, P. A. and Hodgson, D. J. Inorg. Chim. Acta. 1990, 172, 49.

88. Gohdes, J. W. and Armstrong, W. H. Inorg. Chem. 1992, 31, 368.

89. Mikuriya, M.; Yamato, Y. and Tokii, T. Inorg. Chim. Acta. 1991, 181, 1.

90. Gravia-Deibe, A.; Sousa, A.; Bermejo, M. R.; MacRory, P. P.; McAuliffe, C. A.; Pritchard, R. G. and Helliwel, M. J. Chem. Soc. Chem. Commun. 1991, 728.

91. Yu, S. B.; Wang, C. P.; Day, E. P. and Holm, R. H. Inorg. Chem. 1991, 30, 4067.

92. Vincent, J. B.; Folting, K.; Huffman, J. C. and Christou, G. Inorg. Chem. 1986, 25, 996.

93. Mangia, A.; Nardelli, M.; Pelizzi, C. and Pelizzi, G. J. Chem. Soc. Dalton. Trans. 1973, 1141.

94. Larson, E.; Haddy, A.; Kirk, M. L.; Sands, R. H.; Hatfield,

W. E. and Pecoraro, V. L. J. Am. Chem. Soc. 1992, 114, 6263.

95. Larson, E.; Lah, M. S.; Li, X.; Bonadies, J. A. and Pecoraro, V. L. Inorg. Chem. 1992, 31, 373.

96. Mikuriya, M.; Yamato, Y. and Tokii, T. Chem. Lett. 1992, 1571.

97. Bashkin, J. S.; Schake, A. R.; Vincent, J. B.; Chang, H. R.; Li, Q.; Huffman, J. C.; Christou, G. and Hendrickson, D. N. J. Chem. Soc. Chem. Commun. 1988, 700.

98. Libby, E.; Webb, R. J.; Streib, W. E.; Folting, K.; Huffman, J. C.; Hendrickson, D. N. and Christou, G. Inorg. Chem. 1989, 28, 4037

99. Bonadies, J. A.; Kirk, M. L.; Lah, M. S.; Kessissoglu, D. P.; Hatfield, W. E. and Pecoraro, V. L. Inorg. Chem. 1989, 28, 2037.

100 Goodson, P. A.; Glerup, J.; Hodgson, D. J.; Michelsen, K. and Weihe, H. Inorg. Chem. 1991, 30, 4909.

101. Wieghardt, K.; Bossek, U.; Zsolnai, L.; Huttner, G.; Blondin, G.; Girerd, J. J. and Babonneau, F. J. Chem. Soc. Chem. Commun. 1987, 651.

102 Pal, S.; Gohdes, J. W.; Christian, W.; Wilisch, A. and Armstrong, W. H. Inorg. Chem. 1992, 31, 713.

103. Pal, S. and Armstrong, W. H. Inorg. Chem. 1992, 31, 5417.

104. Pal, S.; Chan, M. K. and Armstrong, W. H. J. Am. Chem. Soc.

1992, 114, 6398.

105. Stenkamp, R. E.; Sieker, L. C.; Tensen, L. H. and Sandersloehr, J. Nature. 1981, 291, 263.

106. Stenkamp, R. E.; Sieker, L. C. and Tensen, L. H. J. Am. Chem. Soc. 1984, 106, 618.

107. Wieghardt, K.; Bossek, U.; Ventur, D. and Weiss, J. J. Chem. Soc. Chem. Commun. 1985,347.

108. Wieghardt, K.; Bossek, U.; Nuber, B.; Weiss, J.; Corbella, M.; Vitols, S. E. and Girerd, J. J. J. Am. Chem. Soc. 1988, 110, 7398.

109. Bossek, U. and Wieghardt, K. Inorg. Chim. Acta. 1989, 165, 123.

110. Sheats, J. E.; Czernuszewicz, R. S.; Dismukes, G. C.; Rheingold, A. R.; Petrouleas, V.; Stubbe, J.; Armstrong, W. H.; Beer, R. H. and Lippard, S. J. J. Am. Chem. Soc. 1987, 109, 1435.

111. Menage, S.; Girerd, J. J. and Gleizes, A. J. Chem. Soc. Chem. Commun. 1988, 431.

112. Blackman, A. G.; Huffman, J. C.; Lobkovsky, E. B. and Christou, G. J. Chem. Soc. Chem. Commun. 1991, 989.

113. Wieghardt, K.; Bossek, U.; Bonvoisin, J.; Beauvillain, P.; Girerd, J. J.; Nuber, B.; Weiss, J. and Herinze, J. Angew. Chem. Int. Ed. Engl. 1986, 25, 1030.

114. Wu, F. -J.; Kurtz, Jr.,D. M.; Hagen, K. S.; Nyman, P. D.; Debrunner, P. G. and Vankai, V. A. Inorg. Chem. 1990, 29, 5174.

115. Diril, H.; Chang, H. R.; Zhang, X.; Larsen, S. K.; Potenza, J. A.; Pierpont, C. G.; Schugar, H. J.; Isied. S. S. and Hendrickson, D. N. J. Am. Chem. Soc. 1987, 109, 6207.

116. Chang, H. R.; Diril, H.; Nilges, M. J.; Zhang, X.; Potenza, J. A.; Schugar, H. J.; Hendrickson, D. N. and Iseid, S. S. J. Am. Chem. Soc. 1988, 110, 625.

117. Diril, H.; Chang, H. R.; Nilges, M. J.; Zhang, X.; Potenza, J. A.; Schugar, H. J.; Isied, S. S. and Hendrickson, D. N. J. Am. Chem. Soc. 1989, 111, 5102.

118. Suzuki, M.; Mikuriya, M.; Murata, S.; Uehara, A.; Oshio, H.; Kida, S. and Saito, K. Bull. Chem. Soc. Jpn. 1987, 60, 4305.

119. Buchanan, R. M.; Oberhausen, K. J. and Richardson, J. F. Inorg. Chem. 1988, 27, 971.

120. Mikuriya, M.; Fujii, T.; Tokii, T. and Kawamori, A. Bull. Chem. Soc. Jpn. 1993, 66, 1675.

121. Kipke, C. A.; Scott, M. J.; Gohdes, J. W. and Armstrong, W. H. Inorg. Chem. 1990, 29, 2193.

122. Camenzind, M. J.; Schardt, B. C. and Hill, C. L. Inorg. Chem. 1984, 23, 1984.

123. Vogt, L. H.; Zalkin, A. and Templeton, D. H. Inorg. Chem. 1967, 6, 1725.

124. Bossek, U.; Weyhermuller, T.; Wieghardt, K.; Nuber, B. and Weiss, J. J. Am. Chem. Soc. 1990, 112, 6387.

125. Sarneski, J. E.; Didiuk, M.; Thorp, H. H.; Crabtree, R. H.; Brudvig, G. W.; Faller, J. W. and Schulte, G. K. Inorg. Chem. 1991, 30, 2833.

126. Schardt, B. C., Hollander, F. J. and Hill, C. L. J. Am. Chem. Soc. 1982, 104, 3964.

127. Baikie, A. R. E.; Hursthouse, M. B.; New, D. B. and Thornton, P. J. Chem. Soc. Chem. Commun. 1978, 62.

128. Baikie, A. R. E.; Hursthouse, M. B.; New, L.; Thornton, P. and White, R. G.; J. Chem. Soc. Chem. Commun. 1980, 684.

129. Vincent, J. B.; Chang, H. R.; Folting, K.; Huffman, J. C.; Christou, G. and Hendrickson. D. N. J. Am. Chem. Soc. 1987, 109, 5703.

130. McCusker, J. K.; Jang, H. G.; Wang, S.; Christou, G. and Hendrickson, D. N. Inorg. Chem. 1992, 31, 1874.

131. Auger, N.; Girerd, J. J.; Corbella, M.; Gleizes, A. and Zimmermann, J. L. J. Am. Chem. Soc. 1990, 112, 448.

132. Sarneski, J. E.; Thorp, H. H.; Brudvig, G. W.; Crabtree, R. H. and Schulte, G. K. J. Am. Chem. Soc. 1990, 112, 7255.

133. Mikuriya, M.; Majima, K. and Yamato, Y. Chem. Lett. 1992, 1929.

134. Wieghardt, K.; Bossek, U.; Nuber, B.; Weiss, J.; Gehring, S.

and Haase, W. J. Chem. Soc. Chem. Commun. 1988, 1145.

135. Li, X.; Kessissoglou, D. P.; Kirk, M. L.; Bender, C. J. and Pecoraro, V. L. Inorg. Chem. 1988, 27, 1.

136. Kessissoglou, D. P.; Kirk, M. L.; Bender, C. A.; Lah, M. S. and Pecoraro, V. L. J. Chem. Soc. Chem. Commun. 1989, 84.

137. Kessissoglou, D. P.; Kirk, M. L.; Lah, M. S.; Li, X.; Raptopoulou, C.; Hatfield, W. E. and Pecoraro, V. L. Inorg. Chem. 1992, 31, 5424.

138. Wieghardt, K.; Bossek, U. and Gebert, W. Angew. Chem. Int. Ed. Engl. 1983, 22, 328.

139. Mckee, V. and Shepard, W. B. J. Chem. Soc. Chem. Commun. 1985, 158.

140. Brooker, S.; Mckee, V. and Shepard, W. B. J. Chem. Soc. Dalton. Trans. 1987, 2555.

141. Bashkin, J. S.; Chang, H. R.; Streib, W. E.; Huffman, J. C.; Hendrickson, D. N. and Christou, G. J. Am. Chem. Soc. 1987, 109, 6502.

142. Vincent, J. B.; Christmas, C.; Huffman, J. C.; Christou, G.; Chang, H. R. and Hendrickson, D. N. J. Chem. Soc. Chem. Commun. 1987, 236.

143. Vincent, J. B.; Christmas, C.; Chang, H. R.; Li, Q.; Boyd, P. D. W.; Huffman, J. C.; Hendrickson, D. N. and Christou, G. J. Am. Chem. Soc. 1989, 111, 2086.

144. Li, Q.; Vincent, J. B.; Libby, E.; Chang, H. R.; Huffman, J. C.; Boyd, P. D. W.; Christou, G. and Hendrickson, D. N. Angew. Chem. Int. Ed., Engl. 1988, 27, 1731.

145. Mckee, V. and Tandon, S. S. J. Chem. Soc. Chem. Commun. 1988, 1334.

146. Kulawiec, R. J.; Crabtree, R. H.; Brudvig, G. W. and Schulte, G. K. Inorg. Chem. 1988, 27, 1309.

147. Thorp, H. H.; Sarenski, J. E.; Kulaweic, R. J.; Brudvig, G. W.; Crabtree, R. H. and Papaefthymiou, G. C. Inorg. Chem. 1991, 30, 1153.

148. Suzuki, M.; Sugisawa, T.; Senda, H.; Oshio, H. and Uehara, A. Chem. Lett. 1989, 1091.

149. Chan, M. K. and Armstrong, W. H. J. Am. Chem. Soc. 1990, 112, 4985.

150. Wang, S.; Folting, K.; Streib, W. E.; Schmitt, E. A.; McCusker, J. K.; Hendrickson, D. N. and Christou, G. Angew. Chem. Int.Ed. Engl. 1991, 30, 305.

151. Chan, M. K. and Armstrong, W. H. J. Am. Chem. Soc. 1991, 113, 5055.

152. (a) Mikuriya, M.; Yamato, Y. and Tokii, J. Chem. Lett. 1991, 1929.

(b) Suzuki, M.; Hayashi, Y.; Munezawa, K.; Suenaga, M.; Senda, H and Uehara, A. Chem. Lett. 1991, 1429.

153. Hendrickson, D. N.; Christou, G.; Schmitt, E. A.; Libby, E.; Bashkin, J. S.; Wang, S.; Tsai, H. L.; Vincent, J. B.; Boyd, P. D. W.; Huffman, J. C.; Folting, K.; Li. Q. and Streib, W. E. J. Am. Chem. Soc. 1992, 114, 2455.

154. Schmitt, E. A.; Noodleman, K.; Baerends, E. J. and Hendrickson. D. N. J. Am. Chem. Soc. 1992, 114, 6109.

155. Philouze, C.; Blondin, G.; Menage, S.; Auger, N.; Girerd, J. J.; Vigner, D.; Lance, M. and Nierlich, M. Angew. Chem. Int. Ed. Engl. 1992, 31, 1629.

156. Shindo, K.; Mori, y.; Motoda, K. I.; Sakiyama, H.; Matsumoto, N. and Okawa, H. Inorg. Chem. 1992, 31, 4987.

157. Bouwman, E.; Bolcar, M. A.; Libby, E.; Huffman, J. C.; Folting, K. and Christou, G. Inorg. Chem. 1992, 31, 5185.

158. Wang, S.; Tsai, H. L.; Streib, W. E.; Christou, G. and Hendrickson, D. N. J. Chem. Soc. Chem. Commun. 1992, 1427.

159. Wemple, M. W.; Tsai, H. L.; Folting, K.; Hendrickson D. N. and Christou, G. Inorg. Chem. 1993, 32, 2025.

160. Jiang, Z. H.; Ma, S. L.; Liao, D. Z.; Yan, S. P.; Wang, G. L.; Yao, X. K. and Wang, R. J. J. Chem. Soc. Chem. Commun. 1993, 745.

161. Chandra, S. K.; Chakraborty, P. and Chakravorty, A. J. Chem. Soc. Dalton. Trans. 1993, 863.

162. Low, D. W.; Eichhorn, D. M.; Draganescu, A. and Armstrong, W. H.

Inorg. Chem. 1991, 30, 877.

163. Bhula, R. and Weatherburn, D. C. Angew. Chem. Int. Ed. Engl. 1991, 30, 688.

164. Libby, E.; Folting, K.; Huffman, J. C. and Christou, G. J. Am. Chem. Soc. 1990, 112, 5354.

165. Perlepes, S. P.; Huffman. J. C. and Christou, G. J. Chem. Soc., Chem. Commun. 1991, 1657.

166. Schake, A. R.; Tsai, H. L.; Nadine de Vries.; Webb, R. J.; Folting, K.; Hendrickson, D. N. and Christou, G. J. Chem. Soc. Chem. Commun. 1992, 181.

167. Wang, S.; Tsai, H. L.; Streib, W. E.; Christou, G. and Hendrickson, D. N. J. Chem. Soc. Chem. Commun. 1992, 677.

168. Sessoli, R.; Tsai, H. L.; Schake, A. R.; Wang, S.; Vincent, J. B.; Folting, K.; Gatteschi, D.; Christou, G. and Hendrickson, D. N. J. Am. Chem. Soc. 1993, 115, 1804.

169. Cavaluzzo, M.; Chen, Q. and Zubieta, J. J. Chem. Soc. Chem. Commun. 1993, 131.

170. Ramaraj, R.; Kira, A. and Kaneko, M. Angew. Chem. Int. Ed. Engl. 1986, 25, 825.

171. Chandra, S. K.; Chakraborty, P. and Chakravorty, A. J. Chem. Soc. Dalton. Trans. 1993, 863.

172. Swarnabala, G. and Rajasekharan, M. V. Proc. Ind. Acad. Sci. (Chem Sci) 1990, 102, 87.

173. Furniss, B. S.; Hannaford, A. J.; Rogers, V.; Smith, P. W. G. and Tatchell, A. R. Vogel's Text book of practical Organic Chemistry, Ed., ELBS, 1978.

174. Bassett, J.; Denney, R. C.; Jeffery, G. H. and Mendham, J. Vogel's Textbook of Quantitative Inorganic Analysis, Ed., ELBS, 1978.

175. Dutta, R. L. and Syamal, A. Elements of Magnetochemistry, S. Chand Co. Ltd., 1982.

176. Chandler, J. P. Program 66, Quantum Chemistry Program Exchange, Indiana University, U.S.A.

177. Fair, C. K., MOLEN, Molecular Structure Solution Procedures, Enraf-Nonius, Delft, Netherland, 1990.

178. North, A. C. T.; Phillips, D. C. and Mathews, F. S. Acta Crystallor (A), 1968, A24, 351.

179. Sheldrik, G. M., SHELX-76, Program for Crystal Structure Determination, University of Cambridge, Cambridge, England, 1976.

180. Sheldrik, G. M., SHELXS-86, Program for Crystal Structure Solution, Unversity of Gottingen, Gottingen, Germany, 1986.

181. Johnson, C. K., ORTEP, Report ORNL-3794, Oak Ridge National Laboratory, Oak Ridge, Tennessee, U.S.A., 1965.

182. Sharma, Y. R. and Prakash, P. K. S. Indian. J. Chem. 1980, 19A, 1175.

183. Koikawa, M.; Okawa, H. and Kida, S. J. Chem. Soc. Dalton.

Trans. 1988, 641.

184. Phillips, C. S. G. and Williams, R. J. P. Inorganic Chemistry, Oxford, 1966, Vol. 2, p. 104.

185. Hayward, M. P. and Wells, C. F. Transition. Met. Chem. 1987, 12, 179.

186. O'Connor, C. J. Prog. Inorg. Chem. 1982, 29, 203.

187. Bodner, A.; Drueke, S.; Wieghardt, k.; Nuber, B. and Weiss, J. Angew. Chem. Int. Ed. Engl. 1990, 29, 68.

188. Knopp, P. and Wieghardt, K. Inorg. Chem. 1991, 30, 4061.

189. Martin, L.; Wieghardt, K.; Blondin, G.; Girerd, J. J.; Nuber, B. and Weiss, J. J. Chem. Soc. Chem. Commun. 1990, 1767.

190. Hartman, J. R.; Rardin, R. L.; Chaudhuri, P.; Phol, K.; Wieghardt, K.; Nuber, B.; Weiss, J.; Papaetthymious, A. C.; Frankel, R. B. and Lippard, S. J. Am. Chem. Soc. 1987, 109, 7387.

191. Wieghardt. K.; Bossek, U.; Neves, A.; Nuber, B. and Weiss, J. Inorg. Chem. 1989, 28, 432.

192. Das, B. K. and Chakravarty, A. R. Inorg. Chem. 1991, 30, 4978.

193. Pistorius, E. K. and Schmid, G. H. Biochimica. Biophysica. Acta. 1987, 890, 352.

194. Perlepes, S. P.; Blackman, A. G.; Huffman, J. C. and Christou, G. Inorg. Chem. 1991, 30, 1665.

195. Lumme, P. O. and Lindell, E. Acta. Crystallogr. Sect. A. 1988, 44, 463.

196. Hathaway, B. J. In Comprehensive Coordination Chemistry, Wilkinson, G., Ed., Pergmon Press: Oxoford, England, 1989, Vol 5, P. 611.

197. Williamson, M. M. and Hill, C. L. Inorg. Chem. 1986, 25, 4468.

198. Lis, T.; Matuszewski, J. and Jezowska, B. Acta. Crystallogr. Sect. B. 1977, 33, 1943.

199. Lis, T. and Matuszewski, J. Pol. J. Chem. 1980, 54, 169.

200. Kaucic, V. and Bukovec, P. J. Chem. Soc. Dalton. Trans. 1979, 1512.

201. Swarnabala, G.; Rajender Reddy, K.; Jyotsna, T. and Rajasekharan M. V. Transition. Met. Chem. (Submitted)

202. Dingle, R. Acta. Chim. Scand. 1966, 20, 33.

203. Sarnseki, J. E.; Brzezinski, L. J.; Anderson, B.; Didiuk, M.; Manchanda, R.; Crabtree, R. H.; Brudwig, G. W. and Schulte, G. K. Inorg. Chem. 1993, 32, 3265.

204. Dave, B. C.; Czernuszewicz, R. S.; Bond, M. R. and Carrano, C. J. Inorg. Chem. 1993, 32, 3593.

205. Bossek, U.; Weyhermüller.; Wieghardt, K.; Bonvoisin, J. and Girerd, J. J. J. Chem. Soc Chem. Commun. 1989, 633.

206. Hotzelmann, R.; Wieghardt, K.; Flörke, U.; Haupt, H. J.;

Weatherburn, D. C.; Bonvoisin, J.; Blondin, G. and Girerd, J. J. J. Am. Chem. Soc. 1992, 114, 1681.

207. Chang, H. R.; Larsen, S. K.; Boyd, P. D. W.; Pirepont, C. G. and Hendrickson, D. N. J. Am. Chem. Soc. 1988, 110, 4565.